

Gear shift strategies for automotive transmissions

Citation for published version (APA):

Ngo, D. V. (2012). *Gear shift strategies for automotive transmissions*. [Phd Thesis 1 (Research TU/e / Graduation TU/e), Mechanical Engineering]. Technische Universiteit Eindhoven.
<https://doi.org/10.6100/IR735458>

DOI:

[10.6100/IR735458](https://doi.org/10.6100/IR735458)

Document status and date:

Published: 01/01/2012

Document Version:

Publisher's PDF, also known as Version of Record (includes final page, issue and volume numbers)

Please check the document version of this publication:

- A submitted manuscript is the version of the article upon submission and before peer-review. There can be important differences between the submitted version and the official published version of record. People interested in the research are advised to contact the author for the final version of the publication, or visit the DOI to the publisher's website.
- The final author version and the galley proof are versions of the publication after peer review.
- The final published version features the final layout of the paper including the volume, issue and page numbers.

[Link to publication](#)

General rights

Copyright and moral rights for the publications made accessible in the public portal are retained by the authors and/or other copyright owners and it is a condition of accessing publications that users recognise and abide by the legal requirements associated with these rights.

- Users may download and print one copy of any publication from the public portal for the purpose of private study or research.
- You may not further distribute the material or use it for any profit-making activity or commercial gain
- You may freely distribute the URL identifying the publication in the public portal.

If the publication is distributed under the terms of Article 25fa of the Dutch Copyright Act, indicated by the "Taverne" license above, please follow below link for the End User Agreement:

www.tue.nl/taverne

Take down policy

If you believe that this document breaches copyright please contact us at:

openaccess@tue.nl

providing details and we will investigate your claim.

Gear Shift Strategies
for
Automotive Transmissions

Ngo Dac Viet

Doctoral committee:

prof.dr. L.P.H. de Goey (chairman)
prof.dr.ir. M. Steinbuch (supervisor)
dr.ir. T. Hofman (co-supervisor)
prof. Hyunsoo Kim, PhD (Sungkyunkwan University)
prof. Huei Peng, PhD (University of Michigan)
prof.dr.ir. P.P.J. van den Bosch (Eindhoven University of Technology)
dr.ir. A.F.A. Serrarens (Drivetrain Innovations B.V.)
dr.ir. P.A. Veenhuizen (HAN University of Applied Sciences)

The research leading to this dissertation is part of the project ‘Euro Hybrid’, which is a research project of Drivetrain Innovations B.V., together with Eindhoven University of Technology, The Netherlands. The project is financially supported by Dutch government through AgentschapNL.

Gear Shift Strategies for Automotive Transmissions / by Ngo Dac Viet – Eindhoven University of Technology, 2012 – PhD dissertation.

A catalogue record is available from the Eindhoven University of Technology Library.
ISBN: 978-90-386-3222-3

Copyright © 2012 by Ngo Dac Viet. All rights reserved.

This dissertation was prepared with the PDF \LaTeX documentation system.
Cover design: Oranje Vormgevers, Eindhoven, The Netherlands.
Reproduction: Ipskamp Drukkers B.V., Enschede, The Netherlands.

Gear Shift Strategies
for
Automotive Transmissions

PROEFSCHRIFT

ter verkrijging van de graad van doctor
aan de Technische Universiteit Eindhoven,
op gezag van de rector magnificus, prof.dr.ir. C.J. van Duijn,
voor een commissie aangewezen door het College voor Promoties
in het openbaar te verdedigen
op woensdag 26 september 2012 om 16.00 uur

door

Ngo Dac Viet

geboren te Thua Thien Hue, Vietnam

Dit proefschrift is goedgekeurd door de promotor:

prof.dr.ir. M. Steinbuch

Copromotor:

dr.ir. T. Hofman

Summary

Gear Shift Strategies for Automotive Transmissions

The development history of automotive engineering has shown the essential role of transmissions in road vehicles primarily powered by internal combustion engines. The engine with its physical constraints on the torque and speed requires a transmission to have its power converted to the drive power demand at the wheels. Under dynamic driving conditions, the transmission is required to shift in order to match the engine power with the changing drive power. Furthermore, a gear shift decision is expected to be consistent such that the vehicle can remain in the next gear for a period of time without deteriorating the acceleration capability. Therefore, an optimal conversion of the engine power plays a key role in improving the fuel economy and driveability. Moreover, the consequences of assumptions related to the discrete state variable-dependent losses, e.g. gear shift, clutch slippage and engine start, and their effect on the gear shift control strategies are necessary to be analyzed to yield insights into the fuel usage.

The first part of the dissertation deals with the design of gear shift strategies for electronically controlled discrete ratio transmissions used in both conventional vehicles and Hybrid Electric Vehicles (HEVs). For conventional vehicles, together with the fuel economy, the driveability is systematically addressed in a Dynamic Programming (DP) based optimal gear shift strategy by three methods: i) the weighted inverse of power reserve, ii) the constant power reserve, and iii) the variable power reserve. In addition, a Stochastic Dynamic Programming (SDP) algorithm is utilized to optimize the gear shift strategy, subject to a stochastic distribution of the power request, in order to minimize the expected fuel consumption over an infinite horizon. Hence, the SDP-based gear shift strategy intrinsically respects the driveability and is realtime implementable. By performing a comparative analysis of all proposed gear shift methods, it is shown that the variable power reserve method achieves the highest fuel economy without deteriorating the driveability. Moreover, for HEVs, a novel fuel-optimal control algorithm, consisting of the continuous power split and discrete gear shift, engine on-off problems, based on a combination of DP and Pontryagin's Minimum Principle (PMP) is developed for the corresponding hybrid dynamical system. This so-called DP-PMP gear shift control approach benchmarks the development of an online implementable control strategy in

terms of the optimal tradeoff between calculation accuracy and computational efficiency. Driven by an ultimate goal of realizing an online gear shift strategy, a gear shift map design methodology for discrete ratio transmissions is developed, which is applied for both conventional vehicles and HEVs. The design methodology uses an optimal gear shift algorithm as a basis to derive the optimal gear shift patterns. Accordingly, statistical theory is applied to analyze the optimal gear shift patterns in order to extract the time-invariant shift rules. This alternative two-step design procedure makes the gear shift map: i) improve the fuel economy and driveability, ii) be consistent and robust with respect to shift busyness, and iii) be realtime implementable. The design process is flexible and time efficient such that an applicability to various powertrain systems configured with discrete ratio transmissions is possible. Furthermore, the study in this dissertation addresses the trend of utilizing route information in the powertrain control system by proposing an integrated predictive gear shift strategy concept, consisting of a velocity algorithm and a predictive algorithm. The velocity algorithm improves the fuel economy considerably (in simulation) by proposing a fuel-optimal velocity trajectory over a certain driving horizon for the vehicle to follow. The predictive algorithm successfully utilizes a predefined velocity profile over a certain horizon in order to realize a fuel economy improvement very close to that of the globally optimal algorithm (DP).

In the second part of the dissertation, the energetic losses, involved with the gear shift and engine start events in automated manual transmission-based HEVs, are modeled. The effect of these losses on the control strategies and fuel consumption for (non-)powershift transmission technologies is investigated. Regarding the gear shift loss, the study discloses a perception of a fuel-efficient advantage of the powershift transmissions over the non-powershift ones applied for passenger HEVs. It is also shown that the engine start loss can not be ignored in seeking a fair evaluation of the fuel economy. Moreover, the sensitivity study of the fuel consumption with respect to the prediction horizon reveals that a predictive energy management strategy can realize the highest achievable fuel economy with a horizon of a few seconds ahead. The last part of the dissertation focuses on investigating the sensitivity of an optimal gear shift strategy to the relevant control design objectives, i.e. fuel economy, driveability and comfort. A singular value decomposition based method is introduced to analyze the possible correlations and interdependencies among the design objectives. This allows that some of the possible dependent design objective(s) can be removed from the objective function of the corresponding optimal control problem, hence thereby reducing the design complexity.

Contents

Summary	v
1 Introduction	1
1.1 Automotive Transmissions	1
1.1.1 History	1
1.1.2 Technology Trends	3
1.2 Background	4
1.3 Challenges	6
1.4 Objectives and Contributions	10
1.5 Outline of The Dissertation	12
2 Optimal Gear Shift Strategies for Conventional Vehicles	17
2.1 Introduction	17
2.1.1 Literature Review	18
2.1.2 Research Objectives	19
2.2 Fuel-Optimal Gear Shift Strategy	20
2.2.1 Powertrain Model	20
2.2.2 Powertrain System Dynamics	22
2.2.3 Optimal Gear Shift Control Problem	23
2.2.4 Simulation Results	24
2.3 Driveability-Optimal Gear Shift Strategy	26
2.3.1 Driveability Definition	26
2.3.2 Method 1: The Weighted Inverse of Power Reserve	27
2.3.3 Method 2: The Constant Power Reserve	28
2.3.4 Method 3: The Variable Power Reserve	29
2.3.5 Comparison of Three Methods	35
2.4 Stochastic Gear Shift Strategy	37
2.4.1 Stochastic Modeling of Power Request	37
2.4.2 Stochastic Gear Shift Algorithm	40
2.4.3 Simulation Results and Discussions	41
2.5 Conclusions	43

3	Optimal Gear Shift Strategies for Hybrid Electric Vehicles	45
3.1	Introduction	45
3.2	Powertrain Modeling and Dynamics	47
3.2.1	Powertrain Model	48
3.2.2	Powertrain System Dynamics	50
3.3	Optimal Gear Shift Strategy without Start-Stop Functionality	51
3.3.1	Dynamic Programming	52
3.3.2	Dynamic Programming-Pontryagin's Minimum Principle	53
3.4	Optimal Gear Shift Strategy with Start-Stop Functionality	57
3.4.1	Dynamic Programming	58
3.4.2	Dynamic Programming-Pontryagin's Minimum Principle	58
3.5	Simulation Results and Discussions	60
3.5.1	Baseline Vehicles	60
3.5.2	HEV without the Start-Stop Functionality	63
3.5.3	HEV with the Start-Stop Functionality	65
3.5.4	Simulation Results on FTP75	66
3.6	Conclusions	66
4	Gear Shift Map Design Methodology	67
4.1	Introduction	67
4.2	Powertrain Modeling and Dynamics	70
4.2.1	Powertrain Model	70
4.2.2	Powertrain System Dynamics	72
4.3	Analysis of Gear Shift Contribution to Fuel Economy	73
4.3.1	Conventional Vehicle	73
4.3.2	Hybrid Electric Vehicle	74
4.4	Gear Shift Map Design for Conventional Vehicles	77
4.4.1	Acquisition of Optimal Gear Shift Data	78
4.4.2	Analysis of Shift Data	79
4.4.3	Shift Map Verification	82
4.5	Gear Shift Map Design for Hybrid Electric Vehicles	83
4.5.1	Gear Shift Map for Hybrid Mode	84
4.5.2	Gear Shift Map for E Mode	86
4.5.3	Gear Downshift Map for Regenerative Mode	87
4.5.4	Shift Map Verification	87
4.6	Experimental Validation on Conventional Vehicle	89
4.6.1	Gear Shift Map Generation	90
4.6.2	Description of Gear Shift Pattern	90
4.6.3	Validation in Simulation Environment	92
4.6.4	Experimental Results	95
4.7	Conclusions	96

5	Integrated Predictive Gear Shift Strategy	97
5.1	Benefits of The Preview Route Information	97
5.2	Powertrain Modeling and Dynamics	99
5.2.1	Powertrain Modeling	100
5.2.2	Powertrain System Dynamics	102
5.3	Predictive Algorithm	102
5.3.1	Model Predictive Control	102
5.3.2	Predictive Gear Shift Problem	103
5.3.3	Simulation Results	104
5.4	Velocity Algorithm	106
5.4.1	Travel Requirements on a Preview Route Segment	107
5.4.2	Optimal Velocity Problem	107
5.5	Implementation of the Velocity Algorithm	109
5.5.1	Discretization of Vehicle Longitudinal Dynamics	109
5.5.2	Decoupling of Velocity Algorithm	110
5.5.3	Driving Horizon	111
5.5.4	Simulation Results	112
5.6	Integrated Predictive Gear Shift Strategy	114
5.7	Conclusions	115
6	Effect of Gear Shift and Engine Start Losses	117
6.1	Introduction	117
6.2	Hybrid Powertrain Model	119
6.3	Hybrid Powertrain Control Algorithm	121
6.3.1	Optimal Control Problem Formulation	121
6.3.2	Gear Shift Command Sensitivity	123
6.3.3	Gear Shift Hysteresis	123
6.4	Gear Shift Loss Model and Control Problem	125
6.4.1	Gear Shift Loss Model	125
6.4.2	Optimal Control Problem with Gear Shift Loss	128
6.4.3	Simulation Results	129
6.5	Engine Start Loss Model and Control Problem	131
6.5.1	Engine Start Loss Model	131
6.5.2	Simulation Results	133
6.6	Prediction Horizon Sensitivity Study	134
6.6.1	Predictive Control Algorithm	134
6.6.2	Simulation Results and Discussions	135
6.7	Conclusions	135

7	Structural Analysis of the Control Design Objectives	139
7.1	Introduction	139
7.2	Review of Design Objectives	140
7.3	Powertrain Modeling and Dynamics	142
7.3.1	Powertrain Modeling	143
7.3.2	Powertrain System Dynamics	144
7.4	Optimal Control Problem	145
7.4.1	Vehicular Propulsion Systems	145
7.4.2	Multi-Objective Function	146
7.4.3	Optimal Control Algorithm	147
7.5	SVD-based Structural Analysis	148
7.5.1	Singular Value Decomposition	148
7.5.2	Structural Analysis	149
7.6	Results and Discussions	150
7.6.1	Application of SVD-based Structural Analysis	150
7.6.2	Simulation Results for Conventional Vehicles	151
7.6.3	Simulation Results for Hybrid Electric Vehicles	154
7.7	Conclusions	155
8	Conclusions and Recommendations	157
8.1	Conclusions	157
8.2	Recommendations	162
A	Optimal Power Split Control of HEVs	165
B	State Constrained Optimal Control of the Power Split for HEVs	169
C	Drive Cycles	173
	Bibliography	176
	Acknowledgements	187
	Curriculum Vitae	191

CHAPTER 1

Introduction

Abstract - In this chapter, some historical and technological trends of automotive transmissions used in road vehicles are briefly presented. Moreover, the background and scope of the dissertation are presented. In addition, the challenges related to the gear shift strategy design are discussed, which motivates the research objectives and scientific contributions. Finally, an outline of the dissertation is given.

1.1 Automotive Transmissions

1.1.1 History

Invention of the automobile and utilizing it as a means of transportation have made a great contribution to the growth of society. Automotive engineering and technology have always been subject to evolution. The current state of the art in vehicular propulsion systems is characterized by the following hierarchical interrelations:

environment ↔ traffic ↔ vehicle ↔ engine/transmission.

Since the early phase of the automotive development, the interaction between the environment and the traffic has been represented by an ever increasing number of legal standards related to reducing the exhaust gas pollutants, noise emissions, hazardous substances and waste, etc. The increasingly high traffic density, high demand of mobility and transportation adversely have a significant impact on the environment, causing the large societal problems such as a rapid depleting petroleum resources, an increasing air pollution and global warming. Meanwhile, the traffic and vehicles have been closely connected and have affected each other in a way to meet the required human mobility and transportation needs such as accessibility, destination attainability, maximum fuel economy, maximum driveability and comfort, etc. Hence, vehicular propulsion systems have been designed to satisfy the various human needs, and to match the public and

traffic situations, which have resulted in a strong segmentation of the vehicle classes. Vehicles powered by internal combustion engines require a transmission to transmit the engine power to the drive power at the wheels in accordance with a wide range of operating speeds. Therefore, in the last three decades, many different transmission designs have been developed with competing concepts in terms of the cost, packaging, overall gear ratio, the number of gears, efficiency, comfort and the ease of operation, etc.

Briefly, the development history of automotive transmissions can be roughly split into two stages [89].

- **Until 1980's**

In 1784, James Watt stipulated that the torque and speed of steam or internal combustion engines must be adapted to the load by means of a transmission in order to obtain the maximum drive power at the wheels. From 1884 till 1914, the correct principle for the torque-speed conversion was verified. From 1914 till the 1980's, the geared transmissions, automatic transmissions and continuously variable transmissions were developed. Later, the geared transmissions were more accepted because of their high power-weight ratio. The notion of standardized gearboxes was established. The development had continued until the 1980's in terms of service life, reliability, noise level and the ease of operation. The number of speeds and the overall gear ratio constantly increased.

- **1980's to present**

The transmission research and development have been focused on the individual solutions tailored to a particular usage. Alternative transmissions for passenger cars are competing with each other, e.g. Manual Transmission (MT), Automated Manual Transmission (AMT), Dual Clutch Transmission (DCT), PowerShift-Automated Manual Transmission (PS-AMT) [130], Automatic Transmission (AT), Continuously Variable Transmission (CVT) and Hybrid Transmission¹ (HT), electrically variable transmissions, etc. The number of gears increased up to eight speeds [122] or even nine speeds [36]. In the case of commercial vehicles, the transmissions have 6-16 speeds and cover large overall gear ratios. There are also important developments in integrating the subsystems in both passenger and commercial transmission technologies such as electronics, embedded software, function development, as well as in system and information networking, e.g. CAN bus, applied in vehicles.

¹The electric motor(s), clutch, torsional vibration damper, and hydraulics etc., of a hybrid concept are fitted in the geared transmission in a space-saving and efficient manner to create a Hybrid Transmission (HT).

1.1.2 Technology Trends

The rapid technology developments in electronics and electro-mechanical components and their application in the powertrain system are shaping the future of automotive transmission towards improving the fuel economy, driveability and gear shift comfort. Growth in the vehicle market driven by the increasingly stringent emission norms will create opportunities for the more advanced fuel-efficient transmission technologies such as AMT, PS-AMT, DCT, and CVT, HT, etc., to reach the end consumers.

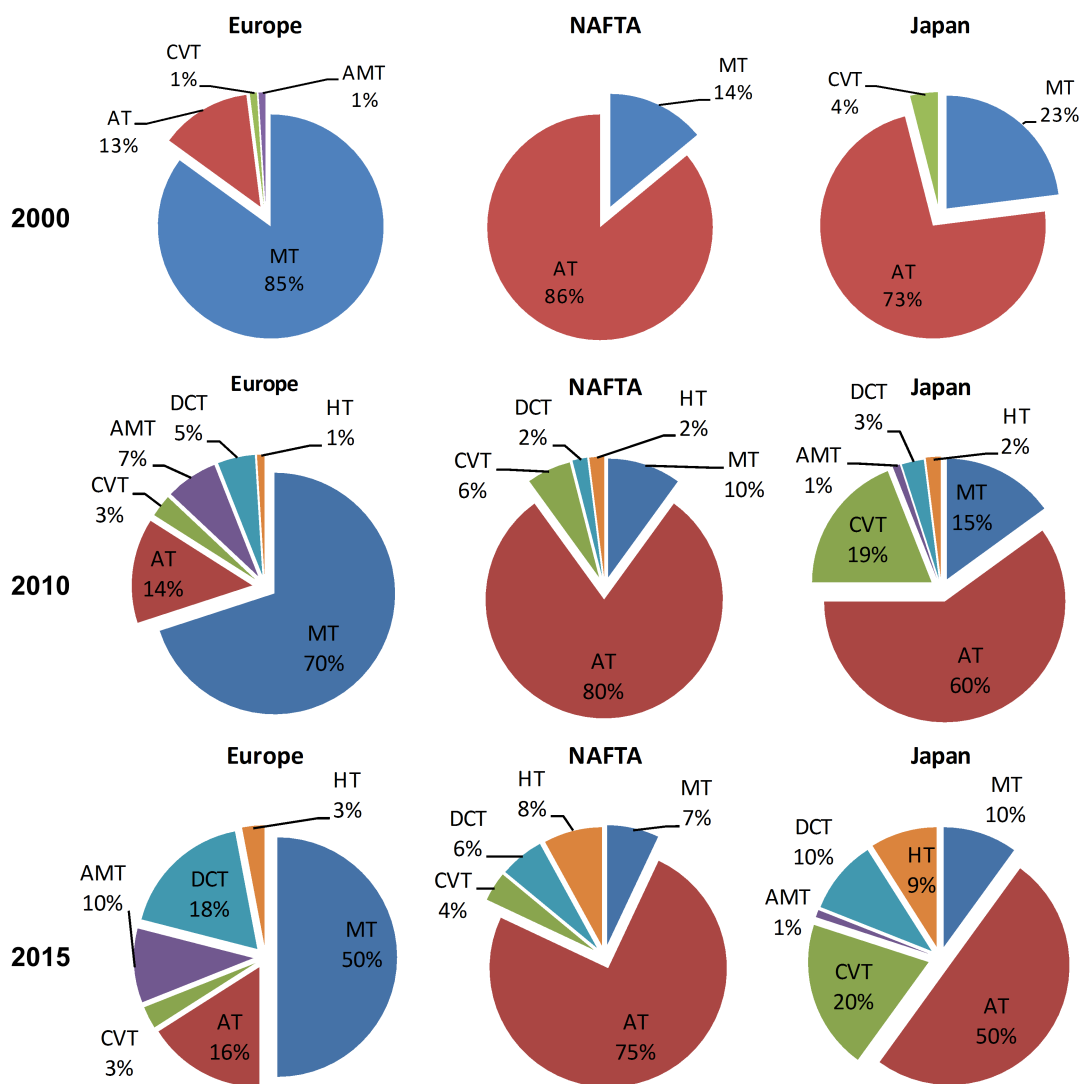


Figure 1.1: Passenger car transmissions: market share and prediction [89] (NAFTA stands for the North American Free Trade Agreement area).

Figure 1.1 illustrates the market share and prediction of the future market share of passenger car transmissions from 2000 till 2015 [89]. From this figure, it can be observed that the market share differs from region to region. Towards the future, it is expected that the diversification in transmission types is increasing. Moreover, the market share related to the automated transmissions is globally expanding, in particular for transmission types with discrete ratio. However, the predicted market share for the CVT and HT is also increasing rapidly. Furthermore, in the China and India markets of automotive transmissions, there is also a strong shift towards the AMT and DCT technologies [109] (not shown in Figure 1.1). Electronic control of the gear shift process in combination with an optimal shift strategy provides a means to further improve the fuel economy, driveability and the reduction of pollutant emissions.

Improvement of the fuel economy has always been an ongoing process of the automobile industry. Hybridization and electrification of powertrains have gained an impressive momentum and will become a leading technological trend for future vehicles. A significant market share of hybrid vehicles of up to 10% of the total vehicle market is expected within 10 to 15 years [37]. Even the full-electric vehicles may benefit from a transmission technology [1]. Currently, two-speed AMT/DCT or even three-speed DCT are being developed. For example, the first gear provides the required acceleration torque from standstill in order to reduce the battery current, which improves the battery lifetime and efficiency. Meanwhile the second gear provides the required operation speed such that the power is constant for a relatively large speed range.

1.2 Background

Every vehicle needs a transmission [89].

An automotive transmission is an inevitable system for a vehicle (even for electric vehicles). From the analysis of the transmission technology trends, the above statement of *every vehicle needs a transmission [89]* can be reaffirmed. To further elaborate on the necessity of a transmission for road vehicles and thereby contributing to the automotive transmission control and design, the research presented in this dissertation focuses on:

- vehicles primarily powered by internal combustion engines; and,
- designing the gear shift strategy for electronically controlled discrete ratio transmissions.

To realize the advantages of the electronically controlled discrete ratio transmissions, such as a high fuel economy, an acceptable driveability, and a shifting automation, a

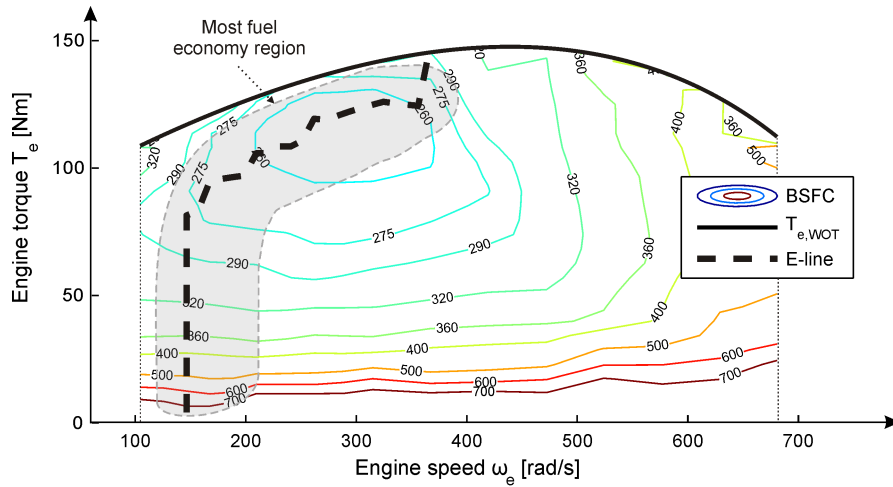


Figure 1.2: Fuel map of the engine: BSFC denotes the Brake Specific Fuel Consumption in [g/kWh]; $T_{e,WOT}$ denotes the engine torque at wide open throttle; E-line denotes the most fuel economic operation line of the engine.

proper gear shift strategy implemented in the transmission control unit is of central importance. The transmission mediates between the engine power and the power demand at the wheels by choosing a suitable gear ratio. Under dynamic driving conditions, the transmission is required to shift in order to match the power conversion requirements, e.g. satisfying the engine torque and speed limitations in the driveline. A gear shift decision is also required to be consistent such that vehicle can remain in the next gear for a period of time without deteriorating the acceleration capability. Otherwise, this will result in an unwanted engine lugging and shift busyness of the gear box. As long as the driving performance is satisfied, the gear shift strategy can utilize the fuel consumption characteristics of the engine in order to improve the operation efficiency of the powertrain. This can be realized by the fact that the engine fuel consumption is strongly dependent on the operating points. In Figure 1.2, the fuel consumption as a function of the engine output torque and speed is shown. The contour lines represent the lines of constant fuel rate per unit output power in [g/kWh], which is denoted as the Brake Specific Fuel Consumption (BSFC). It measures how efficiently the engine is using the fuel supplied to produce work. Operating the engine as close as possible to the E-line² helps realizing the most amount of fuel saving potential. However, the discrete ratio transmission can not change the engine speed smoothly due to the step-changed shifting ratios. Nonetheless, the transmission can exploit the most fuel economy region around the E-line to improve the fuel economy by adopting a fuel-optimal gear shift strategy. However, the driving characteristics, i.e. driveability, needs to be taken into account as well. In many cases high fuel economy and high driveability are contradicting

²E-line denotes the most fuel economic operation line of the engine.

attributes.

Therefore, in the next section, the challenges related to the gear shift problem of discrete ratio transmissions used in conventional and hybrid electric vehicles will be addressed, which motivates the research in this dissertation.

1.3 Challenges

The gear shift strategy for discrete ratio transmissions is a part of the supervisory control algorithm. The supervisory control algorithm generates for example the set points for the gear shift command based on the current powertrain states to improve the operation performance of the powertrain system. In this section, the basic dynamics of the powertrain system is briefly introduced, and some control design challenges are formulated based on, but not limited to:

- the level of which the drive power request is known; and,
- the particular application (i.e., conventional or hybrid vehicle); and,
- the assumptions related to the development of an online strategy; and finally,
- the assumptions related to discrete state variable-dependent losses, such as gear shift and engine start stop losses.

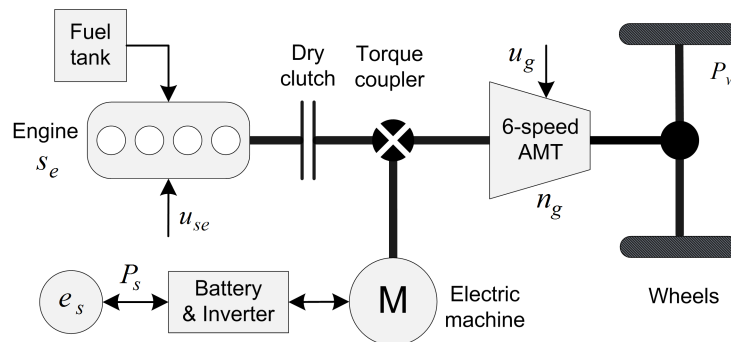


Figure 1.3: Hybrid powertrain topology used in this dissertation, (AMT: Automated Manual Transmission; M: electric machine). The state variables are the engine on-off state s_e , the gear position n_g and the battery state-of-energy e_s . The corresponding control variables are the engine start-stop command u_{se} , the gear shift command u_g and the battery chemical power P_s , respectively. P_w is the power request placed on the wheels.

The hybrid power train topology used in this dissertation is a parallel type and is equipped with an AMT, see Figure 1.3. The secondary power source is connected at

the primary side of the transmission. The quasi static modeling approach [42] is adopted in this dissertation to model the main powertrain components. This approach is very suitable for developing the supervisory control algorithm. Due to the discrete nature of the transmission ratio, the discrete-time dynamics of the powertrain system can be expressed in a generic form by,

$$x(k+1) = f(x(k), u(k), z(k)), \quad (1.1)$$

$$C_{eq}(x(k), u(k), z(k)) = 0, \quad (1.2)$$

$$C_{in}(x(k), u(k), z(k)) < 0, \quad (1.3)$$

wherein: k is the fixed discrete-time step, $x(k)$ and $u(k)$ are the state and control variable vectors, respectively; $z(k)$ is the disturbance vector imposed on the vehicle; f is the function describing the dynamics of the system state. The matrices C_{eq} and C_{in} describe the equality and inequality constraints of the powertrain system, respectively.

From a control point of view, the power request at the wheels P_w is ordinarily referred as the disturbance. In the optimal control problem for the powertrain system, the disturbance can arise from the external disturbing forces acting on the system due to changes of road conditions, traffic conditions, driver behaviors, etc. In general, the power request can be classified into three levels.

1. The power request is known a priori for the whole driving profile.
2. The power request is totally unknown. This case mostly describes a real-life drive mission.
3. The power request is known over a certain preview horizon. This is achieved by means of a prediction technique and onboard route information systems.

Accordingly, the supervisory control algorithm, for example, including the gear shift strategy, is designed such that the disturbance is expectedly attenuated in order to improve the operation performance of the powertrain. The foreseen challenges related to the gear shift strategy design for conventional and hybrid vehicles are discussed next. Moreover, the consequences of the assumptions related to discrete state variable-dependent losses, i.e. gear shift, clutch slippage and engine start, and their effect on the control strategies are addressed in the subsequent sections.

Optimal gear shift strategy for conventional vehicles

The conventional powertrain control consists of one state variable, which is the gear position $n_g(k)$. Hence, an optimal gear shift strategy, allowing the engine to operate in the region closely to the E-line, will reduce the fuel consumption. Consequently, this will

result in a lower speed and a higher torque of the engine, hence reducing the acceleration capability, represented by the power reserve, denoted by $\Delta P_e = (T_{e,WOT} - T_e) \omega_e$. Figure 1.4 demonstrates a tradeoff between a fuel economy improvement potential and a reduction of driveability at three indicated points 1, 2 and 3, with $\Delta P_{e,1} < \Delta P_{e,2} < \Delta P_{e,3}$, respectively. A decision to choose the operating point among three of them should be made on the basis of the ability to remain in the next gear for an acceptable period of time. Therefore, a gear shift strategy needs to be designed such that an optimal tradeoff between the fuel economy and driveability can be realized for the vehicle.

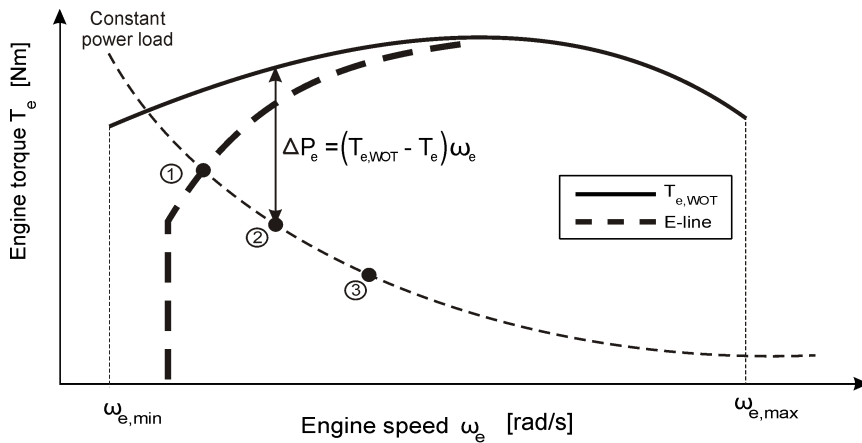


Figure 1.4: Tradeoff between the fuel economy and driveability for a conventional vehicle.

So far, addressing the driveability in the powertrain control can be found in a relatively limited amount of published literature, which mostly focus on satisfying a certain constant power request by cooperatively control the gear shift and throttle opening [66], or satisfying a constraint on a change in the engine power reserve for a given change in the throttle angle by controlling the CVT ratio [135]. Nonetheless, under the effect of the disturbance (changing driver behavior, changing road condition, etc.) the power request varies from time to time, which requires the driveability to be addressed in an optimal gear shift strategy for the whole drive cycle. *Therefore, in this dissertation, the focus is on developing a systematic method to analyze and define the optimal tradeoff between the fuel economy and driveability.*

Optimal gear shift strategy for HEVs

For the hybrid electric powertrain as shown in Figure 1.3, the dynamical system consists of three state variables: the discrete engine on-off state $s_e(k)$, the continuous battery state-of-energy $e_s(k)$, and the discrete gear position $n_g(k)$. The corresponding control variables are the engine start-stop command $u_{se}(k)$ (discrete), the battery power $P_s(k)$

(continuous), and the gear shift command $u_g(k)$ (discrete). Due to the co-existence of the continuous and discrete variables, the dynamical system is a hybrid dynamical system as well. In general, the design of an optimal control algorithm for a hybrid dynamical system with constraints on the state and control variables encounters complex design challenges in terms of optimality, for example, due to the non-smoothness of the objective function [23]. Therefore, the advantages of a HEV could be deteriorated if the gear shift and engine on-off strategies are insufficiently optimized. Moreover, the gear shift command $u_g(k)$ is constrained due to a practical comfort aspect, e.g. not allowing the gear box to shift from the first gear to the highest gear at the next time instant. Besides, the multi-objective character of the problem imposes further control design challenges. The gear shift problem in principle can be solved by discretizing the continuous variables ($s_e(k)$ and $P_s(k)$) and using deterministic Dynamic Programming (DP) [83], yet can result in a computational burden due to the ‘curse of dimensionality’. *Apparently, the tradeoff among optimality, accuracy and the computational efficiency is seen as one of the main challenges for the design of a gear shift control algorithm for HEVs.* In addition, a computationally efficient and optimal Energy Management Strategy (EMS) is very beneficial for accelerating the design process of a HEV at the initial development phase, thus reducing valuable development time and cost.

Realtime gear shift strategy for automotive transmissions

In order to drive the vehicle on road, a real time implementable gear strategy for the transmission is required. When the drive power request is totally unknown, a map-based gear shift strategy is a solution for determining when to shift gears online. A static gear shift map generates the shifting points, defined as a point-wise function of the vehicle speed and the drive power request observed at the transmission input, which determines how to shift gears correspondingly.

For conventional vehicles, the design of a gear shift map is traditionally based on know-how, experience of the calibration engineers and tuning in a heuristic manner [87]. Hence, the gear shift map becomes consistent and relatively robust after a huge effort and relative time-consuming trial-and-error are performed. This experience-based gear shift strategy does not exploit the inherent potential of the powertrain system sufficiently to improve the overall performance of the vehicle, and hence coming with a lower confidence on the optimality with respect to the fuel economy and driveability. A method in order to improve the shift rules can be found in [66]. *Therefore, developing a map-based gear shift strategy which makes the optimal tradeoff between the fuel economy and driveability in a systematic manner is seen as one of the additional research challenges in this dissertation.*

For HEVs, the design of a static gear shift map is more complex compared to conventional vehicles, given that the acceleration capability can be obtained by the hybrid

powertrain system. Therefore, developing an implementable gear shift strategy based on a static map, which is adapted to different operation modes of the hybrid system, would require a rigorous design and analysis.

Recently, using route information is seen as a possibility to significantly further improve the fuel economy for HEVs, for example see, [2, 10, 57, 152]. However, utilizing route information to predict the power request over a certain horizon will increase complexity of the optimization problem by one more state variable, the to-be-optimized vehicle speed. Hence, an optimized map-based gear shift strategy appears as a well-compromised solution for the velocity trajectory optimization problem. When the prediction of the power request over a certain horizon is available, a gear shift strategy incorporated in a predictive EMS will allow the HEV to boost the fuel saving level. Again, this emphasizes on the necessity of a computation-efficient and optimal gear shift strategy such that the predictive EMS can be realtime implementable.

Consequences with respect to the gear shift and engine start events

Incorporation of the gear shift and engine start-stop strategies into an EMS for an AMT-based HEV in order to maximize the fuel economy benefit can result in: i) an earlier upshift pattern and a higher shifting frequency, and ii) a frequent stop and start of the engine. However, it should be noted that the gear shift or engine start-stop induces additional energy losses. For example, the vehicle speed reduces during shifting due to a torque interruption, and higher drive power is needed from the engine to compensate for these dynamic losses later on. Moreover, a certain amount of energy is consumed through cranking the engine from rest. However, in literature, these losses and their effect on the control strategy and fuel consumption are often neglected. This can finally end up with an unfair evaluation on the fuel benefit of HEVs with respect to the gear shift and engine start-stop strategies. *Hence, it is necessary to model these losses and analyze their effect on the control strategies for HEVs.*

Moreover, analysis of the correlation among the design objectives (fuel economy, emissions, driveability, etc.) and investigation of the sensitivity of an optimal control algorithm to the relevant design objectives are essential. The result of this analysis can be used to simplify the multi-objective function. A systematic method, based on Singular Value Decomposition (SVD), for such an analysis is investigated in this dissertation.

1.4 Objectives and Contributions

Motivated by the research challenges related to the gear shift problem for discrete ratio transmissions, used in conventional and hybrid electric vehicles as addressed in Section 1.3, the following six research objectives ($\mathbf{O}_1 - \mathbf{O}_6$) are specifically defined:

- **O₁**: define and address the driveability in a fuel-optimal gear shift strategy for conventional vehicles on drive cycles known a priori.
- **O₂**: design a fuel-optimal control algorithm, including the gear shift strategy, for the hybrid dynamical system of HEVs on drive cycles known a priori.
- **O₃**: develop an online gear shift strategy for conventional and hybrid electric vehicles equipped with discrete ratio transmissions. The strategy improves the fuel economy meanwhile still satisfying an acceptable driveability.
- **O₄**: propose a gear shift strategy for a HEV to further improve the fuel economy by exploiting route information from the GPS-based onboard navigation system.
- **O₅**: analyze the effect of the gear shift and engine start losses on the control strategy and fuel consumption.
- **O₆**: investigate the sensitivity of an optimal gear shift strategy to the relevant control design objectives, such as fuel economy, driveability, comfort, etc.

By fulfilling all the defined research objectives, the work presented in this dissertation systematically tackles all the discussed challenges related to the gear shift problem, thereby making a fundamental contribution in the field of the automotive transmission control design and analysis. Explicitly, the following main contributions (**C₁ – C₆**) are obtained:

- **C₁**: various optimal gear shift strategies with respect to the fuel economy and driveability are proposed for conventional vehicles. A novel concept of variable power reserve is developed to properly address the driveability, meanwhile guaranteeing the highest achievable fuel economy (Chapter 2).
- **C₂**: a novel gear shift control algorithm based on a combination of DP and Pontryagin's Minimum Principle (PMP) is developed for the hybrid dynamical system (consisting of continuous and discrete variables) of HEVs. This so-called DP-PMP algorithm benchmarks the gear shift problem in terms of optimality and computational efficiency (Chapter 3).
- **C₃**: a gear shift map design methodology aiming at a realtime solution for discrete ratio transmissions is developed. The methodology exploits the fuel economy and driveability potential of the optimal gear shift strategies (proposed in Chapters 2 and 3) in order to realize an online gear shift strategy for conventional and hybrid electric vehicles (Chapter 4).
- **C₄**: a concept of integrated predictive gear shift strategy for HEVs, utilizing route information to further explore fuel economy potential, is demonstrated in simulation (Chapter 5).

- C_5 : an analysis of the effect of gear shift and engine start losses on control strategies for AMT-based HEVs. By taking the gear shift loss into account, this study reveals a perception of a fuel-efficient advantage of powershift transmissions (DCT, PS-AMT) over non-powershift transmissions (MT, AMT) applied for passenger HEVs. Furthermore, the effect of the engine start loss can not be ignored in seeking a fair evaluation of the fuel economy for parallel HEVs. A prediction horizon of few seconds can help a predictive EMS to realize the highest achievable fuel economy (Chapter 6).
- C_6 : a Singular Value Decomposition-based technique is introduced to analyze the correlation among the design objectives of an optimal gear shift problem for conventional and hybrid electric vehicles (Chapter 7).

1.5 Outline of The Dissertation

The dissertation consists of six self-contained research chapters, i.e. from Chapter 2 till Chapter 7. The work presented in the dissertation can be categorized into two main parts. The first four chapters together form the first part, related to the gear shift strategy design for automotive transmissions corresponding with three transparent levels of the power request. This is shown in Figure 1.5. Meanwhile the last two chapters form the second part, involved with the analysis of the consequences on the control design objectives with respect to a gear shift strategy and an engine start-stop strategy, see Figure 1.6. On both figures, the arrowed lines indicate the linkage among chapters, meaning that the outcome of a certain chapter is used as input to another chapter. For example, the DP-PMP control approach developed in Chapter 3 is utilized in Chapters 4 and 5 as the corresponding input. The six contributions ($C_1 - C_6$) for six chapters are also shown in the output arrowed lines. Within the context of defining the optimal gear shift points for automotive transmissions, the dissertation is unified by hierarchical interconnections among the chapters. The outline of the dissertation is given next.

In relation to the first part, Chapter 2 deals with the optimal gear shift problem for conventional vehicles. The driveability is systematically analyzed in a DP-based fuel-optimal gear shift strategy by three methods: i) the weighted inverse of power reserve, ii) the constant power reserve, and iii) the variable power reserve. A Stochastic Dynamic Programming (SDP) algorithm optimizes the gear shift strategy, subject to a stochastic distribution of the power request, to minimize the expected fuel consumption over an infinite horizon, hence making the obtained solution intrinsically respect the driveability and be realtime implementable. A comparative analysis of all proposed gear shift methods is given in terms of the fuel economy and driveability improvement. The variable power reserve method achieves the highest fuel economy meaning without sacrificing the driveability. Chapter 3 focuses on a fuel-optimal gear shift strategy for

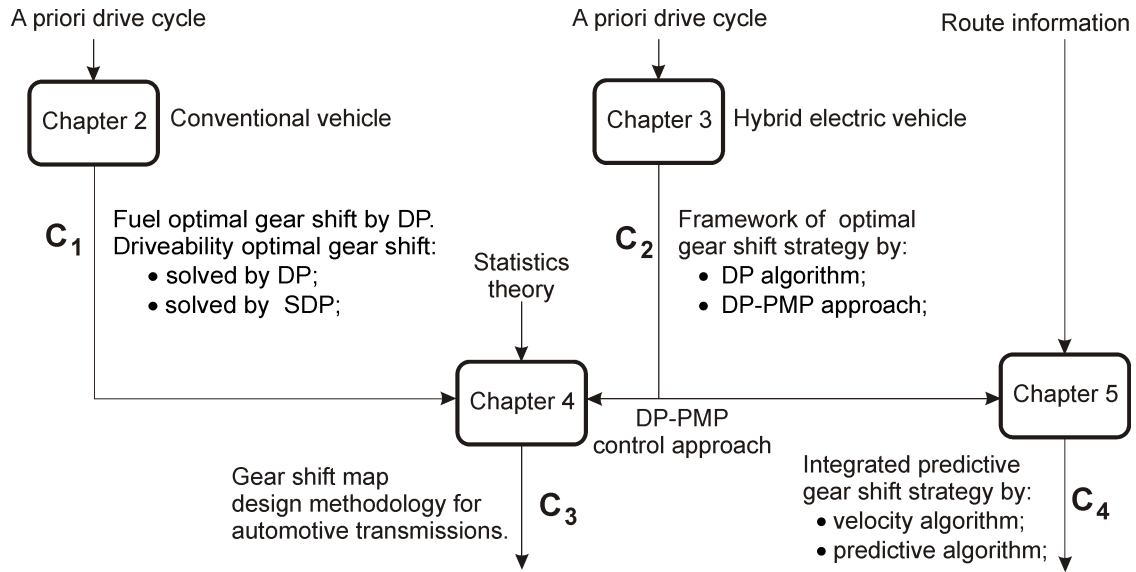


Figure 1.5: Overview of linkage among Chapters 2, 3, 4 and 5 with contributions.

HEVs, wherein a novel control algorithm based on a combination of DP and PMP is developed. The EMS based on DP-PMP control approach benchmarks the development of an online control strategy in terms of the tradeoff between calculation accuracy and computational efficiency. The gear shift strategies proposed in Chapters 2 and 3 are not realtime implementable, yet result in a globally optimal solution on a priori drive cycle. Aiming at a real time implementable solution, Chapter 4 develops a gear shift map design methodology for discrete ratio transmissions, used in conventional and hybrid electric vehicles. The optimal gear shift strategy proposed in Chapters 2 and 3 are utilized as the bases to derive the optimal gear shift patterns. Then statistical theory is applied to analyze the optimal gear shift patterns in order to extract the shift rules. Hence this alternative two-step design procedure makes the gear shift map respect the fuel economy and driveability, consistent and robust with respect to shift busyness. In Chapter 5, a concept of an integrated predictive gear shift strategy for HEVs is demonstrated in simulation environment. The control strategy utilizes route information obtained from a GPS-based onboard navigation system to further explore the fuel economy potential.

In connection with the second part, Chapter 6 addresses the energetic losses, involving with the gear shift and engine start events, in an AMT-based HEV. The effect of these losses on the control strategies and fuel consumption for (non-)powershift transmission technologies is investigated. Moreover, the sensitivity of prediction horizon on the fuel consumption is analyzed. Chapter 7 defines the relevant control design objectives, i.e. fuel economy, driveability and comfort, with respect to an optimal gear shift problem of vehicular propulsion systems. A SVD-based method is introduced to analyze the possible correlations and interdependencies among the design objectives.

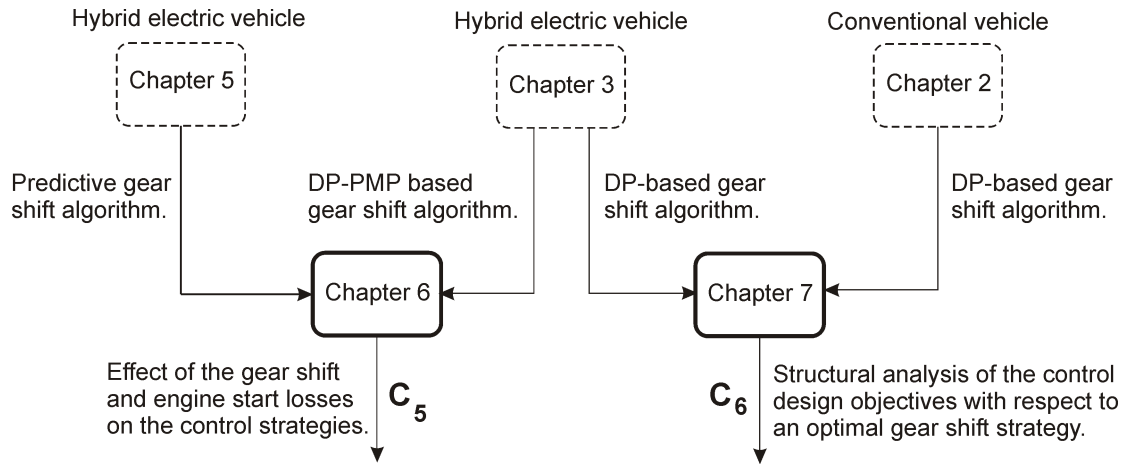


Figure 1.6: Overview of linkage among Chapters 6 and 7 with contributions.

Finally, the conclusions and recommendations of the dissertation are given in Chapter 8.

Publications

In the research leading to this dissertation, the following journals and conference papers have been publishing.

Refereed journal publications

- V. Ngo, J. A. Colin Navarrete, T. Hofman, M. Steinbuch, and A. Serrarens. Optimal Gear Shift Strategies for Conventional Vehicles. *In preparation for journal publication, 2012.* (Chapter 2).
- V. Ngo, T. Hofman, M. Steinbuch, and A. Serrarens. Optimal Control of the Gear Shift Command for Hybrid Electric Vehicles. *IEEE Transactions on Vehicular Technology*, vol. 61, issue 8, 2012. (Chapter 3).
- V. Ngo, T. Hofman, M. Steinbuch, and A. Serrarens. Gear Shift Map Design Methodology for Automotive Transmissions. *In preparation for journal publication, 2012.* (Chapter 4).
- V. Ngo, T. Hofman, M. Steinbuch, and A. Serrarens. Integrated Predictive Gear Shift Strategy for Hybrid Electric Vehicles. *In preparation for journal publication, 2012.* (Chapter 5).
- V. Ngo, T. Hofman, M. Steinbuch, and A. Serrarens. Effect of Gear Shift and Engine Start Losses on Control Strategies for Hybrid Electric Vehicles. *In preparation for journal publication, 2012.* (Chapter 6).

- V. Ngo, T. Hofman, M. Steinbuch, and A. Serrarens. Structural Analysis of Control Design Objectives for Vehicular Propulsion Systems. *In preparation for journal publication, 2012.* (Chapter 7).

Refereed conference publications

- A. Serrarens, R. van Druten, W. van Liempt, N. Weel, P. Kumar, L. Romers, V. Ngo. Light Hybridization of Diesel Powertrains: the most cost-effective route towards 120g/km CO₂ and below. *VDI2008 Innovative Powertrain Systems*, Nov, 2008, Germany.
- V. Ngo, T. Hofman, M. Steinbuch, and A. Serrarens. Shifting Strategy for Stepped-Gear Transmission Vehicle - A Comparative Study and Design Method. *The 24th International Battery, Hybrid and Fuel Cell Electric Vehicle Symposium - EVS24*, Stavanger, Norway, May 2009.
- V. Ngo, T. Hofman, M. Steinbuch, and A. Serrarens. Performance Indices for Vehicular Propulsion Systems. *The 15th Asia Pacific Automotive Engineering Conference - APAC15*, Hanoi, Vietnam, October 2009.
- V. Ngo, T. Hofman, M. Steinbuch, and A. Serrarens. An Optimal Control-Based Algorithm for Hybrid Electric Vehicle Using Preview Route Information. *2010 American Control Conference - ACC2010*, Maryland, USA, June 2010.
- V. Ngo, T. Hofman, M. Steinbuch, and A. Serrarens, L. Merckx. Improvement of Fuel Economy in Power-Shift Automated Manual Transmission through Shift Strategy Optimization - An Experimental Study. *Vehicle Power and Propulsion Conference 2010 - IEEE-VPPC 2010*, Lille, France, September 2010.
- V. Ngo, T. Hofman, M. Steinbuch, and A. Serrarens. Optimal Shifting Strategy for a Parallel Hybrid Electric Vehicle. *The 25th World Battery, Hybrid and Fuel Cell Electric Vehicle Symposium and Exhibition - EVS25*, Shenzhen, China, November 2010.
- V. Ngo, T. Hofman, M. Steinbuch, and A. Serrarens. Analyses of the Performance Index for a Hybrid Electric Vehicle. *2011 American Control Conference - ACC2011*, San Francisco - CA, USA, June 2011.
- V. Ngo, T. Hofman, M. Steinbuch, and A. Serrarens. Predictive Gear Shift Control for a Parallel Hybrid Electric Vehicle. *2011 Vehicle Power and Propulsion Conference - IEEE-VPPC 2011*, Chicago, USA, September 2011.

- V. Ngo, T. Hofman, M. Steinbuch, and A. Serrarens. Effect of Gear Shift and Engine Start Losses on Control Strategies for Hybrid Electric Vehicles. *The 26th Electric Vehicle Symposium - EVS26*, Los Angeles - California, USA, May 2012.

Optimal Gear Shift Strategies for Conventional Vehicles¹

Abstract - This chapter aims at designing optimal gear shift strategies for conventional passenger vehicles equipped with discrete ratio transmissions. The fuel economy and driveability are selected as the design objectives. Three methods of addressing the vehicle driveability are proposed for a fuel-optimal gear shift algorithm based on Dynamic Programming (DP) to quantitatively study the tradeoff between the fuel economy and driveability. Furthermore, another method based on Stochastic Dynamic Programming (SDP) is proposed to derive an optimal gear shift strategy over a number of drive cycles in an average sense, hence making it respect the vehicle driveability. In contrast with the DP-based strategy, the obtained gear shift strategy based on SDP is realtime implementable. A comparative analysis of all proposed gear shift methods is given in terms of the fuel economy and driveability improvements.

2.1 Introduction

For conventional vehicles equipped with discrete ratio transmissions, e.g. automatic, dual clutch, automated (manual) transmissions, etc., a decision on selecting a different gear leads to a sudden change of the engine operating point due to a stepped change of the transmission ratio. With highly nonlinear characteristics of the engine fuel consumption and maximum torque, a change of the engine operating point due to a gear shift can result in a deficient fuel operation state, and/or a low driveability condition for the vehicle thereafter. Hence, an optimal gear shift strategy for a discrete ratio transmission plays an important role in achieving a high performance for the vehicle. In literature, there does not exist a systematic method to quantitatively investigate the

¹This chapter has been prepared for a journal submission in the form as: V. Ngo, J. A. Colin Navarrete, T. Hofman, M. Steinbuch, A. Serrarens. Optimal Gear Shift Strategies for Conventional Vehicles. 2012.

tradeoff between the fuel economy and driveability with respect to an optimal gear shift strategy. Hence, in this chapter, various methods, taking the driveability into account, are proposed for the design of the optimal gear shift strategy. They are comparatively analyzed in terms of the fuel economy and driveability improvements, towards achieving the most optimal method.

2.1.1 Literature Review

In literature, a substantial amount of published research can be found, addressing the design of the ratio control strategy for automotive transmissions. With respect to a fuel economy improvement, the control strategies aim at moving the engine operating points as close as possible to the most fuel economy region. For a push belt Continuously Variable Transmission (CVT), a sequence quadratic programming-based optimization algorithm for an offline optimal ratio strategy, and an online suboptimal feed-forward ratio controller can be found in [105]. For discrete ratio transmissions, a ratio control strategy can be alternatively interpreted as a gear shift strategy. Due to the discrete nature of the ratio, discrete optimization techniques, e.g. Dynamic Programming (DP), can be efficiently utilized to derive an optimal gear shift schedule over a given drive cycle. In addition, the suboptimal gear shift strategy revolves around the methods based on heuristic rules, e.g. genetic algorithm, fuzzy logic, know-how of calibration engineers or from empirical experiments, etc., for example see [18, 99]. The globally optimal gear shift strategy is used to benchmark the fuel economy on a certain drive cycle, and therefore not realtime implementable. Meanwhile the rule-based strategy is less fuel economic, yet realtime implementable.

Improvement of the vehicle driveability, represented by the driver's power demand satisfaction, while simultaneously optimizing the fuel economy is the main challenging aspect for the gear shift strategy design. For a CVT-based vehicle, the authors in [129] suggest that a ratio control strategy with a fuel consumption increase by 15%-20% compared to the E-line (indicating the most fuel-efficient line of the engine) can lead to a good driveability acceptance. The authors in [135] propose a method for choosing the optimum ratio trajectory for a CVT-based passenger vehicle. An optimization problem is formulated focusing on maximizing the fuel economy and driveability, which is defined by a change in the engine power reserve for a given change in the throttle angle. This driveability definition creates a consistent and desirable vehicle response under different road load conditions. The authors claim a good, or improved driveability, while still achieving a fuel economy benefit compared with other ratio control schedules.

For a vehicle equipped with a discrete ratio transmission, the driveability can be improved by an integrated powertrain control approach. In [87], a two-layer fuzzy gear shift strategy for an Automatic Transmission (AT), considering the engine working con-

ditions and the driver's intention, can eliminate unnecessary shifts occurring when the driver's intention is overlooked or unclear. The authors state a better acceleration performance. In [166], a gear shift method, based on pattern recognition and a learning algorithm, is proposed. By utilizing three different dynamic parameters, i.e. the throttle position, vehicle speed and acceleration, the method improves the fuel economy and acceleration capability as claimed by the authors. Another method of combined time-optimal and fuzzy-logic strategies to control the engine during a gear shift process of an Automated Manual Transmission (AMT) is proposed in [167]. By decreasing the engine speed deviation between the controlled target and actual output, and shortening the gear shift time, the proposed control algorithm is claimed to be capable of reducing fuel consumption, engine noise, shift jerk and the clutch friction loss. An integrated powertrain control approach based on an optimization technique to improve the driver's power demand satisfaction for an AT vehicle can be found in [7, 66]. DP is used to solve a fuel-optimal gear shift and throttle control problem over a number of different acceleration profiles. Then, the optimized gear shift map and the throttle open map for the vehicle are extracted to govern the operation of the integrated powertrain. The method is found to be promising in improving the fuel economy without compromising the driveability. Also for an AT, the authors in [6] propose an adaptive gearshift strategy that compensates for variations in the vehicle and road conditions, e.g. the load, trailering, grade, and the curvature. The method utilizes two shift maps: a fuel economy map and a sportive map, in order to dynamically generates the shifting points adapted to the current vehicle and road conditions in achieving the optimal tradeoff between the fuel economy and the driveability.

2.1.2 Research Objectives

For discrete ratio transmissions, it can be observed that improving the fuel economy while not compromising the driveability is still a challenging research problem. There is lack of a proper method to analyze the correlation, and hence not able to define an optimal tradeoff between the fuel economy and driveability through an optimal gear shift strategy. Therefore, in this chapter a systematic approach will be developed consisting of: i) designing a fuel-optimal gear shift strategy, ii) defining the driveability and taking it into the fuel-optimal gear shift problem, and iii) quantitatively evaluating and comparing the fuel economy and driveability among the proposed gear shift strategies.

Firstly, a fuel-optimal gear shift control problem is formulated and solved by using DP to obtain a baseline fuel economy. Secondly, the vehicle driveability represented for an acceleration capability and defined by the power reserve, is addressed in the fuel-optimal gear shift problem by three methods. In the first method, the power reserve is incorporated in the objective function by a weight factor. In the second method, the driveability is respected by imposing an inequality constraint on the power reserve,

which is equal to or larger than a constant threshold value. In the third method, a variable power reserve concept, as a function of the vehicle speed being predefined over a wide range of driving scenarios, is constructed and respected by an inequality constraint to ensure an acceptable driveability. And finally, an optimal tradeoff between the fuel economy and driveability is derived from a comparative analysis of the three methods.

The DP-based gear shift algorithm requires the whole drive cycle to be known a priori. It optimizes the powertrain's operational performance by identifying an optimal gear shift schedule over the given drive cycle. Hence, the obtained gear shift strategy can not be implemented in realtime. Towards an online solution for a gear shift problem, a design method based on Stochastic Dynamic Programming (SDP) is proposed for that purpose. The SDP algorithm formulates and solves an infinite-horizon optimization problem over a probabilistic distribution of the power request from many drive cycles rather than a single drive cycle. The vehicle speed is also considered as a state variable. Hence, the obtained gear shift strategy, in the form of a set of shift maps, is time-invariant and feedback with respect to the state variables (the gear position and the vehicle speed), such that it can be implemented in realtime. The SDP optimization problem, subject to the power request from many drive cycles, renders the stochastic gear shift strategy a driveability satisfaction.

This chapter is organized as follows. The fuel-optimal gear shift problem is formulated and solved in Section 2.2. The driveability-optimal gear shift problem is discussed in Section 2.3. The stochastic gear shift strategy is addressed in Section 2.4. And finally, conclusions and recommendations are given in Section 2.5.

2.2 Fuel-Optimal Gear Shift Strategy

2.2.1 Powertrain Model

In order to derive a supervisory control strategy, the quasi static modeling approach is used to model the main powertrain components. A fixed time step Δt of one second is chosen to simulate the powertrain system. Hence, the powertrain system dynamics faster than $1Hz$ are ignored [42]. The component models in discrete time domain k are described as follows.

- **Engine:** the engine fuel consumption is modeled by a static fuel efficiency map, see Figure 2.2. It indicates the contour lines of constant Brake Specific Fuel Consumption (BSFC), which a static point-wise function of the speed $\omega_e(k)$ and the torque $T_e(k)$. The BSFC describes the fuel rate $\dot{m}_f(k)$ per unit output power of the engine. The engine torque obtained at wide open throttle for the whole

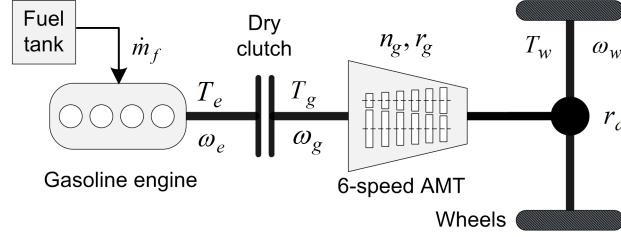


Figure 2.1: The powertrain topology of a conventional vehicle, where T_e is the torque delivered by the engine, ω_e is the engine speed, T_g is the transmission input torque, ω_g is the transmission input speed, n_g is the gear position, r_g is the gear ratio, r_d is the final reduction gear ratio, T_w is the drive torque at the wheels, and ω_w is the wheel rotational speed. AMT stands for Automated Manual Transmission.

engine speed range, denoted by $T_{e,WOT}$, see the black solid line, is equivalent to the engine maximum torque $T_{e,max}$. The most fuel efficient operational region for the engine, denoted by E-line, is the line which connects the points of highest efficiency for a given engine output power (the dashed line). It can be observed that the engine fuel consumption and the maximum torque are both highly nonlinear.

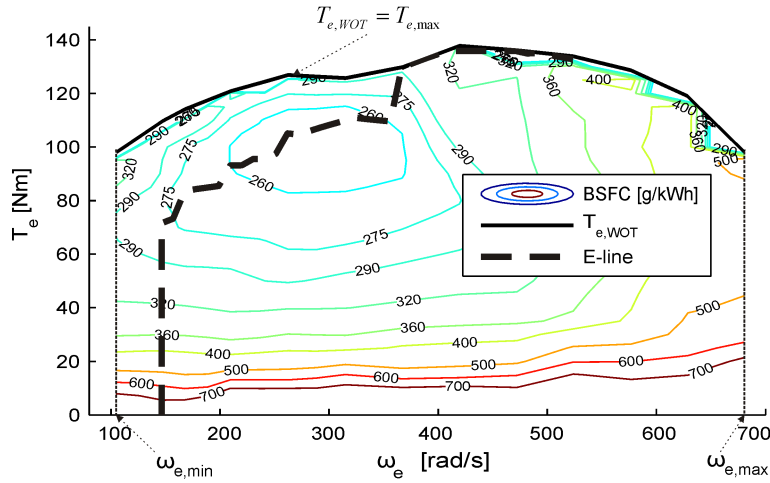


Figure 2.2: Engine fuel efficiency model, where BSFC is the Brake Specific Fuel Consumption in [g/kWh], $T_{e,WOT}$ is the engine torque at wide open throttle, which is equal to the maximum engine torque $T_{e,max}$, E-line is the most fuel efficient operational region, $\omega_{e,min}$ is the minimum engine speed, and $\omega_{e,max}$ is the maximum engine speed.

The constraints on the engine speed $\omega_e(k)$ and the engine torque $T_e(k)$ are,

$$\omega_{e,min} \leq \omega_e(k) \leq \omega_{e,max}, \quad (2.1a)$$

$$0 \leq T_e(k) \leq T_{e,max}(\omega_e(k)), \quad (2.1b)$$

where the engine friction torque, negative value when no combustion taking place, is ignored in the supervisory control strategy for the conventional vehicle.

- **Dry clutch:** the dry clutch is considered as a boolean switch, which connects and disconnects the engine immediately to and from the driveline. Its dynamics and limited power losses during shifting are ignored in this chapter. Note that this study takes no notice of the slippage loss of clutch at vehicle launch. However, analysis of the effect of these losses to the control strategy for a hybrid electric vehicle can be found in Chapter 6.
- **Automated Manual Transmission (AMT):** assuming that the transmission efficiency η is constant for all gears, and the clutch is closed, then the speed and torque relations in both side of the transmission are,

$$\omega_e(k) = \omega_g(k) = \omega_w(k) r_g(n_g(k)) r_d, \quad (2.2a)$$

$$T_w(k) = \eta r_g(n_g(k)) r_d T_g(k) = \eta r_g(n_g(k)) r_d T_e(k), \quad (2.2b)$$

where $\omega_w(k)$ is the wheel rotational speed; $T_w(k)$ is the drive torque at the wheels; $T_g(k)$ is the transmission input torque; $r_g(n_g(k))$ is the gear ratio of the transmission, depend on the gear position $n_g(k)$; r_d is the final reduction gear ratio.

The constraints on the gear position of the 6-speed AMT are,

$$1 \leq n_g(k) \leq 6. \quad (2.3)$$

2.2.2 Powertrain System Dynamics

Gear position dynamics: a next gear position $n_g(k+1)$ is expressed through a current gear position $n_g(k)$ and a gear shift command $u_g(k)$ as follows,

$$n_g(k+1) = n_g(k) + u_g(k). \quad (2.4)$$

Longitudinal motion: the longitudinal motion of the vehicle in discrete time domain is given by,

$$\omega_w(k+1) = \omega_w(k) + \frac{1}{J_{v,eq}} (T_w(k) - F_{load}(k) R_w) \Delta t, \quad (2.5)$$

where F_{load} is the resistance load due to rolling and aerodynamic resistances; $J_{v,eq}$ is an equivalent vehicle inertia at the wheels,

$$F_{load} = c_r m_v g \cos \alpha + m_v g \sin \alpha + \frac{1}{2} \rho_a A_f c_d v^2,$$

$$J_{v,eq} = ((J_e + J_c + J_p) r_g^2 + J_s) r_d^2 + m_v R_w^2,$$

and m_v is the vehicle weight; R_w is the wheel radius; J_e is the engine inertia; J_c is the clutch inertia; J_p is the transmission primary inertia; J_s is the transmission secondary inertia; ρ_a is the air density; A_f is the frontal area of vehicle; c_d is the aerodynamic drag coefficient; c_r is the rolling friction coefficient; g is the gravity coefficient; v is the vehicle velocity; and α is the road slope. It should be noted that the vehicle wheel slip is ignored.

2.2.3 Optimal Gear Shift Control Problem

The powertrain system dynamics, described by (2.1)-(2.5), can be expressed in a generic form by,

$$x(k+1) = f(x(k), u(k)), \quad (2.6)$$

$$C_{eq}(x(k), u(k)) = 0, \quad (2.7)$$

$$C_{in}(x(k), u(k)) < 0, \quad (2.8)$$

where $x(k) = [n_g(k), \omega_v(k)]^T$ and $u(k) = [u_g(k), T_w(k)]^T$ are the vectors of state and control variables, respectively; f is the function describing the dynamic system; C_{eq} and C_{in} are the matrices of equality and inequality constraints of the system, respectively.

Imposing a bound on the discrete gear shift command $u_g(k)$ will influence the gear shift dynamics (2.4), and affect to the optimality. For a 6-speed AMT, $u_g(k)$ belongs to the set $\{-5, \dots, -1, 0, 1, \dots, 5\}$. With a reason for an acceptable driveability, the gear shift command is chosen as,

$$u_g(k) = \begin{cases} -1 & \text{downshift,} \\ 0 & \text{sustaining,} \\ 1 & \text{upshift,} \end{cases} \quad (2.9)$$

to avoid a large variation of the engine speed under a certain shift. One gear upshift ($u_g(k) = 1$) or one gear downshift ($u_g(k) = -1$) for each time step of one second is reasonable, since the average shifting time for an AMT is typically less than one second.

Problem 2.1. *Given a drive cycle $v(k)$ with time length N , implying that the vehicle longitudinal motion (2.5) is deterministic, find an optimal control law $u^*(k) = u_g^*(k)$ to minimize a cost function of fuel consumption over the drive cycle, that is*

$$u^*(k) = \arg \min_{u(k)} \mathbf{J} = \sum_{k=0}^{N-1} \dot{m}_f(k) \Delta t, \quad (2.10)$$

subject to the constraints (2.6)-(2.9).

Dynamic Programming (DP) [11] is well known as a powerful method to solve a non-linear, non-convex optimization problem with mixed constraints while obtaining a globally optimal time-variant, state-feedback solution. In order to apply DP to the proposed optimal control problem, we need to

- grid the state variables $x(k)$;
- grid the corresponding control variables $u(k)$; and,
- calculate $\dot{m}_f(k)$ for the whole drive cycle for every grid point;

Then, the optimal cost-to-go function at any time step k , denoted as \mathcal{J}_k^* , is defined as,

- *step* $k = N$:

$$\mathcal{J}_N^* = 0, \quad (2.11)$$

- *step* $k \in [0, 1, \dots, N - 1]$:

$$\mathcal{J}_k^*(x(k)) = \min_{u(k)} \left[\dot{m}_f(k) \Delta t + \mathcal{J}_{k+1}^*(x(k+1)) \right]. \quad (2.12)$$

The optimal cost-to-go function \mathcal{J}_k^* is defined backwards from $k = N$ until $k = 0$. The optimal solution $u^*(k)$ is obtained correspondingly with a specific value for the end constraint $x(N)$.

2.2.4 Simulation Results

Table 2.1: Relative fuel efficiency improvement of the optimal gear shift strategy compared with the prescribed gear shift schedule.

Drive cycle	NEDC	FTP75
Relative fuel efficiency improvement [%]	14.2	25.4

In order to investigate the fuel-efficient potential of the optimal gear shift strategy, the prescribed gear shift schedules accompanied with the test cycles NEDC and FTP75 (see, Appendix C) are chosen as the baseline shift schedules. These prescribed gear shift schedules, denoted by Pres. and shown by the dashed lines in Figure 2.3, define the shift points for the transmission on NEDC and FTP75 for the standardized test

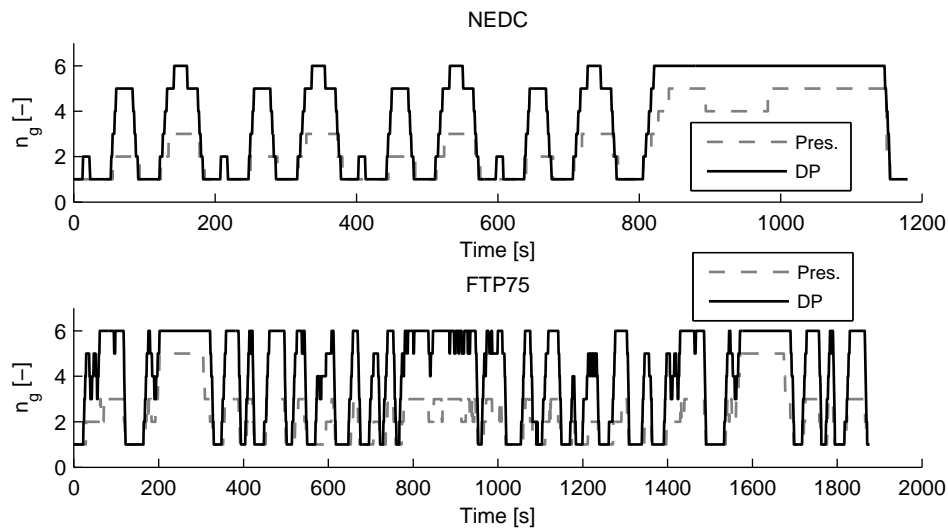


Figure 2.3: Prescribed (Pres.) and the optimal gear positions (DP) over the NEDC and FTP75 cycles.

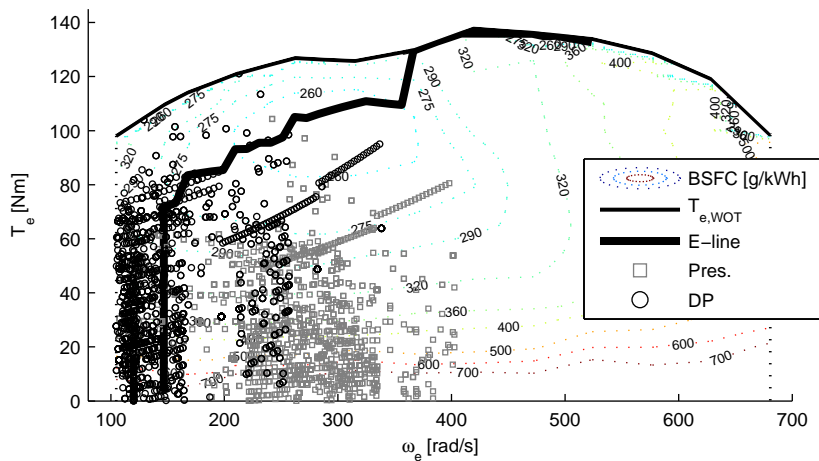


Figure 2.4: Engine operating points corresponding with the prescribed gear shift strategy (Pres.) and the optimal gear shift strategy (DP).

procedure². The optimal gear shift schedule, denoted by DP, is shown by the solid lines in Figure 2.3. It can be observed that, the transmission is shifted at higher rate and to higher values than the prescribed strategy. Obviously, the engine operating points resulted from the optimal gear shift strategy gather around the E-line as much as possible. Meanwhile for the prescribed shift schedules, the engine operating points are more far from the E-line, see Figure 2.4. The relative fuel efficiency improvement of the optimal gear shift strategy compared with the prescribed schedule is of 14.2% and

²NEDC is the standard emission test cycle in Europe, thus the prescribed gear shift schedule is accompanied to give shift signals for geared transmission vehicles. Meanwhile the prescribed gear shift schedule for the standard emission test cycle FTP75 is given by ADVISOR.

25.4% on NEDC and FTP75, respectively, see Table 2.1. Therefore, it can be concluded that by optimizing the gear shift strategy, the fuel economy of conventional vehicles can be improved significantly.

2.3 Driveability-Optimal Gear Shift Strategy

2.3.1 Driveability Definition

The fuel-optimal gear shift strategy, proposed in Section 2.2, yields an early and frequent upshift pattern for the transmission. It renders the engine, on average, to operate at a lower speed and high torque region, and hence improving the fuel economy. As a result, the so-called torque reserve ΔT_e , defined by a difference between the maximum engine torque and the actual engine torque ($\Delta T_e = T_{e,max} - T_e$), tends to decrease. Therefore, if the driver demands a higher acceleration, the engine torque reserve might not be able to fulfil the acceleration surplus. Obviously, this will deteriorate the acceleration capability of the vehicle under certain driving situations. In other words, the fuel economy improvement is gained at a penalty of driveability deterioration. Therefore, in this section, a study on the tradeoff between the fuel economy and the driveability with respect to an optimal gear shift strategy is presented. An appropriate method to address the driveability of conventional vehicles is well defined.

The driveability in general has a broad inference, such as vehicle responsiveness, operating smoothness, driving comfort, vibration, jerk, tip-in tip-out, etc., [158]. Regarding to the gear shift strategy, the engine operating point is changed in a stepwise manner. So, a relevant term for determining the driveability is the acceleration capability, i.e. how much acceleration potential is available for the vehicle *after* a certain gear shift. Since the power reserve, denoted as ΔP_e (2.13) and defined by the product of the engine speed and the torque reserve, represents an instant availability of power for acceleration, it can also be used as a measurement for driveability [92, 135]. Furthermore, the study in [145] also indicates the engine power to be the best parameter representing the driver's demand.

$$\Delta P_e = (T_{e,max} - T_e) \omega_e. \quad (2.13)$$

In this chapter, three different methods are proposed to address driveability of the vehicle,

- Method 1: incorporating the inverse of power reserve with a certain weight factor in the objective function of a fuel-optimal gear shift control problem.
- Method 2: adding an inequality constraint for the power reserve level in a fuel-optimal gear shift control problem in order to ensure that the vehicle actual power

reserve is always above a certain constant threshold.

- Method 3: adding an inequality constraint for the power reserve in a fuel-optimal gear shift control problem. The bound of the power reserve is varied with the vehicle speed.

2.3.2 Method 1: The Weighted Inverse of Power Reserve

Aiming at maximizing the fuel economy and driveability, and then analyzing a tradeoff between them with respect to an optimal gear shift strategy, a corresponding cost function is constructed as,

$$\mathbf{J} = \sum_{k=0}^{N-1} \left[\dot{m}_f(k) + \nu \Delta P_e^{-1}(k) \right] \Delta t, \quad (2.14)$$

where ν is a weight factor imposed on an inverse of the power reserve. The corresponding driveability optimal gear shift control problem is similar to Problem 2.1. Hence, DP is used to solve this control problem.

The fuel consumption, denoted by FC , and the accumulative power reserve, denoted by APR , calculated for the whole drive cycle, are used to quantify the tradeoff between the fuel economy and driveability.

$$FC = \sum_{k=0}^{N-1} \dot{m}_f(k) \Delta t, \quad (2.15a)$$

$$APR = \sum_{k=0}^{N-1} \Delta P_e(k) \Delta t. \quad (2.15b)$$

The weight factor ν is varied as in (2.16) to study a sensitivity of the tradeoff between the fuel economy and driveability to the gear shift strategy.

$$\nu \in \{0, 1, 2, 3, 4, 6, 8, 10, 12, 14\} \cdot 500 \quad [g \cdot W s^{-1}]. \quad (2.16)$$

The drive cycles used for simulation are NEDC, FTP75, LA92, CADC-urban and CADC-road (see, Appendix C). A sensitivity analysis of FC and APR with respect to the weight factor ν is depicted in Figure 2.5a. It can be seen that both FC and APR increase corresponding to an increase of the weight factor for all drive cycles. This means that the vehicle driveability can only be improved at a cost of fuel economy reduction. Figure 2.5b shows a translation of FC and APR to the coordinate origin for a better understanding of the correlation. Basically, a positive linear relation between FC and APR can be seen for almost all selected drive cycles.

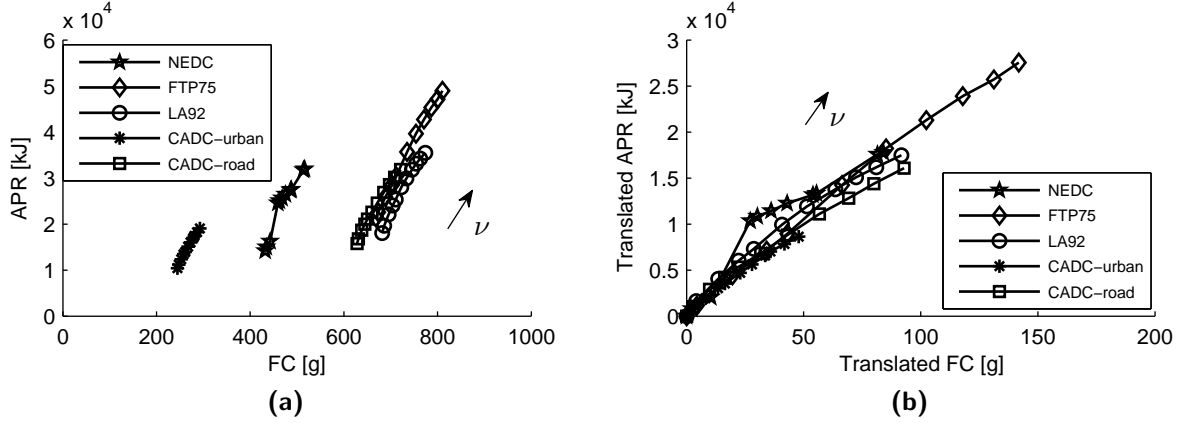


Figure 2.5: Method 1: sensitivity analysis of FC and APR with respect to ν (a); the translation of FC and APR to the coordinate origin (b).

2.3.3 Method 2: The Constant Power Reserve

Instead of introducing the power reserve in the objective function as in method 1, this method proposes that the actual power reserve of the vehicle should be always above a certain constant level in order to ensure a certain driveability level. Hence, an additional inequality constraint for Problem 2.1 is introduced,

$$\Delta P_e(k) \geq \Delta P_{e,lim}, \quad (2.17)$$

where the power reserve limit $\Delta P_{e,lim}$ is varied as in (2.18) to study the sensitivity of the tradeoff between the fuel economy and driveability to the gear shift strategy.

$$\Delta P_{e,lim} \in \{0, 3, 9, 12, 15, 17, 19, 21, 24, 27\} \quad [kW]. \quad (2.18)$$

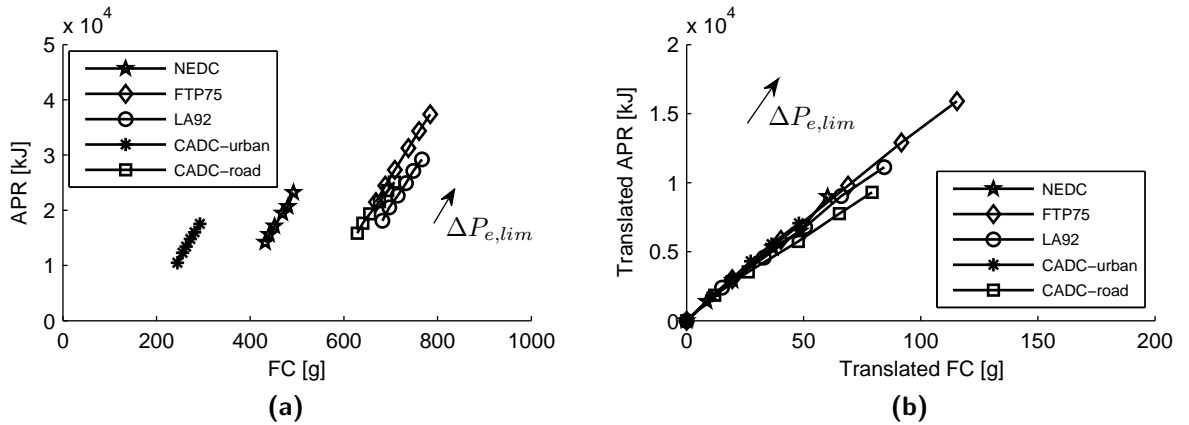


Figure 2.6: Method 2: sensitivity analysis of FC and APR with respect to $\Delta P_{e,lim}$ (a); the translation of FC and APR to the coordinate origin (b).

Simulation results of FC and APR , defined in (2.15), are shown in Figure 2.6a. A translation of FC and APR to the coordinate origin are depicted in Figure 2.6b. It can be observed that an increase of $\Delta P_{e,lim}$ leads to a decrease of the fuel economy. For this method, the higher the value of $\Delta P_{e,lim}$, the better the driveability comes at a cost of fuel economy reduction. Furthermore, it can be concluded that an increase of APR is proportional with an increase of FC with respect to $\Delta P_{e,lim}$.

2.3.4 Method 3: The Variable Power Reserve

Both Methods 1 and 2 show that, the optimal gear shift strategy is sensitive to the weight factor ν and the power reserve limit $\Delta P_{e,lim}$, respectively. These design parameters are kept being constant for the whole drive cycle, and hence making the obtained gear shift strategy become more conservative. To overcome this drawback, the weight factor or the power reserve limit needs to be adapted to the changing driving conditions. Therefore, defining a rule for such an adaptation is a key factor for a fuel-optimal gear shift control strategy to further improve the fuel economy and driveability potentially at the same time. In this section, a method based on a concept of variable power reserve is proposed to address the driveability as put in a fuel-optimal gear shift strategy. The power reserve required for a certain acceleration capability of the vehicle is varied in accordance with its actual speed. In other words, the variable power reserve is a function of the vehicle speed, denoted as $\Delta P_{e,var}(v(k))$. Hence, the gear shift control problem needs to respect the variable power reserve by an inequality constraint as,

$$\Delta P_e(k) \geq \Delta P_{e,var}. \quad (2.19)$$

A novel approach is developed to define the variable power reserve $\Delta P_{e,var}(v(k))$. This approach is based on a statistical analysis of the vehicle acceleration characteristics on various drive cycles. The details are presented next.

Vehicle performance characteristics

In this section, the discrete time variable k is left out of the variables for brevity. For the functional variables, the independent variable is omitted to improve the readability, for example $r_g := r_g(n_g(k))$. Then, if the engine output torque is T_e , the propulsion force available at the wheels is given by,

$$F_w = \eta \frac{r_g r_d T_e}{R_w}. \quad (2.20)$$

Under the influence of road material and driving conditions, e.g. dry, wet, snow, etc., the tractive force at the wheels induced by friction is approximated by

$$F_{fr} = \frac{\mu m_v g (l_b + c_r (h_g - R_w))}{l + \mu h_g}, \quad (2.21)$$

where l is the wheelbase length of the vehicle; l_b is the horizontal distance from the vehicle gravity center to the rear tire; h_g is the height of the vehicle gravity center; μ is the friction coefficient between the tire and road surface.

If we assume that the standard road material of asphalt is used under a dry condition, the corresponding peak friction coefficient μ_p is chosen to calculate a maximum friction force $F_{fr,max}$ at the wheels. The maximum propulsion force at the wheels, denoted as $F_{w,max}$, is calculated by (2.20) with the engine torque at wide open throttle. So, the vehicle maximum acceleration is derived as,

$$a_{max} = \frac{\min(F_{w,max}, F_{fr,max}) - F_{load}}{m_{v,eq}}, \quad (2.22)$$

where $m_{v,eq}$ is the equivalent vehicle mass at the wheels,

$$m_{v,eq} = \frac{((J_e + J_c + J_p) r_g^2 + J_s) r_d^2}{R_w^2} + m_v.$$

Figure 2.7 depicts the maximum acceleration characteristic vs. the vehicle velocity corresponding with each gear position n_g (see, the solid lines). So, the actual accelerations of the vehicle in real-life driving are always inside these bounds. Here, the decelerations are irrelevant for the design method, and therefore neglected.

Variable power reserve

In order to define the variable power reserve $\Delta P_{e,var}$, a statistical analysis of vehicle acceleration characteristics on various drive cycles is performed. Depend on the regions, the driving styles, the driving purposes, etc., the drive cycles are differed from each other. Therefore, the selected drive cycles must encompass a representative driving profile of the vehicle, giving quantitative information of the acceleration level a driver would normally require at every vehicle speed. In this study, to ensure objectiveness, the drive cycles chosen are the standardized ones: ARB02, CADC, FTP75, Hurk, HWFET, JN1015, LA92, NEDC, NYCC, and US06 (see, Appendix C).

The velocity is discretized into a finite number of values N_v with an equal discretized step, thus giving a velocity set,

$$\mathcal{V} = \{v_1, v_2, \dots, v_{N_v}\}. \quad (2.23)$$

For a given drive cycle, at a certain velocity $v(k)$ the corresponding acceleration is approximated as,

$$a(k)|_{v(k)} = \frac{v(k+1) - v(k)}{\Delta t}. \quad (2.24)$$

Sampling the velocity and computing the corresponding acceleration on all chosen drive cycles to create the velocity data. Then clustering the velocity data in accordance with all elements of the velocity set (2.23) to form the corresponding acceleration data. The velocity data and the acceleration data together create the statistical data of the chosen drive cycles. Mapping the statistical data onto the vehicle performance characteristics to realize the representative acceleration characteristics for the vehicle, see, the light blue circles in Figure 2.7. The statistical data falling outside the acceleration bounds are cut off due to infeasible driving situations.

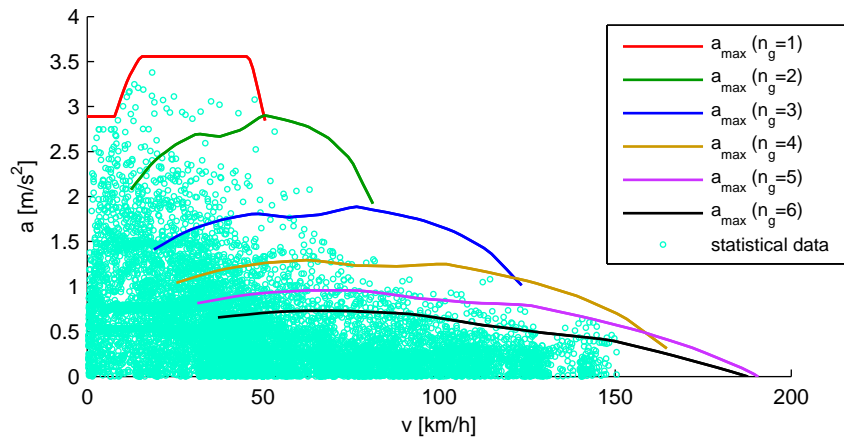


Figure 2.7: Performance characteristics of the vehicle, indicated by the six solid lines corresponding with six gear positions. The representative acceleration characteristics are indicated by the light blue circles. v is the vehicle velocity, a is the vehicle acceleration.

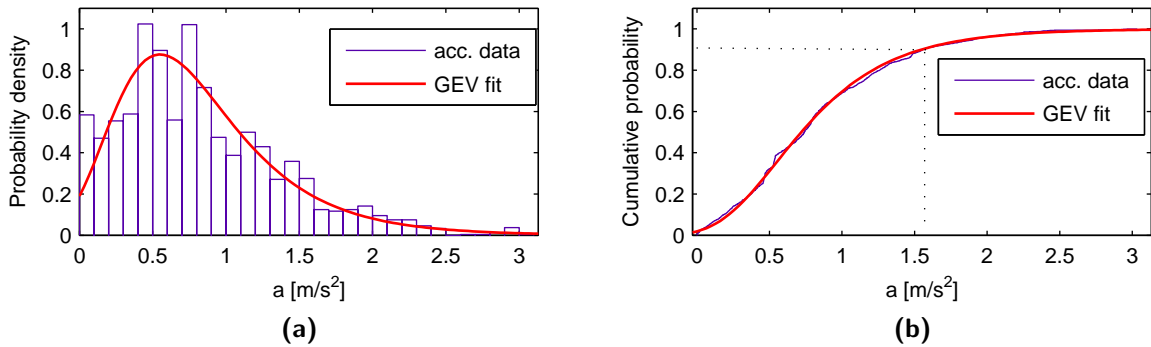


Figure 2.8: Analysis of the acceleration data at the velocity cluster $v_l = 30 [km/h]$. a is the acceleration. Legends: acc. stands for acceleration; GEV stands for generalized extreme value.

The acceleration data is clustered in accordance with $v_l \in \mathcal{V}$, $l = 1, 2, \dots, N_v$. There-

fore, analyzing this cluster can give an insight of a driveability level for the vehicle at the corresponding velocity. The acceleration data at each cluster of velocity is considered as a random variable. In statistics and probability theory [85, 113], probability density function is a function that describes the relative likelihood for a random variable to take on a given value. Hence, probability density function is an appropriate tool to analyze the acceleration data.

As a demonstration, an analysis for the acceleration data at the velocity cluster $v_l = 30 [km/h]$ is given in Figure 2.8: a probability density distribution in (a), and a corresponding cumulative probability in (b). The acceleration data can be fitted by the generalized extreme value distribution having a cumulative distribution function,

$$F_{CD}(a; \kappa, \sigma, \xi) = \exp \left\{ - \left[1 + \xi \left(\frac{a - \kappa}{\sigma} \right) \right]^{-1/\xi} \right\},$$

where a is the vehicle acceleration; κ is the location parameter; σ is the scale parameter; and ξ is the shape parameter.

The fits are shown by the red solid lines. It demonstrates that the acceleration range of $[0.3, 0.9] [m/s^2]$ has the highest probability density, meaning that this acceleration range is where the vehicle acceleration is most likely occurred. Nonetheless, the maximum vehicle acceleration is at $3.1 [m/s^2]$, occurring at very small probability. Whereas, the cumulative probability defines a probability of the vehicle acceleration a to be smaller or equal to a certain value a_{req} , described by,

$$\mathbf{Prob} \left[a \leq a_{req} | v_l \in \mathcal{V} \right] = p_a, \quad (2.25)$$

where **Prob** is a probability of a certain event. Apparently, in order to have $p_a = 1$, a_{req} must be equal to $3.1 [m/s^2]$.

It is observed that, a definition of an acceptable driveability level for the vehicle over the whole velocity range is equivalent to a definition of p_a for each velocity cluster $v_l \in \mathcal{V}$. Drivers would always expect the vehicle to fully meet the acceleration request, which means that $p_a = 1 \forall v_l \in \mathcal{V}$. This would require a gear shift strategy, resulting in a high power reserve, ready for a possible maximum acceleration. Such a high power reserve level will induce a sportive driving behavior, however, it decreases the fuel saving potential considerably. Hence, defining an appropriate value for p_a can improve the fuel economy meanwhile ensuring an acceptable vehicle driveability.

Regarding to the accumulative probability, statistical and probability theories point out that a confidence level associated with a certain p_a is commonly chosen at 90%, or 95%, or 99% [85, 113]. In this study, a confidence level is chosen at 90%. Therefore, if drivers would expect the vehicle to always satisfy the acceleration demand, it's very likely that the vehicle can only meet 90% of the driving demand. Hence, $p_a = 0.9$ is chosen for a fairly acceptable driveability level. In other words, the vehicle can follow

up to 90% of the occurring acceleration situations. Note that 10% excluded represents the very hard, sudden acceleration situations, which are not specifically matched with the powertrain capability at the current gear. Hence, the transmission is required to shift gears (downshift) such that the powertrain can accommodate the high acceleration demand.

Once, the acceptance driveability level represented by p_a has been defined, the required acceleration $a_{req}(v_l)$, $\forall v_l \in \mathcal{V}$ is obtained by solving a reverse problem, defined correspondingly with (2.25). So, a polynomial fit $a_{req,fit}(v)$, as a function of the velocity, can be achieved,

$$a_{req,fit}(v) = p_1 v^6 + p_2 v^5 + p_3 v^4 + p_4 v^3 + p_5 v^2 + p_6 v + p_7, \quad (2.26)$$

where p_1 , p_2 , p_3 , p_4 , p_5 , p_6 and p_7 are the coefficients of the polynomial fit.

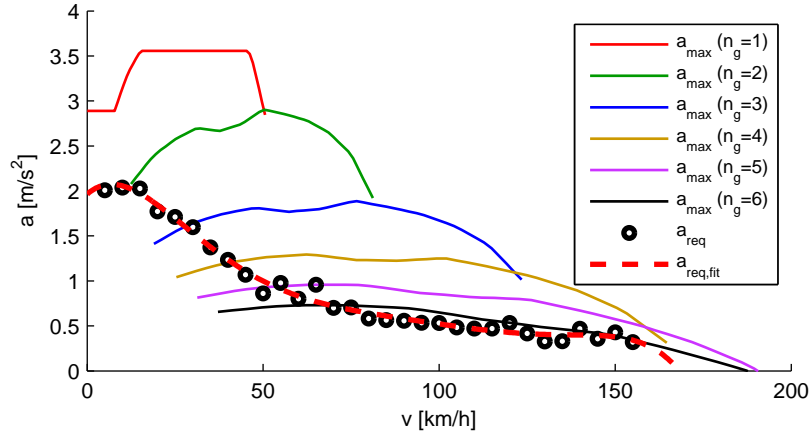


Figure 2.9: Acceleration capability characteristics required to ensure an acceptable driveability level. v is the vehicle speed, a is the vehicle acceleration.

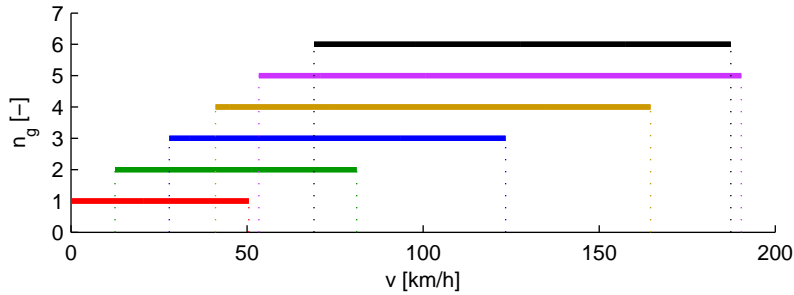


Figure 2.10: Feasible operating regions corresponding with the gear positions for a satisfaction of the vehicle driveability. v is the vehicle speed, n_g is the gear position.

Figure 2.9 depicts the required accelerations $a_{req}(v_l)$ and the corresponding fit poly-

mial $a_{req,fit}(v)$. It represents the acceleration capability characteristics, as a function of the vehicle speed, to ensure that the vehicle can confidently cover 90% of the actual driving situations.

Intersections of $a_{req,fit}(v)$ with the vehicle performance characteristics at a certain gear create the correspondingly feasible operating region for the powertrain at that gear position. Hence, the intersection among the feasible operating regions yields a common operating area for optimally shifting gears meanwhile still ensuring the acceptable driveability level, see Figure 2.10.

Finally, from (2.26), the variable power reserve is derived as,

$$\Delta P_{e,var}(v) = m_{v,eq} a_{req,fit}(v) v. \quad (2.27)$$

Control problem formulation

A fuel-optimal gear shift control problem, taking into account the variable power reserve (2.27) to respect a certain driveability requirement, is formulated as follows.

Problem 2.2. *Given a drive cycle $v(k)$ with time length N , thus making the vehicle longitudinal motion (2.5) deterministic, find an optimal gear shift strategy $u^*(k) = u_g^*(k)$ to minimize the cost function of fuel consumption over the drive cycle, that is,*

$$u^*(k) = \arg \min_{u(k)} \mathbf{J} = \sum_{k=0}^{N-1} \dot{m}_f(k) \Delta t, \quad (2.28)$$

subject to the constraints (2.6)-(2.9), and

$$\Delta P_e(k) \geq \max\left\{0, \Delta P_{e,var}(v(k)) - P_{e,req}(k)\right\}, \quad (2.29)$$

where $P_{e,req}(k)$ is the required power to follow the given drive cycle $v(k)$.

Note that (2.19) refers to a general constraint for meeting the driveability requirement. Therefore, the power $P_{e,req}(k)$, required to follow a given drive cycle, has to be subtracted from $\Delta P_{e,var}(v(k))$ as in (2.29). If $P_{e,req}(k) \geq \Delta P_{e,var}(v(k))$ holds, the constraint (2.29) becomes inactive because the real power reserve $\Delta P_e(k)$ is always larger than zero. For this problem, DP is also used to derive the optimal solution.

Simulation results

Simulation results of Method 3 are given in Table 2.2. The fuel-optimal gear shift strategy, described in Section 2.2, is chosen as a reference. It shows that Method 3 degrades the fuel economy compared to the reference, but benefiting a significant improvement

Table 2.2: Simulation results of FC and APR of Method 3. The relative FC and APR differences are obtained by comparing with the results of the fuel-optimal gear shift strategy. $Rel.$ denotes the relative.

Drive cycle	FC [g]	APR [kJ]	Rel. FC difference [%]	Rel. APR difference [%]
NEDC	457.8	$1.21 \cdot 10^4$	-6.8	47.6
FTP75	722.7	$1.93 \cdot 10^4$	-8.2	58.2
LA92	706.4	$1.37 \cdot 10^4$	-3.3	28.0
CADC-urban	268.1	$0.59 \cdot 10^4$	-7.0	51.3
CADC-road	642.8	$1.39 \cdot 10^4$	-3.6	26.4
CADC-highway	1555.1	$1.67 \cdot 10^4$	-0.3	3.7

of the driveability. It is also observed that on the drive cycles having aggressive acceleration, high speed profiles, e.g. LA92, CADC-road, and CADC-highway, the high drive power demand required to follow the drive cycle is more likely to satisfy the driveability level by default, and thus deteriorating not much fuel economy. However, on the mild and dynamic drive cycles, e.g. NEDC, FTP75 and CADC-urban, the drive power demand is in moderate levels, which is less likely to fulfil the driveability level. Therefore, the transmission tends to shift up late to ensure a driveability satisfaction. This results in a relatively high fuel consumption on NEDC, FTP75 and CADC-urban compared to the other cycles.

2.3.5 Comparison of Three Methods

Three methods to address the driveability in the fuel optimal gearshift control problem were proposed, namely the weighted inverse of power reserve, the constant power reserve, and the variable power reserve, respectively. The first two methods provide control laws more sensitive to the design parameters and more conservative over a certain drive cycle because ν and $\Delta P_{e,lim}$ are kept constant for the whole drive cycle. Meanwhile, the third method, in which $\Delta P_{e,var}(v)$ is varied according to the vehicle speed, seems to yield an optimal compromise. To verify this proposition as well as to evaluate the advantages among the proposed three methods, a procedure is defined as,

Procedure 2.1. *For a certain given drive cycle:*

- *apply Method 3 to get the baseline results of FC and APR , as shown in Table 2.2.*
- *for Method 1: tune the design parameter ν , such that the obtained FC is as close to that of Method 3 as possible. Compute the corresponding APR .*

Table 2.3: Analysis of FC and APR of Methods 1 and 2 in comparison with Method 3. $Rel.$ denotes the relative.

Drive cycle	Method	Parameters	Rel. FC difference [%]	Rel. APR difference [%]
NEDC	1	$\mu = 1730$	0.3	-2.4
	2	$\Delta P_{e,lim} = 11.8[\text{kW}]$	0.2	-8.2
FTP75	1	$\mu = 1730$	0.0	-0.8
	2	$\Delta P_{e,lim} = 11.8[\text{kW}]$	0.0	-8.8
LA92	1	$\mu = 430$	0.3	-16.4
	2	$\Delta P_{e,lim} = 1.0[\text{kW}]$	-0.2	-22.1
CADC-urban	1	$\mu = 1430$	0.6	-1.6
	2	$\Delta P_{e,lim} = 9.8[\text{kW}]$	0.5	-8.1
CADC-road	1	$\mu = 1130$	0.1	-1.3
	2	$\Delta P_{e,lim} = 9.0[\text{kW}]$	0.1	-8.9
CADC-highway	1	$\mu = 1730$	0.5	0.2
	2	$\Delta P_{e,lim} = 8.8[\text{kW}]$	1	-1.2

- for Method 2: tune the design parameter $\Delta P_{e,lim}$, such that the obtained FC is as close to that of Method 3 as possible. Compute the corresponding APR .

Calculate the relative FC and APR differences by comparing the results of Methods 1 and 2 with the baseline results.

Apply Procedure 2.1 for all representative drive cycles, the obtained results are shown in Table 2.3. The relative FC difference is close to zero with an average value of 0.3% and 0.1% for Methods 1 and 2, respectively. Meanwhile, the relative APR difference decreases for almost drive cycles, with an average value of 4.5% and 11.2% for Methods 1 and 2, respectively. In other words, Method 3 gives the highest APR with the same value of FC . Hence, it can be concluded that, Method 3, based on the variable power reserve concept, is the promising solution for achieving the best tradeoff between the fuel economy and driveability. Method 1 gives approximately the same result of FC with a small decrease of APR compared to Method 2. Hence, a weight factor to penalize the power reserve can result in a driveability level better than a constant power reserve constraint.

The concept of variable power reserve, as a function of the vehicle speed and predefined from various driving scenarios, makes the corresponding gear shift strategy independent with the test drive cycles. Hence, the variable power reserve concept reveals itself to be able to apply in realtime by a control approach, e.g. model predictive control [148], to ensure a driveability satisfaction meanwhile still achieving a fuel economy benefit.

Apparently, Methods 1 and 2, yielding solutions sensitive to the design parameters and conservative to a drive cycle, are hard to implement in a realtime controller.

2.4 Stochastic Gear Shift Strategy

A gear shift strategy based on DP requires a knowledge of the whole drive cycle to obtain a globally optimal solution, thus making it not a realtime solution. Meanwhile a realtime implementable gear shift strategy can be achieved by utilizing Model Predictive Control (MPC) or Stochastic Dynamic Programming [11]. The MPC-based algorithm solves the optimal problem over a prediction horizon. Utilizing knowledge of the driving profile over the prediction horizon, and applying the receding principle, the MPC-based strategy is realtime implementable, but yielding a suboptimal solution. Meanwhile SDP-based algorithm formulates and solves an infinite-horizon optimization problem over a probabilistic distribution of the power demand obtained from many drive cycles rather than a single drive cycle. This means that the SDP-based strategy is optimal on an average sense, time-invariant and state variable feedback such that it can be implemented in realtime.

The vehicle driveability can be addressed in a MPC-based gear shift strategy by utilizing the variable power reserve concept (Method 3). Due to suboptimal characteristics, the MPC-based strategy will result in a decrease of the driveability capability compared to the DP-based gear shift strategy. Whereas, the SDP-based gear shift strategy is optimized over many drive cycles on an average sense, which implies that the driveability is intrinsically respected. To compare with Method 3 in terms of the driveability improvement, details and results of the SDP-based gear shift problem are given in the following sections.

2.4.1 Stochastic Modeling of Power Request

Markov model of power request dynamics

In real-life driving, the driver controls the vehicle speed by pressing the throttle and brake pedals. In general, these command signals are interpreted as a power request at the wheels to be satisfied by the powertrain. Hence, the power request, positive or negative, is considered as an input to the powertrain controller. In this section, a model of the power request, as a stochastic dynamic process based on the Markov chain [70,82], is chosen to generate the power request. Assuming that, the power request P_{req} is discretized to create a set,

$$\mathcal{P}_{req} = \{z_1, z_2, \dots, z_{N_p}\}, \quad (2.30)$$

wherein N_p approximates the actual continuum of values of the power request.

The vehicle speed is discretized into a finite number N_v of values, thus giving a set,

$$\mathcal{V} = \{v_1, v_2, \dots, v_{N_v}\}.$$

The Markov chain defines a dynamics of the power request P_{req} by a transition probability matrix $\mathbf{T}_M \in \mathbb{R}^{N_p \times N_p \times N_v}$, whose elements are defined as,

$$\begin{aligned} t_{ij,l} &= \mathbf{Prob} \left[P_{req}(k+1) = z_j \mid P_{req}(k) = z_i, v(k) = v_l \right] \\ &\text{with } i, j = 1, 2, \dots, N_p; \quad l = 1, 2, \dots, N_v \end{aligned} \quad (2.31)$$

where $t_{ij,l}$ is the $(i, j, l)^{th}$ element of \mathbf{T}_M representing one-step transition probability from the current states of $P_{req}(k)$ and $v(k)$ at current time step k to state $P_{req}(k+1)$ at next time step $k+1$.

Note that for a given power request, the vehicle longitudinal dynamics is deterministic. Hence, specifying drive cycle characteristics is equivalent to specifying the transition probability $t_{ij,l}$, which can be estimated from the known drive cycles or the past driving records. In this study, standard drive cycles are used to determine the transition probability matrix \mathbf{T}_M . The maximum likelihood algorithm, a suitable candidate for dealing with the discrete data, is used to derive \mathbf{T}_M .

Algorithm 2.1. Maximum likelihood estimation

1. Chose the drive cycles that represent for actual driving profiles, e.g. suburban, urban, and highway, etc.
2. Sample the vehicle speed $v(k)$, then calculate the corresponding power request at current time step $P_{req}(k)$, and at next time step $P_{req}(k+1)$ by using the quasi-static powertrain model.
3. Cluster $v(k)$ in accordance with all elements of \mathcal{V} to create the velocity cluster at v_l , and collecting the corresponding power request data.
4. For each velocity cluster v_l , cluster the power request $P_{req}(k)$ in accordance with all elements of \mathcal{P}_{req} to create the power request data at cluster z_i , and collecting the corresponding next power request $P_{req}(k+1)$.
5. Then, cluster the corresponding $P_{req}(k+1)$ in accordance with all elements of \mathcal{P}_{req} .
6. Define the transition probability by the maximum likelihood estimator, which counts the observation data as,

$$t_{ij,l} = \frac{n_{ij,l}}{n_{il}} \quad \text{if } n_{il} \neq 0,$$

where $n_{ij,l}$ is the number of occurrences of the transition from z_i to z_j at the velocity cluster v_l ; $n_{i\cdot}$ is the total number of times that z_i has occurred at the velocity cluster v_l . Apparently,

$$n_{i\cdot} = \sum_{j=1}^{N_p} n_{ij,l} \quad \text{and} \quad \sum_{j=1}^{N_p} t_{ij,l} = 1.$$

It is worthwhile to mention that if the observation data are not rich enough to cover the whole state space, $n_{i\cdot}$ may be zero for a specific case of the velocity cluster v_l . Therefore, a fuzzy smoothing algorithm [22] is used to estimate the corresponding transition probabilities.

Algorithm 2.2. Fuzzy smoothing estimation

1. If denote the elements $v_l \in \mathcal{V}$, $l = 1, 2, \dots, N_v$ as the velocity clusters. Then, assume at a certain velocity cluster v_l , there exists N_{obs} observations of the corresponding current and next power requests, obtained from the given drive cycles. Denote a pair of observations of the power request as $x = [x_k, x_{k+1}] \triangleq [P_{req}(k), P_{req}(k+1)]$ giving,

$$x^n \triangleq \{x^1, x^2, \dots, x^{N_{obs}}\}, \quad \text{with } n = 1, 2, \dots, N_{obs}.$$

2. If denote the elements $z_i \in \mathcal{P}_{req}$, $i = 1, 2, \dots, N_p$ as the power request clusters. Then, a membership function of any observed power request x_k with respect to a certain power request cluster z_i is defined as,

$$m_i(x_k) = \left\{ \sum_{m=1}^{N_p} \left[d(x_k, z_i) / d(x_k, z_m) \right]^{1/(F-1)} \right\}^{-1},$$

where $d(x_k, z_i)$ denotes the Euclidean distance between x_k and z_i ; F is a suitable chosen constant greater than one.

3. Use the membership function $m_i(x_k)$, the smoothed transition probabilities of the Markov chain model is estimated as,

$$t_{ij,l} = \frac{\sum_{n=1}^{N_{obs}} [m_i(x_k^n) m_j(x_{k+1}^n)]}{\sum_{n=1}^{N_{obs}} m_i(x_k^n)}, \quad i, j = 1, 2, \dots, N_p.$$

It is apparent that when F tends to one, the fuzzy smooth estimation approaches the maximum likelihood estimation. Figure 2.11 shows an example of the estimated transition probabilities at a velocity cluster $v_l = 80 [km/h]$. The diagonally dominant structure of the transition probabilities reveals a high correlation of the power request separated by one time step. This can be explained that if the vehicle is experiencing some power request level at the current time step, it's likely to experience a similar power request level at the next time step.

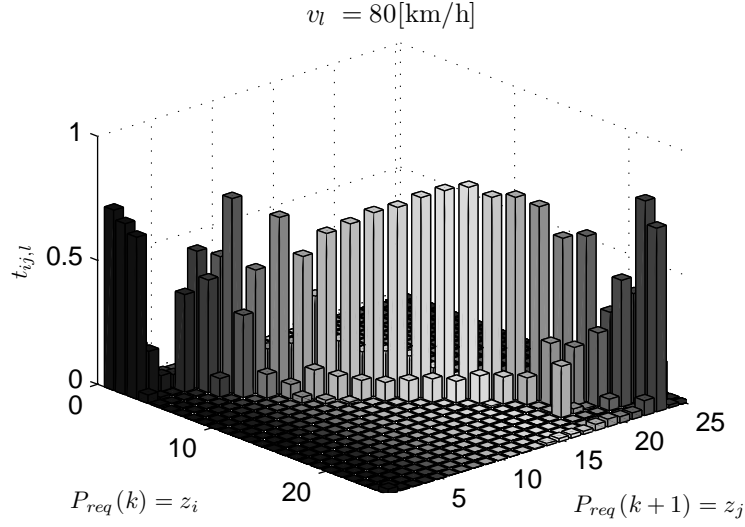


Figure 2.11: Transition probability matrix at a quantized vehicle speed 80[km/h].

Define the stochastic power request

Given a Markov model of the power request, the inverse transform method [26] can be used to define the actual vehicle power request evolution. Given a vehicle speed clustered to v_l and a current power request clustered to z_i at time k , by generating a positive random number u_{rand} with a uniform distribution, ranged $[0, 1]$, the next power request $P_{req}(k+1)$ can be defined as,

$$P_{req}(k+1) = \begin{cases} z_1, & \text{if } 0 \leq u_{rand} < t_{i1,l}, \\ z_2, & \text{if } t_{i1,l} \leq u_{rand} < t_{i1,l} + t_{i2,l}, \\ \dots & \\ z_j, & \text{if } \sum_{q=1}^{j-1} t_{iq,l} \leq u_{rand} < \sum_{q=1}^j t_{iq,l}. \end{cases} \quad (2.32)$$

2.4.2 Stochastic Gear Shift Algorithm

Gear shift problem formulation

Problem 2.3. *Given the powertrain model and a Markov model of the power request evolution, the objective is to define an optimal gear shift strategy $u^* = u_g^*$ that maps the observed states to control decisions to minimize the expected total fuel consumption over an infinite horizon,*

$$\mathbf{J} = \lim_{N \rightarrow \infty} \mathbf{E}_{P_{req}} \left\{ \sum_{k=0}^{N-1} \gamma^k \dot{m}_f(k) \Delta t \right\}, \quad (2.33)$$

subject to the constraints (2.6)-(2.9) and (2.31).

The objective function consists of the instantaneous fuel consumption $\dot{m}_f(k)\Delta t$, accumulated over time, discounted by a factor γ ($0 < \gamma < 1$), averaged over a stochastic distribution of the power request. N is the horizon which approaches infinity for this stochastic algorithm. $\mathbf{E}\{\dots\}$ denotes the expectation with respect to the considered prediction model defined by the time-invariant Markov chain.

Applying the optimality principle of Bellman [11], the stochastic gear shift control problem is solved by a two-step algorithm, namely policy evaluation and policy improvement.

- **Policy evaluation**

In this policy, for each possible state vector value x , given a control policy $u(x)$, the cost-to-go $\mathcal{J}(x)$ is computed recursively as,

$$\mathcal{J}^{s+1}(x) = \dot{m}_f \Delta t + \mathbf{E}_{P_{req}} \left[\gamma \mathcal{J}^s \left(f(x, u(x)) \right) \right] \quad \forall x \in X. \quad (2.34)$$

where s represents an iteration index; X is the set of admissible state value. The recurrence relation is evaluated iteratively for all state vector values in the discretized set of admissible states.

- **Policy improvement**

The optimality principle [11] indicates that an optimal control policy for the stochastic gear shift control problem is also the control policy that minimizes the cost-to-go function $\mathcal{J}(x)$ in (2.34). Hence, the optimal control policy $u^* = u_g^*$ for each state vector value x is defined as,

$$u^*(x) = \arg \min_{u \in U(x)} \left\{ \dot{m}_f \Delta t + \mathbf{E}_{P_{req}} \left[\gamma \mathcal{J} \left(f(x, u) \right) \right] \right\} \quad \forall x \in X, \quad (2.35)$$

where $U(x)$ is the set of admissible control value corresponding to the state value x .

After both policies are completed, the optimal control policy is feedback to the policy evaluation step, and then the entire procedure is repeated iteratively until the optimal cost function converges. In this study, the discount factor is chosen as $\gamma = 0.9$; and the terminate condition for the iteration process is set with $\|\mathcal{J}^{s+1}(x) - \mathcal{J}^s(x)\|_\infty < 1\%$.

2.4.3 Simulation Results and Discussions

The gear shift strategy obtained from the stochastic control algorithm is a set of shift maps. Each shift map, corresponding to each velocity cluster v_l , generates the shift points for the transmission based on the current gear position and the current power

request. Therefore the SDP-based gear shift strategy can be directly implemented in simulation or in realtime.

The stochastic gear shift problem is formulated and solved, subject to a probabilistic distribution of the power request in an average sense. For the stochastic gear shift problem, the power request is considered as a dynamic process, represented by a probability transition. Various drive cycles are used to construct the probability transition matrix T_M for the power request evolution. Therefore, the stochastic-based gear shift strategy by default respects the power request dynamics, meaning that vehicle driveability is taken into account. Therefore the diversity of driving scenarios in the drive cycles will determine a driveability coverage level.

Table 2.4: Simulation results of the SDP method. The relative FC and APR differences are obtained by comparing with Method 3. *Rel.* denotes the relative.

Drive cycle	FC [g]	APR [kJ]	Rel. FC difference [%]	Rel. APR difference [%]
NEDC	450.9	$1.02 \cdot 10^4$	-1.5	-15.7
FTP75	700.2	$1.35 \cdot 10^4$	-3.1	-30.1
LA92	715.8	$1.10 \cdot 10^4$	1.3	-19.7
CADC-urban	285.1	$0.46 \cdot 10^4$	6.3	-22.0
CADC-road	629.1	$1.09 \cdot 10^4$	-2.1	-21.6
CADC-highway	1555.9	$1.58 \cdot 10^4$	0.1	-5.4

Method 3 (see, Section 2.3) gives an optimal tradeoff between the fuel economy and driveability. This method is based on the variable power reserve concept, which is extracted from a statistical analysis of the power request over various drive cycles. As analyzed, the stochastic gear shift strategy intrinsically respects the driveability. Hence, it is necessary to compare the stochastic gear shift strategy with Method 3 for approaching the insight on the driveability aspect among the proposed gear shift strategies.

To do so and to ensure a fair comparison, the standard drive cycles, utilized for building the probability transition matrix of the SDP algorithm, are chosen the same as Method 3, which are ARB02, CADC, FTP75, Hurk, HWFET, JN1015, LA92, NEDC, NYCC, and US06 (see, Appendix C). The stochastic gear shift strategy is tested on the representative drive cycles (also the same as Method 3). Simulation results are displayed in Table 2.4. Compared with the results of Method 3, the stochastic gear shift strategy gives a better fuel economy on NEDC, FTP75 and CADC-road. Meanwhile on LA92, CADC-urban and CADC-highway it reveals a fuel deficiency. On average, the relative FC difference of the stochastic method compared with Method 3 is 0.2%, which renders

the two methods to be nearly equal on the fuel economy aspect. However, the negative relative *APR* differences on all the tested drive cycles mean that the SDP method results in a less acceleration capability compared with Method 3. In conclusion, the variable power reserve concept introduced in Method 3 offers the best way to improve the fuel economy while still satisfying an acceptable driveability level.

2.5 Conclusions

In this chapter, the fuel economy potential of a conventional vehicle equipped with an AMT is explored by a fuel-optimal gear shift strategy based on DP. Simulation results over the standard drive cycles shows a substantial improvement of the fuel economy.

The tradeoff between the fuel economy and driveability with respect to an optimal gear shift strategy is addressed systematically by three methods. In Method 1, the driveability is considered by proposing an objective function consisting of the fuel consumption and the weighted inverse of power reserve. In Method 2, the driveability is respected by imposing an inequality constraint on a constant power reserve level. And in Method 3, the variable power reserve concept, varied with the vehicle speed, is utilized to respect an acceptable driveability level. Simulation results show that Methods 1 and 2 improve the driveability at a cost of a fuel economy reduction in a linear manner. Meanwhile, Method 3 achieves an optimal tradeoff between the fuel economy and driveability compared with Methods 1 and 2. In other words, if applying the concept of variable power reserve in the design of a fuel-optimal gear shift strategy, the fuel economy can be improved without sacrificing the vehicle driveability.

Furthermore, the gear shift strategy based on SDP is capable of handling the vehicle driveability meanwhile improving the fuel economy on an average sense. However, it is not able to compete with the variable power reserve concept proposed in Method 3 for an acceleration capability. Conversely, the SDP method is realtime implementable, which is not held for Method 3. Nonetheless, the variable power reserve concept can be applied in a realtime gear shift approach, e.g. a predictive gear shift strategy, or an optimization-based gear shift map extraction.

The design framework proposed in this study can be applied to other powertrain systems equipped with discrete ratio transmissions to address the driveability in an optimal gear shift strategy.

Optimal Gear Shift Strategies for Hybrid Electric Vehicles¹

Abstract - This chapter proposes a control algorithm for the Energy Management Strategy to explore the potential fuel saving of Hybrid Electric Vehicles (HEVs) equipped with an Automated Manual Transmission. The control algorithm is developed based on a combination of Dynamic Programming (DP) and Pontryagin's Minimum Principle (PMP) to optimally control the discrete gear shift command, in addition to the continuous power split between the internal combustion engine and electric machine. The proposed algorithm outperforms the DP algorithm in terms of computational efficiency without loss of accuracy. Simulation results for the DP-PMP algorithm show that by further optimizing the gear shift strategy, additional fuel savings of 20.3% and 31.6% can be reached compared to the prescribed gear shift strategies on the drive cycles NEDC and FTP75, respectively.

Furthermore, with the start-stop functionality available, it is shown that the two-point boundary value problem following from the PMP can not be solved with sufficient accuracy without loss of optimality. This means that the finding of a constant value for the Lagrange multiplier while satisfying the battery state-of-energy at the terminal time is not always guaranteed. Therefore an alternative approach of state-of-energy feedback control to adapt the Lagrange multiplier is adopted. The obtained results are very close to the globally optimal solution of the DP algorithm. Simulation results show the relative fuel savings can be up to 26.8% and 36.4% compared to the prescribed gear shift strategies on NEDC and FTP75, respectively.

3.1 Introduction

Design of the Energy Management Strategies (EMSs) for Hybrid Electric Vehicles (HEVs) to improve vehicle performance, such as fuel economy, driveability, comfort and emissions has received considerable attentions in literature [126]. Regardless the

¹This chapter has been accepted for a journal publication in the form of a paper as [98]: V. Ngo, T. Hofman, M. Steinbuch, A. Serrarens. Optimal Control of Gear Shift Command for Hybrid Electric Vehicles. *IEEE Transactions on Vehicular Technology*, vol. 61, issue 8, 2012.

powertrain topology, the EMS controls the power flow of the powertrain system to satisfy the driver's power request while minimizing a certain cost function over a drive cycle under system constraints. For example, the control strategy aims at optimally choosing the power split between the internal combustion engine and electric machine in order to minimize fuel consumption. Many control solutions have been proposed for the EMSs in literature, such as heuristic controllers based on predefined rules, fuzzy logics, neural networks; optimal controllers based on deterministic Dynamic Programming (DP) or optimal control, such as Pontryagin's Minimum Principle (PMP) [3, 50, 51, 63, 67, 73, 118, 125–127, 134].

For HEVs equipped with discrete ratio transmissions, such as an Automated Manual Transmission (AMT), the instantaneous operating points of the hybrid driveline are not only defined by the power split but also defined by the gear position of the transmission. Therefore, a control algorithm including an optimized gear shift strategy would result in a fuel economy improvement. In [107], a heuristic gear shift strategy is proposed by selecting the highest possible gear position capable of delivering the required power from the engine given a vehicle speed. In [83], the authors use DP to derive optimal trajectories of the power split and gear shift sequence to minimize the weighted cost function of fuel consumption and pollution emissions for a hybrid electric truck. In [25], the authors utilize optimal control to derive the combined optimal torque distribution and gear position to minimize fuel consumption for a parallel HEV. In this way, the optimal solution can be computed very fast. However, the control algorithm allows the transmission to freely shift within the admissible set of gear positions. This shift strategy is not realistic and unreasonable in terms of the vehicle driveability. The authors in [156] propose an EMS for a parallel HEV to optimize the torque distribution and gear shift separately. Given the optimal torque distribution, pre-defined for minimizing the powertrain equivalent specific fuel consumption, the gear shift strategy is designed to maximize the powertrain efficiency. By doing so, the authors acknowledge the designed EMS to be suboptimal despite a claim of significant fuel economy improvement.

Nevertheless, none of the mentioned research papers has discussed a systematic method to optimize the gear shift strategy for HEVs in order to address its potential fuel saving compared to the case of a standard gear shift strategy. Moreover, the constraints on the gear shift command, affecting to the vehicle driveability [98], are not taken into account in synthesizing the control algorithm. Another issue related to the shift strategy is how fast such a control algorithm can compute the optimal solution when comparing with the DP. Therefore, in this study, a framework of designing the optimal control algorithm for the gear shift problem and analyzing its contribution to the fuel economy of a parallel HEV is presented. Firstly, DP is used to obtain the globally optimal solution of the gear shift position and power split despite the fact that it requires a heavy computation. Secondly, a control algorithm based on a combination of DP and PMP is proposed to achieve fast computation meanwhile attaining the globally optimal

solution. This so-called DP-PMP control algorithm is a novel method for the gear shift problem of HEVs equipped with discrete ratio transmissions. It is seen as a suitable alternative applied for a realtime implementable control algorithm, such as a model predictive control algorithm.

Furthermore, HEVs can utilize a start-stop functionality to stop and re-start the engine during the driving mission. This functionality enables further fuel consumption reduction by turning off the engine when needed. When the drive power request is beyond the electric machine capacity, the engine is assumed to be re-started immediately and supplies propulsive power to the wheels. Incorporating the start-stop functionality into the synthesis of an optimal control algorithm can be found in published studies, for example see [3, 63, 67, 118, 134]. The PMP method is commonly chosen for the control algorithm to achieve the global optimal solution with fast computation. However, in the mentioned research works, there are two points which have not been addressed fully and sufficiently: i) the gear shift problem is not taken into account; ii) the constant Lagrange multiplier (or the costate or the equivalent factor between the fuel energy cost and the battery energy cost) is assumed to exist which is not always correct. Therefore, the gear shift control problem will be extended to the hybrid powertrain including the start-stop functionality to explore the potential fuel saving. The DP-PMP control algorithm is still applied to achieve the solution at fast computing manner. The followed two-point boundary value problem from PMP will be addressed explicitly in terms of the start-stop functionality (through the engine on-off state variable). Consequently, the design rule for finding the (constant) Lagrange multiplier to satisfy the battery state-of-energy at the terminal time will be achieved.

This chapter is organized as follows. The powertrain modeling and dynamics are given in Section 3.2. The optimal gear shift strategy for the HEV without the start-stop functionality is designed in Section 3.3. Meanwhile the optimal gear shift strategy for the HEV with the start-stop functionality is proposed in Section 3.4. Simulation results and discussions are given in Section 3.5. And finally, conclusions are given in Section 3.6.

3.2 Powertrain Modeling and Dynamics

The hybrid powertrain topology is shown in Figure 3.1. The main parameters of the powertrain components are given in Table 3.1. Aiming at deriving an EMS, the quasi-static models of the powertrain components are used and simulated with a fixed time step of one second. The system dynamics faster than $1Hz$ are ignored [42]. The clutch system is considered as a discrete switch to connect and disconnect the engine immediately to and from the driveline. Its dynamics and limited power losses during a gear shift or an engine start are ignored. Notice of the slippage loss of clutch at vehicle

launch is also not taken into account. However, analysis of the effect of these losses to the control strategy can be found in Chapter 6.

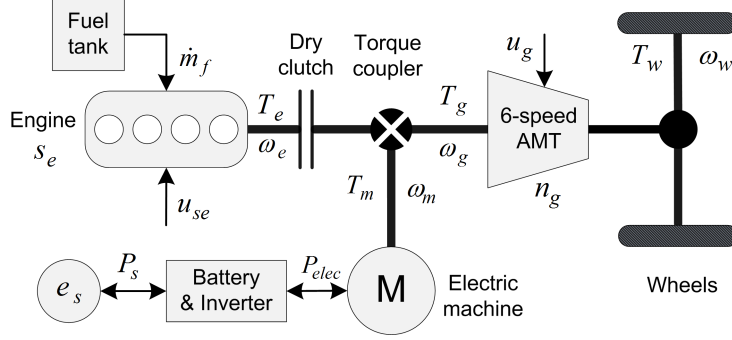


Figure 3.1: A parallel hybrid electric vehicle topology, (AMT: Automated Manual Transmission; M: Electric machine).

Table 3.1: Prototype HEV specifications.

Item	Description/Quantity
Engine	type: diesel, maximum torque of 200Nm, maximum power of 68kW.
Electric machine	maximum torque of 40Nm, maximum power of 6kW.
Battery	Lithium-ion, capacity of 6Ah, 110V.
Transmission	6-speed automated manual transmission, $r_g = [3.817, 2.053, 1.302, 0.959, 0.744, 0.614]$.
Vehicle mass	1320kg.

3.2.1 Powertrain Model

- **Engine:** the engine fuel consumption model used in this study is based on the static fuel rate map as shown in Figure 3.2. For a certain engine speed $\omega_e(k)$, the fuel mass flow $\dot{m}_f(k)$ is approximated as an affine piece-wise second order function of the power as expressed in (3.1),

$$\dot{m}_f(k) \approx a_0(k)P_e^2(k) + a_1(k)P_e(k) + a_2(k). \quad (3.1)$$

in which the coefficients $a_0(k)$, $a_1(k)$ and $a_2(k)$ are functions of the engine speed. If assume during braking, the engine is switched off and decoupled from the drive-

line, then the engine braking is neglected. Therefore, the constraints on the engine speed $\omega_e(k)$ power $P_e(k)$ are as follows,

$$\omega_{e,min} \leq \omega_e(k) \leq \omega_{e,max}, \quad (3.2a)$$

$$0 \leq P_e(k) \leq P_{e,max}(\omega_e(k)). \quad (3.2b)$$

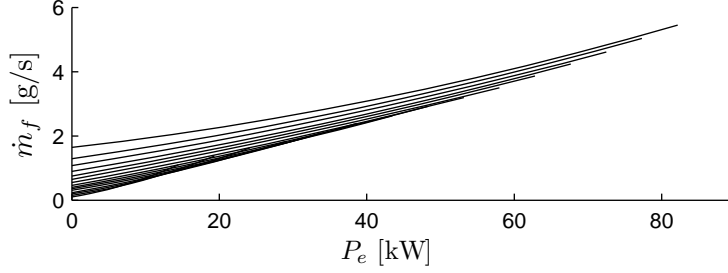


Figure 3.2: Engine fuel consumption model.

- **Electric machine:** the machine efficiency η is assumed to be constant under normal operating state in both normal bidirectional conversion. Therefore, the power flow in motoring and generating modes is expressed as,

$$P_m(k) = \eta P_{elec}(k) \quad \text{in motoring}, \quad (3.3a)$$

$$P_m(k) = \frac{1}{\eta} P_{elec}(k) \quad \text{in generating}. \quad (3.3b)$$

The constraints on the speed $\omega_m(k)$ and power $P_m(k)$ are,

$$0 \leq \omega_m(k) \leq \omega_{m,max}, \quad (3.4a)$$

$$P_{m,min}(\omega_m(k)) \leq P_m(k) \leq P_{m,max}(\omega_m(k)). \quad (3.4b)$$

- **Battery system:** in this study, the battery energy capacity is chosen properly such that its state of energy never exceeds its bounds for increasing lifetime and reliable operation. This means that $e_s(k)$ is assumed to be in a nominal range $[E_{s,min}, E_{s,max}]$. In addition, the battery operating temperature is assumed to be constant under tight control. Therefore, a center battery energy flow depicted in Figure 3.3 is chosen to model the nominal battery efficiency. The battery electrical power $P_{elec}(k)$ is approximated as a quadratic function of the battery chemical power $P_s(k)$,

$$P_{elec}(k) \approx b_0 P_s^2(k) + b_1 P_s(k) + b_2. \quad (3.5)$$

The constraints imposing on the battery system,

$$P_{s,min} \leq P_s(k) \leq P_{s,max}. \quad (3.6)$$

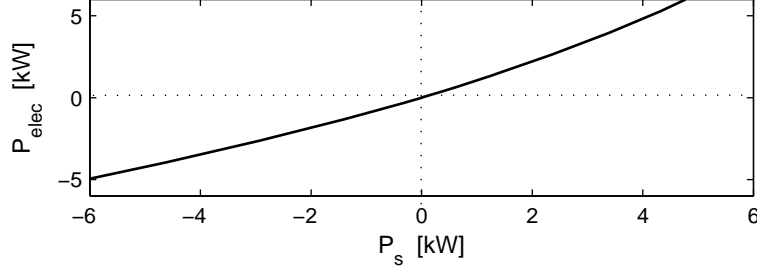


Figure 3.3: Battery efficiency model.

- **Automated Manual Transmission (AMT):** the transmission efficiency η is assumed to be constant for all gears, the speed and torque relations in both side of transmission when the clutch closed are,

$$\omega_e(k) = \omega_g(k) = \omega_w(k)r_g(k), \quad (3.7a)$$

$$T_w(k) = \eta r_g(k) T_g(k) = \eta r_g(k) T_e(k). \quad (3.7b)$$

wherein: $\omega_w(k)$ is the wheel rotational speed; $T_w(k)$ is the drive torque at the wheels; $T_g(k)$ is the transmission input torque; $r_g(k)$ denotes the gear ratio. The final reduction gear ratio is merged into the transmission ratio for a simplification.

The constraints on the gear position of the 6-speed transmission are,

$$1 \leq n_g(k) \leq 6. \quad (3.8)$$

- **Power flow model:** the power flow equilibrium at the transmission input of the powertrain is expressed as,

$$P_e(k) = P_g(k) + P_m(k). \quad (3.9)$$

3.2.2 Powertrain System Dynamics

The powertrain system consists of the continuous battery state-of-energy $e_s(k)$, and the discrete gear position $n_g(k)$. Their dynamics are governed by the two corresponding control variables $P_s(k)$ and $u_g(k)$ as,

$$e_s(k+1) = e_s(k) + P_s(k)\Delta t, \quad (3.10)$$

$$n_g(k+1) = n_g(k) + u_g(k). \quad (3.11)$$

Apparently, due to co-existence of the continuous and discrete variables, the powertrain system is a hybrid dynamical system as well.

Vehicle longitudinal dynamics: the longitudinal motion of the vehicle in discrete time domain is given by,

$$\omega_w(k+1) = \omega_w(k) + \frac{1}{J_{v,eq}}(T_w(k) - F_{load}(k)R_w)\Delta t, \quad (3.12)$$

where F_{load} is the resistance loads due to rolling and aerodynamic resistances; $J_{v,eq}$ is an equivalent vehicle inertia at the wheel,

$$J_{v,eq} = ((J_e + J_c + J_p)r_g^2 + J_s)r_d^2 + m_v R_w^2,$$

$$F_{load} = c_r m_v g \cos \alpha + m_v g \sin \alpha + \frac{1}{2} \rho_a A_f c_d v^2,$$

and m_v is the vehicle weight; R_w is the wheel radius; J_e is the engine inertia; J_c is the clutch inertia; J_p is the transmission primary inertia; J_s is the transmission secondary inertia; ρ_a is the air density; A_f is the frontal area of vehicle; c_d is the aerodynamic drag coefficient; c_r is the rolling friction coefficient; g is the gravity coefficient; v is the vehicle speed; α is the slope of the road.

3.3 Optimal Gear Shift Strategy without Start-Stop Functionality

Initially, the start-stop functionality is assumed to be not available. The operating points of the hybrid powertrain are governed by the power split between the engine and electric machine, and the gear position. The power split is alternatively controlled by the continuous engine power which varies in the boundary interval determined by (3.2b), (3.4b), (3.6) and (3.9). Detail of the power split control is given in Section 3.3.2. The gear position is controlled by the discrete gear shift command through the gear shift dynamics expressed by (3.11). The discrete gear shift command $u_g(k)$ belongs to the set $\{u_{g,min}, \dots, -1, 0, 1, \dots, u_{g,max}\}$. Under the constraints (3.11) and (3.8), for a 6-speed AMT, $[u_{g,min}, u_{g,max}] = [-5, 5]$.

From a control point of view, the bounds $u_{g,min}$ and $u_{g,max}$ have effect on the optimality. However, defining the optimum bounds for the gear shift command $u_g(k)$ is out of the scope of this study. For reasons of an acceptable driveability, the gear shift command is chosen as,

$$u_g(k) = \begin{cases} -1, & \text{downshift,} \\ 0, & \text{sustaining,} \\ 1, & \text{upshift,} \end{cases} \quad (3.13)$$

to avoid a large variation of the engine speed under a certain shift at a certain time step k . One gear upshift ($u_g(k) = 1$) or downshift ($u_g(k) = -1$) for each time step of one second is reasonable, because the average shift time for an AMT is typically less than one second.

Note that the gear shift event will lead to a change of the engine torque due to a changed engine speed, which may cost additional fuel affecting the optimal control solution. In

this study, this phenomenon is ignored as well. This effect will be investigated in Chapter 6.

The optimization problem is formulated as follows.

Problem 3.1. *Given a priori drive cycle $v(k)$ with a time length of N , implying that the vehicle longitudinal dynamics (3.12) is deterministic, find an optimal control law $u^*(k) = [P_s^*(k), u_g^*(k)]$, that minimize the cost function of fuel consumption over the entire drive cycle, defined as,*

$$\mathbf{J} = \sum_{k=0}^{N-1} \dot{m}_f(P_e(k), \omega_e(k), k) \Delta t, \quad (3.14)$$

subject to the constraints (3.12) - (3.9) and

$$e_s(N) = e_s(0), \quad (3.15)$$

$$n_g(N) = n_g(0). \quad (3.16)$$

In the next section, two optimization solvers for Problem 3.1 will be presented. The first one is based on DP. The second one is based on a combination of DP and PMP.

3.3.1 Dynamic Programming

DP [11, 14] is well known as a powerful numerical method on optimal state feedback control to solve a non-linear, non-convex optimization problem with constraints while obtaining a globally optimal time-variant solution. To apply DP to Problem 3.1, we need,

- to grid the state variables $x(k) = [e_s(k), n_g(k)]$;
- to grid the corresponding control variables $u(k) = [P_s(k), u_g(k)]$;
- to calculate the instantaneous cost $\dot{m}_f(P_e(k), \omega_e(k), k) \Delta t$ for the whole drive cycle;

The states $x(k) \in X(k)$, the control inputs $u(k) \in U(k)$ are discrete variables both in time (index k) and value. Exactly, the subset $U(k)$ depends on the states $x(k)$, i.e. $u(k) \in U(x(k))$. Then, the optimal cost-to-go function is defined backwards as the following steps.

Step $k = N$:

$$\mathcal{J}_N^* = 0; \quad (3.17)$$

Step $k, 0 \leq k < N$:

$$\mathcal{J}_k^*(x(k)) = \min_{u(k) \in U(x(k))} \left[m_f(P_e(k), \omega_e(k), k) \Delta t + \mathcal{J}_{k+1}^*(x(k+1)) \right]; \quad (3.18)$$

Solving the above procedure backward until $k = 0$, the optimal solution $u^*(k)$ is obtained correspondingly with a specific end constraint on $x(N)$.

3.3.2 Dynamic Programming-Pontryagin's Minimum Principle

It is noticed that solving Problem 3.1 by discretizing the continuous variables, $s_e(k)$ and $P_s(k)$, and using deterministic DP can lead to a computational burden due to the 'curse of dimensionality'. Applying optimal control theory (PMP method) to Problem 3.1 is possible if a continuously variable ratio model for the AMT can be obtained, such that the cost function is differentiable with respect to the transmission ratio. Then, the continuous optimal solution will be derived in a fast computational manner. However, rounding off the continuous optimal ratio to the corresponding gear ratio for the AMT will definitely lead to a sub-optimality. Furthermore, respecting the constraints on the ratio variation speed is another factor affecting the rounded-off solution. Apparently, the tradeoff between optimality, accuracy and the computational efficiency is seen as one of the main challenges for the design of a gear shift control algorithm for HEVs.

Respecting the discrete nature of ratio of the AMT, and taking into account the advantages of the DP and PMP, a control algorithm based on a combination of DP and PMP is proposed for the gear shift problem of HEVs. The globally optimal solutions of $P_s^*(k)$ (or $P_e^*(k)$ alternatively) and $u_g^*(k)$ are obtained and the computational time is significantly reduced. The control method consists of: deriving the optimal engine power based on the PMP in the inner loop, meanwhile the gear position dynamics, under the mixed-constraints (3.8) and (3.13) is optimally controlled by using DP in the outer loop. The structure of the DP-PMP control algorithm is illustrated in Figure 3.4. The optimal control problem is formulated and solved in the form of a power flow based model for consistency. This algorithm is presented next.

PMP for an optimal power split

Assume at a certain time step k , given the vehicle speed $v(k)$, the required power $P_w(k)$ at the wheels is computed from (3.12). With a given admissible gear position $n_g(k)$, assume that the constraints on engine speed and electric machine speed, (3.2a) and (3.4a), are satisfied and $P_w(k)$ can be produced by the powertrain, i.e., by both the engine and electric machine. The lower and upper bounds of the electric machine power and battery power can be incorporated with the bounds of engine power to create the

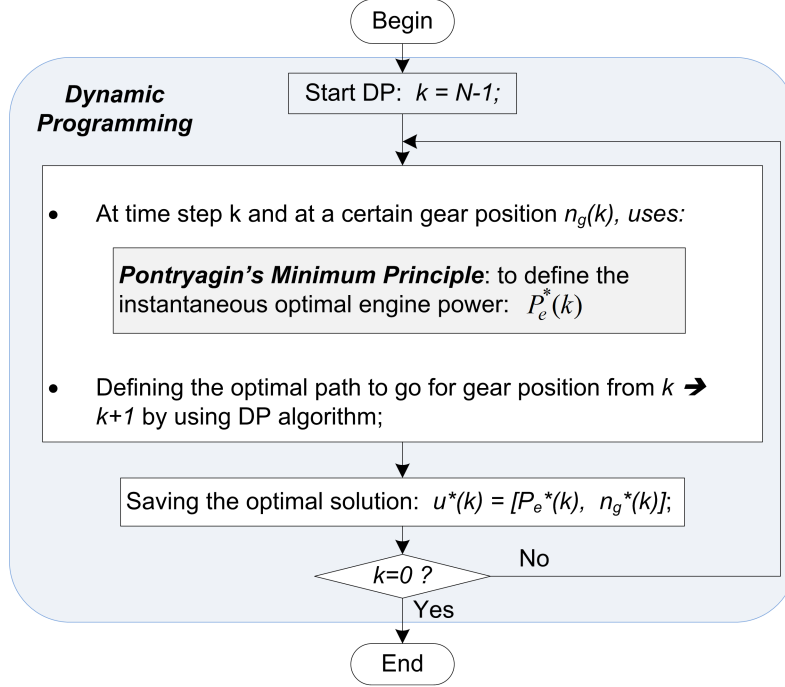


Figure 3.4: The DP-PMP control algorithm.

new bounds for the control variable $P_e(k)$,

$$P'_{e,min}(k) \leq P_e(k) \leq P'_{e,max}(k). \quad (3.19)$$

The new lower bound and upper bound of the engine power are defined as follows,

$$P'_{e,min}(k) = \max\{0; P_g(k) + P_{EM,min}(k)\}, \quad (3.20)$$

$$P'_{e,max}(k) = \min\{P_{e,max}(k); P_g(k) + P_{EM,max}(k)\}, \quad (3.21)$$

wherein:

$$P_{EM,min}(k) = \max\{P_{m,min}(k); \eta(b_0 P_{s,min}^2 + b_1 P_{s,min} + b_2)\}, \quad (3.22)$$

$$P_{EM,max}(k) = \min\{\eta P_{m,max}(k); (b_0 P_{s,max}^2 + b_1 P_{s,max} + b_2)\}. \quad (3.23)$$

For compact notation, let us denote the engine fuel rate $\mathcal{F}_r(P_e(k), k) := \dot{m}_f(P_e(k), \omega_e(k), k)$ and the chemical battery power $\mathcal{P}_s(P_e(k), k) := P_s(k)$ as functions of the engine power.

The optimal control problem is reformulated as follows.

Problem 3.2. *Given a prior drive cycle with a time length N , with a given admissible gear sequence $n_g(k)$ along the drive cycle, find an optimal engine power $P_e^*(k)$ that minimizes the cost function \mathbf{J}_1 of fuel consumption over the entire drive cycle, defined*

as,

$$\mathbf{J}_1 = \sum_{k=0}^{N-1} \mathcal{F}_r(P_e(k), k) \Delta t, \quad (3.24)$$

subject to constraints:

$$\begin{aligned} e_s(k+1) &= e_s(k) + \mathcal{P}_s(P_e(k), k) \Delta t, \\ P'_{e,min}(k) &\leq P_e(k) \leq P'_{e,max}(k). \end{aligned}$$

In this study, the upper and lower bounds of state variable $e_s(k)$ are ignored by assuming that the battery capacity is chosen properly such that it never exceeds its bounds. The Lagrange multiplier is used to take into account the dynamics of battery. This leads to the Hamiltonian function (3.25) at each time step needs to be minimized, see Appendix A for the proof.

$$\mathbf{H}(P_e(k), \lambda_{opt}, k) = \left[\mathcal{F}_r(P_e(k), k) + \lambda_{opt} \mathcal{P}_s(P_e(k), k) \right] \Delta t. \quad (3.25)$$

From the model approximations of engine fuel rate and battery efficiency model, $\mathcal{F}_r(P_e(k), k)$ and $\mathcal{P}_s(P_e(k), k)$ can be approximated as affine piecewise second-order functions of engine power at a certain engine speed. Therefore, if the constant optimal Lagrange multiplier λ_{opt} is known, the globally instantaneous optimal engine power $P_e^*(k)$ can be obtained analytically. Therefore, the globally instantaneous equivalent optimal cost value is defined correspondingly by

$$\mathbf{C}_{eq}(k) = \left[\mathcal{F}_r(P_e^*(k), k) + \lambda_{opt} \mathcal{P}_s(P_e^*(k), k) \right]. \quad (3.26)$$

However, it should be noticed that for the gear shift control problem with constraints on the battery state-of-energy $e_s(k)$, a derivation of the optimal solution can be found in Appendix B. It is observed that when the battery state-of-energy reaches its bounds, then the Lagrange multiplier changes its value. Between the two consecutive points of reaching the bounds of the state of energy, the Lagrange multiplier is kept constant.

DP for an optimal gear shift strategy

The PMP proposed in Section 3.3.2 solves only the globally optimal power split along a drive cycle with any certain gear shift sequence by choosing a proper Lagrange multiplier λ_{opt} , satisfying the constraint (3.15) on the battery energy at the terminal time. This means that the optimal solution of the power split is independent with the gear position if λ_{opt} is known in advance. Therefore the gear shift sequence can be optimized along the drive cycle to further improve the fuel economy. Due to the characteristic of discrete ratio of the AMT, a DP-based control algorithm applied to define the optimal gear shift strategy is presented as follows.

Problem 3.3. Given a drive cycle with a time length N , at a certain time step k with the vehicle speed $v(k)$ and a certain gear position $n_g(k)$; suppose that the instantaneous optimal engine power $P_e^*(k)$ and the instantaneous equivalent optimal cost value $C_{eq}(k)$ are obtained by solving Problem 3.2; the control problem is to find an optimal gear shift command $u_g^*(k)$ resulting in a next optimal gear position $n_g^*(k+1)$ that minimizes the cost function \mathbf{J}_2 described by,

$$\mathbf{J}_2 = \sum_{k=0}^{N-1} C_{eq}(k) = \sum_{k=0}^{N-1} \left[\mathcal{F}_r(P_e^*(k), k) + \lambda_{opt} \mathcal{P}_s(P_e^*(k), k) \right] \Delta t, \quad (3.27)$$

subject to constraints (3.11), (3.8), (3.13) and (3.16).

The DP algorithm is implemented in the same manner as presented in Section 3.3.1. The state and control variables are the gear position $n_g(k)$ and gear shift command $u_g(k)$, respectively. The instantaneous optimal cost value $C_{eq}(k)$ is calculated for the whole drive cycle. Then, the optimal cost-to-go function is defined backwards as the following steps.

Step $k = N$:

$$\mathcal{J}_{2,N}^* = 0; \quad (3.28)$$

Step k , $0 \leq k < N$:

$$\mathcal{J}_{2,k}^*(n_g(k)) = \min_{u_g(k)} \left[C_{eq}(k) + \mathcal{J}_{2,k+1}^*(n_g(k+1)) \right]; \quad (3.29)$$

Solving the above procedure backwards until $k = 0$, the optimal solution $u_g^*(k)$ is obtained correspondingly with a predefined end constraint on $n_g(N)$.

The end constraint on battery state-of-energy

The end constraint (3.15) on the battery energy should be respected when finishing the drive cycle to ensure a fair comparison of fuel economy. This leads to a choice of λ_{opt} resulted from the two-point boundary value problem of the optimal control problem. Hereinafter, the normalized battery state-of-energy, denoted as $SOE(k)$

$$SOE(k) = e_s(k) / E_{s,cap},$$

is chosen to represent the current battery state-of-energy relative to the battery energy capacity $E_{s,cap}$. A sensitivity study of the normalized battery state-of-energy at the terminal time $SOE(N)$ with respect to the Lagrange multiplier λ over the drive cycle NEDC (see Appendix C) is shown in Figure 3.5. $SOE(0) = 0.5$ is chosen for this study.

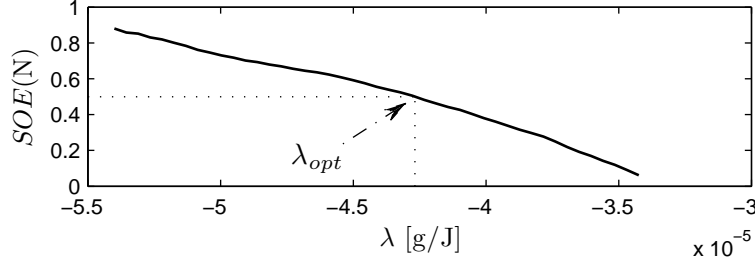


Figure 3.5: $SOE(N)$ vs. λ of the HEV without start-stop functionality.

We can see that $SOE(N)$ monotonously decreases with λ . At $\lambda > \lambda_{opt}$, the powertrain tends to use more electrical power that leads to a battery discharge. Vice versa, at $\lambda < \lambda_{opt}$, the vehicle tends to generate electrical power that leads to a battery charge.

Therefore a search method (bisection search method) is utilized in this study to find the optimal Lagrange multiplier λ_{opt} to satisfy the end constraint (3.15) at $SOE(N) = 0.5$. The search condition is stopped at $|\Delta SOE| = |SOE(N) - SOE(0)| < \xi$ with ξ is a predefined positive small number.

3.4 Optimal Gear Shift Strategy with Start-Stop Functionality

One of the advantages of HEVs is the availability of the start-stop functionality to further reduce the fuel consumption by shutting down the engine whenever feasible. The start-stop functionality describes the engine on-off state by a state variable $s_e(k)$,

$$s_e(k) = \begin{cases} 1, & \text{engine on,} \\ 0, & \text{engine off.} \end{cases} \quad (3.30)$$

with the state dynamics and the constraints on the control variable are correspondingly given by,

$$s_e(k+1) = s_e(k) + u_{se}(k), \quad (3.31)$$

$$u_{se}(k) = \begin{cases} [0, 1] & \text{if } s_e(k) = 0, \\ [-1, 0] & \text{if } s_e(k) = 1. \end{cases} \quad (3.32)$$

When the engine is on, the fuel rate at a certain engine speed is defined by (3.1) and the engine power is larger than zero. When engine is off, the fuel rate is zero and the engine power is zero. Therefore the fuel rate model of the engine at a certain engine speed $\omega_e(k)$ is expressed as

$$\dot{m}_f(P_e(k), k) = \begin{cases} a_0 P_e^2(k) + a_1 P_e(k) + a_2, & \text{if } s_e(k) = 1, \\ 0, & \text{if } s_e(k) = 0, \end{cases} \quad (3.33)$$

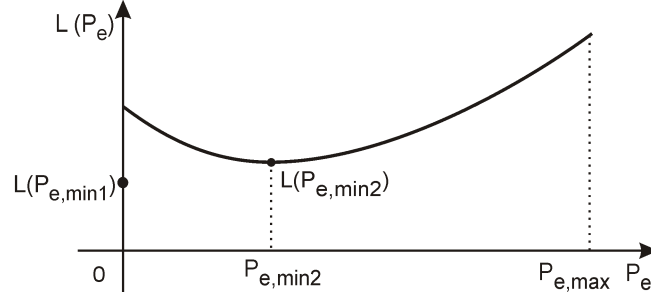


Figure 3.6: Cost functional $L(P_e)$

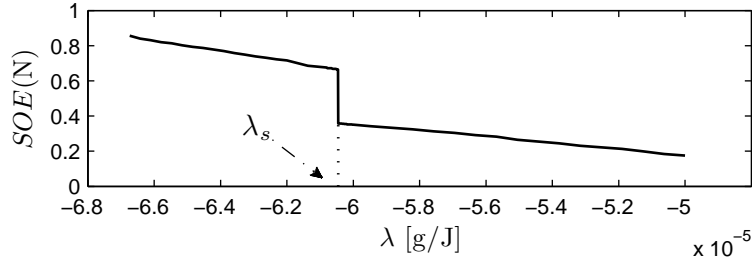


Figure 3.7: $SOE(N)$ vs. λ of the HEV with start-stop functionality.

or equivalently

$$\dot{m}_f(P_e(k), k) = \begin{cases} a_0 P_e^2(k) + a_1 P_e(k) + a_2, & \text{if } 0 < P_e(k) \leq P_{e,max}(k), \\ 0, & \text{if } P_e(k) = 0, \end{cases} \quad (3.34)$$

which clearly shows that there is a discontinuous point of fuel rate model at $P_e(k) = 0$.

3.4.1 Dynamic Programming

Designing the EMS to optimize the gear shift command for the HEV with the start-stop functionality can be done by using the DP method despite the fact that intensively computational demand is required due to the presence of one more state variable $s_e(k)$. The dynamic system consists of three state variables, $x(k) = [s_e(k), e_s(k), n_g(k)]$, and three corresponding control variables $u(k) = [u_{se}(k), P_s(k), u_g(k)]$. The same procedure as in Section 3.3.1 is used to implement the DP-based control algorithm in simulation.

3.4.2 Dynamic Programming-Pontryagin's Minimum Principle

The computational burden due to the curse of dimensionality of DP can be reduced significantly by using the DP-PMP control algorithm as presented in Section 3.3.2. Utilizing the PMP method in designing the EMS is followed by solving the two-point

boundary value problem to find an initial value of the Lagrange multiplier such that the end constraint of the battery state of energy is respected. This issue is analyzed next.

At a certain time step k , assuming that the power demand from the wheels is P_w , then the admissible range of engine power can be defined as $0 \leq P_e \leq P_{e,max}$ by using (3.20)-(3.21). Let $L(P_e)$ denote the augmented Lagrange cost functional as

$$L(P_e) = \begin{cases} \mathcal{F}_r(P_e) + \lambda \mathcal{P}_s(P_e) & \text{if } 0 < P_e \leq P_{e,max}, \\ \lambda \mathcal{P}_s(P_e) & \text{if } P_e = 0, \end{cases} \quad (3.35)$$

which is discontinuous at $P_e = 0$ due to the characteristic of fuel rate model as described by (3.34). Apparently, $L(P_e)$ is non-differentiable at $P_e = 0$. However, the PMP method is still applicable to define the global optimal solution regardless the discontinuity of the cost functional. Figure 3.6 gives a demonstration for the augmented cost functional $L(P_e)$ at a certain λ . There are two local minima for the cost functional $L(P_e)$: one is at $P_{e,min1} = 0$ and the other is assumed at $P_{e,min2} \in (0, P_{e,max}]$. The minimum one is chosen by comparing the $L(P_{e,min1})$ and $L(P_{e,min2})$. It can be either at $P_{e,min1} = 0$ or at $P_{e,min2}$ such that the augmented Lagrange cost functional is global minimum.

Due to the discontinuous characteristic, the optimal solution depends on the value of Lagrange multiplier λ . There exists a switching point of Lagrange multiplier denoted as λ_s whereby $L(P_{e,min1}) = L(P_{e,min2})$ occurs. In other words, such a λ_s does not exist with respect to the optimal solution. Therefore, for a variation of λ around the point λ_s , there is a jump in optimal solution of P_e by an amount of $P_{e,min2} - P_{e,min1}$, thus $P_{e,min2} \delta$. As a result, the same consequence holds for the optimal solution of the battery power P_s which yields a jump in the normalized battery energy SOE .

Figure 3.7 shows the sensitivity of the normalized battery state-of-energy at the terminal time $SOE(N)$ with respect to the λ over the NEDC. The $SOE(N)$ is discontinuous at λ_s . Therefore, a constant optimal Lagrange multiplier λ_{opt} does not exist if the end constraint on the normalized battery state-of-energy $SOE(N) = 0.5$ is required at the terminal time.

The DP-PMP control algorithm is used in the same manner as described in Section 3.3.2 for the gear shift control problem. The PMP is used in the inner loop to define the instantaneous optimal power split. The DP is used in the outer loop to define the optimal gear position and the engine on-off state from the beginning until the end of the drive cycle. Due to the non-existence of a constant Lagrange multiplier, to respect the end constraint on battery state-of-energy (3.15), the costate $\lambda(k)$ is controlled by using an integral regulator (I controller) as in (3.36). This leads to the fact that the obtained solution is not globally optimal.

$$\lambda(k+1) = \lambda(k) + K_I(e_s(k) - e_s(0)). \quad (3.36)$$

3.5 Simulation Results and Discussions

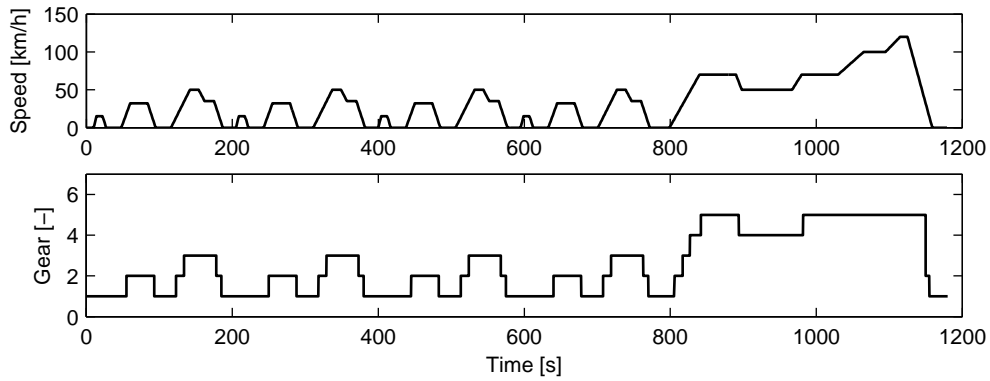


Figure 3.8: NEDC cycle (top) and a prescribed gear shift schedule (bottom).

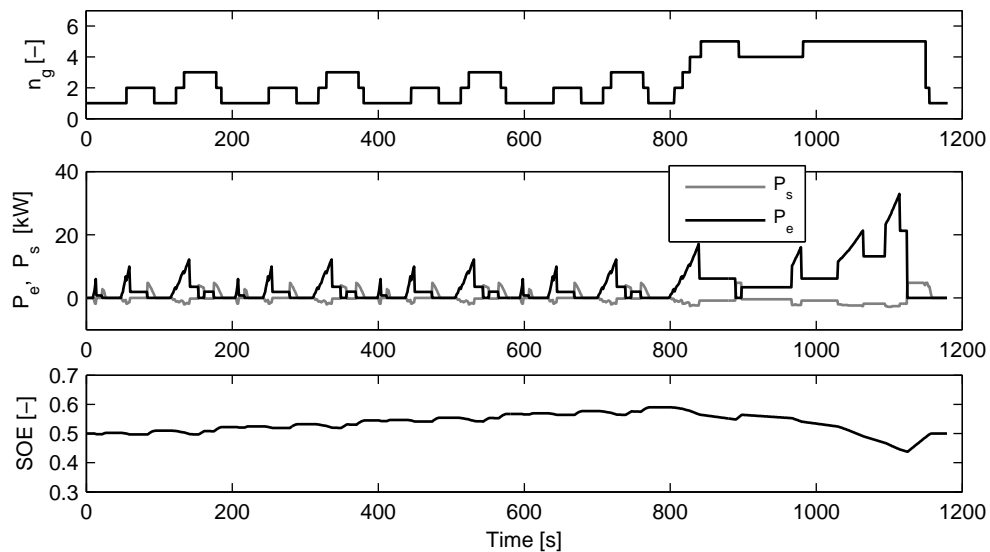


Figure 3.9: Test 1: DP algorithm for only the power split optimization.

3.5.1 Baseline Vehicles

The drive cycle NEDC is chosen for simulation, see Figure 3.8. This drive cycle is a standardized emission test cycle in Europe. There is a prescribed gear shift schedule accompanied along with this cycle to signal the gear shift for vehicles with manual transmission [42].

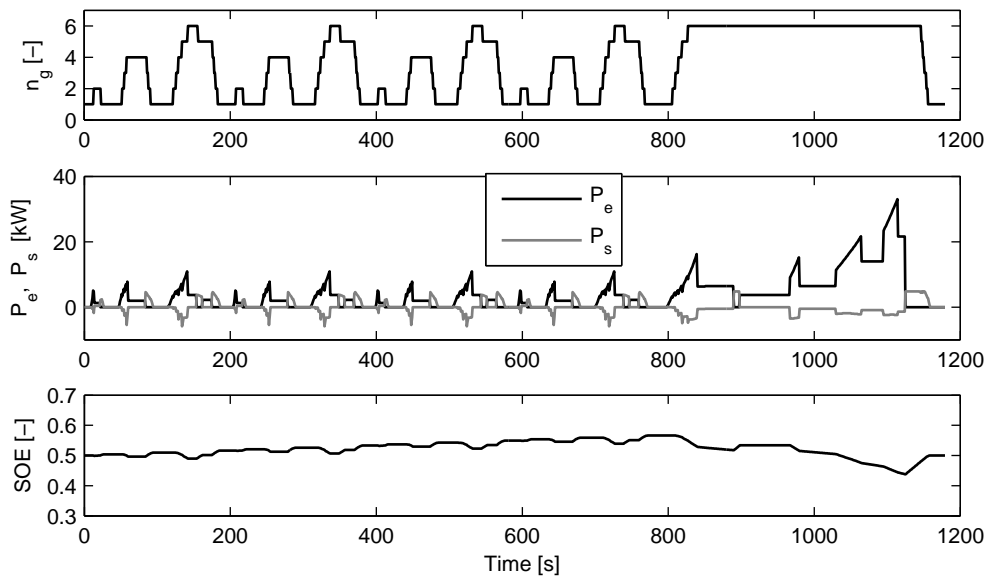


Figure 3.10: Test 2: DP algorithm for the power split and gear shift optimization.

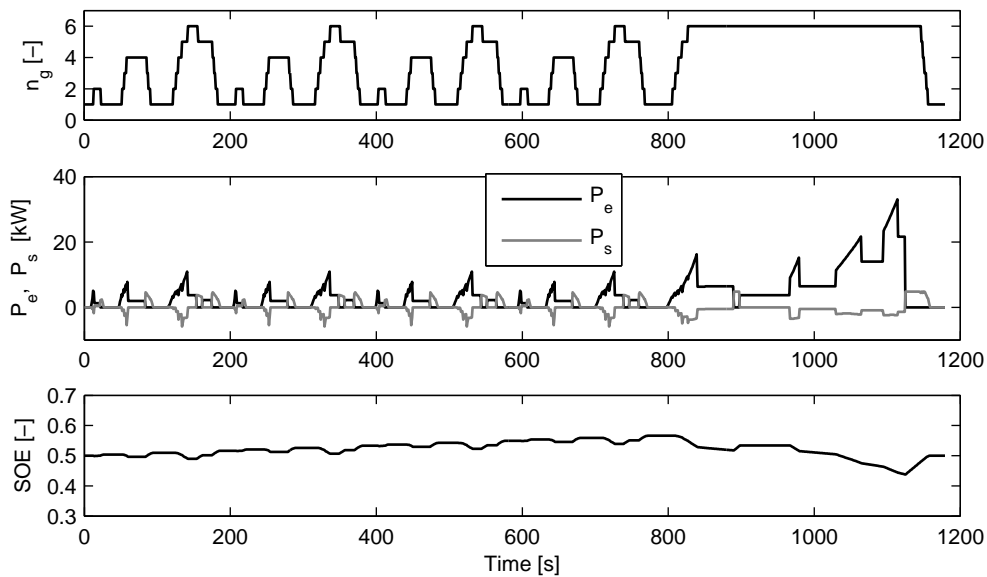


Figure 3.11: Test 3: DP-PMP algorithm for the power split and gear shift optimization.

One of the purposes of this study is to evaluate the contribution of the gear shift strategy to a fuel economy improvement of HEVs. Therefore, two baseline vehicles are defined: 1) a baseline-conventional vehicle with the same parameters of the hybrid vehicle except for the secondary power source; 2) a baseline-HEV is simulated whereby the EMS is designed by DP to optimize only the power split. The prescribed gear shift schedule

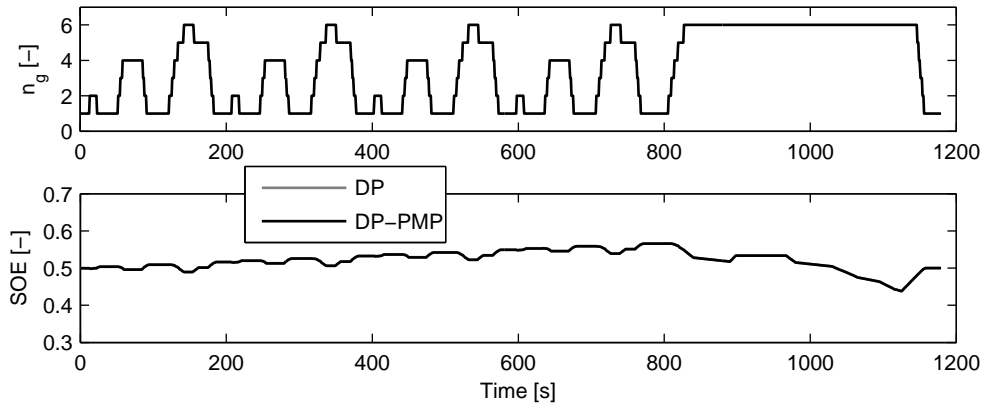


Figure 3.12: Comparison of Tests 2 and 3.

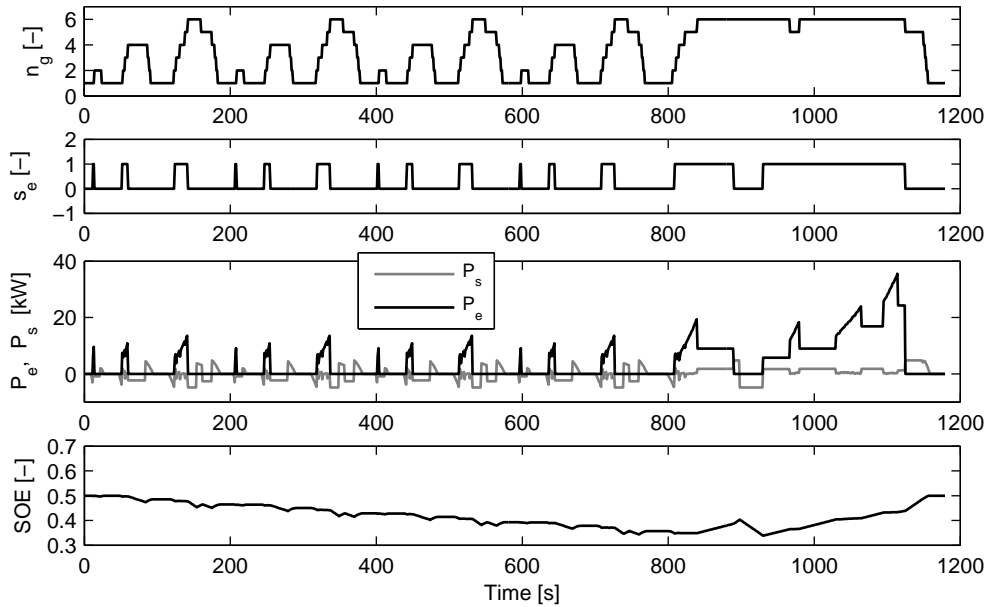


Figure 3.13: Test 4: DP algorithm for the power split, gear shift and start-stop functionality optimization.

(accompanied along with drive cycle) is used to shift gears in both baseline vehicles. The start-stop functionality is assumed to be not available for the baseline-HEV. This is only theoretical because the start-stop functionality is always available in HEVs. Simulation results of the baseline-HEV are shown in Figure 3.9. The battery state-of-energy at the end of drive cycle satisfies its end constraint. The fuel economy improvement is of 12.2% compared to the baseline-conventional vehicle, see Table 3.2.

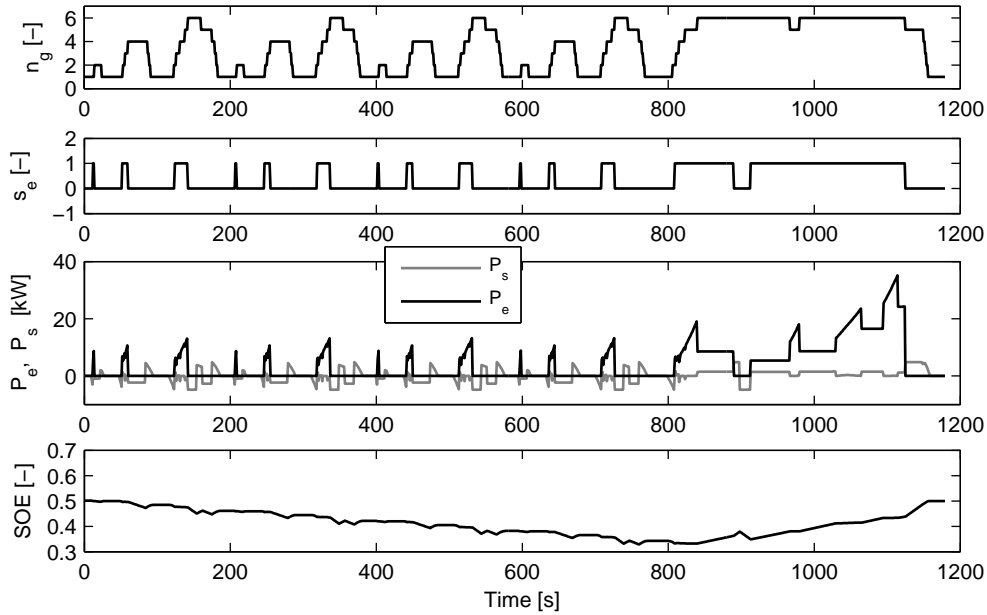


Figure 3.14: Test 5: DP-PMP algorithm for the power split, gear shift and start-stop functionality optimization.

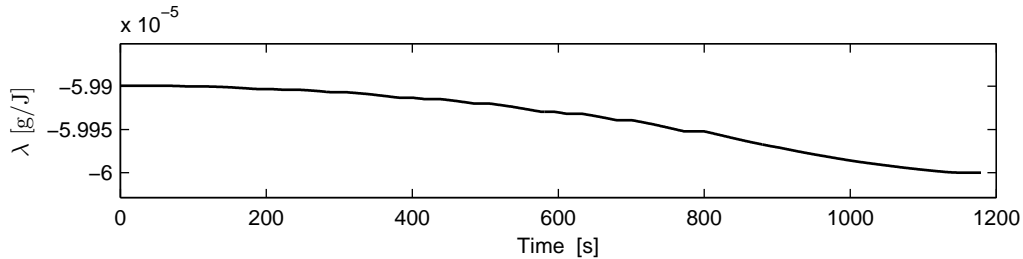


Figure 3.15: $\lambda(k)$ of the DP-PMP algorithm for Test 5.

3.5.2 HEV without the Start-Stop Functionality

Simulation results of two algorithms, the DP and DP-PMP, are illustrated in Figures 3.10 and 3.11, respectively. The gear shift patterns of both approaches are totally different from the prescribed gear shift schedule. The proposed control algorithms allow the vehicle to shift to higher gear and earlier which contribute to fuel economy improvement. Figure 3.12 shows a comparison of the gear position and the battery state-of-energy of both approaches. The obtained optimal solutions are almost the same. The state of energy in both cases satisfies the end constraint to ensure the fair comparisons of fuel economy.

From Table 3.2, we see that fuel economy for both approaches are improved up to 30% relatively to the case of the baseline conventional vehicle. By optimally shifting the gear, potential fuel savings can be obtained up to 20.3% compared to the case of baseline-HEV. There is a small difference in the fuel economy between these two methods. This

is due to the numerical errors of gridding the control variables in the DP algorithm. Meanwhile, the DP-PMP algorithm improves the computation efficiency significantly by a factor of 171 compared with the DP algorithm.

It appears that an optimal gear shift strategy for the hybrid vehicle can improve the fuel economy substantially, up to 20.3% and 30% compared to the baseline-HEV and baseline conventional vehicle, respectively. The optimal gear shift strategy owns its fuel efficiency to: i) much motor assist during acceleration, and ii) lowering the engine speed during constant speed phase. Furthermore, it should be emphasized that the baseline gear shift strategy (the prescribed gear shift schedule) is less efficient due to its late-upshift strategy. During acceleration or cruising (constant speed), the optimal gear shift strategy triggers the upshift to occur earlier, more frequent and to higher values, which will allow the engine to operate at low speed region for more fuel efficient. Another issue contributing to the significant values of fuel economy improvement is a chosen minimum engine speed. In this study, the minimum engine speed is set at 800[rpm] to provide theoretical value of fuel saving.

In real-life driving, the minimum engine speed for passenger cars during driving can be somewhere between 800[rpm]-1200[rpm], which will result in a less fuel saving compared to the obtained theoretical value. For example, in previous experimental research work for an AMT conventional vehicle [99], it showed that 11.2% fuel economy improvement on the ECE cycle (urban part of NEDC) can be realized by using an optimized shifting strategy. The 11.2% fuel economy improvement is compared with the baseline gear shift strategy (the prescribed gear shift schedule).

Table 3.2: Comparison of simulation results on NEDC.

Test	Algorithms	Fuel [g]	Improvement [%]		Time [s] ²
0	Baseline-conventional vehicle	468.7	-		1
1	Baseline-HEV: optimizing only the power split by DP algorithm	411.7	12.2	-	460
2	HEV: optimizing the power split and gear shift by DP algorithm	328.0	30.0	20.3	1540
3	HEV: optimizing the power split and gear shift by DP-PMP algorithm	328.1	30.0	20.3	9
4	HEV: optimizing the power split, gear shift and start-stop functionality by DP algorithm	300.2	35.9	27.1	3964
5	HEV: optimizing the power split, gear shift and start-stop functionality by DP-PMP algorithm	301.3	35.7	26.8	9

3.5.3 HEV with the Start-Stop Functionality

Figure 3.13 depicts simulation results of the HEV with start-stop functionality when using the DP algorithm. The start-stop signal indicates the engine is allowed to turn off during the drive cycle to save fuel. By optimizing further the gear shift, the fuel economy can be improved: up to 35.9% relative to the baseline conventional vehicle, up to 27.1% relative to the baseline hybrid vehicle. The battery state-of-energy is different with that of the hybrid powertrain without start-stop functionality.

Simulation results of the DP-PMP algorithm are shown in Figure 3.14. Despite the fact of suboptimal method, it still yields the very close results to the case of DP algorithm. Fuel economy can improved up to 35.7%. However, computational efficiency is reduced drastically by the factor of 440 which brings realtime implementation of this control method into a realistic viewpoint.

The Lagrange multiplier $\lambda(k)$ regulated by a state-feedback controller is depicted in Figure 3.15. It is observed that when the $SOE(k)$ tends to deplete from the nominal value (the initial value), the I controller will be more active to decrease the Lagrange multiplier to enhance charging the battery, which finally results in meeting the battery end constraint.

Table 3.3: Comparison of simulation results on FTP75

Test	Algorithms	Fuel [g]	Improvement [%]		Time [s]
0	Baseline-conventional vehicle	836.5	-		2
1	Baseline-HEV: optimizing only the power split by DP algorithm	745.4	10.9	-	757
2	HEV: optimizing the power split and gear shift by DP algorithm	509.8	39.1	31.6	3595
3	HEV: optimizing the power split and gear shift by DP-PMP algorithm	509.6	39.1	31.6	12
4	HEV: optimizing the power split, gear shift and start-stop functionality by DP algorithm	472.6	43.5	36.6	4799
5	HEV: optimizing the power split, gear shift and start-stop functionality by DP-PMP algorithm	474.3	43.3	36.4	12

²HP EliteBook 8530w, Core 2 Duo, CPU T9600 @ 2.8GHz, RAM 4.0GB

3.5.4 Simulation Results on FTP75

FTP75, representing a more realistic drive cycle, is also chosen for testing on simulation platform. The results are shown in Table 3.3. It can be seen from Tests 2 and 4 that, by optimally shifting gears, potential fuel savings can be achieved up to 31.6% and 36.6% (compared with the baseline HEV) for the HEV without and with the start-stop functionality, respectively. From Tests 3 and 5, it also shows that the DP-PMP algorithm improves the same fuel economy with the DP algorithm. Meanwhile the DP-PMP algorithm reduces computational burden significantly by the factors of 300 and 415 compared with the DP algorithm for the HEV without and with the start-stop functionality, respectively.

3.6 Conclusions

This chapter presented a control algorithm based on a combination of DP and PMP for HEVs to further optimize the gear shift command. The proposed control algorithm reduces the computation time significantly compared with the DP algorithm. It shows that by further optimally controlling the gear shift command, the potential fuel saving can be increased significantly.

Applying the DP-PMP control algorithm for the HEV was addressed explicitly in terms of the start-stop functionality. For the hybrid powertrain without the start-stop functionality, it is found that a unique constant Lagrange multiplier exists such that the end constraint of the battery state-of-energy is respected, and the globally optimal solution is guaranteed. For the hybrid powertrain with the start-stop functionality, the constant Lagrange multiplier for the optimal control problem does not always exist. Therefore, the obtained results of the proposed control algorithm are suboptimal, despite the fact that they are very close to the globally optimal results obtained from the DP algorithm.

The DP-PMP control algorithm is considered as a novel control algorithm for the optimal gear shift problem of HEVs. From an engineering point of view, the DP-PMP algorithm can be considered as a globally optimal method applied for HEVs. The algorithm is executed fast enough such that it can be seen as a potential candidate applied in a realtime implementable control algorithm, such as a model predictive control.

Gear Shift Map Design Methodology¹

Abstract - In this chapter, a design methodology is developed to build the gear shift map for automotive transmissions used in conventional and hybrid electric vehicles. The methodology utilizes an optimal gear shift strategy to derive the optimal gear shift patterns over a wide range of driving profiles. Then, statistical theory is applied to analyze the obtained gear shift patterns towards a gear shift map. The designed gear shift map improves the fuel economy and driveability. It is consistent, robust to shift busyness, and realtime implementable. The design process is flexible and time-efficient such that an applicability to various powertrain systems configured with discrete ratio transmissions is possible. Validation on a test vehicle proves the effectiveness of the design methodology.

4.1 Introduction

Gear shift strategy has been proved to be crucial for vehicles to improve the fuel economy, driveability, etc. A supervisory control algorithm, including an optimal gear shift strategy, based on optimal control algorithms, such as Dynamic Programming (DP), Pontryagin's Minimum Principle (PMP), Dynamic Programming-Pontryagin's Minimum Principle (DP-PMP), Model Predictive Control (MPC), etc., can guarantee an optimal operation of the powertrain system over a priori drive cycle. Therefore, the obtained gear shift strategy is not optimal, consistent and robust for other drive cycles. Furthermore, disturbances involved with the powertrain system, e.g. driving conditions and driver behaviors, etc., are not considered and addressed in the algorithm, thus making the corresponding gear shift strategy hard to be reliably realtime implemented. Hence, a gear shift strategy based on a static shift map has been widely adopted as a standard solution for shifting gears online. A static shift map defines the shift points based on the current vehicle speed and the engine torque (sensing via the acceleration

¹This chapter has been prepared for a journal publication in the form as: V. Ngo, T. Hofman, M. Steinbuch, A. Serrarens. Gear Shift Map Design Methodology for Automotive Transmissions. 2012.

pedal position, throttle opening, etc.). Design of a gear shift map is traditionally based on know-how, experience of the calibration engineers and tunings in heuristic manner. Hence, the gear shift map is consistent and robust after a huge trial-and-error effort. This so-called experience-based gear shift strategy does not exploit the inherent potential of the powertrain system sufficiently to improve the overall performance of the vehicle, and thus coming with a lower confidence on optimality with respect to the fuel economy and driveability. In this research, a gear shift map design methodology is developed for discrete ratio transmissions used in road vehicles. The methodology takes advantages of: i) the optimal-based gear shift strategy, and ii) the statistical theory, to build an optimized gear shift map, which is consistent, robust and realtime implementable.

In literature, there is a small number of studies addressing about the gear shift map design methods for conventional vehicles. Besides an essential requirement on fuel economy improvement, ensuring an acceptable driveability level is also an important index for the design of a map-based gear shift strategy. The study in [168] analyzes the influence of different vehicle weights on the gear shift point control. In order to ensure the driveability, the authors adopt a policy of maintaining the same acceleration level after shifting, which requires an unchanged throttle position right after shifting. The most fuel economy points are derived to create a gear shift map. Also focusing on the driveability, the authors in [55] present an approach based on DP to define an optimal gear shift sequence. The optimization criterion aims at minimizing the acceleration time of the vehicle. Meanwhile the authors in [66] also put the driveability into consideration when designing a gear shift map for an automatic transmission. An optimization problem for the gear shift and throttle opening strategies is formulated on a prescribed launch profile with a constant engine power, representing a driveability constraint. DP is used to obtain the optimal results at different constant engine power levels, which are then combined to form the gear shift and throttle opening maps. These two maps will govern the operation of the integrated powertrain. The authors claim an improved fuel economy for the designed gear shift map meanwhile still meeting a sufficient driveability level.

Regarding Hybrid Electric Vehicles (HEVs), where a certain driveability level can be satisfied by an assistance from the secondary power source, the gear shift strategy in general can aim at further improving the fuel economy. However, there is not much published research dedicating on the design of a map-based gear shift strategy for discrete ratio transmissions. Due to the availability of the secondary power source, the gear shift map for HEVs should be composed from the different gear shift strategies in different driving modes, as discussed in [78]. However that paper does not describe the design of such a gear shift strategy. In [157], the authors propose a method to design a gear shift map for an Automated Manual Transmission (AMT). A gear shift problem is formulated and solved by using static programming to derive the most fuel-economic

shift points corresponding with a prescribed constant acceleration profile. The method takes the vehicle speed, engine torque (or mechanical braking torque), and motor torque into account to form a three-dimension gear shift map, which is designed correspondingly with the driving modes. The authors claim a fuel economy improvement compared to a traditional shift map of a conventional vehicle. However the optimization problem is not well formulated in terms of the system constraints to guarantee optimality. Furthermore, an optimization-based gear shift map extraction for HEVs can be found in [75, 83]. The authors utilize DP to design an optimal Energy Management Strategy (EMS) to derive the optimal gear shift solution. Then, a near optimal map-based gear shift strategy is built by observation and extraction. An improvement of the driveability for the designed gear shift map compared to an original, intuitive algorithm-based shift map is claimed by the authors.

Through literature review, it is observed that the gear shift map design methods proposed in the published studies have not taken a wide range of driving scenarios, i.e. the driving behavior dynamics and road dynamics, into account. For conventional vehicles, the driveability is not systematically addressed in the gear shift map due to lack of a driveability-optimal gear shift strategy design method. For HEVs, coupling among the operating modes and the resulted dominant gear shift pattern(s) have not been analyzed in order to achieve an overall, consistent, robust and optimized gear shift map over a wide range of driving scenarios. Furthermore, there is lack of an approach to properly analyze the optimal gear shift data towards extracting the representative optimal gear shift lines of the gear shift map. In this study, a gear shift map design methodology for discrete ratio transmissions used in conventional and hybrid electric vehicles is developed. Aiming at designing a gear shift map improving both the fuel economy and driveability, the methodology utilizes an optimal gear shift strategy to derive the optimal gear shift patterns over a wide range of driving profiles. Statistical theory is then applied to analyse the optimal gear shift patterns, towards extracting the optimal gear shift lines of the gear shift map. Robustness and consistency of the gear shift map are considered in the step of statistical analysis and shifting line extraction. The design methodology is described and demonstrated by applying for the prototype conventional and hybrid electric vehicles. Experimental validation on a test conventional vehicle, different from the prototype vehicle, is performed to verify the applicability and flexibility of the design method.

This chapter is organized as follows. The powertrain modeling and dynamics are given in Section 4.2. An analysis of gear shift contribution to the fuel economy of conventional and hybrid electric vehicles is given in Section 4.3. Gear shift map design methodology applied for conventional vehicles is described in Section 4.4. Meanwhile application of the gear shift map design methodology for HEVs is discussed in Section 4.5. An experimental validation of the design methodology on a test conventional vehicle is presented in Section 4.6. And finally, conclusions are given in Section 4.7.

4.2 Powertrain Modeling and Dynamics

4.2.1 Powertrain Model

The hybrid powertrain topology is shown in Figure 4.1. This study focuses on both conventional and hybrid electric vehicle, so a conventional powertrain topology can be realized by removing or deactivating the battery, inverter and electric machine from the hybrid driveline. The main parameters of the powertrain components are given in Table 4.1.

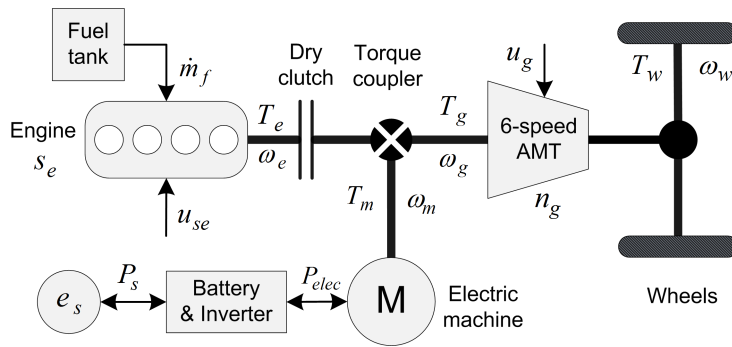


Figure 4.1: The hybrid powertrain topology, (AMT: Automated Manual Transmission; M: Electric machine).

Table 4.1: Specifications of the prototype vehicle.

Item	Description/Quantity
Engine	diesel type, maximum torque of 200Nm, maximum power of 68kW.
Electric machine	maximum torque of 40Nm, maximum power of 6kW.
Battery	lithium-ion; capacity of 6Ah, 110V.
Transmission	6-speed automated manual transmission, $r_g = [3.817, 2.053, 1.302, 0.959, 0.744, 0.614]$.
Vehicle mass	1320kg.

Aiming at designing an EMS, the quasi static modeling approach is used to model the main powertrain components. Hence, a time step Δt of one second is chosen to simulate the powertrain system, thus ignoring the system dynamics faster than $1Hz$ [42]. The clutch is modeled as a boolean switch to connect and to disconnect the engine

immediately to and from the driveline. Its dynamics and limited power losses during a gear shift or an engine start are ignored. Notice of the slippage loss of clutch at vehicle launch is also not taken into account. However, analysis of the effect of these losses to the control strategy can be found in Chapter 6.

- **Start-stop system:** the start-stop system can be modeled by a decision variable $s_e(k)$ to control the engine on-off state.

$$s_e(k) = \begin{cases} 1 & \text{if engine on,} \\ 0 & \text{if engine off.} \end{cases} \quad (4.1)$$

- **Engine:** for a certain engine speed $\omega_e(k)$, the fuel mass flow $\dot{m}_f(k)$ is modeled as an affine piece-wise second order function of the engine power, as expressed in (4.2),

$$\dot{m}_f(k) \approx \left(a_0(k)P_e^2(k) + a_1(k)P_e(k) + a_2(k) \right) s_e(k). \quad (4.2)$$

in which the coefficients $a_0(k)$, $a_1(k)$ and $a_2(k)$ are functions of the engine speed. When the engine is off, no fuel is consumed. If assume during braking, the engine is switched off and decoupled from the driveline, then the engine braking is neglected. Therefore, the constraints on the speed $\omega_e(k)$ and the power $P_e(k)$ are as follows,

$$\omega_{e,min} \leq \omega_e(k) \leq \omega_{e,max}, \quad (4.3a)$$

$$0 \leq P_e(k) \leq P_{e,max}(\omega_e(k)). \quad (4.3b)$$

- **Electric machine:** the machine efficiency η is assumed to be constant in a normal operating state. Therefore, the power flow in motoring and generating modes is expressed as,

$$P_m(k) = \eta P_{elec}(k) \quad \text{in motoring,} \quad (4.4a)$$

$$P_m(k) = \frac{1}{\eta} P_{elec}(k) \quad \text{in generating.} \quad (4.4b)$$

The constraints on the speed $\omega_m(k)$ and the power $P_m(k)$ are,

$$0 \leq \omega_m(k) \leq \omega_{m,max}, \quad (4.5a)$$

$$P_{m,min}(\omega_m(k)) \leq P_m(k) \leq P_{m,max}(\omega_m(k)). \quad (4.5b)$$

- **Battery system:** the electrical power $P_{elec}(k)$ is modeled as a quadratic function of the storage power $P_s(k)$,

$$P_{elec}(k) \approx b_0 P_s^2(k) + b_1 P_s(k) + b_2. \quad (4.6)$$

The constraints on the battery storage power,

$$P_{s,min} \leq P_s(k) \leq P_{s,max}. \quad (4.7)$$

Notice that the battery capacity is chosen properly such that its state never exceeds the predefined upper and lower bounds for increasing lifetime and reliable operation. Battery operating temperature is assumed to be under tight control.

- **Automated Manual Transmission (AMT):** transmission efficiency η is assumed to be constant for all gears. The speed and torque relations in both side of transmission when the clutch closed are,

$$\omega_e(k) = \omega_g(k) = \omega_w(k)r_g(k), \quad (4.8a)$$

$$T_w(k) = \eta r_g(k) T_g(k) = \eta r_g(k) T_e(k). \quad (4.8b)$$

wherein: $\omega_w(k)$ is the wheel rotational speed; $T_w(k)$ is the drive torque at the wheels; $T_g(k)$ is the transmission input torque; $r_g(k)$ denotes the gear ratio. The final reduction gear ratio is merged into the transmission ratio for a simplification.

The constraints on the gear position of the 6-speed transmission are,

$$1 \leq n_g(k) \leq 6. \quad (4.9)$$

- **Power flow model:** the power flow equilibrium at the transmission input of the powertrain is expressed as,

$$P_e(k) = P_g(k) + P_m(k). \quad (4.10)$$

where $P_m(k) = 0$ if the conventional powertrain is under consideration.

4.2.2 Powertrain System Dynamics

The powertrain dynamic system consist of three state variables: the start-stop state $s_e(k)$, battery state-of-energy $e_s(k)$ and gear position $n_g(k)$. Their dynamics are governed by three corresponding control variables $u_{se}(k)$, $P_s(k)$ and $u_g(k)$ as,

$$s_e(k+1) = s_e(k) + u_{se}(k), \quad (4.11)$$

$$e_s(k+1) = e_s(k) + P_s(k)\Delta t, \quad (4.12)$$

$$n_g(k+1) = n_g(k) + u_g(k). \quad (4.13)$$

Vehicle longitudinal dynamics: the discrete longitudinal motion of the vehicle is given by,

$$\omega_w(k+1) = \omega_w(k) + \frac{1}{J_{v,eq}}(T_w(k) - F_{load}(k)R_w)\Delta t, \quad (4.14)$$

where F_{load} is the resistant loads due to rolling and aerodynamic resistances; $J_{v,eq}$ is an equivalent vehicle inertia at the wheels,

$$J_{v,eq} = ((J_e + J_c + J_p)r_g^2 + J_s)r_d^2 + m_v R_w^2,$$

$$F_{load} = c_r m_v g \cos \alpha + m_v g \sin \alpha + \frac{1}{2} \rho_a A_f c_d v^2,$$

and m_v is the vehicle weight; R_w is the wheel radius; J_e is the engine inertia; J_c is the clutch inertia; J_p is the transmission primary inertia; J_s is the transmission secondary inertia; ρ_a is the air density; A_f is the frontal area of vehicle; c_d is the aerodynamic drag coefficient; c_r is the rolling friction coefficient; g is the gravity coefficient; v is the vehicle speed; α is the slope of the road.

4.3 Analysis of Gear Shift Contribution to Fuel Economy

Under an optimal EMS, the engine tends to operate at low speed and high torque areas for a fuel economy improvement, see Chapters 2 and 3. A gear shift decision can only be made if the engine speed at the next gear is above the minimum engine speed $\omega_{e,min}(k)$, as imposed by the inequality constraint (4.3a). This lower bound will definitely influence a gear shift decision, and thus considerably affect the fuel economy improvement. Raising this threshold will render the engine to operate at higher speed than it would do for a lower value, which will result in an inefficient operation state of the engine. Hence, a design methodology, which is based on the optimal shift data to analyze and extract the gear shift lines, is influenced by the lower bound of the engine speed. Therefore, its sensitivity study on fuel economy is necessary within the framework of developing a gear shift map design methodology.

4.3.1 Conventional Vehicle

For a supervisory control algorithm over a given drive cycle, the gear shift command is the only control variable for the conventional powertrain system. Hence, an analysis of the fuel economy improvement is straightforward, which can be done by an optimal gear shift strategy.

Problem 4.1. *Given a drive cycle $v(k)$ with time length N , find an optimal control law of the gear shift command $u^*(k) = u_g^*(k)$ to minimize the cost function of fuel consumption over the entire drive cycle, defined as,*

$$\mathbf{J}_{CV} = \sum_{k=0}^{N-1} \dot{m}_f(k) \Delta t, \quad (4.15)$$

subject to the system dynamics and constraints (4.2), (4.3), (4.8), (4.9), (4.10) and (4.13),

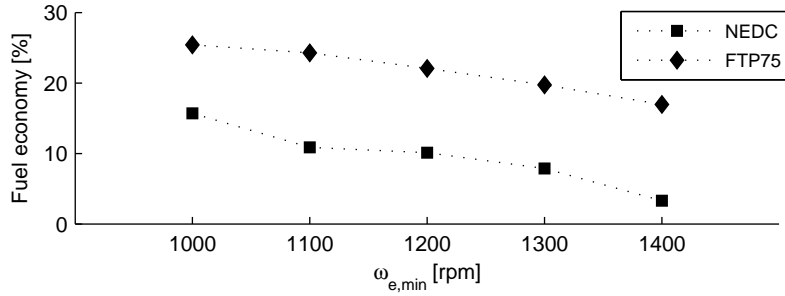


Figure 4.2: Sensitivity study of the fuel economy with respect to $\omega_{e,min}$ for a conventional vehicle.

Problem 4.1 is solved by using DP to achieve a globally optimal solution on a given drive cycle. A sensitivity study of the fuel economy improvement with respect to the minimum engine speed $\omega_{e,min}$, as in the constraint (4.3a), is given in Figure 4.2. The prescribed gear shift schedule accompanied with the drive cycles is chosen as the baseline strategy. In both cycles, NEDC and FTP75, it shows that the fuel economy decreases linearly with respect to an increase of the minimum engine speed by an approximated factor of $-2.5\%/100\text{rpm}$. Hence, in the design of a gear shift map, this factor needs to be taken into account when seeking and evaluating fuel economy improvement.

4.3.2 Hybrid Electric Vehicle

For a HEV, the fuel economy improvement can be achieved not only by an optimal gear shift strategy but also by hybridization. It is realized by an optimal EMS proposed as follows,

Problem 4.2. *Given a drive cycle $v(k)$ with time length of N , find an optimal control law $u^*(k) = [u_{se}^*(k), P_s^*(k), u_g^*(k)]$, which are the optimal control variables for the start-stop system, battery state-of-energy and gear position respectively, that minimize the cost function of fuel consumption over the entire drive cycle, defined as,*

$$\mathbf{J}_{HEV} = \sum_{k=0}^{N-1} \dot{m}_f(k) \Delta t, \quad (4.16)$$

subject to the system dynamics and constraints (4.1)-(4.13).

Problem 4.2 is well defined and solved by a control algorithm based on a combination of Dynamic Programming and Pontryagin's Minimum Principle [98], as described in Chapter 3. The control algorithm is computationally efficient and guarantees an optimal solution.

A sensitivity investigation of the fuel economy improvement with respect to the minimum engine speed is shown in Figure 4.3. The baseline result is obtained by applying

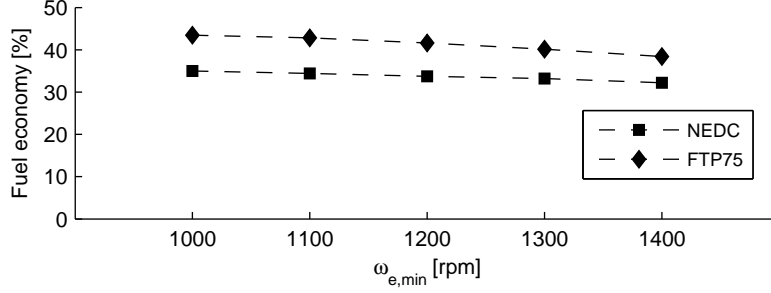


Figure 4.3: Sensitivity study of the fuel economy with respect to $\omega_{e,min}$ for a HEV.

the prescribed gear shift schedule accompanied with the drive cycles on a corresponding conventional vehicle. An increase of the minimum engine speed will result in a decrease of the relative fuel economy with an approximated factor of $-1.0\%/100\text{rpm}$. Comparing to the conventional vehicle, the fuel economy improvement of the hybrid electric vehicle is less sensitive to the minimum engine speed. Assuming that the start-stop functionality in the hybrid powertrain can be done by using the electric machine to crank up the engine from rest, the corresponding fuel benefit can be appointed to the hybridization factor. This implies that there are two factors contributing to the fuel economy improvement of HEVs: the gear shift and the hybridization. In order to investigate the share of these two factors in the fuel economy improvement, an algorithm is proposed for this purpose.

Algorithm 4.1. *Given a drive cycle, Problem 4.2 is formulated and solved. Then at every time step k ,*

- compute the instantaneous optimal fuel rate $\dot{m}_f^*(k)$;
- given the optimal gear position $n_g^*(k)$, compute the required engine power without hybridization,

$$P_{e,gs}(k)|n_g^*(k);$$

- compute the corresponding fuel rate without hybridization, given $n_g^*(k)$ and $P_{e,gs}(k)$,

$$\dot{m}_{f,gs}(k)|P_{e,gs}(k), n_g^*(k).$$

Define the fuel consumption for two powertrain systems:

- the hybrid powertrain, $m_f = \sum_0^{N-1} \dot{m}_f^*(k)\Delta t$;
- the conventional powertrain utilizing the corresponding optimal gear shift strategy obtained from the EMS of the hybrid powertrain, $m_{f,gs} = \sum_0^{N-1} \dot{m}_{f,gs}(k)\Delta t$.

Here $m_{f,base}$ denotes fuel consumption of the baseline vehicle. Then, contributions of the gear shift and hybridization to the total fuel economy are defined as,

- the fuel economy improvement due to the gear shift: $m_{f,base} - m_{f,gs}$;
- the fuel economy improvement due to the hybridization: $m_{f,gs} - m_f$;
- the total fuel economy improvement: $m_{f,base} - m_f$.

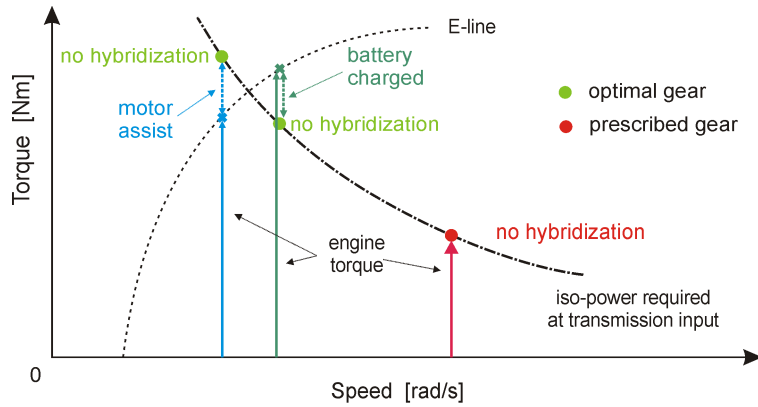


Figure 4.4: Contributions of the gear shift and hybridization to the fuel economy.

Algorithm 4.1 can be graphically explained through a demonstration shown in Figure 4.4. Under a certain power request at the wheels, a corresponding power at the transmission input can be expressed in the form of a hyperbolic torque-speed curve, the dashed dotted black line. For the conventional powertrain, if a prescribed gear schedule is used for shifting, the engine operating point is positioned at the red dot. Hybridization of the powertrain with an optimal EMS allows i) the engine operating point to move to the green dot due to an optimal gear shift strategy, ii) a further load balance sharing (power split) between the engine and electric machine to move the engine operating point as close to the E-line as possible, see the corresponding battery charged or motor assist point due to a certain power split strategy. Factors i) and ii) help improving the hybrid powertrain efficiency compared to the conventional one.

Calculation results of Algorithm 4.1 on NEDC and FTP75 are shown in Figure 4.5. Therein, the fuel economy improvement of the optimal gear shift strategy for the conventional vehicle, as discussed in Section 4.3.1, is also plotted for reference, see the marked dotted lines. The dark grey bars indicate contribution of the gear shift; meanwhile the light grey bars indicate contribution of the hybridization. It can be seen that contribution of the gear shift in the hybrid vehicle is almost equal to the optimal gear shift strategy for the conventional vehicle. Hence, from an engineering point of view, it can be inferred that the gear shift factor is independent from the hybridization factor

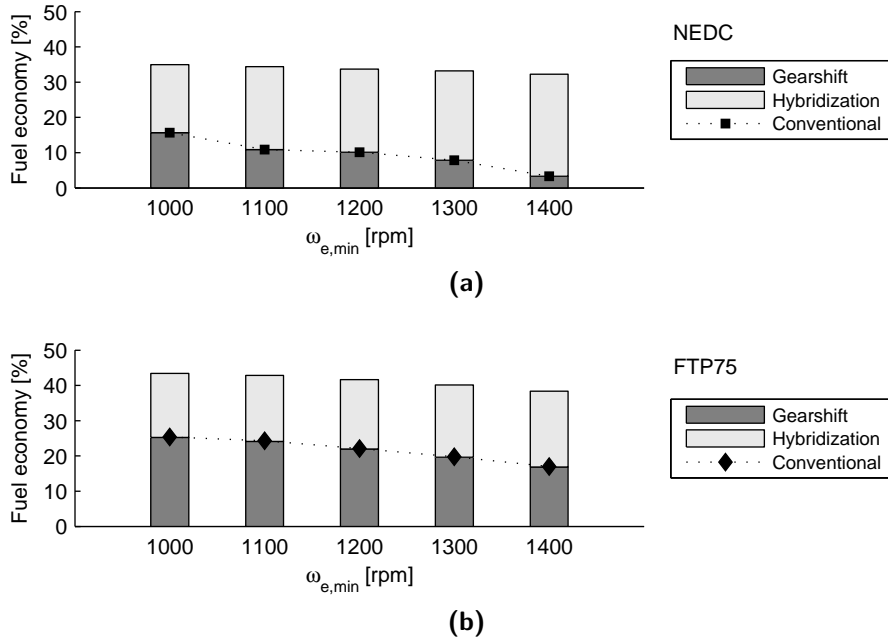


Figure 4.5: Contributions of the gear shift and hybridization to the fuel economy of the HEV. Simulation results on NEDC and FTP75 are shown in (a) and (b), respectively.

for the HEV. Furthermore, when raising the minimum engine speed, contribution of the gear shift factor is reduced but the hybridization factor is more active to maintain the fuel economy level. This helps neutralizing the fuel economy sensitivity to $\omega_{e,min}$ for the hybrid vehicle compared to the conventional vehicle.

4.4 Gear Shift Map Design for Conventional Vehicles

The optimal gear shift strategies for the conventional vehicle, proposed in Chapter 2, are benchmark solutions rather than realtime implementable ones. Despite the fact that the stochastic-based strategy is realtime implementable, a rigorous implementation approach is required to deal with the uncertainties and disturbances of the powertrain system to ensure a robust and fuel-efficient gear shift pattern. Therefore, a map-based gear shift strategy, which can be implemented directly to the production vehicles and ensures optimality, appears as a promising solution. This section describes a novel methodology which is used to generate an optimized gear shift map for conventional vehicles equipped with discrete ratio transmissions.

4.4.1 Acquisition of Optimal Gear Shift Data

This is the first step of the design methodology. The fuel optimal gear shift problem, see Problem 4.1, is formulated and solved to obtain the optimal gear shift points on various drive cycles. The higher the number of drive cycles used to acquire the optimal gear shift points, the higher level of optimality the designed gear shift map is. In this study, the standard test drive cycles in Europe, Japan and United States, e.g. ARB02, CADC, FTP75, HWFET, Hurk, JN1015, LA92, NEDC, NYCC, and US06, are chosen to objectively represent the drive profiles of vehicles. Note that the driveability optimal gear shift problem, see Problem 2.2 in Chapter 2, is applied if a driveability-optimal gear shift map is required. The optimal shift points, as point-wise functions of the engine torque and vehicle speed, for all gear upshift patterns are shown in Figure 4.6. The optimal shift points, hereafter called the shift data, scatter around a specific area for a certain upshift pattern. With the upshift patterns of $1 \rightarrow 2$, $2 \rightarrow 3$ and $3 \rightarrow 4$, the scatter areas are less dispersed than that of the upshift patterns of $4 \rightarrow 5$ and $5 \rightarrow 6$. Nonetheless, an inference of a shift pattern characteristic based on a rigorous analysis of the corresponding shift data is necessary, such that representative shift lines can be extracted.

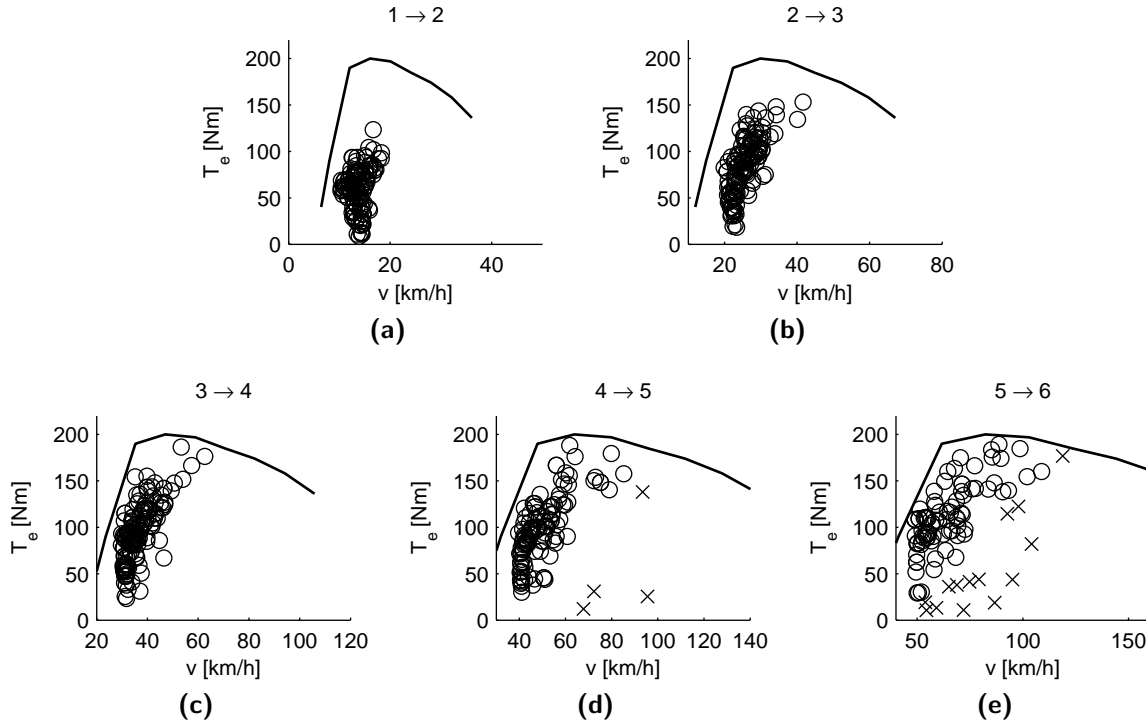


Figure 4.6: Optimal upshift points of the conventional vehicle, wherein the x-mark points denote the outliers.

4.4.2 Analysis of Shift Data

Once the shift data have been collected, an analysis of the shift data based on statistical theory is performed to infer a shift characteristic behind the representative information. Furthermore, statistical analysis gives a way to quantify the confidence level we can have on this inference. Details of statistical theory and analysis method can be found in the reference books, for example see [85, 113].

Outlier examination

In statistical theory, a sum of the squared error, based on Euclidean distance, is commonly used to measure a scatter degree of the shift data. A data that is numerically distant from the rest is referred as an outlier. So, an outlier can unduly influence the clusters of the shift data. The resulting cluster centroids may not be as representative as they otherwise would be, and thus the sum of the squared error will be higher as well. Because of this, it is often useful to examine the outliers and eliminate them if necessary.

Problem 4.1 aims at maximizing the fuel economy, thus making the shift data scatter around the most fuel economy region of the engine. This helps identifying the outliers easily. Therefore, a visual inspection approach [113] can be used effectively to examine the shift data and remove the outliers before clustering. As shown in Figures 4.6a-4.6c, it can be seen that no outlier arises for the gear upshift patterns of $1 \rightarrow 2$, $2 \rightarrow 3$ and $3 \rightarrow 4$. However, for the gear upshift patterns of $4 \rightarrow 5$ and $5 \rightarrow 6$, the outliers can be the upshifts occurring at a high vehicle speed or at a high required engine torque. They are located far from the rest of the shift data in the corresponding clusters, see the x-marks in Figures 4.6d-4.6e.

Cluster analysis method

After removing the outliers, the shift data still have a dispersion degree over the design space. Hence, clustering the shift data into groups, whose data in each group have a similar information and are different from other groups, is required to properly define the correspondingly central tendencies. In statistical theory, there are a number of different methods that can be used to carry out a cluster analysis. These methods can be classified as hierarchical and non-hierarchical methods [29], as shortly brief as follows.

- **Hierarchical clustering**

Hierarchical clustering technique is the most important category of clustering methods, wherein an agglomerative technique is used more often for generating

clusters. The working principle of this technique is to start with individual points as clusters, then successively merge the two closest clusters until only one cluster remains. This clustering technique is basically described in Algorithm 4.2.

Algorithm 4.2. Agglomerative clustering method

define the cluster proximity matrix, if necessary;
repeat
 - merge the two closest clusters,
 - update the cluster proximity matrix to reflect the proximity between the new clusters and the original clusters,
until only one cluster remains.

- **Non-hierarchical clustering**

This clustering technique is most often known as a K-means clustering method. The K-means method defines the data prototype in terms of a centroid, which is usually a mean of a group of points. The K-means clustering technique is described by Algorithm 4.3.

Algorithm 4.3. K-means clustering method

select K points as initial centroids;
repeat
 - form K clusters by assigning each point to its closest centroid,
 - recompute the centroid of each cluster,
until the centroids do not change.

In this study, an effective approach of combining two clustering methods is used to analyze the shift data [29]. The hierarchical agglomerative method is used to define the optimum number of clusters. Then the non-hierarchical K-means method is used to compute the centroid of each cluster. All cluster centroids will form a central tendency of the gear shift pattern. Figures 4.7a-4.7b show an exemplary cluster analysis for a gear upshift pattern from 2 \rightarrow 3. There are seven clusters resulting in seven centroids, indicated by the blue circled x-marks. The centroids create a basis for building a shift line by a curve best fitting these points.

Shift line extraction

For a conventional vehicle, a gear shift map consists of the upshift lines and the corresponding downshift lines.

- **Upshift:** the upshift line is built from the centroids of the corresponding upshift patterns by a best fitting curve. Figure 4.7c typically depicts an upshift line from 2 \rightarrow 3.

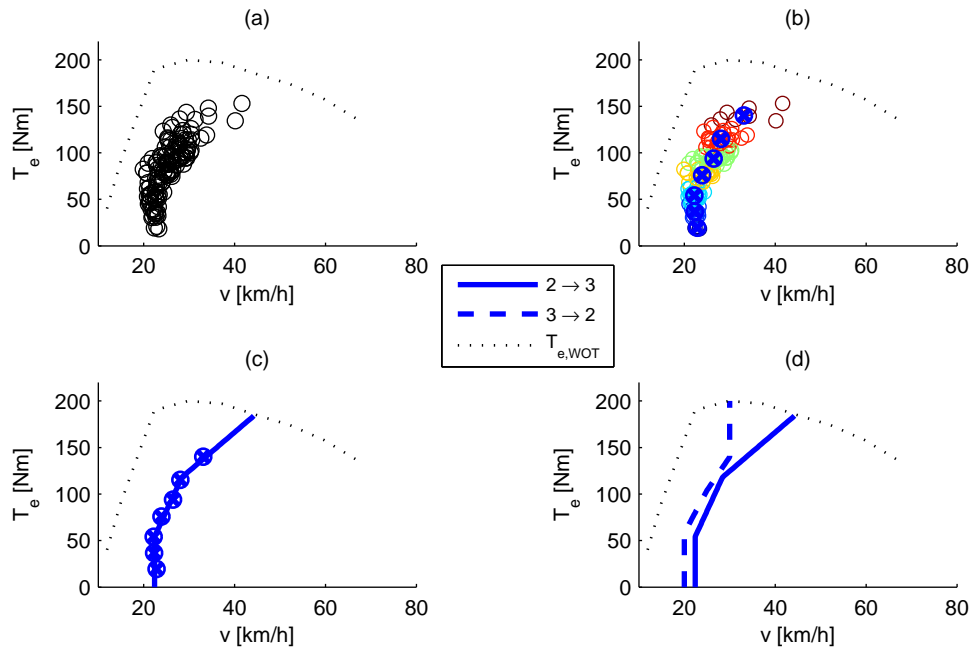


Figure 4.7: Exemplary analysis of the shift data of the conventional vehicle: the shift data of 2 \rightarrow 3 in (a); cluster analysis in (b); an extraction of the upshift line in (c), a corresponding downshift line of 3 \rightarrow 2 in (d).

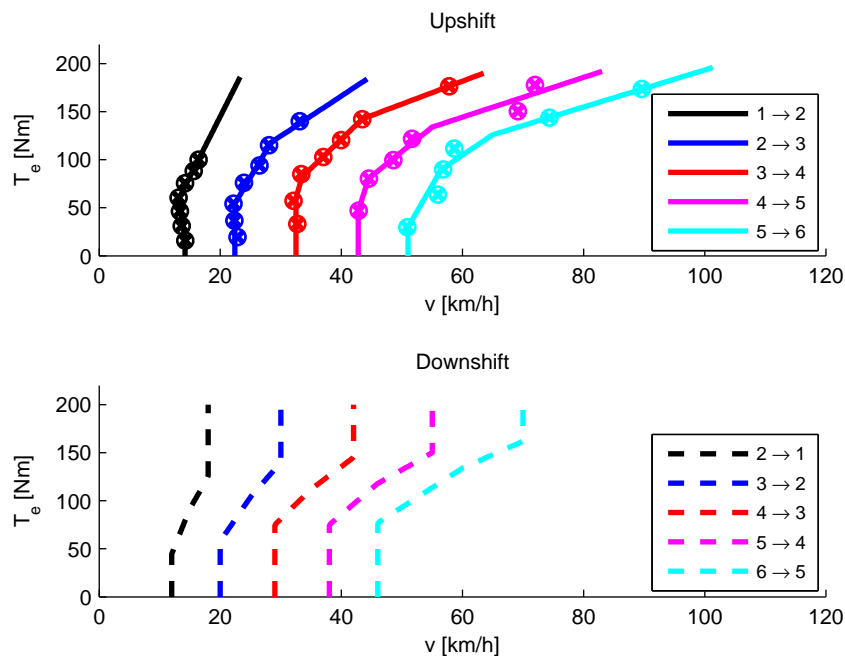


Figure 4.8: A gear shift map for the conventional vehicle.

- **Downshift:** a downshift line is built by considering two cases: i) a normal downshift occurs to avoid engine stalling due to a reduction of the vehicle speed; ii)

a power downshift, called kick-downshift, is required to meet a high torque demand at the wheels, which is not fulfilled by the powertrain at the current gear position. Taking these two factors into account, a downshift pattern, for example from $3 \rightarrow 2$, is built, see Figure 4.7d.

Figure 4.7d depicts the upshift pattern $2 \rightarrow 3$, and the corresponding downshift pattern $3 \rightarrow 2$. At a certain engine torque, there always exists a difference in the vehicle speed at the upshift and downshift lines. This results in a shifting hysteresis phenomenon, required for a consistent and robust shifting pattern.

4.4.3 Shift Map Verification

Applying the procedure described in Section 4.4.2 for the other shift patterns to extract the shift lines, a gear shift map is obtained and shown in Figure 4.8. Detail description of the typical upshift and downshift lines is given in Section 4.6.2. This gear shift map can be implemented directly in simulation or realtime environment.

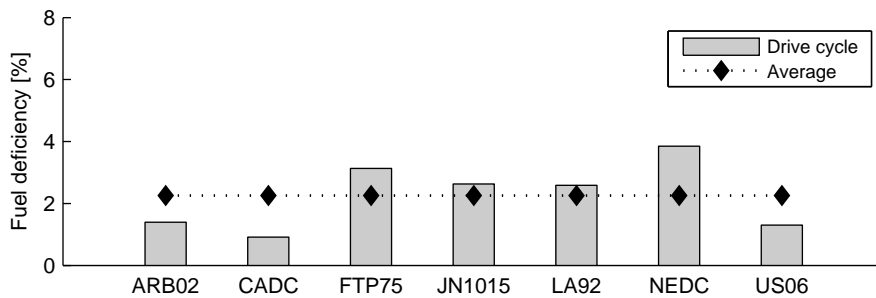


Figure 4.9: Fuel deficiency of the gear shift map compared to the DP-based optimal shift strategy for the conventional vehicle.

The obtained gear shift map is implemented in a simulation model of the conventional vehicle to verify a fuel economy improvement. The drive cycles are chosen to consist of the urban, suburban and highway parts, which represent the typical driving missions for the vehicle. By comparing with a globally optimal result (DP result), a fuel deficiency of the gear shift map is realized, as shown in Figure 4.9. Depend on the drive cycles, the fuel deficiency varies from 0.9% to 3.9%. On average, the gear shift map, which is consistent, robust and realtime implementable, degrades the fuel economy of 2.3% compared with a globally optimal gear shift algorithm based on DP.

4.5 Gear Shift Map Design for Hybrid Electric Vehicles

HEVs, having a secondary power source offer, more operation modes, e.g. engine mode, assisting mode, charging mode, electrically driving mode and regenerative mode, to improve the fuel economy, driveability, etc., compared to conventional vehicles. Therefore, a gear shift strategy for HEVs is required to match with all operation modes. This can be achieved by an advanced EMS to optimally govern the operation of the hybrid powertrain. The EMS proposed in [98] is computationally efficient and guarantees an optimal solution. Hence, it is highly suitable for the gear shift design methodology for HEVs. The obtained optimal gear shift data will ensure an optimality of the gear shift map, compatible with all operation modes of the hybrid vehicle. The design process is highly accelerated due to a computationally efficient property of the EMS.

Gear shift map characteristics

- *Shift map coordinate:* the gear shift map coordinate for a conventional vehicle is based on the vehicle speed and engine torque. However, for a HEV, the equilibrium point of the power flow is at the transmission input. Hence it is reasonable to define a gear shift map coordinate based on the vehicle speed and the transmission input torque.
- *Hybrid mode:* this mode in general can be referred to an engine mode or an assisting mode or a charging mode. Basically, in hybrid mode, the engine primarily supplies the propulsive power for the vehicle. Hence, the design of gear shift map in hybrid mode is thus similar to that of a conventional vehicle.
- *E mode:* this mode refers to a situation of electrically driving the vehicle. The electric machine is placed in front of the transmission. Therefore, a gear shift strategy in E mode can expand the operating range for the electric machine with respect to the vehicle speed range, and thus gaining a fuel benefit.
- *Regenerative mode:* in this mode the electric machine functions as a generator to recuperate the vehicle kinetic energy. A gear shift strategy in this mode can increase the energy conversion efficiency of the generator and thus further contributing for a fuel benefit.

Note that the transition among the operating modes in the HEV is assumed to be well defined and properly controlled. In addition, this kind of mode shifting is irrelevant to a gear shift map design, and thus ignored in this study.

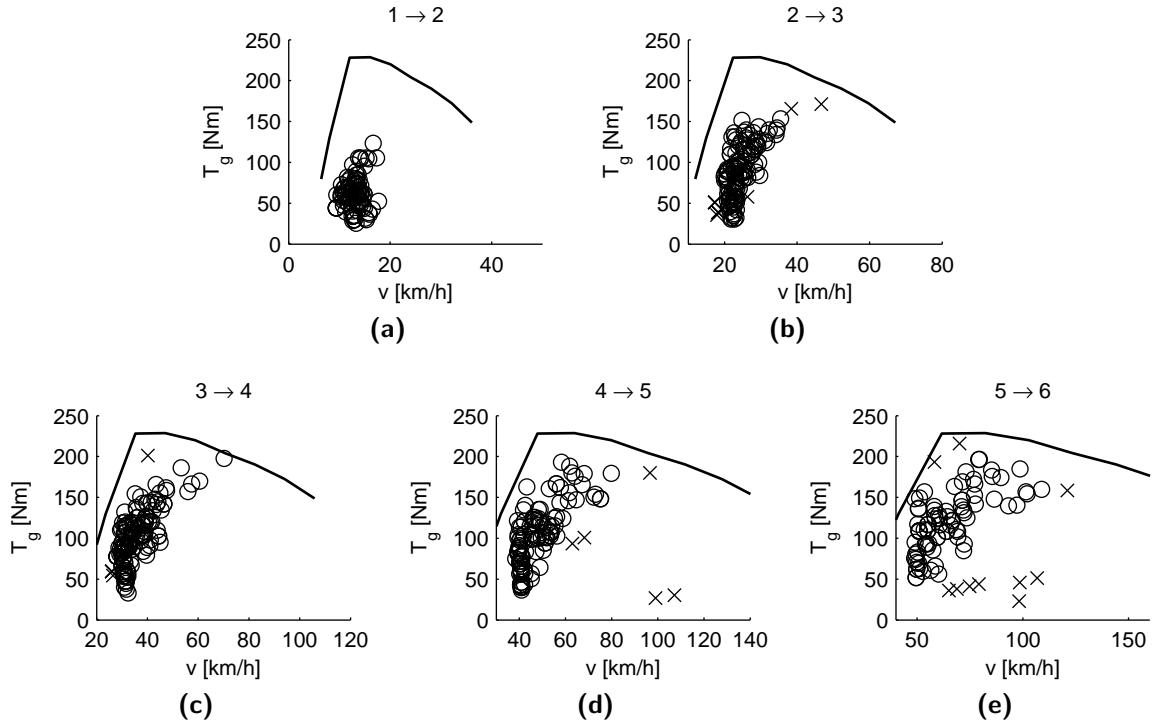


Figure 4.10: Optimal upshift points of the HEV, wherein the x-mark points denote the outliers.

4.5.1 Gear Shift Map for Hybrid Mode

A gear shift map of hybrid mode is designed similar to that of a conventional vehicle. Hence, the design process is taken through three steps as follows.

1. *Gear shift data acquisition*

Applying the optimal EMS, described in Chapter 3, for Problem 4.2, the optimal gear shift points, as point-wise functions of the vehicle speed and the transmission input torque, in hybrid mode are obtained. Figure 4.10 shows the corresponding upshift data.

2. *Analysis of the shift data*

By using the visual inspection technique [113], the outliers for each upshift pattern, indicated by x-marks, are removed from the upshift data. The cluster analysis method, as introduced in the conventional vehicle application, is used to extract a shifting pattern characteristic. Then the upshift and downshift lines are built correspondingly. Figure 4.11 illustrates a sequence from the shift data acquisition to the shift line extraction for the shift patterns of $3 \rightarrow 4$ and $4 \rightarrow 3$.

3. *Shift line extraction*

Applying the second step for the remained gear shift patterns. The gear shift map

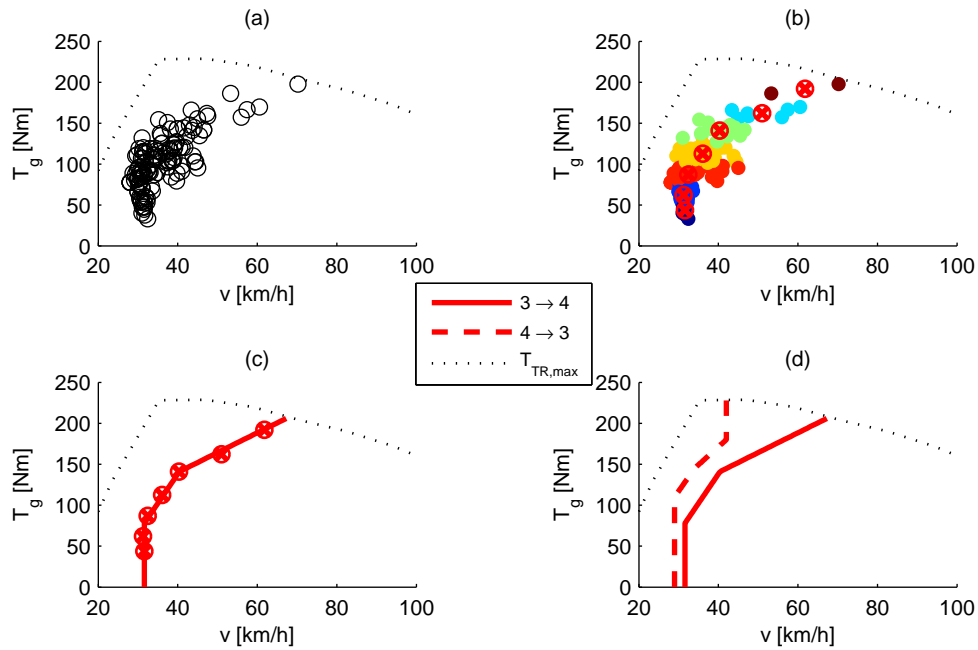


Figure 4.11: Exemplary analysis of the shift data of the HEV: the shift data of 3 → 4 in (a); cluster analysis in (b); an extraction of the upshift line in (c), a corresponding downshift line of 4 → 3 in (d).

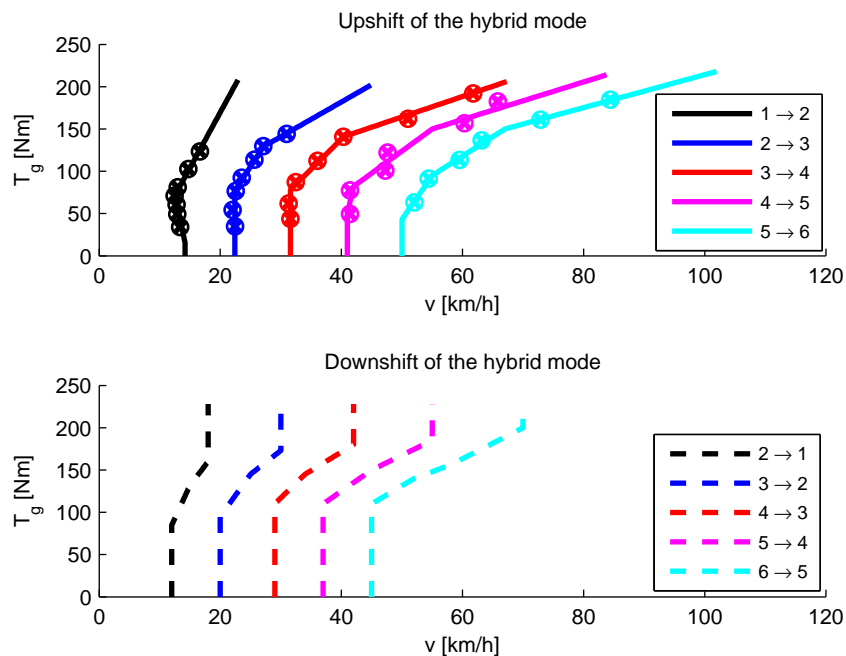


Figure 4.12: A gear shift map for hybrid mode of the HEV.

in hybrid mode is obtained and depicted in Figure 4.12.

4.5.2 Gear Shift Map for E Mode

A gear shift strategy in E mode helps expanding the electric machine operating range with respect to the vehicle speed range. The proposed EMS for the HEV does not derive the optimal gear shift strategy separated from the engine on-off and power split strategies. Furthermore, the gear shift patterns in all operation modes are coupled together to create an optimal gear shift strategy for the whole drive cycle.

For a HEV where the engine is the main traction source, E mode occurs if a low drive power is required. When a high drive power is needed, the vehicle transits to hybrid mode to meet the high demand traction. In this situation, a gear shift is occurred in hybrid mode instead of E mode. Therefore the electric machine can take advantage of the gear shift strategy in hybrid mode to expand its operating range. Apparently, the relative size of the electric machine, compared to the engine size, is a decisive factor for a coupling between the gear shift patterns in E mode and hybrid mode. Taking the mentioned issues into account, the design of gear shift map of E mode should be considered in the light of the gear shift map of hybrid mode.

Hence, a gear shift map of E mode is built in accordance with a procedure given as follows.

1. *E mode data*

Collect the transition data (from E mode to hybrid mode) and the gear shift data (occurring within E mode). Figure 4.13 shows the obtained data separating in each gear position. The transition data creates a boundary between E mode and hybrid mode, indicated by the dashed line. Meanwhile the upshift data is not rich enough to clearly define the shift patterns within E mode. This implies that a gear shift in E mode would not further improve the fuel economy rather than an operation in E mode would do. However, the operating region of the electric machine, corresponding with each gear position, can yield the possible gear shift patterns in E mode, indicated by vertical solid lines.

2. *Upshift patterns*

By comparing with the upshift lines of hybrid mode, there are identical upshift patterns for E mode. This reveals that hybrid mode dominates E mode. In other words, an improvement of the combustion efficiency is much more important than an improvement of the electro-mechanical conversion efficiency of the electric machine with respect to an optimal gear shift strategy. Therefore, the electric machine can take advantage of the upshift strategy occurred in hybrid mode to expand its operating range, thus increasing the portion of the traveled distance in E mode.

3. *Downshift patterns*

The downshift patterns in E mode can be defined as the corresponding upshift patterns, due to the fact that there is no clutch operation in a shift process in E mode. However, the downshift patterns of E mode are chosen as the downshift patterns of hybrid mode to respect a gear shift hysteresis.

4.5.3 Gear Downshift Map for Regenerative Mode

Figure 4.14 shows the obtained downshift data in regenerative mode. For each downshift pattern, the corresponding downshift points create an optimal downshift region. Basically, the downshift line can be extracted by using the cluster analysis technique applied for the conventional vehicle. However, to approach a downshift pattern robust to driving uncertainties, e.g. an upshift request induced right after a regenerative downshift, a left boundary linear line of each downshift region is defined for a corresponding downshift pattern, see the circled-mark solid lines.

It can be seen that the downshift lines are not vertical, meaning that a downshift point is a function of the vehicle speed and the brake torque. A higher a brake torque requires at the wheels, an earlier a regenerative downshift would occur to exploit the high efficient region of the electric machine. Crossing points of the downshift lines with the vehicle speed axis nearly coincide with that of the upshift lines in hybrid mode. This discloses that the downshift points in regenerative mode occur earlier than that of hybrid mode. Actually, an earlier downshift in regenerative mode will rapidly raise up the speed of electric machine, thus avoiding operating at the power limit region (at low speed) and approach an efficient operating region. Hence, a gear downshift strategy in regenerative mode can further improve the fuel economy of hybrid vehicles.

4.5.4 Shift Map Verification

A gear shift map of the HEV, consisting of all gear shift maps corresponding with all operating modes, is constructed as shown in Figure 4.15. As analyzed, the shift map of E mode is considered as a lower part of hybrid mode shift map (at a low transmission torque area). Therefore, hybrid mode shift map governs the gear shift when the driving torque is positive; the shift map of regenerative mode governs the gear downshift when the driving torque is negative (regenerative braking). When the driving torque is zero, e.g. the vehicle coasts down smoothly by the aerodynamic drag and rolling friction resistances, the shift strategy of hybrid mode at zero torque will govern a downshift for the transmission.

The gear shift map is verified by implementing it in a simulation model of the HEV. The DP-PMP approach [98] is applied to control the engine start-stop and power split. Compared to the optimal gear shift strategy, the gear shift map reduces the fuel economy

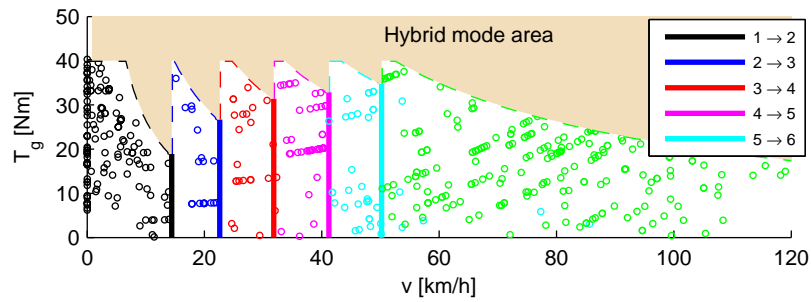


Figure 4.13: A gear shift map for E mode.

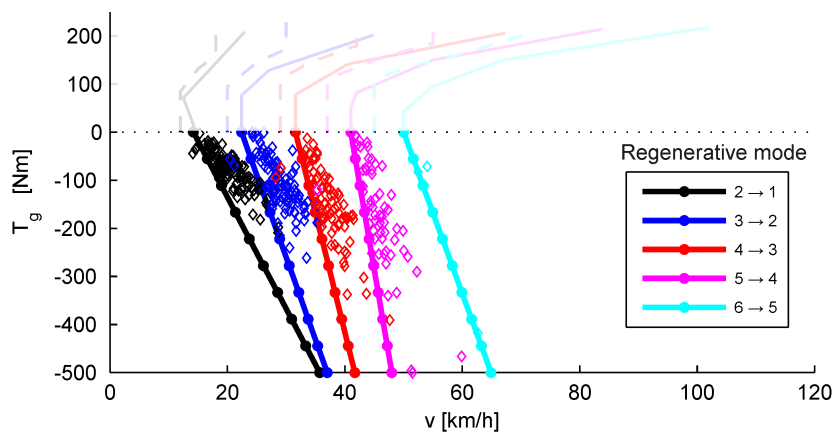


Figure 4.14: A gear downshift map for regenerative mode.

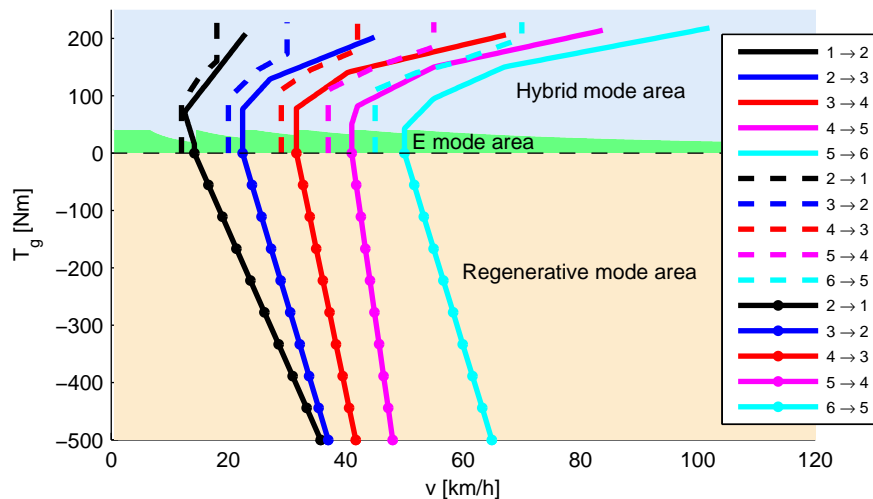


Figure 4.15: A gear shift map for the HEV.

from 2.5% to 5.9% on all simulated drive cycles, see Figure 4.16. On average, a fuel deficiency of 4.1% is obtained in return for a consistent, robust and realtime map-based gear shift strategy for the HEV.

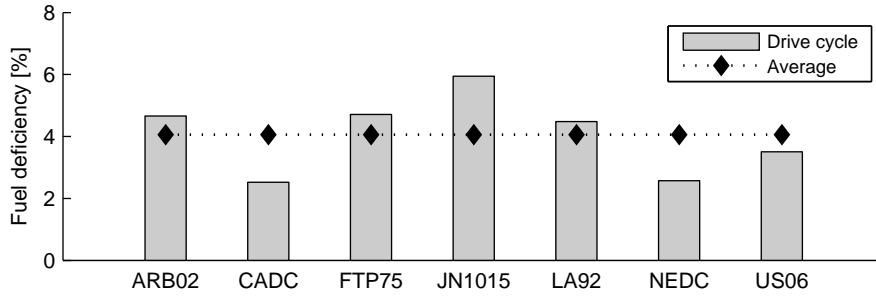


Figure 4.16: Fuel deficiency of the gear shift map compared with the DP-PMP gear shift strategy for the HEV.

4.6 Experimental Validation on Conventional Vehicle

The gear shift map design methodology is applied to produce a gear shift map for a test conventional vehicle. The test vehicle is different from the prototype vehicle, used for demonstrating the development of in the design methodology. The test vehicle is powered by a gasoline engine, meanwhile the prototype vehicle is diesel-based powered. Two gear shift maps, based on the fuel-optimal and driveability-optimal gear shift strategies, are produced and tested to verify the fuel economy and driveability improvements. This helps to validate the applicability of the design methodology on various vehicle propulsion technologies.

Figure 4.17 shows the test vehicle for which the designed gear shift maps will be implemented for an experimental validation. In the right is the original gear shift map implemented on the vehicle at production. This map, denoted as a ‘BASE’ map, is used to obtain the baseline results for a comparative analysis with the designed gear shift maps. The parameters of the test vehicle are given in Table 4.2. Note that the equipped 6-speed AMT has a powershift module activated for all gear shift patterns among the first four gears [132], thus avoiding the torque interruption at the corresponding gear shift.

Table 4.2: Main parameters of the test vehicle.

Item	Description/Quantity
Engine	type: gasoline, maximum torque of 140Nm, maximum power of 70kW.
Transmission	6-speed PowerShift (PS) AMT, $r_g = [3.071, 1.913, 1.258, 0.943, 0.763, 0.643]$.
Vehicle mass	1120kg.

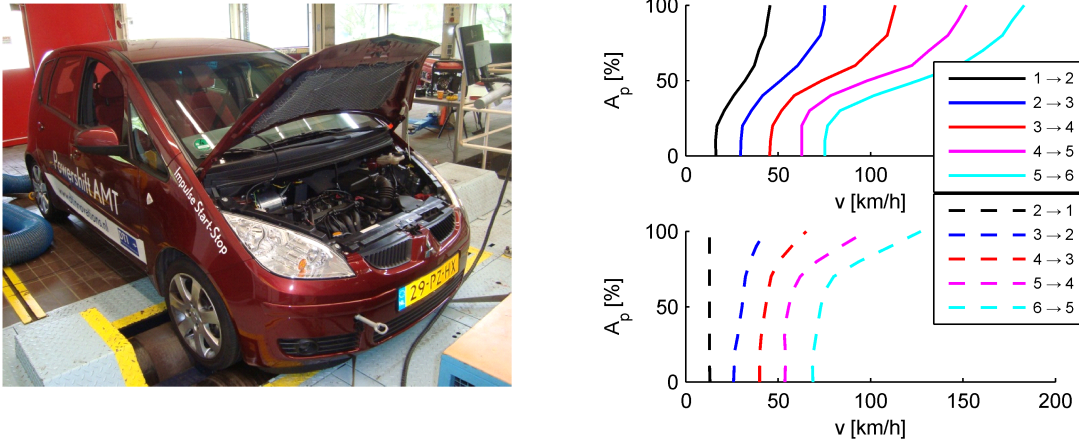


Figure 4.17: The test vehicle (left). The gear shift map at production (right), denoted as ‘BASE’ map.

4.6.1 Gear Shift Map Generation

Two gear shift maps are built for the test vehicle.

- **ECO map:** this map refers to a gear shift strategy, aiming at improving the fuel economy. Therefore, the whole procedure introduced in Section 4.4 is applied to generate ECO map.
- **ECO^S map:** this map refers to a gear shift strategy aiming at improving the fuel economy meanwhile still satisfying an acceptable driveability level. The method to address the driveability, based on the variable power reserve concept (see Section 2.3 of Chapter 2), is utilized in the gear shift design methodology to generate ECO^S map.

Figures 4.18 and 4.19 illustrate ECO and ECO^S maps, respectively. Note that the vertical axis of the shift map denotes the accelerator pedal position A_p , ranged 0%-100%, instead of the engine torque. A conversion from the engine torque to the accelerator pedal position is done by using two conversion maps: i) the first map describes the engine torque as a function of the engine speed and throttle position, ii) the second map describes the throttle position as a function of the accelerator pedal position. Hence, a gear shift point for the test vehicle is generated based on the vehicle speed and accelerator pedal position.

4.6.2 Description of Gear Shift Pattern

The gear shift patterns are extracted from ECO and ECO^S maps, called ECO and ECO^S shift patterns, and shown in Figure 4.20. It can be seen that ECO shift pattern

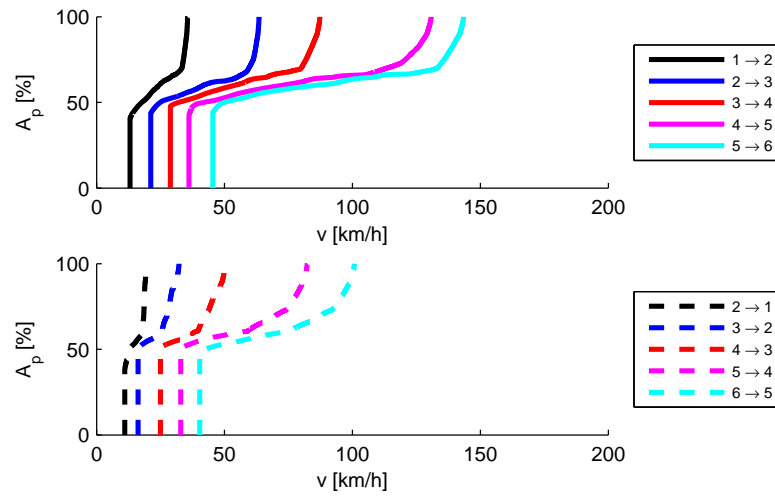


Figure 4.18: ECO map, aiming at a fuel economy improvement.

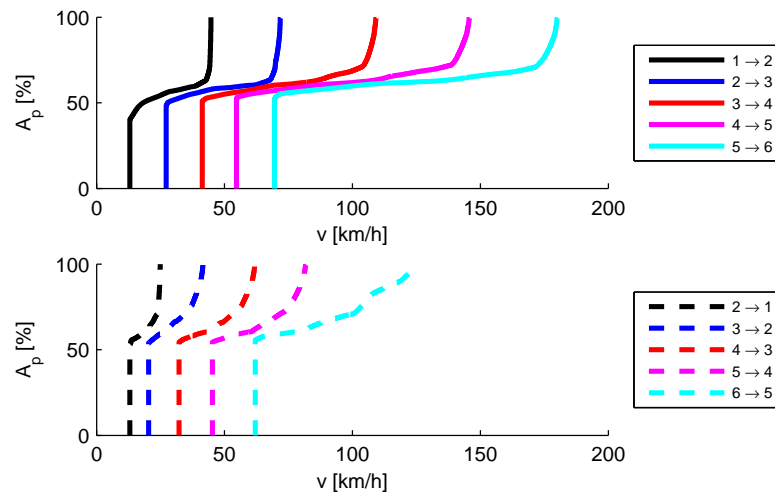


Figure 4.19: ECO^S map, aiming at improving the fuel economy meanwhile satisfying an acceptable driveability level.

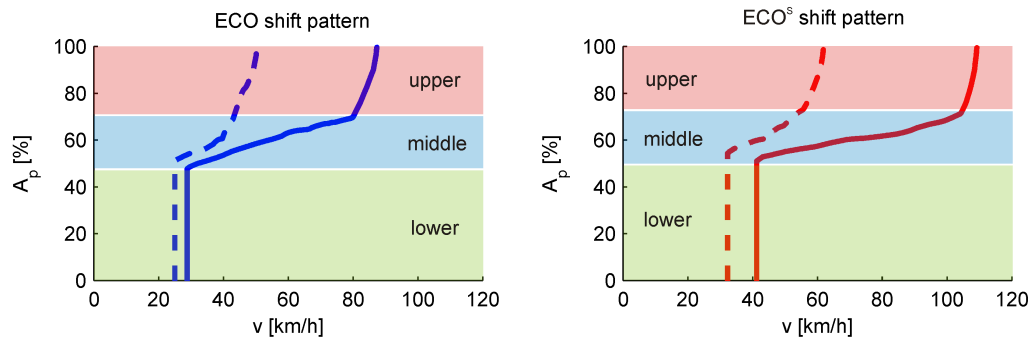


Figure 4.20: Description of the gearshift patterns in ECO map (left) and ECO^S map (right).

occurs earlier than ECO^S shift pattern with respect to the vehicle speed. Hence, the engine will operate at lower engine speed region under ECO map compared to ECO^S map. In general, a shift pattern can be divided into three parts: lower, middle and upper.

- *Lower part* is an area where the shift patterns are parallel with the Y-axis. It represents shift conditions for the vehicle independent of the acceleration pedal input. In this area, a gear shift takes place depending on the current vehicle speed. Under mild driving situations, e.g. maintaining the vehicle speed, following a traffic stream, etc., an upshift is triggered when the vehicle speed is larger than the upshift threshold. Under a coasting down, when the vehicle speed is smaller than a downshift threshold, a downshift is triggered to sustain the engine speed above a limit.
- *Upper part* defines an area where the gearshift patterns are relative steep with respect to the X-axis. In this area, the driver requests a high or full engine power to satisfy its driving styles. An upshift can occur if the engine satisfies the power request and the vehicle speed is higher than a shift threshold. If the power request is high at the current gear, a kick-downshift is performed such that the engine can meet this high power request at the lower gear.
- *Middle part* where the lower and upper parts are linked together. The obtained gearshift patterns in this area depict an optimal tradeoff among the design objectives, e.g. fuel economy, driveability, etc. It can be seen that the upshift pattern of ECO^S map is less steep than that of ECO map to improve the vehicle performance.

4.6.3 Validation in Simulation Environment

Fuel economy test

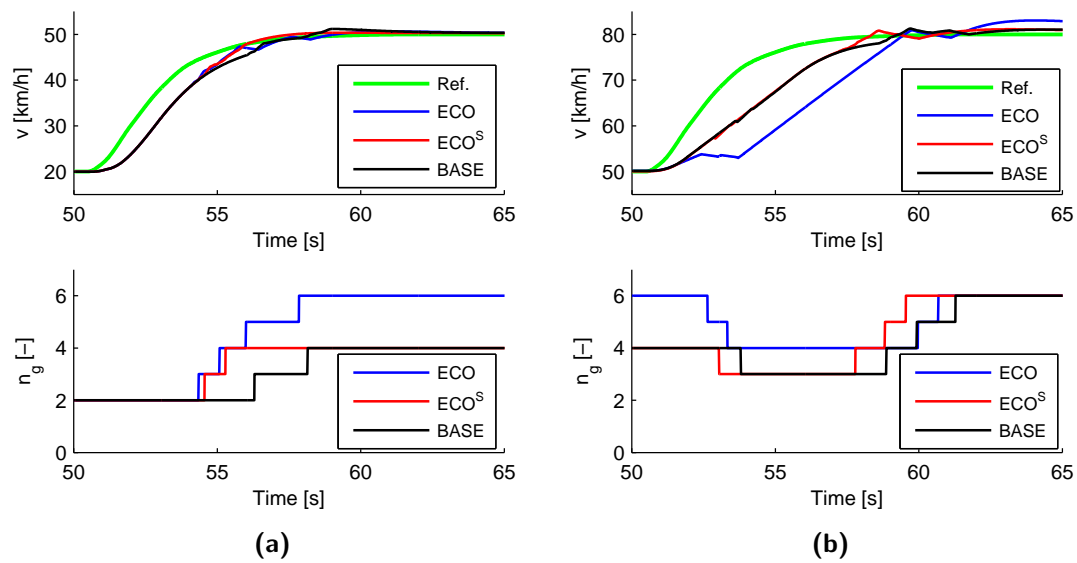
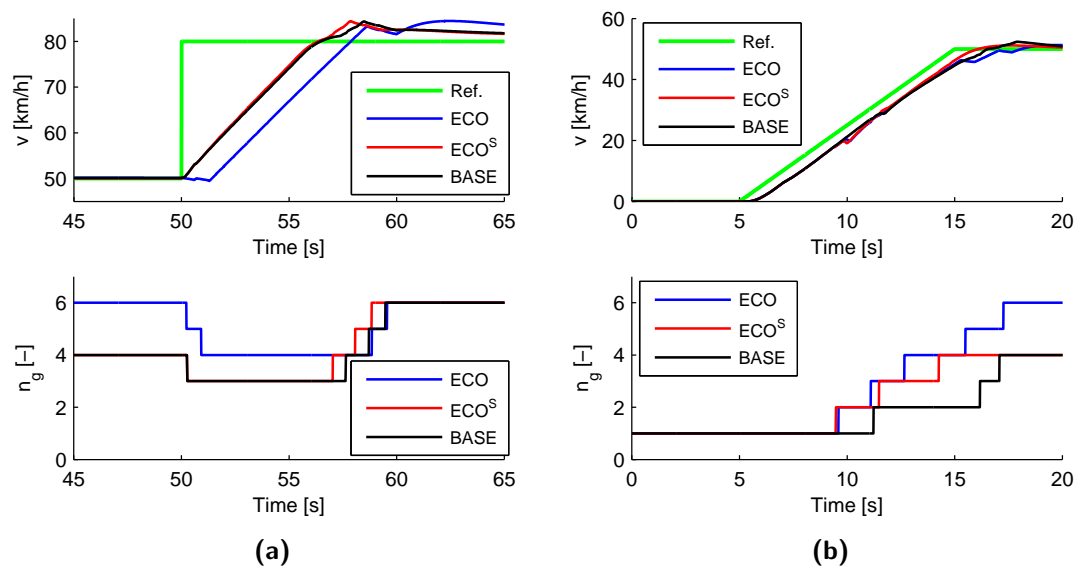
ECO and ECO^S maps are implemented on a forward facing simulation model of the test vehicle, built in Matlab/Simulink, to test the fuel economy. Compared to BASE map, a fuel economy improvement is achieved for both designed gear shift maps on the drive cycles NEDC and JN1015, see Table 4.3. As expected, ECO map gains more fuel benefit than ECO^S map.

Driveability test

Forward facing simulation results of the relative fuel economy improvement show a very promising prospect for the gear shift map design methodology in generating the gear shift map, especially for ECO^S map with a considerable improvement of the fuel

Table 4.3: Simulation results of the relative fuel economy improvement.

Shift Map	NEDC	JN1015
BASE (manufacturer)	-	-
ECO	7.3 %	9.9 %
ECO ^S	4.3 %	3.7 %

**Figure 4.21:** Mild acceleration tests.**Figure 4.22:** High acceleration tests.

economy. In order to evaluate the driveability characteristic of ECO^S map, several acceleration profiles are tested with three gear shift maps.

- *Mild acceleration profiles* consist of two tests, as shown in Figure 4.21.

For the first test, see Figure 4.21a, ECO^S map gives a better acceleration response. ECO map triggers earlier upshift to higher gear. Therefore, there is a torque interruption at the shifts $4 \rightarrow 5$ and $5 \rightarrow 6$, which causes a velocity tracking loss. Meanwhile BASE map reveals a latest upshift compared to the other two. The PS-AMT maintains at the second gear for a long period, thus bringing the engine speed to a high revolution. Therefore, at high engine speed, the reduced maximum engine torque could not continue to accommodate the vehicle with velocity tracking until an upshift to the third gear occurs.

For the second test, see Figure 4.21b, due to a high power demand, the three maps require a kick-downshift for the transmission to improve the engine traction capability by raising the engine speed. However, ECO map triggers a kick-downshift two times from the sixth gear to the fourth gear, thus resulting in a velocity loss due to a torque interruption in the PS-AMT. It is observed that when nearly approaching 80[km/h], ECO^S map allows an upshift pattern earlier than BASE map, thus improving the fuel economy. BASE map keeps the transmission at the third gear longer, thus bringing the engine speed to a high revolution. Therefore the reduced maximum torque degrades the vehicle acceleration capability compared to ECO^S map.

- *High acceleration profiles* consist of two tests, as shown in Figure 4.22.

For the first test, see Figure 4.22a, ECO^S and BASE maps result in a nearly equal velocity response. Meanwhile ECO map reveals a poor driveability followed by a torque interruption due to a two-gear kick-downshift occurrence, from the sixth gear to the fourth gear. Right after reaching the setpoint velocity, ECO^S map produces upshifts earlier than BASE map to contribute to a fuel economy improvement.

For the second test, see Figure 4.22b, ECO^S map possesses a good driveability property compared to the other maps. The results also show an earlier upshift, at higher rate to higher gear position, is held for ECO map. Meanwhile, ECO^S map is better than BASE map in terms of an upshift trigger.

In summary, the driveability tests reveal that ECO^S map is better than BASE map in fulfilling the vehicle performance. Furthermore, ECO^S map yields an earlier upshift pattern compared to BASE map, thus coming with a considerable gain in the fuel economy. Meanwhile a superior fuel economy property of ECO map is penalized by a low driveability capability.

4.6.4 Experimental Results

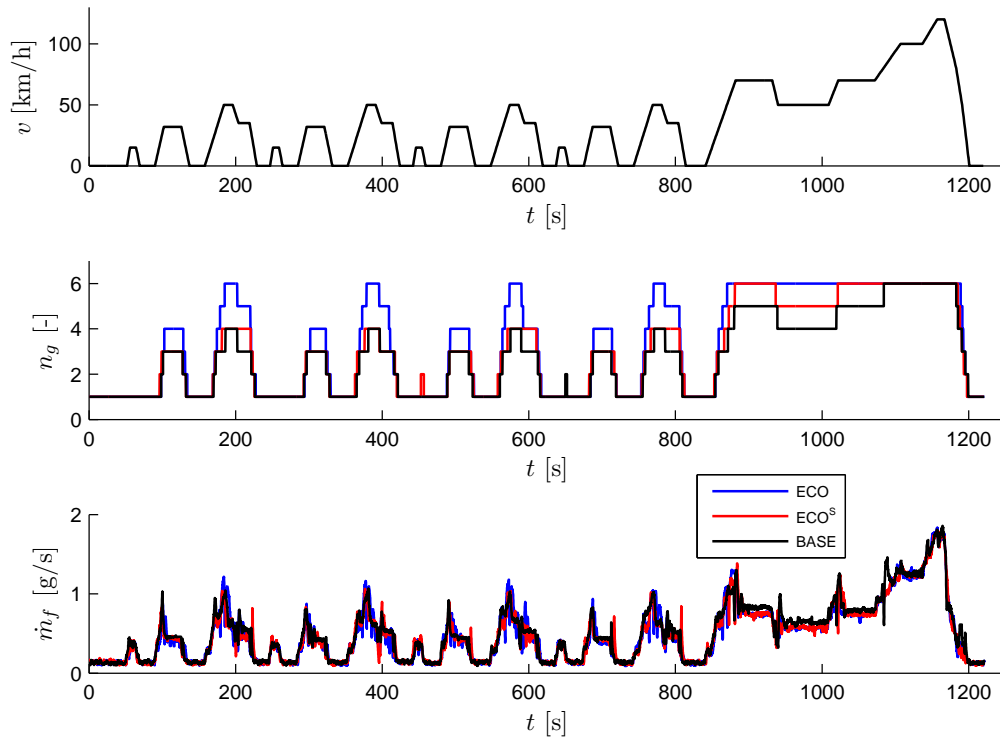


Figure 4.23: Experimental test results on NEDC.

Table 4.4: Experimental results of the relative fuel economy improvement.

Shift Map	NEDC	JN1015
BASE (manufacturer)	-	-
ECO	7.4 %	8.7 %
ECO ^S	4.8 %	3.9 %

Experimental tests of the vehicle are performed on the roller bench for the drive cycles NEDC and JN1015. The gear position and fuel rate on NEDC, corresponding with the three gear shift maps, are illustrated in Figure 4.23. ECO map yields a highest upshift frequency and allows the transmission to go to a highest gear. ECO^S map triggers an upshift earlier and stays longer at the same gear position compared to BASE map. The relative fuel economy improvement on NEDC and JN1015 are given in Table 4.4. ECO map possesses a highest fuel economy property compared to the other two. ECO^S map also improves the fuel economy considerably compared to BASE map.

By comparing the simulation results (in Table 4.3) with the experimental results (in Table 4.4), the relative fuel economy improvement on NEDC is almost equal together for both cases. The biggest difference between the simulation and experiment is realized at ECO map on JN1015, with absolute difference of 1.2%. In general, it can be observed that there is not much difference of the relative fuel economy improvement between the two validation approaches. Hence, the match between simulation and experimental results validates the effectiveness of the gear shift map design methodology.

4.7 Conclusions

In this chapter, a gear shift map design methodology for road vehicles equipped with discrete ratio transmissions was developed. The fuel economy, driveability, consistency and robustness of the designed gear shift map are guaranteed by combining an optimal gear shift strategy with a statistical gear shift pattern extraction method in the design process. The design methodology is model-based, thus giving a flexibility with changes, modifications of the powertrain specifications, and being time-efficient for the design process. Therefore, the design methodology is applicable to various powertrain configurations.

Furthermore, it is found that the minimum operable engine speed considerably affects to the fuel economy. Due to the hybridization factor, HEVs diminish the sensitivity of fuel economy to the minimum engine speed compared to conventional vehicles. The early downshift strategy in regenerative mode of HEVs will boost the energy conversion efficiency of the electric machine in generation mode, and thus further improving the fuel economy.

Integrated Predictive Gear Shift Strategy¹

Abstract - This study focuses on utilizing route information obtained from an onboard navigation system and a Global Positioning System (GPS) in the design of an Energy Management Strategy (EMS) to improve the fuel economy of Hybrid Electric Vehicles (HEVs). Given a priori driving profile over a horizon, assumed as an output of the onboard navigation system, a predictive algorithm is proposed to control the gear shift command, besides the power split and engine start-stop decision, to further improve the fuel economy. Given route information over a driving horizon in the form of road characteristics, speed limits, average speed, traveled distance, etc., a velocity algorithm is proposed to derive a fuel-optimal vehicle speed as a function of time. The two algorithms supplement each other to create a so-called integrated predictive gear shift strategy to explore the fuel saving potential of HEVs.

5.1 Benefits of The Preview Route Information

An onboard navigation system combined with a Global Positioning System (GPS) helps gaining route information, such as road characteristics, speed limits, etc., over a certain driving horizon, thus making this information available as an extra input to the Energy Management Strategy (EMS) of Hybrid Electric Vehicles (HEVs). Hence, by exploiting this route information in the design of an EMS, a further significant fuel economy improvement can be realized.

Depending on the built-in technology of the onboard navigation system, the obtained route information can be classified into two categories. In the first category, the route information is processed to yield a driving profile in terms of the vehicle speed and time within a certain horizon, which becomes a priori cycle information for the EMS. At this

¹This chapter has been prepared for a journal publication in the form as: V. Ngo, T. Hofman, M. Steinbuch, A. Serrarens. Integrated Predictive Gear Shift Strategy for Hybrid Electric Vehicles. 2012.

level, the onboard navigation system supplies a velocity setpoint for the vehicle to follow. In the second category, the route information is not well processed. It is characterized in the form of the speed limits, average speed, traveling time, etc., within a certain driving horizon. Corresponding to the first category, a so-called predictive algorithm is proposed for the EMS to anticipate the gear shift command, besides the power split and engine start-stop decisions, to further improve the fuel economy. Regarding the second category, a so-called velocity algorithm is proposed to derive a fuel-optimal velocity profile over a driving horizon. This algorithm is seen as a promising solution to be implemented in the onboard navigation system to yield a fuel-optimal velocity trajectory, which is a priori to the predictive algorithm. The two algorithms supplement each other for realizing an integrated predictive gear shift strategy achieving the highest possible fuel economy for HEVs in real-life driving.

In the literature, there is an increasing amount of studies utilizing preview route information to improve the fuel economy for HEVs. In [5, 10], the authors assume that the velocity profile over a preview route segment is available for a formulation of a predictive power split control problem. Meanwhile in [2], the authors exploit route information in the form of topographic profiles and average traveling speed to predict a reference signal for battery state of charge. This predicted battery state of charge is then used to maximize the recuperated energy despite the constraints on battery state of charge, thus improving the fuel economy. At another aspect, utilizing route information to predict the velocity trajectory over a preview route segment has increasingly gained much attention. A fuzzy-based control algorithm to compute a weighted average velocity over a look-ahead zone is seen in [111]. Markov chain is also used to model a stochastic process of the vehicle speed on a specific traveling route [57]. The authors divide this specific route into a number of intervals and define the vehicle speed at the end of each interval by a predefined Markov model. The authors in [152] formulate a velocity trajectory optimization problem for a truck application. A simple non-smooth cost function together with assumptions of constant acceleration and deceleration rates, and speed limits for every consecutive route segment, are used to derive a velocity profile over a route segment. Furthermore, in [61], the authors propose a method for building a velocity profile along the preview route cycle by dividing it into a series of segments. The speed for each segment is defined from statistical features, e.g. mean, variance, etc. Accordingly, a path forecasting-based control algorithm is proposed to optimize the battery charging and discharging for a fuel economy improvement. Nonetheless, for all mentioned studies, the obtained velocity profile along a preview route cycle or segment is not optimal in terms of fuel consumption and traveling time.

In this study, firstly, it is assumed that a prediction of the velocity profile over a certain horizon is available thanks to a GPS-based onboard navigation system. This facilitates a study of designing a predictive algorithm [96], based on Model Predictive Control (MPC), to anticipate the gear shift command besides the start-stop decision and power

split strategy for the HEV. The Dynamic Programming-Pontryagin's Minimum Principle (DP-PMP) optimal control solver, described in Chapter 3 [98], is utilized to derive the optimal solution over a certain horizon. The predictive algorithm is implemented in a receding horizon manner to reveal a suitable candidate for a realtime implementable strategy. Subsequently, involving with a definition of a velocity profile over a certain horizon, another algorithm is proposed for the HEV to derive a fuel-optimal velocity trajectory satisfying the required traveling time over a preview route segment. This so-called velocity algorithm [93] is also based on a combination of DP and PMP. PMP is used to derive an instantaneous optimal power split, meanwhile DP is used to attain an optimal velocity profile.

This chapter is organized as follows. Powertrain modeling and dynamics are outlined in Section 5.2. Formulation of a predictive gear shift problem and synthesis of a corresponding algorithm are given in Section 5.3. A velocity profile optimization algorithm is presented in Section 5.4. Implementation of the velocity algorithm in simulation environment and discussions are given in Section 5.5. Outlook of an integrated predictive gear shift strategy based on preview route information is addressed in Section 5.6. Finally, conclusions are given in Section 5.7.

5.2 Powertrain Modeling and Dynamics

The hybrid powertrain topology used in this study is shown in Figure 5.1. The main parameters of the powertrain are given in Table 5.1.

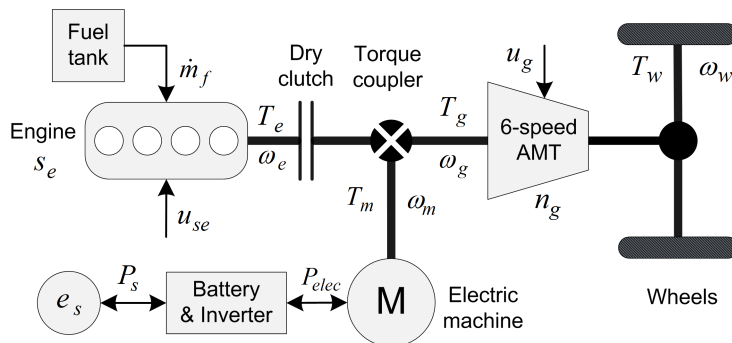


Figure 5.1: The hybrid powertrain topology, (AMT: Automated Manual Transmission; M: Electric machine).

Aiming at designing an EMS, the quasi static modeling approach is used to model the main powertrain components. Hence, the time step Δt is chosen to be equal to one second to simulate the powertrain system, thus ignoring the system dynamics faster than $1Hz$ [42]. The clutch is modeled as a switch to connect and to disconnect the

Table 5.1: The prototype vehicle specifications.

Item	Description/Quantity
Engine	diesel type, maximum torque of 200Nm, maximum power of 68kW.
Electric machine	maximum torque of 40Nm, maximum power of 6kW.
Battery	lithium-ion; capacity of 6Ah, 110V.
Transmission	6-speed automated manual transmission, $r_g = [3.817, 2.053, 1.302, 0.959, 0.744, 0.614]$.
Vehicle mass	1320kg.

engine immediately to and from the driveline. Its dynamics and limited power losses during a gear shift or an engine start are ignored in this chapter. Notice of the slippage loss of clutch at vehicle launch is also not taken into account. However, analysis of the effect of these losses to the control strategy can be found in Chapter 6.

5.2.1 Powertrain Modeling

- **Start-stop system:** the start-stop system can be modeled by a decision variable $s_e(k)$ to control the engine on-off state. When the engine is off, no fuel is consumed by the engine.

$$s_e(k) = \begin{cases} 1 & \text{if engine on,} \\ 0 & \text{if engine off.} \end{cases} \quad (5.1)$$

- **Engine:** for a certain engine speed $\omega_e(k)$, the fuel mass flow $\dot{m}_f(k)$ is modeled as an affine piece-wise second order function of the power as expressed in (5.2),

$$\dot{m}_f(k) \approx \left(a_0(k)P_e^2(k) + a_1(k)P_e(k) + a_2(k) \right) s_e(k). \quad (5.2)$$

in which the coefficients $a_0(k)$, $a_1(k)$ and $a_2(k)$ are functions of the engine speed. If assume during braking, the engine is switched off and decoupled from the driveline, then the engine braking is neglected. Therefore, the constraints on the engine speed $\omega_e(k)$ power $P_e(k)$ are as follows,

$$\omega_{e,min} \leq \omega_e(k) \leq \omega_{e,max}, \quad (5.3a)$$

$$0 \leq P_e(k) \leq P_{e,max}(\omega_e(k)). \quad (5.3b)$$

- **Electric machine:** the machine efficiency η is assumed to be constant in a normal operating state. Therefore, the power flow in motoring and generating modes is expressed as,

$$P_m(k) = \eta P_{elec}(k) \quad \text{in motoring,} \quad (5.4a)$$

$$P_m(k) = \frac{1}{\eta} P_{elec}(k) \quad \text{in generating.} \quad (5.4b)$$

The constraints on the speed $\omega_m(k)$ and power $P_m(k)$ are,

$$0 \leq \omega_m(k) \leq \omega_{m,max}, \quad (5.5a)$$

$$P_{m,min}(\omega_m(k)) \leq P_m(k) \leq P_{m,max}(\omega_m(k)). \quad (5.5b)$$

- **Battery system:** the electrical power $P_{elec}(k)$ is modeled as a quadratic function of the storage power $P_s(k)$,

$$P_{elec}(k) \approx b_0 P_s^2(k) + b_1 P_s(k) + b_2. \quad (5.6)$$

The constraints imposing on the battery system,

$$P_{s,min} \leq P_s(k) \leq P_{s,max}. \quad (5.7)$$

Notice that the battery capacity is chosen properly such that its state never exceeds a predefined lower bound $E_{s,min}$ and an upper bound $E_{s,max}$ for increasing lifetime and reliable operation. Battery operating temperature is assumed to be under tight control.

- **Automated Manual Transmission (AMT):** the transmission efficiency η is assumed to be constant for all gears. The speed and torque relations in the driveline when the clutch closed are,

$$\omega_e(k) = \omega_g(k) = \omega_w(k) r_g(k), \quad (5.8a)$$

$$T_w(k) = \eta r_g(k) T_g(k) = \eta r_g(k) T_e(k). \quad (5.8b)$$

wherein: $\omega_w(k)$ is the wheel rotational speed; $T_w(k)$ is a drive torque at the wheels; $T_g(k)$ is a transmission input torque; $r_g(k)$ denotes a gear ratio, depend on the gear position $n_g(k)$. The final reduction gear ratio is merged into the transmission ratio for a simplification.

The constraints on the gear position of a 6-speed transmission are,

$$1 \leq n_g(k) \leq 6. \quad (5.9)$$

- **Power flow model:** the power flow equilibrium at the transmission input of the powertrain is expressed as,

$$P_e(k) = P_g(k) + P_m(k). \quad (5.10)$$

5.2.2 Powertrain System Dynamics

The powertrain dynamic system consists of three state variables: the start-stop $s_e(k)$, the battery state-of-energy $e_s(k)$ and the gear position $n_g(k)$. Their dynamics are governed by three corresponding control variables $u_{se}(k)$, $P_s(k)$ and $u_g(k)$ as,

$$s_e(k+1) = s_e(k) + u_{se}(k), \quad (5.11)$$

$$e_s(k+1) = e_s(k) + P_s(k)\Delta t, \quad (5.12)$$

$$n_g(k+1) = n_g(k) + u_g(k). \quad (5.13)$$

Longitudinal dynamics: it represents the motion of the vehicle, given by:

$$v(k+1) = v(k) + a(k)\Delta t; \quad (5.14)$$

wherein the vehicle acceleration $a(k)$ is calculated by,

$$a(k) = \frac{1}{J_{v,eq}} \left(\frac{T_w(k)}{R_w} - F_{load}(k) \right),$$

where F_{load} is a resistance load due to rolling and aerodynamic resistances; $J_{v,eq}$ is an equivalent vehicle inertia at the wheel,

$$J_{v,eq} = ((J_e + J_c + J_p)r_g^2 + J_s)r_d^2 + m_v R_w^2,$$

$$F_{load} = c_r m_v g \cos \alpha + m_v g \sin \alpha + \frac{1}{2} \rho_a A_f c_d v^2,$$

and m_v is the vehicle weight; R_w is the wheel radius; J_e is the engine inertia; J_c is the clutch inertia; J_p is the transmission primary inertia; J_s is the transmission secondary inertia; ρ_a is the air density; A_f is the frontal area of vehicle; c_d is the aerodynamic drag coefficient; c_r is the rolling friction coefficient; g is the gravity coefficient; v is the vehicle speed; α is the slope of the road. It should be noted that vehicle wheel slip is ignored.

5.3 Predictive Algorithm

5.3.1 Model Predictive Control

The Model Predictive Control (MPC) methodology involves solving online an open-loop finite horizon optimal control problem subject to input, state and/or output constraints. At each discrete-time instant k , the measured variables and the process model (linear, nonlinear or hybrid) are used to calculate (predict) a future behavior of the controlled plant over a specified time horizon, which is usually called the prediction horizon and

is denoted by N_p . This is achieved by considering a future control scenario as the input sequence applied to the process model, which must be calculated such that certain desired constraints and objectives are fulfilled. To do that, a cost function is minimized subject to constraints, yielding an optimal sequence of control inputs over a specified time horizon, which is usually called control horizon and is denoted by N_c . According to the receding horizon control principle, only the first element of the computed optimal sequence of control inputs is then applied to the plant and this sequence of steps is repeated at the next discrete-time step, for the updated state [148].

5.3.2 Predictive Gear Shift Problem

To apply the MPC principle for a predictive gear shift problem in the HEV, the following assumptions are made:

- the prediction horizon and the control horizon are assumed to be equal, and is defined by the length of a preview route segment.
- a velocity profile over the horizon is assumed to be known a priori.
- a certain available drive cycle is utilized as a reference drive profile, which is assumed to be constructed from consecutive preview route segments of the whole drive mission.

The predictive gear shift problem based on MPC principle for the prototype HEV is formulated as follows.

Problem 5.1. *Assuming that at current time step k , a prediction of the vehicle speed $\tilde{v}(k) = [\hat{v}(k+1|k), \hat{v}(k+2|k), \dots, \hat{v}(k+N_c|k)]^T$ is available over a horizon N_c , find an optimal control law $\tilde{u}^*(k) = [\tilde{u}_{se}^*(k), \tilde{P}_s^*(k), \tilde{u}_g^*(k)]$, that minimize the fuel cost function $\hat{J}(k)$ accumulated over the entire driving horizon,*

$$\hat{J}(k) = \sum_{i=0}^{N_c-1} m_f \left(\hat{s}_e(k+i|k), \hat{P}_e(k+i|k), \hat{\omega}_e(k+i|k) \right) \Delta t, \quad (5.15)$$

subject to the constraints (5.1) - (5.13) and,

$$E_{s,min} \leq \hat{e}_s(k+N_c|k) \leq E_{s,max}, \quad (5.16)$$

wherein

$$\hat{e}_s(k+N_c|k) = e_s(k) + \sum_{i=0}^{N_c-1} \hat{P}_s(k+i|k) \Delta t \quad (5.17)$$

denotes the prediction of battery state-of-energy at the end of horizon; $\tilde{u}_{se}^*(k)$, $\tilde{P}_s^*(k)$ and $\tilde{u}_g^*(k)$ denote the vectors of predictive optimal control sequences over the horizon N_c at a time step k .

Problem 5.1 is solved by utilizing the Dynamic Programming-Pontryagin's Minimum Principle (DP-PMP) control approach [98]. This control approach, described in Chapter 3, appears to be a suitable candidate for solving the predictive gear shift problem due to its optimality and computational efficiency on a given drive cycle. To summarize this method, PMP is used in the inner loop to solve the instantaneous optimal solution of the engine power at every time step with a certain given gear position and engine on-off state. DP is used in the outer loop to solve the optimal gear position and engine on-off state for the whole drive cycle.

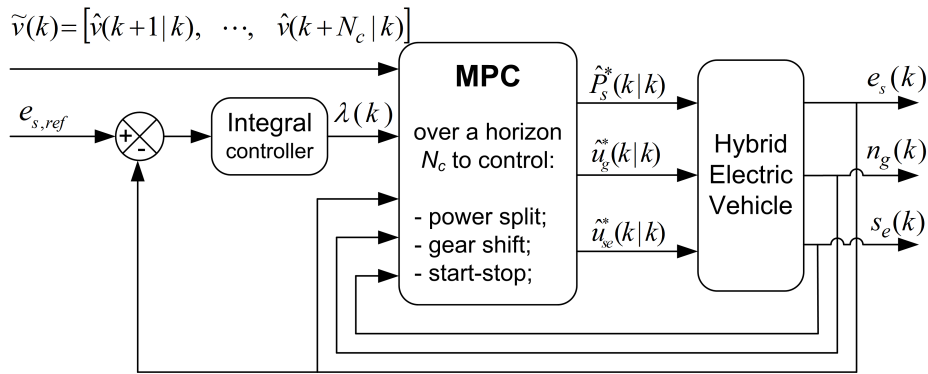


Figure 5.2: MPC-based realtime implementable control algorithm.

Implementation of the predictive gear shift strategy is shown in Figure 5.2. With a prediction over a horizon N_c of the vehicle speed $\tilde{v}(k) = [\hat{v}(k+1|k), \dots, \hat{v}(k+N_c|k)]^T$ is available at any time step k , the future optimal sequences of the gear shift command as well as the power split and the engine on-off decision are obtained by solving Problem 5.1. The receding horizon control strategy utilizes only the first elements of $\tilde{u}_g^*(k|k)$, $\tilde{P}_s^*(k|k)$ and $\tilde{u}_{se}^*(k|k)$ of the defined optimal trajectories to apply to the hybrid powertrain system for updated state; for the next step $k+1$, the whole optimization process is repeated using the updated prediction of route horizon. The Lagrange multiplier $\lambda(k)$ is kept constant during the optimization process over the horizon N_c . Due to a slow dynamics of the battery state-of-energy, an Integral (I) controller is chosen to adapt $\lambda(k)$ at every time step with respect to a reference input of the battery state-of-energy [73, 98, 150].

5.3.3 Simulation Results

For a comparison purpose, two more control strategies proposed for the gear shift problem based on DP and DP-PMP methods are simulated. These two approaches are not discussed here, so the details are referred to [98], as described in Chapter 3.

The battery state-of-energy on both NEDC and FTP75 are shown in Figure 5.3. The

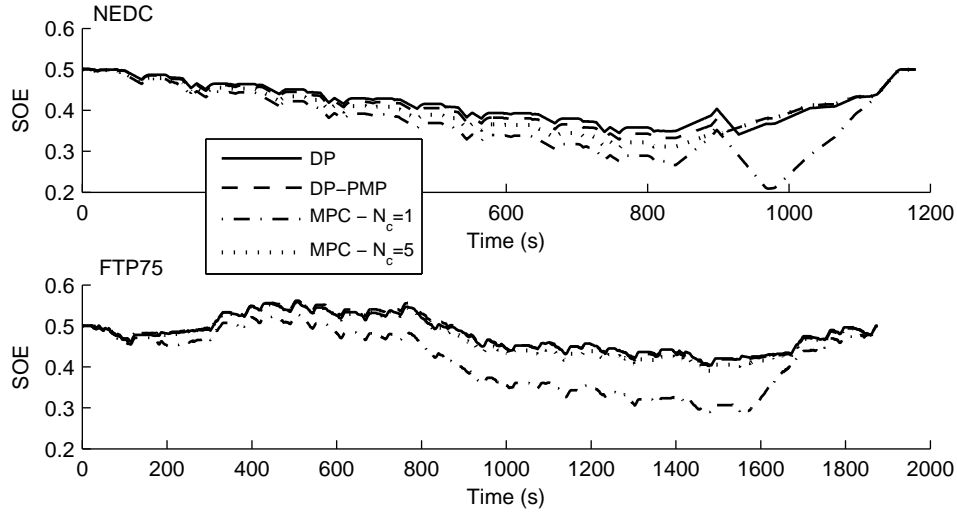


Figure 5.3: Battery state-of-energy $e_s(k)$ on NEDC and FTP75

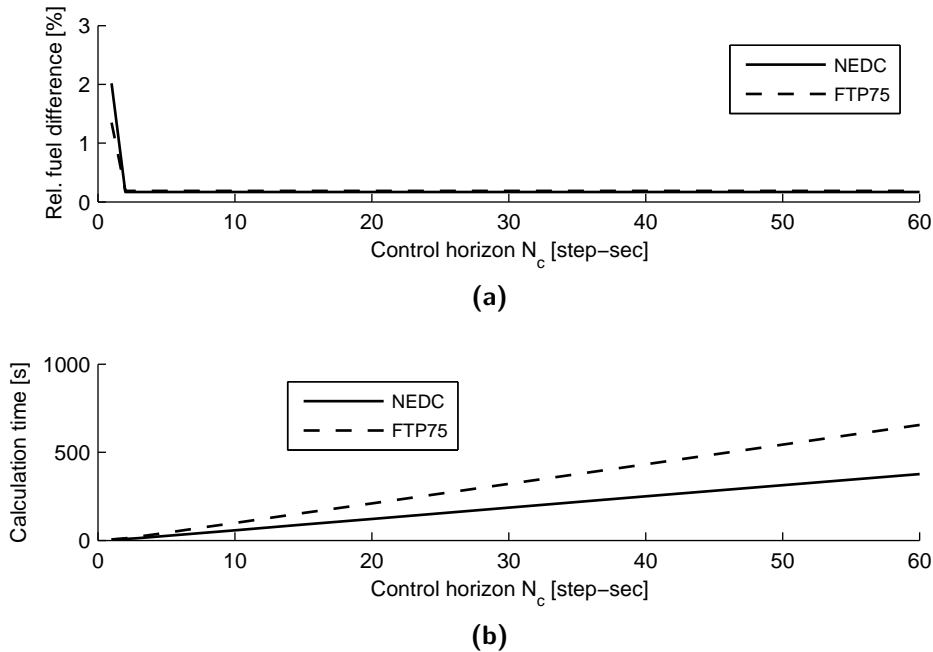


Figure 5.4: Relative fuel difference [%] and calculation time [s] vs. the control horizon N_c are shown in (a) and (b), respectively.

coefficient of the integral controller is properly tuned such that the battery state-of-energy at the end of drive cycle is equal to its initial value to ensure fair comparisons among the control approaches. The DP results (the solid lines) almost overlap the results of the DP-PMP method (the dashed lines), which renders the DP-PMP almost globally optimal from an engineering point of view. For the predictive gear shift strategy, two cases of $N_c = 1$ and $N_c = 5$ are chosen for demonstration. For the case of $N_c = 1$ (the dashed-dotted lines), $e_s(k)$ is more different from the globally optimal result. Meanwhile

for the case of $N_c = 5$ (the dotted lines), it is very close to the globally optimal result. The MPC-based approach tends to use as much electric energy as possible to minimize the fuel cost function over the driving horizon. This results in a more depletion of SOE corresponding with a shorter horizon. The online-updated Lagrange multiplier will allow the EMS to bring the battery state-of-energy back to its initial value at the end of the drive mission.

Figure 5.4a depicts simulation results of the relative fuel difference vs. the control horizon N_c on both NEDC and FTP75. The relative fuel difference is derived by comparing to the fuel consumption of the predictive gear shift strategy with that of a globally optimal strategy based on DP. With $N_c = 1$ (one time step ahead), the maximum relative fuel difference is 2% on the NEDC. It shows that with $N_c \geq 2$, the predictive gear shift strategy achieves a fuel consumption level almost close to the globally optimal solution. This reveals that the MPC-based controller can use only the vehicle model and accelerator pedal position to estimate the next vehicle speed in order to achieve a significant fuel economy improvement. Moreover, a prediction of the vehicle speed over a short horizon, for example with a horizon of 5s, is realistic with the current technology of the onboard navigation firmware. This shows the possibility of implementing such a controller in realtime without requirement of knowing (a large part of) the drive cycle a priori.

Figure 5.4b indicates an increased calculation time vs. an increased control horizon N_c for the predictive gear shift strategy. Nevertheless, the calculation time for all surveyed cases of N_c is smaller than the time length of the driving profiles. Especially, with a very short control horizon, e.g. $N_c \leq 10$, the fuel consumption is steadily close to the global optimal solution meanwhile the computation time is very small compared to the length of the drive profiles. This reveals that the MPC-based gear shift strategy is seen as a realtime implementable control algorithm from an execution time point of view.

5.4 Velocity Algorithm

Based on the onboard navigation system in combination with the GPS, the obtained route information is given in the form of a route segment length \mathcal{L} , a minimum allowable speed v_{min} and a maximum allowable speed v_{max} . The objective is to propose an algorithm to derive a fuel-optimal velocity profile over a preview route segment, such that the vehicle can finish this preview route segment at a given traveling time N_c in the most fuel efficient way.

5.4.1 Travel Requirements on a Preview Route Segment

Given the route information, the constraints imposed on the vehicle longitudinal dynamics is,

$$a_{min} \leq a(k) \leq a_{max}, \quad (5.18a)$$

$$v_{min} \leq v(k) \leq v_{max}. \quad (5.18b)$$

wherein a_{min} stands for the highest deceleration rate due to safety condition, and a_{max} represents for the highest acceleration rate due to the powertrain traction capacity and friction traction.

The traveled distance of the vehicle is defined as,

$$s(k+1) = s(k) + v(k)\Delta t + \frac{a(k)}{2}\Delta t^2,$$

wherein $a(k)$ is assumed to be constant in the time interval $k \rightarrow k+1$. The end constraint on traveled distance at the end of horizon is defined as,

$$s(N_c) = \mathcal{L}. \quad (5.19)$$

5.4.2 Optimal Velocity Problem

For an optimal velocity problem, the hybrid powertrain system are determined by four state variables $v(k)$, $s_e(k)$, $n_g(k)$, $e_s(k)$ which are controlled by $a(k)$, $u_{se}(k)$, $u_g(k)$, $P_s(k)$, respectively. The powertrain system consists of two continuous and two discrete state variables which make the optimal velocity problem really challenging for the design of a corresponding solver in terms of the optimality and computational efficiency. By discretizing all the continuous state and corresponding control variables and applying Dynamic Programming, the globally optimal solution can be obtained. Apparently, for the powertrain dynamic system with four state variables, the ‘curse of dimensionality’ is still a remained issue for the DP algorithm whose requirements on computational accuracy and efficiency are highly contradictory.

Inspired by the novel control algorithm for the hybrid dynamical system [98], described in Chapter 3, the concept of combining DP and PMP is utilized to synthesize the solver for the optimal velocity problem. However, aiming at demonstrating the generation of an optimal velocity profile over a driving horizon, the engine start-stop and gear shift strategies are excluded in the problem formulation to reduce the system dimension, and thus reducing the computational burden for the DP-PMP algorithm. The engine is assumed to stop and re-start immediately matching with driving conditions, e.g. electrically driving at low vehicle speed or low power demand, regenerative braking, engine stop idling, etc. A fuel-efficient gear shift map, discussed in Chapter 4, is applied

to shift gears. Therefore, it will render the obtained solution of the corresponding velocity algorithm suboptimal.

The optimal velocity algorithm is formulated as follows.

Problem 5.2. *Given a driving horizon length \mathcal{L} with a required traveling time not longer than N_c , find an optimal control law $u^*(k) = [a^*(k), P_e^*(k)]$, which are the vehicle acceleration and engine power sequences over the time horizon N_c , that govern the vehicle to finish the driving horizon in the most fuel economy way, or equivalently minimize the fuel cost function,*

$$\mathbf{J} = \sum_{k=0}^{N-1} \dot{m}_f(k) \Delta t \quad (5.20)$$

subject to the constraints (5.2)-(5.8), (5.10), (5.12), (5.14), (5.18) and (5.19).

Problem 5.2 is separated into two problems. The PMP is utilized in the first problem to define an instantaneous optimal power split between the engine and electric machine. The DP is applied in the second problem to define an optimal acceleration sequence over the whole driving horizon.

PMP for optimal power split

Problem 5.3. *At a certain time step k , under a certain engine on-off state $s_e(k)$ and gear position $n_g(k)$, given a possible vehicle speed from $v^i(k)$ to $v^j(k+1)$, find an optimal control law of engine power $P_e^*(k)$ that minimizes the instantaneous fuel cost function,*

$$\mathbf{J}_1(k) = \dot{m}_f(k) \Delta t, \quad (5.21)$$

subject to the dynamics and constraints described in (5.2)-(5.8), (5.10).

Assuming with a given admissible gear position $n_g(k)$ at any time step k , the constraints on engine speed and electric machine speed, (5.3a) and (5.5a), are satisfied and the required power at the wheel $P_w(k)$ can be produced by the powertrain, i.e., by both the engine and electric machine. The constraints on the electric machine and battery power (5.5b), (5.7) can be incorporated with the constraints of the engine power (5.3b) to create the new bounds for the control variable $P_e(k)$, as follows,

$$P'_{e.min}(k) \leq P_e(k) \leq P'_{e.max}(k). \quad (5.22)$$

The fuel rate (5.2) and battery efficiency model (5.6) can be approximated as affine piecewise second-order functions of engine power at a certain engine speed, and thus denoted as $\mathcal{F}_r(P_e(k), k) := \dot{m}_f(k)$ and $\mathcal{P}_s(P_e(k), k) := P_s(k)$ for compact notations.

Applying the PMP method, the objective is to find an instantaneous optimal engine power $P_e^*(k) > 0$ that minimizes an equivalent fuel cost functional $\mathbf{C}_{eq}(k)$,

$$\mathbf{C}_{eq}(k) = \left[\mathcal{F}_r(P_e(k), k) + \lambda(k) \cdot \mathcal{P}_s(P_e(k), k) \right] \cdot \Delta t, \quad (5.23)$$

Therefore, if the Lagrange multiplier $\lambda(k)$ is known, the globally instantaneous optimal engine power $P_e^*(k)$ can be obtained analytically. The globally instantaneous equivalent optimal cost value is defined correspondingly by

$$\mathbf{C}_{eq}^*(k) = \left[\mathcal{F}_r(P_e^*(k), k) + \lambda(k) \cdot \mathcal{P}_s(P_e^*(k), k) \right] \cdot \Delta t. \quad (5.24)$$

DP for optimal acceleration sequence

Problem 5.4. Find an optimal acceleration profile $a^*(k)$, resulting in an optimal velocity profile $v^*(k)$, along the driving horizon that minimizes the cost functional,

$$\mathbf{J}_2 = \sum_{k=0}^{N-1} \mathbf{C}_{eq}^*(k) \quad (5.25)$$

subject to constraints: (5.12), (5.14), (5.18) and (5.19).

The implementation of the DP algorithm is performed by discretizing the state variable $v(k)$ and the corresponding control variable $a(k)$, and then calculating the cost functional \mathbf{J}_2 for the whole driving profile. The optimal cost-to-go path is solved backwards as the following steps.

- Step $k = N_c$:

$$\mathcal{J}_2^*(N_c) = 0. \quad (5.26)$$

- Step k , $0 \leq k < N$:

$$\mathcal{J}_2^*(v^i(k), k) = \min_{a_{ij}(k)} \left[\mathbf{C}_{eq}^*(k) + \mathcal{J}_2^*(v^j(k+1), k+1) \right]. \quad (5.27)$$

Solving the above procedure backward until $k = 0$, the optimal solutions of $a^*(k)$ and $v^*(k)$ are obtained correspondingly with a specific end value of $v(N_c)$.

5.5 Implementation of the Velocity Algorithm

5.5.1 Discretization of Vehicle Longitudinal Dynamics

To apply DP for Problem 5.4, the control variable for the vehicle dynamics is required to be discretized. From the constraint (5.18a), the deceleration and acceleration grid

vectors are defined with a grid step δa as,

$$A_{dec} = \{a_{min}, a_{min} + \delta a, \dots, -\delta a\}, \quad (5.28)$$

$$A_{acc} = \{\delta a, \dots, a_{max} - \delta a, a_{max}\}. \quad (5.29)$$

For any pair of $a_{dec} \in A_{dec}$ and $a_{acc} \in A_{acc}$, the grid space a_{grid} of control variable $a(k)$ is formed

$$a_{grid} = \{a_{dec}, a_{dec} - \delta a, \dots, 0, \dots, a_{acc} - \delta a, a_{acc}\}, \quad (5.30)$$

If we define $\delta v = \delta a \Delta t$, taking into account the velocity constraint (5.18b), the grid space of velocity v_{grid} is thus in the form,

$$v_{grid} = \{v_{min}, v_{min} + \delta v, \dots, v_{max} - \delta v, v_{max}\}. \quad (5.31)$$

Furthermore, the velocity grid $v_{grid}(k)$ at any time step k is reduced further by reconstructing the minimum speed $v_{min}(k)$ and maximum speed $v_{max}(k)$ as follows,

$$v_{min}(k) = \max\{v_{min}(k-1) + a_{min}\Delta t, 0\}, \quad (5.32)$$

$$v_{max}(k) = \min\{v_{max}(k-1) + a_{max}\Delta t, v_{max}\}. \quad (5.33)$$

5.5.2 Decoupling of Velocity Algorithm

Due to a coupling of the vehicle acceleration and drive power demand, solving Problem 5.2 by separating it into Problems 5.3 and 5.4, and solving them by the PMP and DP respectively, does not guarantee a globally optimal solution.

The vehicle acceleration determines the drive power demand, which influences the power split and thus directly affecting the fuel consumption in (5.21). Meanwhile the vehicle acceleration influences the longitudinal dynamics, as in (5.14). Therefore, to ensure an optimality when decoupling Problem 5.2, an equivalent factor, denoting a rate of change of the vehicle acceleration $a(k)$ with respect to a change of the instantaneous equivalent fuel cost functional $C_{eq}^*(k)$, must be defined. Furthermore, to satisfy the end constraint on traveled distance (5.19), it requires the solver to know the rate of change of the instantaneous equivalent fuel cost functional $C_{eq}^*(k)$ with respect to a change of the vehicle speed $v(k)$.

An alternative technique is introduced to deal with this coupling in the DP algorithm. The lower and upper bounds on a_{grid} are varied by changing the values of a_{dec} and a_{acc} . Then, construct a boundary region of the feasible traveled distance profiles along the preview route segment, such that any traveled profile falling within this region will meet the constraints (5.18) and (5.19). The upper bound is constructed based on the

fastest traveling situation. Vice versa, the lower bound is based on the slowest traveling situation. This region forms a state space where the DP algorithm can find an optimal acceleration sequence. Figure 5.5 shows a boundary region of the feasible traveled distance profiles along for a certain set of $\{a_{dec}, a_{acc}\}$. An optimal traveled distance is indicated by $s^*(k)$.

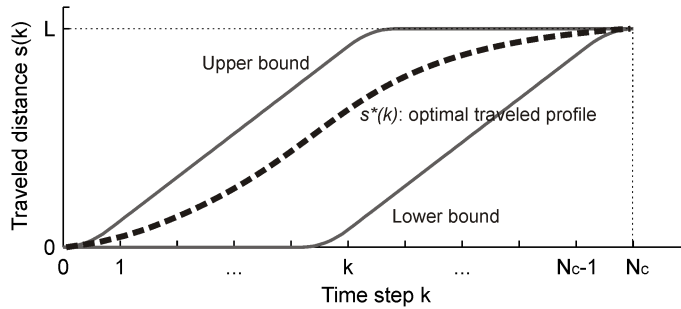


Figure 5.5: Boundary region for the feasible traveled distance profile. $s^*(k)$ indicates the optimal traveled distance profile.

By repeating this procedure with another pair of lower and upper bounds on a_{grid} , the final optimal solution is defined at the pair giving the smallest value of fuel consumption. An implementation of the proposed control algorithm is graphically given in Figure 5.6.

5.5.3 Driving Horizon

An arbitrary driving horizon, describing a final part of urban driving cycle in Europe (ECE), see the profile v_1 in Figure 5.8, is chosen for simulation and clarification. This route has a length of 626m and required time of traveling of 71s. Aiming at demonstrating a fuel economy improvement of the velocity algorithm, the end constraint on battery state-of-energy (5.34) should be respected when finishing the driving horizon for a fair comparison,

$$e_s(N_c) = e_s(0), \quad (5.34)$$

which can be achieved by an integral controller as in (5.35) to online adapt the Lagrange multiplier $\lambda(k)$,

$$\lambda(k+1) = \lambda(k) + K_I(e_s(k) - e_s(0)). \quad (5.35)$$

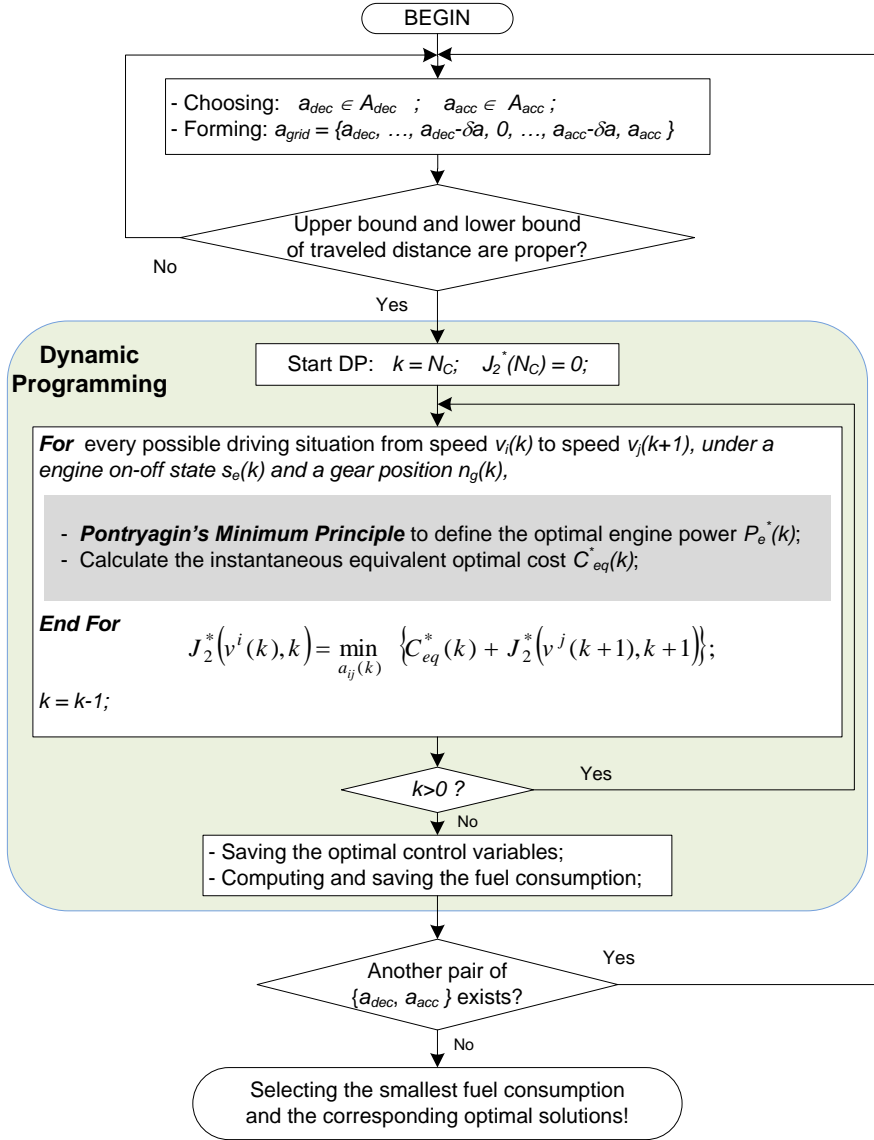


Figure 5.6: Structural implementation of the velocity algorithm.

5.5.4 Simulation Results

Sensitivity investigation of the fuel consumption with respect to a variation of $\{a_{dec}, a_{acc}\}$ is depicted in Figure 5.7. It shows that the smallest fuel consumption is realized approximately at $a_{acc} \approx 1.5m/s^2$ for all surveyed values of a_{dec} .

Figure 5.8 shows the simulation results of the traveled distance profiles (to sub-figure) and the velocity profiles (bottom sub-figure). The optimal traveled distance s_{opt} and velocity v_{opt} profiles are indicated by the circled-mark thick solid lines. Simulation results of the other three arbitrary driving profiles, denoted as v_1, v_2, v_3 , are also given for a comparison. Note that these three driving profiles are not the results of the velocity algorithm. The traveled distance requirement on the given driving segment is satisfied

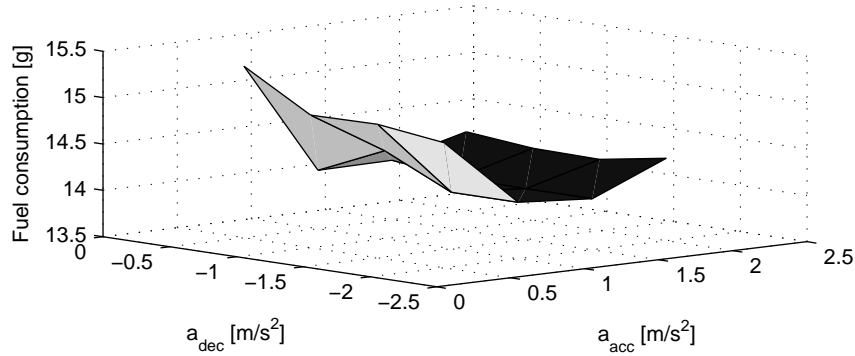


Figure 5.7: Sensitivity study of the fuel consumption with respect to a variation of $\{a_{dec}, a_{acc}\}$.

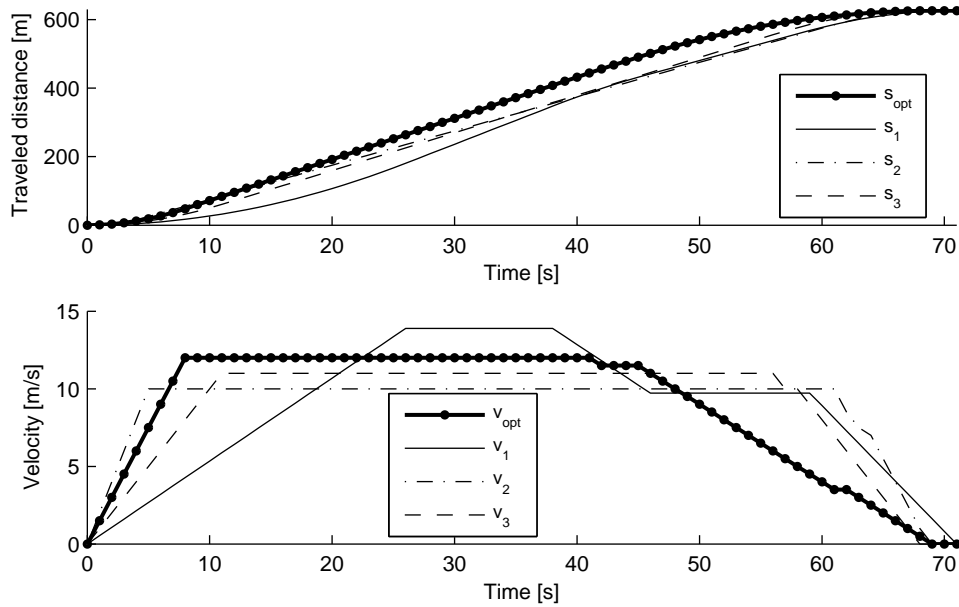


Figure 5.8: Comparison of the optimal driving profile (circled-mark thick solid line) with other three profiles along the given route segment.

by the four driving profiles (top sub-figure). The optimal velocity profile possesses a moderate acceleration and the smallest deceleration. Its deceleration phase lasts longer than the other three to take advantage of regenerative braking.

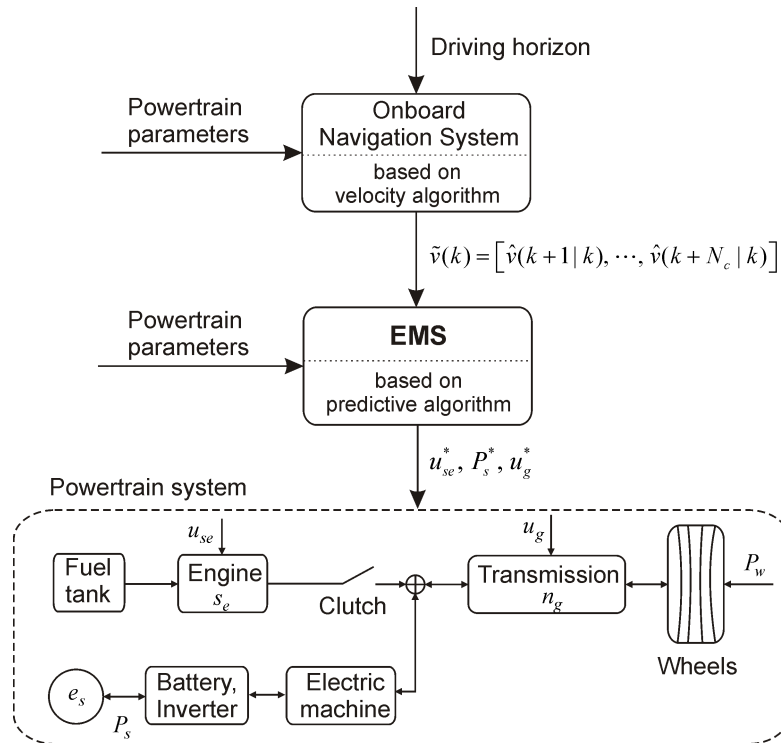
As given in Table 5.2, the fuel economy of the driving profile v_1 is 11.5% lower compared with that of the optimal profile v_{opt} . Meanwhile, for the other two arbitrary driving profiles v_2 and v_3 , a severe reduction in fuel economy is 15.1% and 16.5%, respectively. The end constraint of the battery state-of-energy is guaranteed by the condition $|\Delta e_s| = |e_s(N_c) - e_s(0)| / e_s(0) * 100 < 1\%$. Although, the optimal velocity problem is partly solved using a surface response model to find an optimal setting for the bounds on a_{grid} , and creates a suboptimal solution, it shows a significant fuel economy improvement.

Table 5.2: Fuel consumption of four driving profiles along the route segment.

Profile	$ \Delta e_s $ [%]	Fuel [g]	Fuel economy [%]
v_{opt}	0.5	14.14	baseline
v_1 (ECE)	0.6	15.76	-11.5
v_2	0.6	16.28	-15.1
v_3	0.8	16.48	-16.6

5.6 Integrated Predictive Gear Shift Strategy

A concept of an integrated predictive gear shift strategy for the transmission equipped in a HEV is created by i) embedding the velocity algorithm on an onboard navigation system, ii) implementing the predictive algorithm for a corresponding EMS. Output of the onboard navigation system is a prediction of the velocity profile over a driving horizon. This prediction information is put into the EMS based on the predictive algorithm controlling the gear shift besides the engine on-off decision and power split strategy. Figure 5.9 graphically demonstrates this concept. Validated by a fuel economy improvement for each separated algorithm, the concept is proved to work in principle.

**Figure 5.9:** Schematic diagram of the concept of integrated predictive gear shift strategy.

5.7 Conclusions

In this study, a concept of integrated predictive gear shift strategy for the transmission equipped in a HEV was demonstrated and validated in simulation environment. Despite the fact of being not globally optimal, the velocity algorithm significantly improves the fuel economy for the HEV by proposing an optimized velocity profile for the vehicle to follow. The predictive algorithm successfully utilizes a short preview horizon to realize a fuel economy improvement very close to that of the globally optimal control algorithm.

Future work should focus on implementing the velocity algorithm on a preview route segment with a relatively short horizon, e.g. an acceleration phase, a cruise phase or a deceleration phase, etc., to analyze the effect of the horizon length on the optimal solution. Upgrading the velocity algorithm such that it is able to handle with a free final state of the vehicle speed and battery state-of-energy (at the end of each driving horizon) is also required. This makes the upgraded velocity algorithm applicable for a certain driving mission consisting of consecutive fuel-optimal driving segments, while still achieving a desired finishing time.

Effect of Gear Shift and Engine Start Losses¹

Abstract - In this study, the energetic loss models involved with gear shift and engine start in a parallel Hybrid Electric Vehicle (HEV) equipped with an Automated Manual Transmission (AMT) will be introduced. An optimal control algorithm for the start-stop, power split and gear shift problem based on the Dynamic Programming-Pontryagin's Minimum Principle control approach is utilized to evaluate the effect of the gear shift and engine start losses on the optimal solution. Furthermore, with preview route information available, a Model Predictive Control (MPC) algorithm is applied to investigate an achievable fuel saving with respect to the prediction horizon. Under the influence of the gear shift loss, simulation results of a passenger HEV disclose a superior fuel efficient property of the powershift-AMT over the AMT. It also shows that by reducing the interruption time in the gear shift process as much as possible, the AMT vehicle can reduce the fuel consumption noticeably compared to the PS-AMT vehicle. The study also reveals a minimum prediction length of 5s required for the design of a MPC-based realtime implementable controller to get the possible maximum fuel economy under the impact of the engine start loss.

6.1 Introduction

Design of the Energy Management Strategies (EMSs) for Hybrid Electric Vehicles (HEVs) in general aims at optimally choosing the power split between the internal combustion engine and electric machine to improve the fuel economy, for example see, [3, 25, 50, 63, 67, 73, 83, 96, 98, 107, 118, 125, 126, 134, 156]. For HEVs equipped with discrete ratio transmissions, e.g. an Automated Manual Transmission (AMT), the operating points of the hybrid powertrain are not only defined by the power split but also by

¹This chapter has been prepared for a journal publication in the form as: V. Ngo, T. Hofman, M. Steinbuch, A. Serrarens. Effect of Gear Shift and Engine Start Losses on Control Strategies for Hybrid Electric Vehicles. 2012.

the start-stop state and gear position. Hence, by further optimizing the start-stop and gear shift strategies, the fuel economy is improved substantially compared to the EMSs optimizing only the power split. Consequently, the controller allows i) the transmission to shift up earlier with higher frequency and to higher values, and ii) the engine to stop and restart more frequently, for a fuel benefit [3,25,63,67,83,96,98,107,118,125,134,156]. At a gear shift or engine start event, an amount of energy related to clutch slippage, vehicle velocity loss during shifting, and engine cranking, is lost. So, it is worthwhile to concern these losses when the number of shifts and starts is at a considerable amount for a certain drive cycle. However, none of the mentioned published papers has been addressing the relevant gear shift and engine start losses, and thus analyzing their effect on the control strategies and fuel consumption. Therefore, this study will focus on these challenges.

Regarding to the gear shift, a shift decision will encounter a change of the engine rotating dynamics, a possible clutch operation loss and a consequent vehicle velocity loss due to an interrupted tractive torque. Hence, compensation for the gear shift loss might cost additional fuel. For a decision of restarting the engine, apart from the tractive torque required at the wheels, an extra torque from the electric machine is needed for cranking up the engine from stand still and compensating the friction loss in the clutch. This would consume an amount of electric energy which sometime later can cost fuel for recharging. Engine combustion takeover after the cranking phase for each engine start process should also be considered. In summary, on highly dynamic drive cycles with frequent stop-go patterns, the number of gear shifts and engine restarts will increase. Hence, the fuel consumption might increase.

Therefore, this study will bring the aforementioned aspects, regarding to the losses of shifting gears and restarting engine, into the EMS [98] to analyze their influence on the fuel economy. It's worthwhile to mention that the proposed EMS for a parallel HEV equipped with an AMT, optimally control not only the power split but also the engine start-stop and gear shift. The control algorithm based on a combination of Dynamic Programming (DP) and Pontryagin's Minimum Principle (PMP) guarantees an optimality and is computationally efficient. First of all, a sensitivity study of the fuel economy with respect to the gear shift command is conducted towards a gear shift hysteresis strategy implementation to get rid of the shift busyness and hunt. A gear shift loss model capturing the main shifting characteristics is introduced and incorporated in the EMS for a fuel economy evaluation. Then, a sensitivity study with respect to the interruption time of tractive torque during a gear shift process reveals a perception of a fuel-efficient advantage of the powershift transmissions (Dual Clutch Transmission (DCT), PowerShift-AMT (PS-AMT) [132], etc.) compared to non-powershift ones (Manual Transmission (MT), AMT). In addition, an engine start loss model corresponding to the prototype HEV is built and embedded in the EMS design to reflect its effect on fuel consumption. Moreover, Model Predictive Control (MPC) for the HEV appears

to be a possible candidate for a realtime implementation when using preview route information [96]. Therefore, the impact of the prediction horizon length on the achievable fuel saving of the HEV with the engine start loss modeled will be investigated for this realtime implementable control algorithm.

The content of this research work is organized as follows. The hybrid powertrain model is given in Section 6.2. The optimal control problem for the engine start-stop decision, power split and gear shift strategies is formulated in Section 6.3. Gear shift loss model and its influence on the fuel economy will be discussed in Section 6.4. Engine start loss model and the related optimal control problem are addressed in Section 6.5. Prediction horizon length sensitivity study on the fuel economy resulted from the corresponding predictive control algorithm under the impact of engine start loss is given in Section 6.6. Finally, conclusions are given in Section 6.7.

6.2 Hybrid Powertrain Model

Aiming at deriving an EMS, the quasi-static models of the powertrain components are used and simulated with a time step of one second. The system dynamics faster than $1Hz$ are ignored [42]. The clutch system is considered as a discrete switch to connect and to disconnect the engine immediately to and from the driveline. The energy losses during the clutching process of the gear shift and engine start are addressed explicitly in Sections 6.4 and 6.5, respectively.

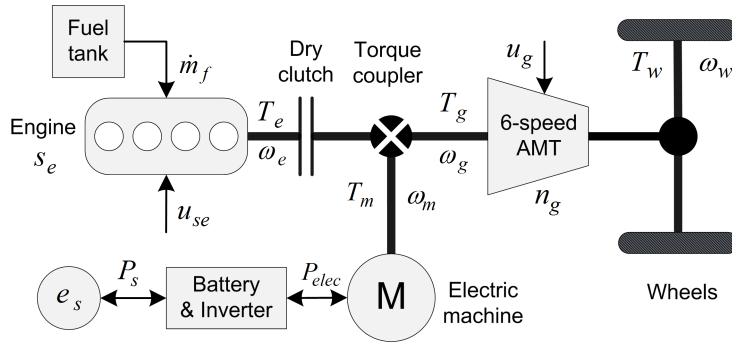


Figure 6.1: A parallel hybrid electric vehicle topology, (AMT: Automated Manual Transmission; M: Electric machine).

The start-stop system can be modeled by using a discrete state variable $s_e(k)$ to represent the engine on-off state,

$$s_e(k) = \begin{cases} 1 & \text{if engine on,} \\ 0 & \text{if engine off.} \end{cases} \quad (6.1)$$

We ignore the engine drag torque during deceleration phase due to a disconnection of

the engine from the driveline and the engine is shut down. For a certain engine speed $\omega_e(k)$, the fuel consumption model is approximated as an affine piece-wise second order function of the engine power $P_e(k)$. The fit coefficients a_0 , a_1 , and a_2 are dependent on the engine speed,

$$\dot{m}_f(P_e(k), k) \approx (a_0 P_e^2(k) + a_1 P_e(k) + a_2) s_e(k). \quad (6.2)$$

The electric machine efficiency η_m is assumed to be constant. Therefore the power $P_m(k)$ flowing in and out of the electric machine in motoring mode and generating mode is expressed as follows,

$$\begin{aligned} P_m(k) &= \eta_m P_{elec}(k) \quad (\text{if motoring}); \\ P_m(k) &= \frac{1}{\eta_m} P_{elec}(k) \quad (\text{generating}). \end{aligned} \quad (6.3)$$

We assume the battery state-of-energy $e_s(k)$ to be in a nominal range $[E_{s,min}, E_{s,max}]$ such that its effect to the battery efficiency model can be ignored. Hence, the electrical power $P_{elec}(k)$ can be approximated as a quadratic function of the chemical power $P_s(k)$ as,

$$P_{elec}(k) \approx b_0 P_s^2(k) + b_1 P_s(k) + b_2. \quad (6.4)$$

The gearbox efficiency model is assumed to be constant η for all gears. The torque and speed relations in the driveline (the clutch is closed) are given by,

$$T_w(k) = T_g(k) r_g(k) \eta, \quad (6.5)$$

$$\omega_w(k) = \frac{\omega_m(k)}{r_g(k)}, \quad \omega_m(k) = \omega_g(k), \quad (6.6)$$

where $T_w(k)$ is the transferred torque at the wheels (assumed equal to output torque of the transmission); $T_g(k)$ is the input torque of the transmission; $r_g(n_g(k))$ denotes the discrete gear ratio depending on the gear position $n_g(k)$; $\omega_w(k)$ is the wheel speed; $\omega_m(k)$ is the electric machine speed and $\omega_g(k)$ is the transmission input speed.

At any time step k , the power flow equilibrium in the parallel hybrid powertrain topology is expressed as,

$$P_e(k) = P_g(k) + P_m(k), \quad (6.7)$$

with $P_g(k)$ is the power flow at the transmission input.

The vehicle longitudinal motion dynamics in discrete time domain is given by,

$$\omega_w(k+1) = \omega_w(k) + \frac{1}{J_{v,eq}} (T_w(k) - F_{load}(k) R_w) \Delta t, \quad (6.8)$$

where F_{load} is the resistance loads due to rolling and aerodynamic resistances; $J_{v,eq}$ is an equivalent vehicle inertia at the wheel,

$$J_{v,eq} = ((J_e + J_c + J_p)r_g^2 + J_s)r_d^2 + m_v R_w^2,$$

$$F_{load} = c_r m_v g \cos \alpha + m_v g \sin \alpha + \frac{1}{2} \rho_a A_f c_d v^2,$$

and m_v is the vehicle weight; R_w is the wheel radius; J_e is the engine inertia; J_c is the clutch inertia; J_p is the transmission primary inertia; J_s is the transmission secondary inertia; ρ_a is the air density; A_f is the frontal area of vehicle; c_d is the aerodynamic drag coefficient; c_r is the rolling friction coefficient; g is the gravity coefficient; v is the vehicle speed; α is the slope of the road.

6.3 Hybrid Powertrain Control Algorithm

6.3.1 Optimal Control Problem Formulation

Problem 6.1. *Given a drive cycle $v(k)$ with a time length of N , implying that the vehicle longitudinal dynamics (6.8) is deterministic, find an optimal control law $u^*(k) = [u_{se}^*(k), P_s^*(k), u_g^*(k)]$, which are the optimal control variables for the start-stop system, battery state-of-energy, and gear shift, respectively, that minimize the fuel cost function described by,*

$$\mathbf{J} = \sum_{k=0}^{N-1} m_f(P_e(k), \omega_e(k), k) \Delta t, \quad (6.9)$$

subject to:

1. the hybrid powertrain dynamics,

$$s_e(k+1) = s_e(k) + u_{se}(k), \quad (6.10)$$

$$e_s(k+1) = e_s(k) + P_s(k) \Delta t, \quad (6.11)$$

$$n_g(k+1) = n_g(k) + u_g(k), \quad (6.12)$$

2. the constraints on the speeds of the drivetrain components,

$$\omega_{e,min} \leq \omega_e(k) \leq \omega_{e,max}, \quad (6.13a)$$

$$0 \leq \omega_m(k) \leq \omega_{m,max}, \quad (6.13b)$$

3. the constraints on the engine power $P_e(k)$, electric machine power $P_m(k)$ and battery power $P_s(k)$ are,

$$0 \leq P_e(k) \leq P_{e,max}(\omega_e(k)), \quad (6.14a)$$

$$P_{m,min}(\omega_m(k)) \leq P_m(k) \leq P_{m,max}(\omega_m(k)), \quad (6.14b)$$

$$P_{s,min} \leq P_s(k) \leq P_{s,max}, \quad (6.14c)$$

4. the constraints on the system states, which are the engine start-stop state and gear position,

$$0 \leq s_e(k) \leq 1, \quad (6.15)$$

$$1 \leq n_g(k) \leq 6, \quad (6.16)$$

here, note that the constraints on the engine on-off state are described by (6.1).

5. the end constraint of the battery state-of-energy,

$$e_s(N) = e_s(0) + \sum_{k=0}^{N-1} P_s(k)\Delta t = e_s(0), \quad (6.17)$$

6. the constraints on the control variables,

$$u_{se}(k) = \begin{cases} [0, 1] & \text{if } s_e(k) = 0, \\ [-1, 0] & \text{if } s_e(k) = 1; \end{cases} \quad (6.18)$$

$$u_g(k) \in \{u_{g,min}, \dots, -1, 0, 1, \dots, u_{g,max}\}, \quad (6.19)$$

wherein Δt is the time step of the discrete system; $u_{g,min}$ and $u_{g,max}$ are the lower and upper bounds for the gear shift command $u_g(k)$.

In this study, the upper and lower bounds of the state variable $e_s(k)$ are ignored by an assumption that the battery capacity $E_{s,cap}$ is chosen properly such that $e_s(k)$ never exceeds its bounds for increasing the battery lifetime and reliable operation. Battery operating temperature is assumed to be under tight control.

Dynamic Programming-Pontryagin's Minimum Principle (DP-PMP) control approach, described in Chapter 3, appears to be a suitable candidate to solve the formulated optimal control problem. For further details of this approach, interested readers are referred to [98]. In summary, PMP is used in the inner loop to solve the instantaneous optimal solution of the battery power (or the engine power alternatively) at every time step with a certain gear position and engine on-off state. DP is used in the outer loop to solve the optimal gear position and the engine on-off state for the whole drive cycle.

6.3.2 Gear Shift Command Sensitivity

From (6.12), the bounds of the gear shift command $u_g(k)$ determine the dynamic behavior of the next gear position $n_g(k+1)$, which eventually affects the fuel economy. From (6.19), $u_{g,min}$ and $u_{g,max}$ are varied to investigate a sensitivity of the optimal solution with respect to the gear shift dynamics. With a 6-speed transmission, the upper bound and the lower bound on $u_g(k)$ are 5 and -5 respectively which leads to five main cases of consideration as in (6.20),

$$\begin{bmatrix} u_{g,min} \\ u_{g,max} \end{bmatrix} \in \left\{ \begin{bmatrix} -1 \\ 1 \end{bmatrix}, \begin{bmatrix} -2 \\ 2 \end{bmatrix}, \begin{bmatrix} -3 \\ 3 \end{bmatrix}, \begin{bmatrix} -4 \\ 4 \end{bmatrix}, \begin{bmatrix} -5 \\ 5 \end{bmatrix} \right\}. \quad (6.20)$$

The drive cycles chosen for testing the control algorithm are NEDC, FTP75, LA92 and CADC to represent real-life driving scenarios (see, Appendix C). Simulation results of the fuel consumption for the case $[u_{g,min}; u_{g,max}] = [-1; 1]$ are shown in Table 6.1. Compared to this case, the relative fuel economy of the other cases mentioned in (6.20) is very small ($\approx 0\%$). This means that increasing the bounds on the gear shift command does not affect the fuel economy. In other words, choosing $u_g(k) \in \{-1, 0, 1\}$ is the optimum gear shift command in terms of the fuel economy and the engine speed variation reduction during shifting.

Table 6.1: Fuel consumption with the gear shift command bound $[u_{g,min}; u_{g,max}] = [-1; 1]$.

Cycle	NEDC	FTP75	LA92	CADC
Fuel [g]	300.5	480.3	530.8	1873.9

Depicted in Figure 6.2 are the results of the gear position, engine on-off state and battery state-of-energy on the NEDC. They are almost the same for five cases of $[u_{g,min}; u_{g,max}]$, described in (6.20), which further demonstrates the robustness of the controlled powertrain system with respect to the uncertainty of the gear shift command bounds.

6.3.3 Gear Shift Hysteresis

The proposed control strategy allows the transmission to shift as much as possible with a maximum shift frequency equal to the frequency of the discrete powertrain system for fuel savings. Actually, vehicles equipped with an AMT can only shift the transmission under the respect of so-called shift hysteresis to prevent the gear hunting, i.e. shifting up and down at two consecutive time steps, and avoid losing the driveability. This practical

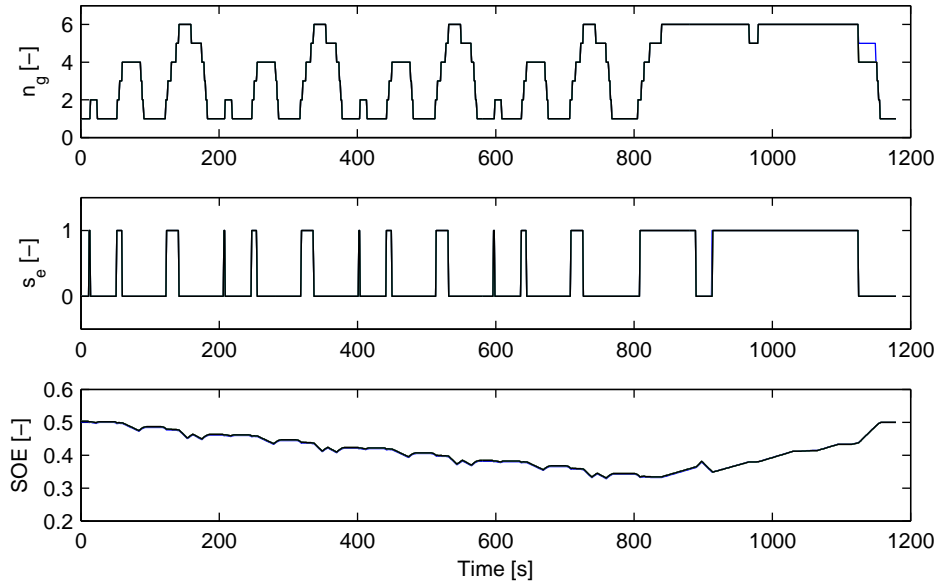


Figure 6.2: Simulation results on the NEDC for five cases of the gear shift command bounds $[u_{g,min}; u_{g,max}]$.

issue can be implemented into the EMS by imposing a constraint of not changing gear within n_{hys} time steps after each previous shifting, described by a general shift condition,

$$\begin{array}{l}
 \textit{general shift condition} \\
 \hline
 u_{hys} = u_g(k - n_{hys}) + \dots + u_g(k - 1); \\
 \textbf{if } u_{hys} == 0 \\
 \quad u_g(k) \in \{-1, 0, 1\}, \\
 \textbf{else} \\
 \quad u_g(k) = 0, \\
 \textbf{end} \\
 \hline
 \end{array}$$

This means that a gear shift decision can be only made when a hysteresis time n_{hys} is respected. The powertrain dynamic system for control will increase in dimension by an order of $n_{hys} - 1$. Therefore, $n_{hys} > 1$ will make the control system more complicated and affect to the computation load of the control algorithm. Hence, in this study $n_{hys} = 1$ is adopted for a reasonable compromise, which leads to a simplified shift hysteresis condition as in (6.21),

$$u_g(k - 1)u_g(k) = 0. \quad (6.21)$$

Simulation results are given in Table 6.2. The relative difference of the shift hysteresis case compared to the baseline is indicated in the parenthesis. It depicts that the shift hysteresis strategy reduces the number of shifts significantly, meanwhile the fuel econ-

Table 6.2: Simulation results corresponding with a study on the gear shift hysteresis. Relative difference is indicated in the parenthesis

Cycle	Baseline		Shift hysteresis	
	Fuel [g]	No. shift	Fuel [g]	No. shift
NEDC	300.5	73	301.8 (0.4%)	71 (-2.7%)
FTP75	480.3	423	481.5 (0.3%)	197 (-53.4%)
LA92	530.8	358	531.8 (0.2%)	179 (-50%)
CADC	1873.9	651	1876.2 (0.1%)	244 (-62.5%)

omy impact is small. The obtained results reveal an essential role of the shift hysteresis in removing the unnecessary shifts not affecting the fuel economy considerably.

6.4 Gear Shift Loss Model and Control Problem

The gear shift process of an AMT-based vehicle includes three chronological phases: 1) disengaging the clutch and lowering the engine torque; 2) shifting to the expected gear; and 3) engaging the clutch while increasing the engine torque again. The speed and torque profiles of both clutch and engine during the shifting process are assumed to be properly controlled in every phase to ensure quick shifting, more comfort and and less friction losses, etc. [39, 132]. The energetic loss model involved with the gear shift process is described next.

6.4.1 Gear Shift Loss Model

A decision of shifting gears is meaningful when the vehicle is in acceleration or cruising modes, wherein the engine is used as a primary mover to meet the required positive drive torque at the wheels. The transmission can: i) shift up to accommodate the engine speed to the changing vehicle speed and improve the fuel economy, or ii) even shift down, called kick-downshift, if a higher acceleration or driving uphill is required.

During electrically driving mode (the electric machine is used to solely propel the vehicle) or deceleration mode (the electric machine operates as a generator to recuperate the kinetic energy), the hybrid powertrain with a start-stop functionality can turn the engine off and disconnect it from the driveline. The clutch is opened. Apparently, there is no slippage phenomena in clutch which leads to no energy loss involved. The gear

shift during these driving modes can be assumed to occur immediately.

In summary, only upshift and kick-downshift events are considered for modeling the gear shift loss which is described next.

Upshift

Figure 6.3a demonstrates the simplified uniform profiles of the speed and torque of the engine and clutch in an upshift process. Three phases of the shifting process occurring in the interval Δt_{shift} are indicated. In phases 1 (disengagement) and 3 (engagement), the engine torque and clutch transferred torque are controlled to have a declined and inclined patterns to allow a comfort disengagement and engagement, respectively. Hence, there exists a slippage phenomena at the clutch to transfer the tractive torque to the wheels during these phases. The speed difference between the engine and clutch during these phases is small enough, thus assuming to be zero [34,39,132,165]. In phase 2, the clutch is fully disengaged for shifting gears, and there is an interruption of the tractive torque which finally results in a velocity loss for an interval Δt_{int} . Due to the engine drag torque, the engine speed is assumed to reduce to a synchronization point corresponding to the clutch speed at the next higher gear. Denoting the engine torque right before and after shifting is T_e , then the engine torque and tractive torque transferred to the wheels during an upshift process can be modeled as,

- in phases 1, 2 and 3, the corresponding engine torque can be averaged as,

$$\begin{aligned} T_{e,1} &= \frac{T_e}{2}, \\ T_{e,2} &= 0, \\ T_{e,3} &= \frac{T_e}{2}; \end{aligned} \tag{6.22}$$

- the average tractive torque transferred to the wheels during an upshift process (due to a clutch slippage in phases 1 and 3),

$$T_{e,shift} = \frac{T_e}{2} \frac{\Delta t_{shift} - \Delta t_{int}}{2\Delta t_{shift}}. \tag{6.23}$$

Kick-downshift

Figure 6.3b shows the typical profiles of the engine and clutch torque for a kick-downshift process [34,39,132,165]. It also consists of three phases. In phases 1 and 3, the engine and clutch torque profiles are similar to an upshift. In phase 2, the clutch torque is zero, meanwhile the engine torque is maintained above zero to increase the engine speed

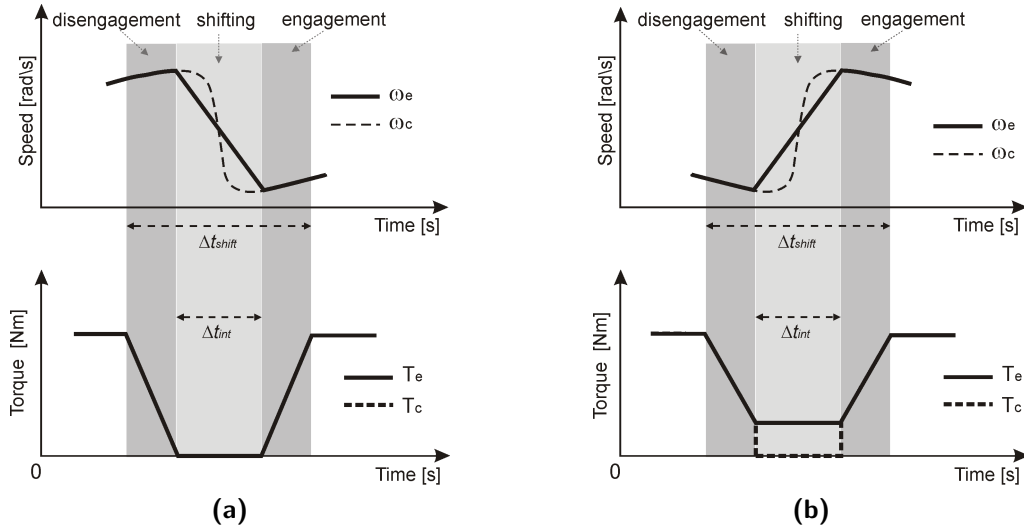


Figure 6.3: Simplified engine and clutch profiles during an upshift process (a), and a kick-downshift process (b).

up to the synchronization point corresponding to the clutch speed at next lower gear. Hence the engine torque and tractive torque transferred to the wheels during an upshift process can be modeled as,

- in phases 1, 2 and 3, the corresponding engine torque can be averaged as,

$$\begin{aligned} T_{e,1} &= \frac{T_e + T_{e,2}}{2}, \\ T_{e,2} &= J_e \frac{\omega_{e,3} - \omega_{e,1}}{\Delta t_{int}}, \\ T_{e,3} &= \frac{T_e + T_{e,2}}{2}, \end{aligned} \quad (6.24)$$

where J_e is the equivalent inertia on the engine side (seen from the clutch); $\omega_{e,1}$ is the engine speed in phase 1 (right before shifting); $\omega_{e,3}$ is the engine speed in phase 3 (right after shifting);

- the average tractive torque transferred to the wheels during a kick-downshift process (due to a clutch slippage in phases 1 and 3),

$$T_{e,shift} = \frac{T_e + T_{e,2}}{2} \frac{\Delta t_{shift} - \Delta t_{int}}{\Delta t_{shift}}. \quad (6.25)$$

Note that the engine torque in phase 2 does not constitute the tractive torque, but it still results in additional fuel consumption.

Velocity tracking loss

As analyzed in the upshift and kick-downshift and demonstrated in Figure 6.3, the tractive torque is totally lost during phase 2 of the shifting process due to a clutch

opening. During phases 1 and 3, the tractive torque transferred to the wheels is defined by (6.23) and (6.25). Taking all these tractive torque characteristics into account will result in a velocity loss for each upshift or kick-downshift event. Therefore, the vehicle needs to accelerate more, later in the driving mission, in order to compensate for the loss in each gear shift. This will definitely influence the fuel economy of the vehicle.

Apparently, the length of the power interruption in phase 2, denoted by Δt_{int} , mainly decide the effect level of the gear shift loss on the vehicle performance. In reality, the interruption time Δt_{int} is varied according to the types of vehicles and the clutch operation conditions [39,132]. Therefore, a sensitivity study with respect to Δt_{int} should be done for a thorough analysis of the gear shift loss effect.

6.4.2 Optimal Control Problem with Gear Shift Loss

The design of EMSs for AMT-based HEVs always assumes the gear shift to occur instantly, which means that there is no torque interruption at the wheels when shifting and the vehicle keeps tracking the velocity and acceleration profiles. This is only true when the transmission possesses a powershift technology, e.g. PS-AMT, DCT, AT, etc., to enable the tractive torque to be transferred to the wheels during shifting. As said for AMTs, the consequence of a gear shift activity is loss of velocity tracking. To arrive the final destination on time, the vehicle must accelerate more after each gear shift to compensate for the velocity loss accumulated during shifting.

As shown in Section 6.3.3, the optimal control strategy for the HEV yields many shifts for fuel economy improvement. Therefore, it's a fair evaluation to include AMT gear shift loss model to the fuel-optimal EMS. Note that, as a consequence of the velocity tracking loss, the vehicle can not exactly follow a given drive cycle, and thus the next vehicle speed is gear shift dependent. An EMS optimizing further the driving profile (velocity, traveled time) [93,151] is an appropriate solution for the control problem with the gear shift loss model involved. Such a control algorithm is complicated and out of scope of this study. In order to cope with the velocity tracking loss, an appropriate approach to investigate effect of the gear shift loss on fuel economy and evaluate powershift technology is introduced as follows.

PS-AMT: the EMS is designed with no gear shift loss model taken into account. This means the AMT has a powershift technology to ensure a velocity tracking. The designed EMS optimizes the engine on-off state, power split and gear shift.

AMT: the hybrid powertrain is equipped with an AMT. The gear shift loss model is respected during the design process of the EMS. The optimal gear shift strategy obtained from the PS-AMT is now used as a prescribed one for the AMT. To ensure the same average speed with the PS-AMT in order to get a fair comparison on the fuel economy, the next vehicle speed is controlled by an integral regulator. The powertrain

is simulated in a forward-facing manner and the EMS optimizes the engine on-off state and power split.

6.4.3 Simulation Results

The gear shift hysteresis strategy is taken into account in the case of the PS-AMT to avoid any gear shift hunting pattern. Figure 6.4 depicts a zoom-in of one part of the simulation results on the NEDC. It can be seen that when an upshift occurs, the AMT vehicle loses velocity tracking, represented by the corresponding flat vehicle speed (the dotted line). Right after each upshift, the AMT vehicle accelerates higher than the PS-AMT vehicle to compensate for the velocity tracking loss during the gear shift before.

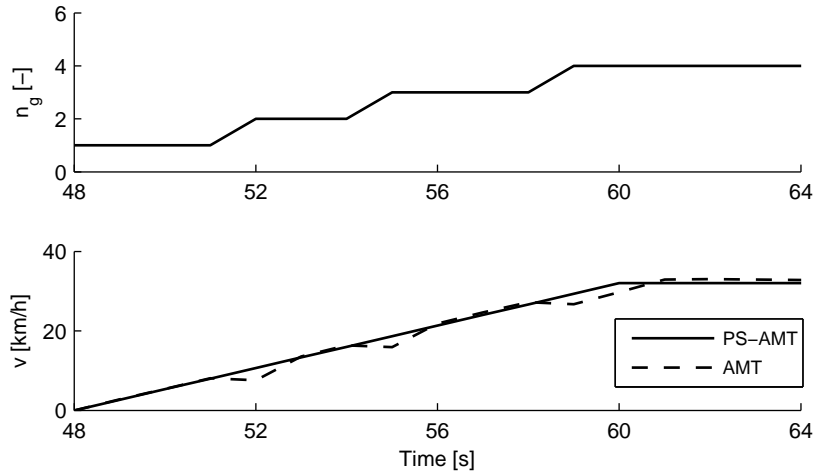


Figure 6.4: Zoom-in on the NEDC of the velocity tracking for the PS-AMT vs. the AMT.

Sensitivity study of the relative fuel difference (by comparing the fuel consumption of the AMT vehicle with that of the PS-AMT vehicle) with respect to a variation in interruption time Δt_{int} over the tested drive cycles is shown in Figure 6.5. The interruption is varied as,

$$\Delta t_{int} \in \{0.3, 0.4, 0.5, 0.6, 0.7, 0.8, 0.9, 1\}[s] \quad (6.26)$$

to reflect the possible interruption time of the actual gear shift activity. Herein $\Delta t_{int} = 0.3s$ represents the possible smallest time of actuating the synchronizer for a gear change. Meanwhile $\Delta t_{int} = 1s$ represents the longest interruption time for passenger cars. It is noticed that the slopes of the torque profiles during disengagement and engagement phases are unchanged for a comfort reason. In this study, the slope time for each phase is chosen to equal to 0.2s. The AMT vehicle speed is controlled to finish the drive cycle

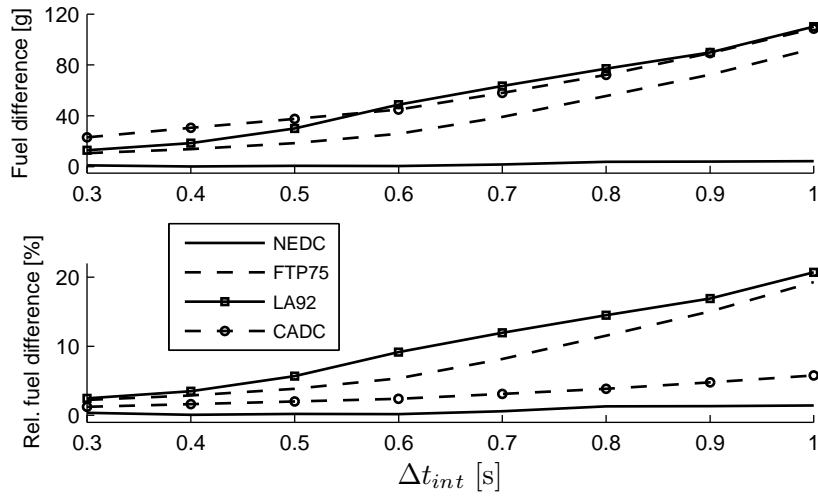


Figure 6.5: Sensitivity study of the fuel difference (comparing the AMT vehicle with the PS-AMT vehicle) with respect to a variation in interruption time Δt_{int} .

on time to ensure a fair comparison with the PS-AMT vehicle.

- The results shown in Figure 6.5 reveal that, the longer the interruption time, the more the AMT vehicle consumes fuel compared to the PS-AMT vehicle. The results on the drive cycles FTP75, LA92 and CADC, representing real-life driving missions, demonstrate a superior fuel economy property of the PS-AMT compared to the AMT. Therefore, reducing the interruption time in the gear shift process of the AMT would reduce the fuel consumption at a considerable amount.
- On NEDC, the relative fuel difference is very small and even equal to zero at $\Delta t_{int} = 0.4$. This means that the obtained driving profile from the AMT vehicle is equivalent with the NEDC in terms of fuel consumption. This characteristic discloses the possibility of further boosting the fuel economy for HEVs by optimizing the vehicle velocity profile while still satisfying the requirements on traveled distance and time.
- In an attempt to find the rationale of fuel advantage of the PS-AMT vehicle over the AMT one, dynamical analysis (mean and standard deviation) of acceleration characteristics of the drive cycles is conducted and shown in Figure 6.6. It can be seen that the NEDC is less dynamic, represented by the lowest mean and standard deviation compared to the other drive cycles. This corresponds with the lowest relative fuel difference on the NEDC. Meanwhile, the LA92 has the highest dynamical property, represented by the highest mean and standard deviation. This is matched with the highest relative fuel difference on the LA92, see Figure 6.5. An analogous correlation between the dynamical property of drive cycle and the relative fuel difference is also held for FTP75 and CADC. Hence, it can be

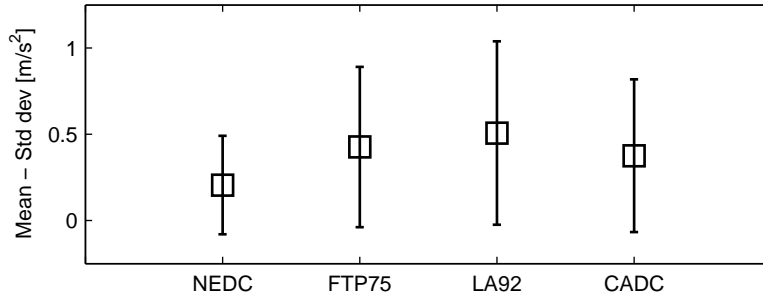


Figure 6.6: Dynamic characteristics (mean and standard deviation (std dev)) of the drive cycles.

concluded that, the more dynamic the drive cycle, the more fuel-efficient the PS-AMT vehicle (compared to the AMT vehicle). In other words, a drive cycle with many shifts required, e.g. driving in urban area, is fuel economy potential for the PS-AMT vehicle.

6.5 Engine Start Loss Model and Control Problem

6.5.1 Engine Start Loss Model

A full parallel HEV can utilize the electric machine, positioned right after the clutch, to start the engine. By exploiting this advantage, the parallel hybrid powertrain can eliminate the traditional engine starter. The starting process can be done through two chronological steps: 1) engaging the clutch to crank the engine from rest to a start-speed by the torque from electric machine; 2) after reaching the start-speed, the engine will takeover the combustion process to synchronize its speed with the transmission input speed before fully engaging the clutch. Consequently, a decision of starting the engine would consume an amount of electric energy and fuel. Moreover in the first step of turning the engine speed up to the start-speed, the friction loss occurring in the clutch is also compensated through the electrical path. For a simplification of modeling the start loss, the friction loss in the second step can be neglected due to an assumption of quickly engaging the clutch at the synchronization point.

In the context of designing an EMS, it can be assumed that the whole starting process occurs in one time step. Any decision to start the engine at any time step k means that, the engine will be ready to propel the vehicle on the next time step $k + \Delta t$. The model of the engine start is graphically displayed in Figure 6.7. Therefore, the loss model can be described as follows.

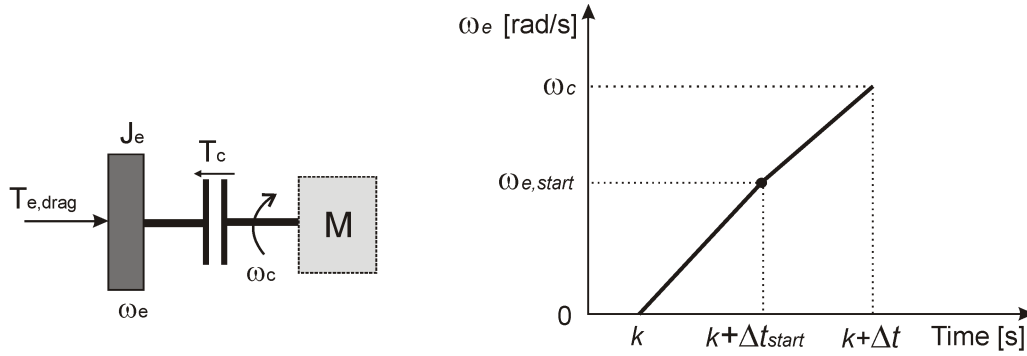


Figure 6.7: Engine start model.

Cranking phase

We assume that cranking phase can last within an average time interval Δt_{start} . The torque required for cranking the engine up to the start-speed $\omega_{e,start}$ is the torque transferred through clutch T_c , defined as,

$$\begin{aligned} T_{c,crank} &= J_e \frac{\omega_{e,start}}{\Delta t_{start}} + T_{e,drag}, \\ \Rightarrow P_{c,crank} &= \frac{\int_0^{\Delta t_{start}} T_{c,crank} \omega_e dt}{\Delta t_{start}} = T_{c,crank} \frac{\omega_{e,start}}{2}, \end{aligned} \quad (6.27)$$

wherein $T_{e,drag}$ is the engine drag torque.

The transferred torque T_c is obtained by a clutch slippage, thus inducing a friction loss. Assuming the engine speed at the end of the starting process is the clutch speed ω_c , the clutch friction loss is,

$$\begin{aligned} E_{c,loss} &= \int_0^{\Delta t_{start}} T_{c,crank} (\omega_c - \omega_e) dt = \int_0^{\Delta t_{start}} T_{c,crank} \left(\omega_c - \frac{\omega_{e,start}}{\Delta t_{start}} \cdot t \right) dt \\ &= T_{c,crank} \left(\omega_c - \frac{\omega_{e,start}}{2} \right) \Delta t_{start}, \end{aligned}$$

wherein $\omega_c = \omega_g$.

The averaged power loss at the clutch,

$$P_{c,loss} = \frac{E_{c,loss}}{\Delta t_{start}} = T_{c,crank} \left(\omega_c - \frac{\omega_{e,start}}{2} \right). \quad (6.28)$$

From (6.27) and (6.28), the total average required power placed at the electric machine for cranking phase is,

$$P_{m,crank} = P_{c,crank} + P_{c,loss}. \quad (6.29)$$

Synchronization phase

After reaching the start speed $\omega_{e,start}$, the engine takes over the synchronization with the transmission input speed by combustion. The energy loss can be derived from the corresponding engine power,

$$\begin{aligned} T_{e,syn} &= J_e \frac{\omega_c - \omega_{e,start}}{\Delta t - \Delta t_{start}}, \\ \Rightarrow P_{e,syn} &= T_{e,syn} \frac{\omega_c + \omega_{e,start}}{2}. \end{aligned} \quad (6.30)$$

It should be noticed that, the electric machine is assumed to operate under a nominal condition. Therefore even in the case of electrically driving, if an engine start is required, the surplus power from nominal to peak values of the electric machine can fulfill the required power (6.29) for the cranking phase.

6.5.2 Simulation Results

Table 6.3: Simulation results corresponding with a study on the engine start loss and gear shift hysteresis. Relative difference is indicated in the parenthesis

Cycle	Baseline		Shift hysteresis, start loss	
	Fuel [g]	No. start	Fuel [g]	No. start
NEDC	300.5	14	303.8 (0.9%)	14 (0%)
FTP75	480.3	107	489.9 (2%)	85 (-20.6%)
LA92	530.8	99	540.2 (1.8%)	86 (-13.1%)
CADC	1873.9	229	1898.9 (1.3%)	196 (-14.4%)

The engine start loss model is incorporated in the optimal control problem, described in Section 6.3. The gear shift hysteresis is active to avoid unrealistic shifting patterns. Simulation results are shown in Table 6.3. It can be seen that, compared to the baseline vehicle of no engine start loss and no gear shift hysteresis, the maximum relative fuel difference is 2% on the FTP75; the minimum relative fuel is 0.9% on the NEDC. Nonetheless, the absolute different fuel on the CADC is the biggest one (25g), corresponding to the largest number of starts. Apparently, the more the engine start, the more the vehicle lost the fuel economy. It's also observed that, by including the start loss model the EMSs reduces the number of starts considerably. Referring back to the

simulation results of the study on gear shift hysteresis shown in Table 6.2, it can be recognized that, the engine start loss deteriorates the fuel economy more than the gear shift hysteresis. In summary, the effect of engine start loss can not be ignored in seeking a fair evaluation of the fuel economy for hybrid vehicles.

6.6 Prediction Horizon Sensitivity Study

Losses involved with a discrete decision of either shifting gears or starting engine have been considered in the design of an EMS to find out a theoretical value of the fuel saving. However, knowledge of the whole drive cycle, required for the EMS design, is almost impossible to obtain in advance. In reality, only a driving profile over a certain horizon can be known by a prediction technique. Therefore, with a preview route information available, a predictive control algorithm for hybrid powertrain systems appears to be a suitable candidate to realize a highest fuel saving as much close as possible to the theoretical value (see, Chapter 5).

6.6.1 Predictive Control Algorithm

We use a certain available drive cycle as a reference driving profile which is assumed to be constructed from the consecutive preview route segments of the whole driving mission. Model Predictive Control (MPC) problem for the prototype parallel HEV is formulated as follows.

Problem 6.2. *Assuming that at current time step k , a prediction of the vehicle speed $\tilde{v}(k) = [\hat{v}(k+1|k), \hat{v}(k+2|k), \dots, \hat{v}(k+N_c|k)]^T$ is known over a certain horizon N_c , find an optimal control law $\tilde{u}^*(k) = [\tilde{u}_{se}^*(k), \tilde{P}_s^*(k), \tilde{u}_g^*(k)]$, that minimize the fuel cost functional $\hat{J}(k)$ over the entire prediction horizon,*

$$\hat{J}(k) = \sum_{i=0}^{N_c-1} \dot{m}_f(\hat{s}_e(k+i|k), \hat{P}_e(k+i|k), \hat{\omega}_e(k+i|k)) \Delta t, \quad (6.31)$$

subject to the constraints (6.10) - (6.19) and,

$$E_{s_min} \leq \hat{e}_s(k+N_c|k) \leq E_{s_max}, \quad (6.32)$$

with

$$\hat{e}_s(k+N_c|k) = e_s(k) + \sum_{i=0}^{N_c-1} \hat{P}_s(k+i|k) \Delta t, \quad (6.33)$$

wherein: $\tilde{u}_{se}^*(k)$, $\tilde{P}_s^*(k)$ and $\tilde{u}_g^*(k)$ denote the vectors of predictive optimal control sequences over the horizon N_c at time step k .

The MPC problem is solved by using the DP-PMP algorithm, described Chapter 3. The predictive control approach is implemented in a receding horizon control manner to realize a real-time implementable algorithm when utilizing the route information. Only the first element of the defined optimal trajectories of $\tilde{u}_{se}^*(k)$, $\tilde{P}_s^*(k)$ and $\tilde{u}_g^*(k)$ is applied to the hybrid powertrain system; for the next step $k+1$, the whole optimization process is repeated with the updated system states and new prediction of the route horizon.

The gear shift loss model can not be incorporated in the MPC due to the velocity loss at each gear shift, resulting in the next vehicle speed to be dependent on the gear position. Hence, we assume that the PS-AMT is used in the hybrid powertrain. The gear shift hysteresis and the engine start loss model are respected under the control algorithm.

6.6.2 Simulation Results and Discussions

Sensitivity study of the relative fuel difference with respect to the prediction horizon N_c is shown in Figure 6.8. The relative fuel difference is obtained by comparing the result of the MPC approach with that of an optimal approach (based on the DP-PMP algorithm). The MPC without the gear shift hysteresis and engine start loss model included (see, the upper plot) indicates that with a short horizon of $N_c = 2$, the predictive controller realizes a result very close to the optimal solution. The relative fuel difference steadily approaches a small value around 0.2% from $N_c \geq 2$. However, for the case of the MPC with the gear shift hysteresis and the engine start loss model included (see, the lower plot), from the horizons $N_c \geq 4$, the relative fuel difference is steady, ranged from 1% (NEDC) until 3% (FTP75). The obtained results reveal that at least a prediction horizon of 5s ahead the vehicle is necessary to achieve the most possible fuel economy. Fortunately a prediction of the velocity profile over a preview route segment of 5s is almost possible for current technology of the vehicle onboard navigation system nowadays.

Sensitivity study of the calculation time with respect to the prediction horizon for the MPC strategy, including the gear shift hysteresis and the engine start loss, is shown in Figure 6.9. The calculation time is almost linear with the prediction horizon and smaller than the drive cycle length itself. This brings a realtime implementation possibility to the MPC-based control algorithm.

6.7 Conclusions

Design of the EMSs for passenger HEVs equipped with discrete ratio transmissions requires an optimal gear shift strategy for a fuel economy benefit. One gear up or down per shift is the most optimum gear shift command in terms of the fuel economy and

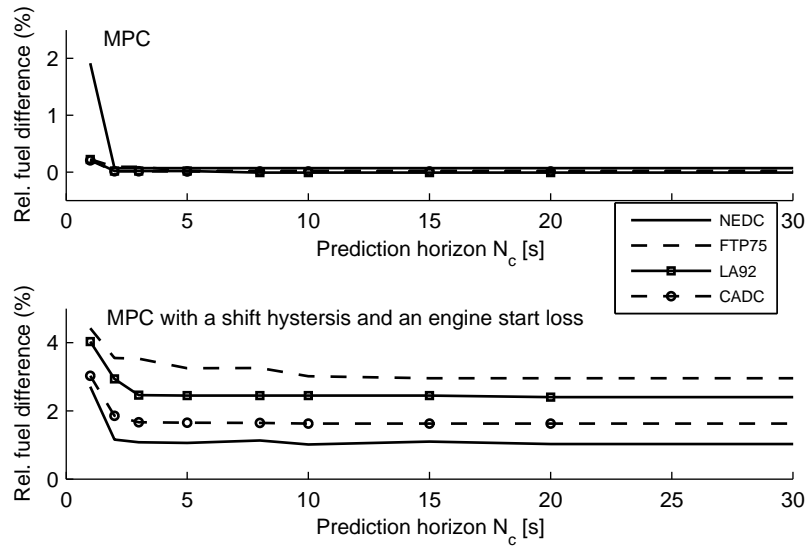


Figure 6.8: Sensitivity result of the relative fuel difference with respect to the prediction horizon N_c of the MPC approach.

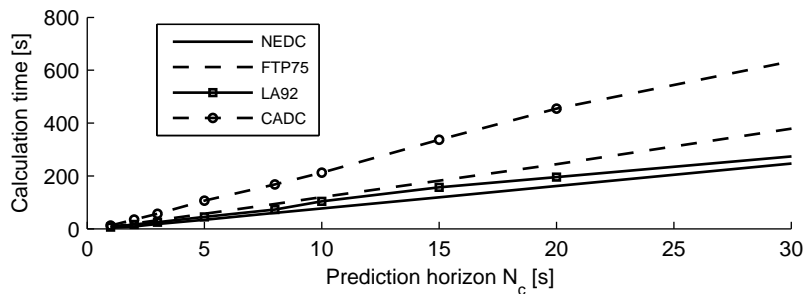


Figure 6.9: Sensitivity result of the calculation time for the MPC, including the gear shift hysteresis and engine start loss, with respect to the prediction horizon N_c .

engine operation comfort. Gear shift hysteresis strategy plays a crucial role in reducing the shift busyness and hunt in a way not deteriorating the fuel economy.

Regarding the loss involved with the gear shift, it is found by simulation that a perception of a fuel-efficient advantage of powershift transmissions (DCT, PS-AMT) over non-powershift transmissions (MT, AMT) is realized for passenger HEVs.

Any discrete decision of starting the engine in a parallel HEV will induce an energy loss which finally affects the optimal solution. This loss can not be ignored in a proper EMS to ensure a fair evaluation of the fuel economy. The model predictive control algorithm utilizes the engine start loss model effectively in yielding the possible shortest prediction horizon (five seconds) such that the highest possible fuel economy level can be realized.

Prospects of future research continued from this study are very diverse. An investigation of the effect of gear shift and engine start losses on the control strategies for commercial

vehicles equipped with an AT or a DCT is an example. This helps verifying whether the fuel benefit of powershift transmissions compared to non-powershift ones is held for the commercial vehicle class.

Structural Analysis of the Control Design Objectives¹

Abstract - In the optimal control design for vehicular propulsion systems, the objective function describing the design objectives (fuel economy, driveability, comfort, emissions, battery operation, battery aging, etc.) plays an important role in defining the optimal solution. However, the definition of the objective function is not often analyzed explicitly and thoroughly. In this study, a method of objectively analyzing and evaluating the objective function is introduced. The method uses the Singular Value Decomposition (SVD) technique to analyze the correlations among the design objectives and investigate their sensitivity to an optimal control algorithm. Accordingly, the dependent design objective(s) will be omitted such that the objective function can be simplified. This will reduce the complexity of the control design. The method is then applied to the optimal control design for a conventional vehicle and a hybrid electric vehicle. It is found that, instead of introducing an objective function including the fuel consumption, comfort (the weighted gear shift frequency), and driveability (the weighted inverse of power reserve), a simplified objective function consisting of the fuel consumption and comfort can be proposed for the control design, such that the driveability is not sacrificed noticeably at the obtained optimal solution.

7.1 Introduction

Design of vehicular propulsion systems boils down to choices of topology, technology, size of the components (in terms of power or energy) and control strategy to achieve the design objectives, such as fuel economy, driveability, comfort, emissions, battery operation, battery aging, etc. Regarding the control strategy which governs the operations of individual components of vehicular propulsion systems at each time instant,

¹This chapter has been prepared for a journal publication in the form as: V. Ngo, T. Hofman, M. Steinbuch, A. Serrarens. Structural Analysis of the Control Design Objectives for Vehicular Propulsion Systems. 2012.

optimal control [42, 49] is widely used to achieve the optimal solution with respect to the specified control design objectives. Therefore, the starting point of formulating a certain optimal control problem is to define an objective function, which consists of a single or multiple design objectives. For the case of a multi-objective problem, the objective function can be created by summing the relevant objectives multiplied by the corresponding weight factors defining the relative importance. However, defining an appropriate objective function with suitable weight factors for a specific propulsion system is an ambiguous task. This is due to the fact that there might be strong interdependencies of the design parameters, unknown sensitivities of the design parameters to the design objectives, and the possibility of finding multiple sets of weight factors resulting in an equal overall design performance [49]. Hence, an objective function is appropriate when it can diminish the interdependent design objective(s), and finally, it can balance the tradeoff(s) among the design objectives of the design process [49, 91, 121, 158].

In literature, the objective function is generally defined based upon the powertrain configurations (conventional, hybrid, etc.), the control strategy, and the subjective reasonings of the designers about relative impacts among the design objectives. In this research work, a method of objectively analyzing the design objectives for the control design of vehicular propulsion systems (conventional and hybrid powertrains) is proposed. The method uses the Singular Value Decomposition (SVD) technique to analyze: i) the sensitivity of the design objectives with respect to an optimal control problem, and ii) the correlation among the design objectives. Herein the optimal control problem also takes the gear shift problem into account. Then, the dependent design objective(s) will be omitted such that the objective function for the optimal control problem can be simplified in order to reduce the design complexity.

This study is organized as follows. In Section 7.2, the design objectives for the optimal control problem of vehicular propulsion systems are reviewed. In Section 7.3, the quasi static models of the main components of conventional and hybrid powertrain systems are given. In Section 7.4, a multi-objective optimal control problem is formulated for the powertrain systems. In Section 7.5, a SVD-based structural analysis method is introduced. Analysis of the interdependencies among the design objectives is also presented. Simulation results together with discussion are given in Section 7.6. Finally, conclusions and future research can be found in Section 7.7.

7.2 Review of Design Objectives

The design objectives for the control design of vehicular propulsion systems can be, e.g. fuel economy, driveability, comfort, emission, battery operation, battery aging, etc. Table 7.1 shows the possible design objectives, denoted by $DO_1 - DO_6$, and the corresponding performance metrics.

- DO_1 - fuel economy is evaluated by the amount of fuel consumed over a given drive cycle.
- DO_2 - driveability is a comprehensive terminology for vehicle responsiveness. It can be determined as the instant power reserve, or the instant torque reserve, or vehicle acceleration, or velocity tracking of the vehicle, etc.
- DO_3 - the main comfort metrics can be listed as jerk, gear shift time or gear shift frequency, etc.
- DO_4 - emission standard have been increasingly tightened due to the environmental problem. Hence, Carbon Dioxide (CO_2), mono-Nitrogen Oxides (NO_x), Carbon Monoxide (CO), Particulate Matter (PM) and Hydro Carbons (HC), etc., can be used as metrics for engine emissions.
- DO_5 - regarding hybrid electric vehicles, to ensure the reliable operation of battery, its state of charge needs to stay within a predefined operating range to avoid any damage.
- DO_6 - battery aging (battery wear) represents the overall reduction of battery life.

Table 7.1: Design objectives and the corresponding metrics.

Design objective	Metric
DO_1 - Fuel economy	fuel consumption.
DO_2 - Driveability	power reserve, acceleration, velocity tracking.
DO_3 - Comfort	jerk, shifting time, shifting frequency.
DO_4 - Emissions	CO_2, NO_x, CO, PM, HC .
DO_5 - Battery operation	state of charge.
DO_6 - Battery aging	effective Ah-throughput.

Table 7.2 shows how an objective function has been composed in literature. The first column indicates which design objective(s) is (are) utilized in building a certain objective function. The second column gives a literature overview of objective functions proposed for Conventional Vehicle (CV); meanwhile the third column indicates the references wherein objective functions are proposed for Hybrid Electric Vehicle (HEV). The objective functions vary according to the types of powertrain configurations, design method, control algorithms, etc. However fuel economy and driveability are the most concerned design objectives.

Table 7.2: Literature review of the design objective composition. CV denotes Conventional Vehicle; HEV represents Hybrid Electric Vehicle.

Objective composition	CV	HEV
DO_1	[60, 92, 105] [12, 48, 135]	[8, 41, 73, 88, 136, 144, 169–171] [3, 25, 67, 76, 98, 107, 126, 156, 164]
$DO_1 + DO_2$	[47, 135]	[158]
$DO_1 + DO_3$	[133]	-
$DO_1 + DO_4$	[12, 60]	[19, 52, 53, 112, 147]
$DO_1 + DO_5$	-	[4, 69, 159, 163]
$DO_1 + DO_6$	-	[128]
$DO_1 + DO_2 + DO_3$	[92]	-
$DO_1 + DO_2 + DO_5$	-	[21]
$DO_1 + DO_4 + DO_5$	-	[56, 81, 82, 162]
$DO_1 + DO_2 + DO_3 + DO_5$	-	[158]
$DO_1 + DO_3 + DO_4 + DO_5$	-	[17, 80, 83, 106, 172]

7.3 Powertrain Modeling and Dynamics

The hybrid powertrain topology used in this study is shown in Figure 7.1. This study focuses on both conventional and hybrid electric vehicle, so a conventional powertrain topology can be realized by removing the battery, the inverter and the electric machine from the driveline.

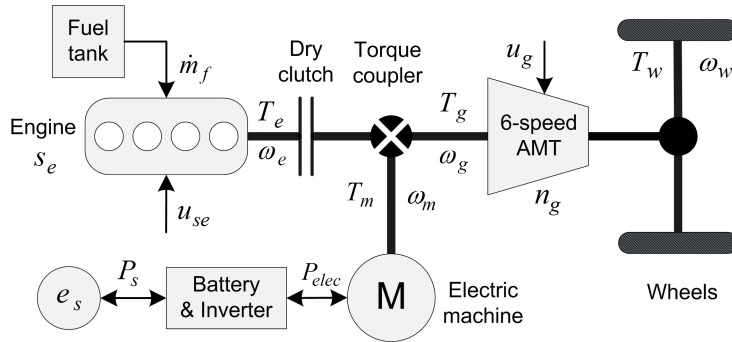


Figure 7.1: The hybrid powertrain topology, (AMT: Automated Manual Transmission; M: Electric machine).

With aiming at deriving the appropriate Energy Management Strategy (EMS), quasi static models of the main powertrain components are used. The length of time step Δt of one second is chosen to simulate the powertrain, hence the dynamics faster than $1Hz$ are ignored [42]. The clutch system is considered as a boolean switch to connect and to

disconnect the engine immediately to and from the driveline. Its dynamics and limited power losses during a gear shift or an engine start are ignored in this chapter.

7.3.1 Powertrain Modeling

- **Start-stop system:** the start-stop system can be modeled by a decision variable $s_e(k)$ to control the engine on-off state. When the engine is off, no fuel is consumed by the engine.

$$s_e(k) = \begin{cases} 1 & \text{if engine on,} \\ 0 & \text{if engine off.} \end{cases} \quad (7.1)$$

- **Engine:** for a certain engine speed $\omega_e(k)$, the fuel mass flow $\dot{m}_f(k)$ is modeled as an affine piece-wise second order function of the power as expressed in (7.2),

$$\dot{m}_f(k) \approx \left(a_0(k)P_e^2(k) + a_1(k)P_e(k) + a_2(k) \right) s_e(k). \quad (7.2)$$

in which the coefficients $a_0(k)$, $a_1(k)$ and $a_2(k)$ are functions of the engine speed. When the engine is off, no fuel is consumed. If assume during braking, the engine is switched off and decoupled from the driveline, then the engine braking is neglected. Therefore, the constraints on the engine speed $\omega_e(k)$ power $P_e(k)$ are as follows,

$$\omega_{e,min} \leq \omega_e(k) \leq \omega_{e,max}, \quad (7.3a)$$

$$0 \leq P_e(k) \leq P_{e,max}(\omega_e(k)). \quad (7.3b)$$

- **Electric machine:** the machine efficiency η is assumed to be constant in a normal operating state. Therefore, the power flow in motoring and generating modes is expressed as,

$$P_m(k) = \eta P_{elec}(k) \quad \text{in motoring,} \quad (7.4a)$$

$$P_m(k) = \frac{1}{\eta} P_{elec}(k) \quad \text{in generating.} \quad (7.4b)$$

The constraints on the speed $\omega_m(k)$ and power $P_m(k)$ are,

$$0 \leq \omega_m(k) \leq \omega_{m,max}, \quad (7.5a)$$

$$P_{m,min}(\omega_m(k)) \leq P_m(k) \leq P_{m,max}(\omega_m(k)). \quad (7.5b)$$

- **Battery system:** the electrical power $P_{elec}(k)$ is modeled as a quadratic function of the storage power $P_s(k)$,

$$P_{elec}(k) \approx b_0 P_s^2(k) + b_1 P_s(k) + b_2. \quad (7.6)$$

The constraints imposing on the battery system,

$$P_{s,min} \leq P_s(k) \leq P_{s,max}, \quad (7.7a)$$

$$E_{s,min} \leq e_s(k) \leq E_{s,max}. \quad (7.7b)$$

- **Automated Manual Transmission (AMT):** the transmission efficiency η is assumed to be constant for all gears, the speed and torque relations in both side of transmission are (when clutch is closed),

$$\omega_e(k) = \omega_g(k) = \omega_w(k)r_g(k), \quad (7.8a)$$

$$T_w(k) = \eta r_g(k) T_g(k) = \eta r_g(k) T_e(k). \quad (7.8b)$$

wherein: $\omega_w(k)$ is the wheel rotational speed; $T_w(k)$ is the drive torque at the wheels; $T_g(k)$ is the transmission input torque; $r_g(k)$ denotes the gear ratio. The final reduction gear ratio is merged into the transmission ratio for a simplification.

The constraints on the gear position of the 6-speed transmission are,

$$1 \leq n_g(k) \leq 6. \quad (7.9)$$

- **Power flow model:** the power flow equilibrium at the transmission input of the powertrain is expressed as,

$$P_e(k) = P_g(k) + P_m(k). \quad (7.10)$$

where $P_m(k) = 0$ if the conventional powertrain is considered.

7.3.2 Powertrain System Dynamics

The powertrain dynamic system consists of three state variables: the start-stop $s_e(k)$, the battery state-of-energy $e_s(k)$ and the gear position $n_g(k)$. Their dynamics are governed by three corresponding control variables $u_{se}(k)$, $P_s(k)$ and $u_g(k)$ as,

$$s_e(k+1) = s_e(k) + u_{se}(k), \quad (7.11)$$

$$e_s(k+1) = e_s(k) + P_s(k)\Delta t, \quad (7.12)$$

$$n_g(k+1) = n_g(k) + u_g(k). \quad (7.13)$$

Vehicle longitudinal dynamics: the longitudinal motion of the vehicle in discrete time domain is given by,

$$\omega_w(k+1) = \omega_w(k) + \frac{1}{J_{v,eq}}(T_w(k) - F_{load}(k)R_w)\Delta t, \quad (7.14)$$

where F_{load} is the resistance loads due to rolling and aerodynamic resistances; $J_{v,eq}$ is an equivalent vehicle inertia at the wheel,

$$J_{v,eq} = ((J_e + J_c + J_p)r_g^2 + J_s)r_d^2 + m_v R_w^2,$$

$$F_{load} = c_r m_v g \cos \alpha + m_v g \sin \alpha + \frac{1}{2} \rho_a A_f c_d v^2,$$

and m_v is the vehicle weight; R_w is the wheel radius; J_e is the engine inertia; J_c is the clutch inertia; J_p is the transmission primary inertia; J_s is the transmission secondary inertia; ρ_a is the air density; A_f is the frontal area of vehicle; c_d is the aerodynamic drag coefficient; c_r is the rolling friction coefficient; g is the gravity coefficient; v is the vehicle speed; α is the slope of the road.

7.4 Optimal Control Problem

7.4.1 Vehicular Propulsion Systems

The dynamic behavior of the vehicular propulsion systems for conventional and hybrid vehicles can be expressed in a generic form by

$$x(k+1) = f(x(k), u(k), z(k)), \quad (7.15)$$

$$C_{eq}(x(k), u(k), z(k)) = 0, \quad (7.16)$$

$$C_{in}(x(k), u(k), z(k)) < 0, \quad (7.17)$$

wherein $x(k)$ and $u(k)$ are the state variable vector and control variable vector, respectively; $z(k)$ is the disturbance to the powertrain system which is defined by a priori drive cycle. f is the function describing the dynamics of the system state. C_{eq} and C_{in} are the functions describing the equality and inequality constraints of the systems.

The conventional powertrain system is described by, (7.2)-(7.3),(7.8)-(7.10), (7.13), (7.14). The state and control variables are,

$$x(k) = [n_g(k)],$$

$$u(k) = [u_g(k)].$$

The hybrid powertrain system is described by (7.1)-(7.14). The state and control variables are,

$$x(k) = [s_e(k), e_s(k), n_g(k)],$$

$$u(k) = [u_{se}(k), P_s(k), u_g(k)].$$

From (7.13), the constraints on the discrete gear shift command $u_g(k)$ influence the gear shift dynamics and have effect on the optimality. Under the constraints (7.9), with a

6-speed AMT, $u_g(k)$ belongs to the set $\{-5, \dots, -1, 0, 1, \dots, 5\}$. For reasons of an acceptable driveability, the gear shift command is chosen as,

$$u_g(k) = \begin{cases} -1 & \text{downshift,} \\ 0 & \text{sustaining,} \\ 1 & \text{upshift,} \end{cases} \quad (7.18)$$

to avoid a large variation of the engine speed under a certain shifting at a certain time step k . One gear upshift ($u_g(k) = 1$) or downshift ($u_g(k) = -1$) for each time step of one second are reasonable, since the average shifting time for an AMT is typically less than one second.

7.4.2 Multi-Objective Function

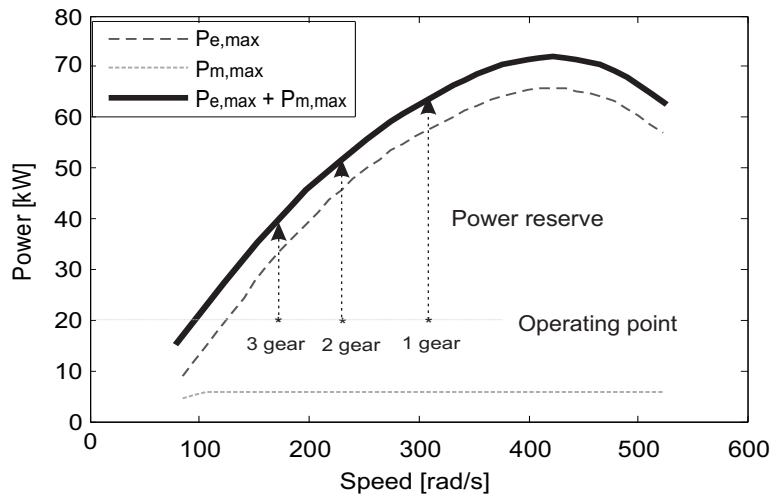


Figure 7.2: Demonstration of the power reserve in relation with the gear position for the hybrid powertrain.

Within the context of design an optimal control problem including the gear shift strategy, the relevant design objectives are required to be well-defined. Figure 7.2 graphically shows the correlation between the gear position and the power reserve of the hybrid powertrain. It can be seen that the power reserve is decreased when the transmission performs an upshift and vice versa. Intuitively, when the controller allows more upshifts, the engine operating points will be moved to a region of higher nominal torque and lower speed, which results in a lower power reserve. Furthermore, the fuel mass flow is a function of the engine power. Therefore, the engine power reserve has a correlation with the fuel consumption. It can be seen that changing the operating points by further optimizing the gear shift would affect the driveability (power reserve) and comfort (shift frequency or number of shifts) of the hybrid powertrain system. This reasoning holds also for the conventional powertrain system.

Therefore, an objective function is proposed by the weighted sum of the fuel consumption, comfort and driveability, as follows,

$$\mathbf{J} = \sum_{k=0}^{N-1} \mathbf{L}(k) = \sum_{k=0}^{N-1} \left[\dot{m}_f(k) + w_1 |u_g(k)| + w_2 (\Delta P_e(k) + \Delta P_m(k))^{-1} \right] \Delta t, \quad (7.19)$$

in which, N is the length of the drive cycle; w_1 and w_2 are the weight factors; $\Delta P_e(k)$ and $\Delta P_m(k)$ are the power reserve of the engine and electric machine, respectively; $w_1 |u_g(k)|$ represents the comfort cost related to the gear shift frequency; $w_2 (\Delta P_e(k) + \Delta P_m(k))^{-1}$ stands for the driveability cost related to the power reserve.

7.4.3 Optimal Control Algorithm

Problem 7.1. *Given a drive cycle with a time length N , implying that the vehicle longitudinal dynamics (7.14) is deterministic, find an optimal control law $u^*(k)$ that minimizes the objective function (7.19):*

$$u^*(k) = \arg \min_{u(k)} \mathbf{J} = \sum_{k=0}^{N-1} \mathbf{L}(k)$$

subject to the constraints (7.15)-(7.18) and

$$x(N) = x(0). \quad (7.20)$$

Dynamic Programming (DP) [14] is well known as a powerful method to solve a non-linear, non convex optimization problem with mixed constraints while obtaining a globally optimal time-variant, state feedback solution. To apply DP to the proposed optimal control problem, we need to

- grid the state variables $x(k)$;
- grid the corresponding control variables $u(k)$;
- calculate $\mathbf{L}(k)$ in (7.19) for the whole drive cycle for every grid point;

Then, the optimal cost-to-go function is defined as,

- *step* $k = N$:

$$\mathcal{J}_N^* = 0, \quad (7.21)$$

- *step* $k \in [0, 1, \dots, N - 1]$:

$$\mathcal{J}_k^*(x(k)) = \min_{u(k)} \left[\mathbf{L}(k) + \mathcal{J}_{k+1}^*(x(k+1)) \right]. \quad (7.22)$$

By solving the optimal cost-to-go function backwards until $k = 0$, the optimal solution $u^*(k)$ is obtained correspondingly with a specific value for the end constraint $x(N)$.

Reducing the objective function to a simple form so that the weight factors can be tuned easily meanwhile the control algorithm can achieve the desired performances is the ultimate goal. In order to do so, we need to study the correlations and dependencies among the design objectives of the objective function. Then the dependent ones can be eliminated so that a simplified objective function can be obtained. Clearly, this boils down to a rank analysis which will be introduced next.

7.5 SVD-based Structural Analysis

SVD is a widely used method in the structural and rank analysis of the dynamic system. A similar usage of rank conditions using the SVD is to measure the interactions between the inputs and the outputs of the dynamic system [103, 117, 143]. Furthermore, a special application of the SVD method is that it can be used to evaluate the system's performances by doing the data-based structural analysis [43]. A brief introduction of the SVD-based structural analysis is given next.

7.5.1 Singular Value Decomposition

Consider a linear algebraic equation as,

$$\mathbf{A}\mathbf{x} = \mathbf{b}; \quad \mathbf{A} \in \mathbf{R}^{N \times M}. \quad (7.23)$$

SVD of the matrix \mathbf{A} is given

$$\mathbf{A} = \mathbf{U}\mathbf{\Sigma}\mathbf{V}^T$$

wherein:

$$\begin{aligned} \mathbf{U} &= [u_1, u_2, \dots, u_N] \in \mathbf{R}^{N \times N}, \\ \mathbf{V} &= [v_1, v_2, \dots, v_M] \in \mathbf{R}^{M \times M}, \\ \mathbf{\Sigma} &= \text{diag}(\sigma_i | 0) \in \mathbf{R}^{N \times M}. \end{aligned} \quad (7.24)$$

The column vectors v_i of \mathbf{V} and u_i of \mathbf{U} are known as the right input singular vectors and left output singular vectors of matrix \mathbf{A} , respectively. They hold an important relation:

$$\mathbf{A}v_i = \sigma_i u_i. \quad (7.25)$$

This equation states that each right input singular vector is mapped by the system \mathbf{A} onto the corresponding left output singular vector with the magnification factor being

the corresponding singular value. From (7.25), if $\sigma_i = 0$, then $\mathbf{A}v_i = 0$, i.e., v_i forms the null space of \mathbf{A} . Thus any change made in the direction corresponding to the singular value $\sigma_i = 0$ maps into the zero vector in the output space. In other words, any input in that direction is not reflected in the output space.

By using (7.24), the solution \mathbf{x} to (7.23) is directly obtained as linear combination of the scaled right input singular vectors,

$$\mathbf{x} = \sum_i^{\text{rank}(\mathbf{A})} \frac{u_i^T \cdot \mathbf{b}}{\sigma_i} v_i = \sum_i^{\text{rank}(\mathbf{A})} q_i v_i. \quad (7.26)$$

Any target vector \mathbf{b} can be achieved by a linear combination of the scaled left output singular vectors as

$$\mathbf{b} = \sum_i^{\text{rank}(\mathbf{A})} \sigma_i q_i u_i = \sum_i^{\text{rank}(\mathbf{A})} (u_i^T \cdot \mathbf{b}) u_i. \quad (7.27)$$

7.5.2 Structural Analysis

In the structural analysis of this study, v_i is called the input mode vector, and u_i is called the output mode vector. From (7.26) the control input vector \mathbf{x} is a linear combination of the input mode vectors v_i multiplied by the corresponding input weight factors q_i . So, the designer can assess the control input distribution pattern through the input weight factors q_i . Similarity, we can use the output mode vectors u_i to assess tradeoffs among the contributions of them to the target vector \mathbf{b} as in (7.27).

For example, consider the input weight factor q_1 in (7.27) to be much larger than the other weight factors in the linear combination. Since σ_1 is the largest singular value, $q_1 \sigma_1$ is dominant among the coefficients of the linear combination, then the actual target vector \mathbf{b} will be largely dependent on the first output mode vector u_1 .

The input mode vectors v_i and output mode vectors u_i obtained from SVD are paired by the corresponding singular values σ_i . Thus, truncating any input mode vector v_i would affect the corresponding output mode vector u_i , and vice versa. Truncating the output mode vector u_i that is part of the linear combination of the target vector \mathbf{b} would degrade the total performance. If, however, the truncated output mode vector contributes little to the target vector \mathbf{b} , then there would be little performance degradation and it would be possible to save control effort equal in size to the weighted input mode vector that is paired with the truncated output mode vector.

Cutting off any input mode vector v_i that consumes a large control input, i.e., one with a large weight factor q_i , but contributes little to the total performance of the target vector \mathbf{b} , will reduce the design complexity at a little performance degradation.

From (7.27), it is clear that the output mode vector u_i that lines up more towards the target vector \mathbf{b} will contribute more to \mathbf{b} . Therefore, the value of inner product of two vector u_i and \mathbf{b} , which is called the *collinearity* and denoted by $col_i \triangleq (u_i^T \cdot \mathbf{b})$, can be used to measure the performance dependency of the target vector \mathbf{b} on each output mode vector u_i . Using this indicator, we can identify which output mode vector u_i is dominant in achieving the target vector \mathbf{b} and which output mode vector u_i contributes little. Furthermore, the normalized target vector $\bar{\mathbf{b}}$ should be used to compare the collinearities for simplicity since they span from 0 to 1.

7.6 Results and Discussions

7.6.1 Application of SVD-based Structural Analysis

The structural analysis for the powertrain systems will be carried out by using the SVD technique. The analysis is not based on the system model, but is based on data obtained from simulating the system model governed by the optimal control algorithm, as described in Section 7.4. The concerned data is the discrete optimal cost values along the drive cycle.

Objective function analysis: the optimal objective function (7.19) is rewritten as follows.

$$\mathbf{J}^* = \sum_{k=0}^{N-1} \mathbf{L}^*(k) = \sum_{k=0}^{N-1} \left[m_{fe}^*(k) + m_{sh}^*(k) + m_{pr}^*(k) \right], \quad (7.28)$$

wherein the asterisk (*) denotes the optimal solution and

$$\begin{aligned} m_{fe}^*(k) &\triangleq \dot{m}_f^*(k) \Delta t, \\ m_{sh}^*(k) &\triangleq w_1 |u_g^*(k)| \Delta t, \\ m_{pr}^*(k) &\triangleq w_2 (\Delta P_e^*(k) + \Delta P_m^*(k))^{-1} \Delta t. \end{aligned}$$

The discrete optimal cost values of (7.28) are stacked along the discrete time dimension of the drive cycle to create the linear algebraic equation $\mathbf{A}\mathbf{x} = \mathbf{b}$, with

$$\mathbf{A} = \begin{bmatrix} m_{fe}^*(0) & m_{sh}^*(0) & m_{pr}^*(0) \\ m_{fe}^*(1) & m_{sh}^*(1) & m_{pr}^*(1) \\ \vdots & \vdots & \vdots \\ m_{fe}^*(N-1) & m_{sh}^*(N-1) & m_{pr}^*(N-1) \end{bmatrix}, \quad \mathbf{b} = \begin{bmatrix} \mathbf{L}^*(0) \\ \mathbf{L}^*(1) \\ \vdots \\ \mathbf{L}^*(N-1) \end{bmatrix}, \quad (7.29)$$

$$\mathbf{x} = [1 \quad 1 \quad 1]^T.$$

In (7.29), the vector \mathbf{x} acts as the control vector imposed on the weighted objectives, so it is chosen as $\mathbf{x} = [1 \ 1 \ 1]^T$ to respect the original optimal values of the objectives.

The target vector \mathbf{b} contains the instantaneous optimal values of the objective function at every time step. SVD-based structural analysis method is applied to study the sensitivity of the design objectives to the weight factors w_1 and w_2 .

7.6.2 Simulation Results for Conventional Vehicles

The main parameters of a prototype conventional vehicle are given in Table 7.3.

Table 7.3: Main parameters of a prototype conventional vehicle.

Item	Description/Quantity
Engine	type: gasoline, maximum torque of 140Nm, maximum power of 70kW.
Transmission	6-speed automated manual transmission, $r_g = [3.071, 1.913, 1.258, 0.943, 0.763, 0.643]$.
Vehicle mass	1120kg.

- **The NEDC cycle:** the weight factors w_1 and w_2 are chosen as,

$$w_1 \in \{0.6, 1, 1.5, 2, 3\}, \quad (7.30)$$

$$w_2 \in \{250, 500, 750, 1000, 1500, 2000\}. \quad (7.31)$$

Computational results of SVD analyses for the input weight factors q_i and the normalized collinearities col_i for all combinations of w_1 and w_2 are shown in Figure 7.3.

In Figure 7.3a, q_1 varies from $0.89 \rightarrow 0.99$, q_2 varies from $0.72 \rightarrow 0.94$ and q_3 varies from $0.48 \rightarrow 0.87$. By looking at the normalized collinearities in Figure 7.3b, we can recognize that the values of col_i are totally different from each other. col_1 approximately varies from $0.90 \rightarrow 0.99$; col_2 approximately varies from $0.13 \rightarrow 0.44$ whereas col_3 roughly varies from $0.02 \rightarrow 0.09$.

From col_2 and col_3 , it is observed that the maximum contributions of the output mode vectors u_2 and u_3 to the target vector \mathbf{b} are 19.4% ($= 0.44^2 * 100\%$) and 0.8% ($= 0.09^2 * 100\%$) respectively. Meanwhile, the maximum contributions of input mode vectors v_2 and v_3 to the control input vector \mathbf{x} are almost equivalent to that of v_1 (observed from q_1 , q_2 and q_3). This is an important observation on the fact that the output mode vector u_3 pays only a very small contribution to

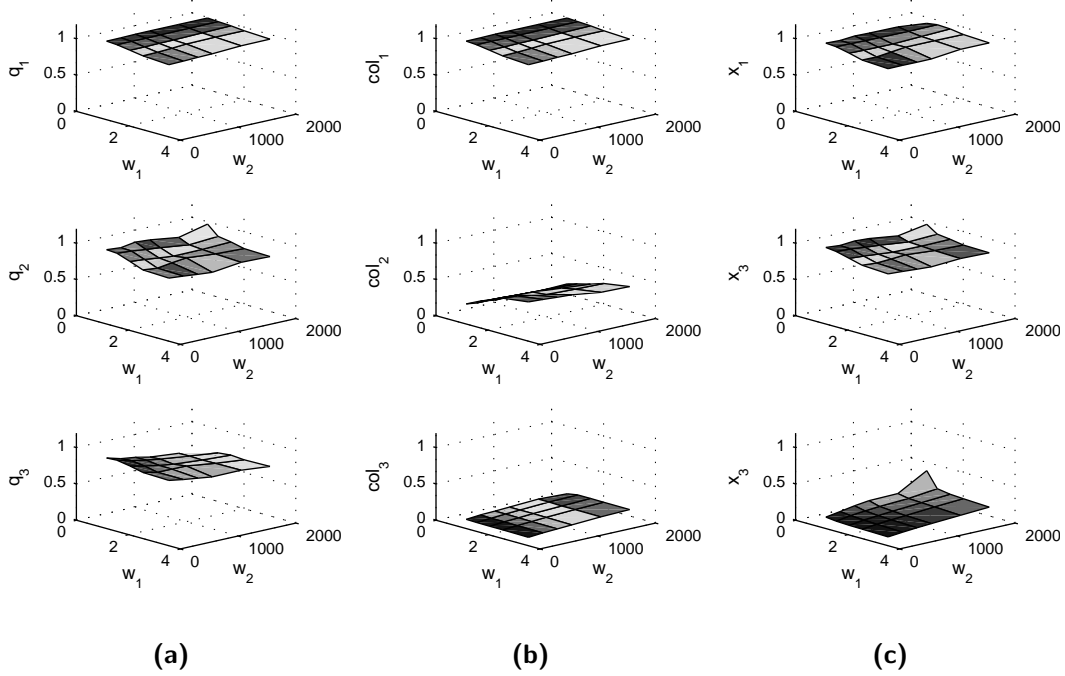


Figure 7.3: Results of the conventional powertrain on NEDC: the input weight factors q_i in (a); the collinearities col_i in (b); the three directions x_1 , x_2 and x_3 of the reconstructed \mathbf{x} in (c).

the target vector \mathbf{b} . Therefore, truncating the input mode vector v_3 will save a large amount of control effort without seriously degrading the performance.

From the observations and analyses above, we can come up with a design decision to truncate the input mode vector v_3 out of the control input vector \mathbf{x} . Therefore, \mathbf{x} can be approximated as,

$$\mathbf{x} \approx q_1 \cdot v_1 + q_2 \cdot v_2 \triangleq [x_1 \quad x_2 \quad x_3]^T. \quad (7.32)$$

Using the obtained simulation results, the reconstructed control input vector \mathbf{x} is depicted in Figure 7.3c. We can see that x_1 varies from 0.84 \rightarrow 0.96; x_2 varies from 0.8 \rightarrow 0.96. Meanwhile, x_3 varies from 0.02 \rightarrow 0.18. Or the control input vector \mathbf{x} can be re-designed as,

$$\mathbf{x} \approx [1 \quad 1 \quad 0]^T. \quad (7.33)$$

- **The FTP75 cycle:** the weight factors w_1 and w_2 are chosen as,

$$w_1 \in \{1, 2, 3, 4, 5\}, \quad (7.34)$$

$$w_2 \in \{250, 500, 750, 1000, 1250, 1500\}. \quad (7.35)$$

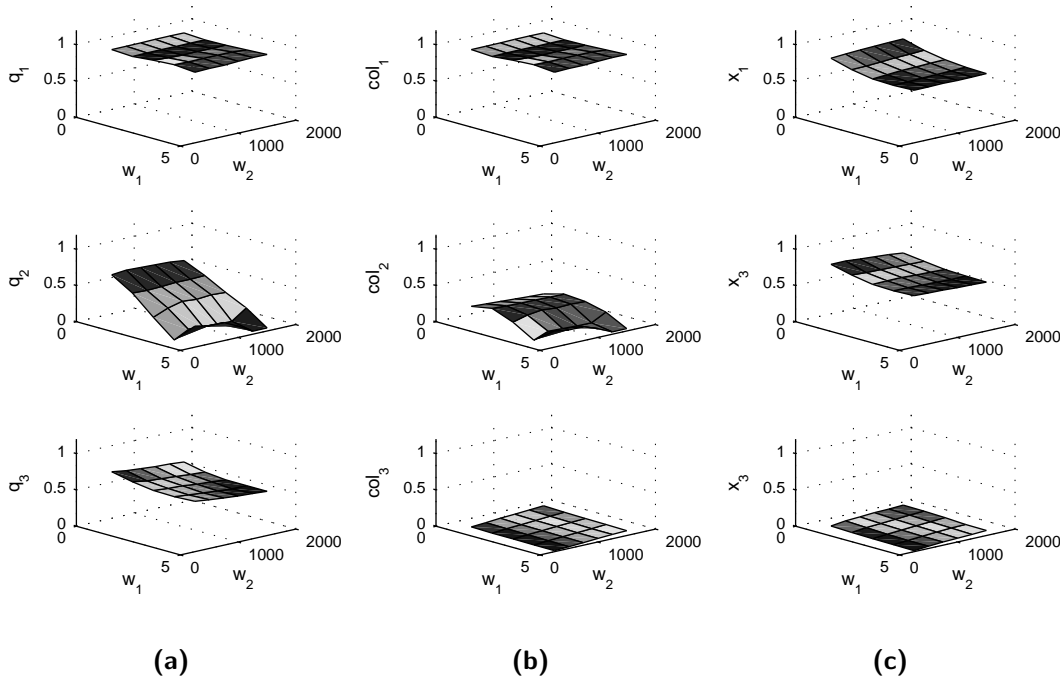


Figure 7.4: Results of the conventional powertrain on FTP75: the input weight factors q_i in (a); the collinearities col_i in (b); three directions x_1 , x_2 and x_3 of the reconstructed \mathbf{x} in (c).

Computational results of SVD analyses for the input weight factors q_i and the normalized collinearities col_i are shown in Figure 7.4. By using the same analysis technique applied on the NEDC cycle, the control input vector \mathbf{x} is reconstructed and depicted in Figure 7.4c. Or the control input vector \mathbf{x} can be approximately re-designed as

$$\mathbf{x} \approx [1 \quad 1 \quad 0]^T. \quad (7.36)$$

From (7.33) and (7.36), it can be concluded that the third design objective, i.e. the power reserve term, can be eliminated from the objective function (7.28) due to its small contribution to the objective function. In other words, the objective function for the optimal control problem can be simplified as,

$$\mathbf{J}_{CV} = \sum_{k=0}^{N-1} [\dot{m}_f(k) + w_1 |u_g(k)|] \Delta t. \quad (7.37)$$

Therefore, it would be easy to tune only one weight factor w_1 such that the Pareto optimal solution is achieved to satisfy the expected design objectives.

7.6.3 Simulation Results for Hybrid Electric Vehicles

Another case study of the SVD-based structural analysis is applied for a prototype HEV, see Table 7.4 for the main parameters, to investigate the correlations among of the design objectives. NEDC and FTP75 are still used to test the analysis approach.

Table 7.4: Main parameters of a prototype HEV.

Item	Description/Quantity
Engine	diesel type, maximum torque of 200Nm, maximum power of 68kW.
Electric machine	maximum torque of 40Nm, maximum power of 6kW.
Battery	lithium-ion; capacity of 6Ah, 110V.
Transmission	6-speed automated manual transmission, $r_g = [3.817, 2.053, 1.302, 0.959, 0.744, 0.614]$.
Vehicle mass	1320kg.

Table 7.5: The weight factors w_1 and w_2 for the HEV optimal control problem on NEDC and FTP75.

Cycle	w_1	w_2
NEDC	$\in \{1, 2, 3, 4\}$	$\in 100 * \{2, 4, 6, 8, 10\}$
FTP75	$\in \{2, 6, 10, 14, 20\}$	$\in 1000 * \{1, 3, 5, 8, 10\}$

The results of SVD analyses on the NEDC and FTP75 are shown in Figure 7.5 and Figure 7.6 respectively. Using the same analysis technique applied for the conventional vehicle, it's still able to achieve the reconstructed control input vector \mathbf{x} as depicted in Figure 7.5c and Figure 7.6c for the NEDC and FTP75 respectively. Notice the reconstructed control input vector \mathbf{x} for the case of FTP75, in which, x_1 varies from $0.74 \rightarrow 1.08$; x_2 varies from $0.6 \rightarrow 0.95$; and x_3 varies from $0.04 \rightarrow 0.35$. In this case study, x_3 is not approximated to zero for the whole ranges of w_1 and w_2 . Therefore, the three directions are normalized by the $\|\mathbf{x}\|_2$ to evaluate their relative contributions to the input vector \mathbf{x} . The maximum relative contribution of x_3 is 10% which is relative small compared to the contributions of x_1 and x_2 , such that x_3 can be ignored from an engineering point of view. Meaning that, the control input vector \mathbf{x} can be re-designed

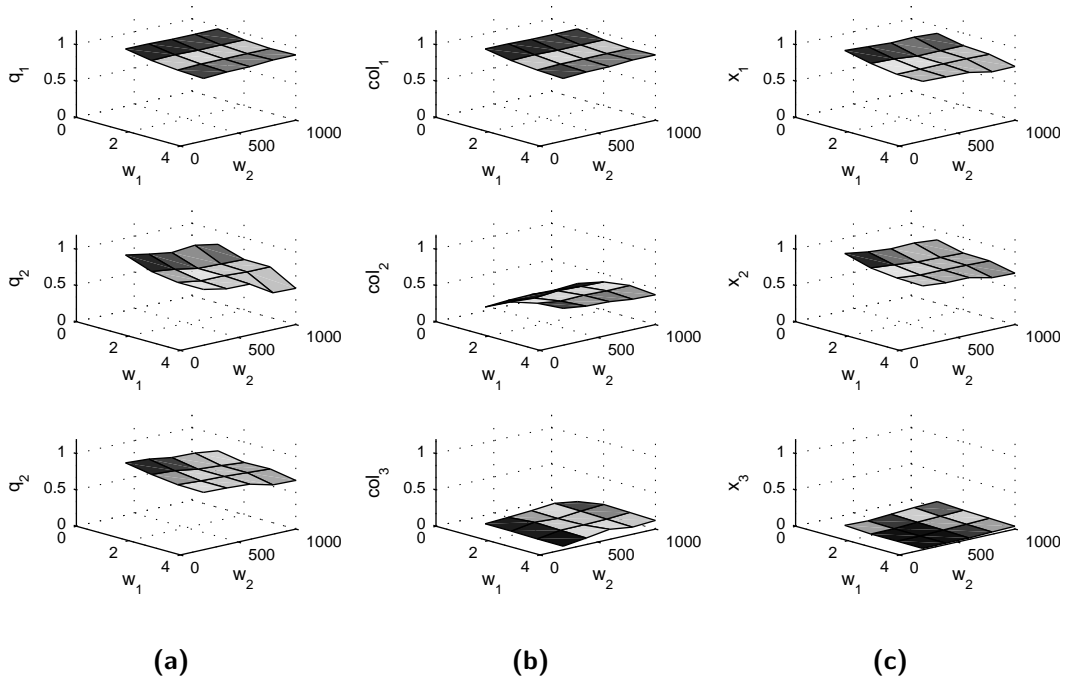


Figure 7.5: Results of the hybrid powertrain on NEDC: the input weight factors q_i in (a); the collinearities col_i in (b); three directions x_1 , x_2 and x_3 of the reconstructed \mathbf{x} in (c).

as follows,

$$\mathbf{x} \approx [1 \ 1 \ 0]^T. \quad (7.38)$$

So, it is observed that for the optimal control problem of HEVs, the driveability, defined by the weighted inverse of power reserve, pays a very small contribution to the objective function. Therefore, the objective function is simplified as,

$$\mathbf{J}_{HEV} = \sum_{k=0}^{N-1} [\dot{m}_f(k) + w_1 |u_g(k)|] \Delta t. \quad (7.39)$$

7.7 Conclusions

A method of objectively analyzing and evaluating the objective function of an optimal control problem for vehicular propulsion systems was proposed. The method utilizes the SVD-based structural analysis approach to study the correlations among the design objectives and investigate their sensitivity to the optimal control algorithm of vehicular propulsion systems. It helps identifying the possibly dependent design objective(s) among the originally concerned ones, such that an objective function can be properly

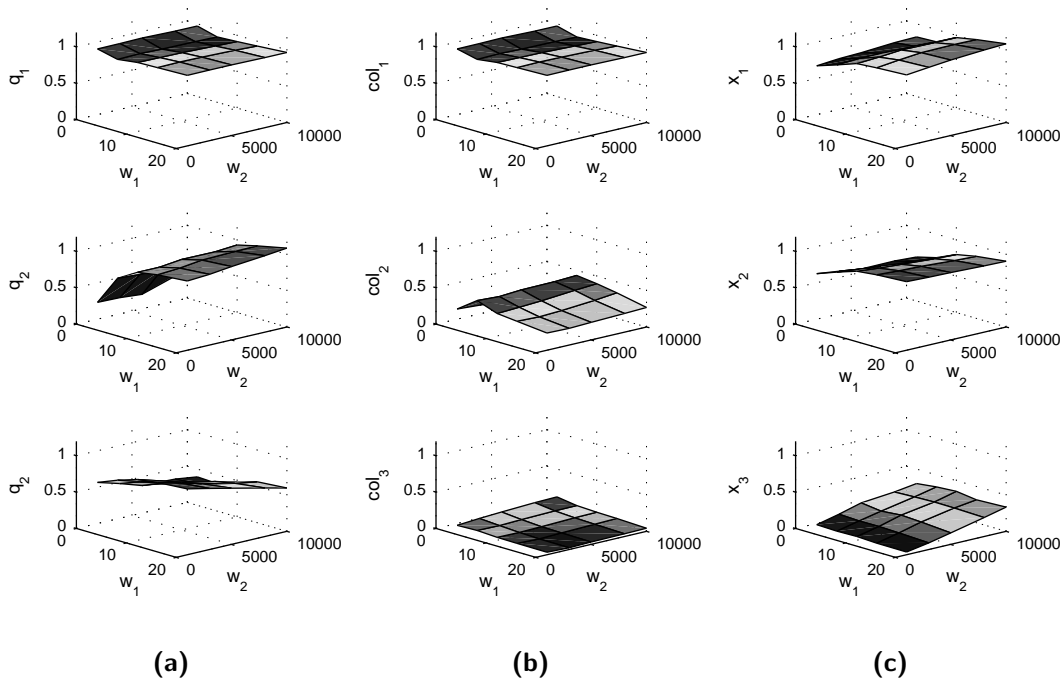


Figure 7.6: Results of the hybrid powertrain on FTP75: the input weight factors q_i in (a); the collinearity col_i in (b); three directions x_1 , x_2 and x_3 of the reconstructed \mathbf{x} in (c).

defined in terms of reducing the complexity of the optimal control design. From the simulation results of the two case-studies, one for conventional vehicle with a gasoline engine, and the other for hybrid electric vehicle with a diesel engine, it can be concluded that the driveability (the weighted inverse of power reserve) is the dependent design objective and has a very small influence on the objective function in defining the optimal solution. Therefore, the objective function consisting of the fuel economy (the fuel consumption) and the comfort (the weighted gear shift frequency) can be proposed for the control design of both powertrain systems.

The proposed method shows itself as an effective method to be able to analyze the objective function. The proposed method is not limited to a specific powertrain topology. In principle, it can be extended to other types of vehicle configurations.

Conclusions and Recommendations

Abstract - In this chapter, the main conclusions following from the previous chapters are drawn and the recommendations for future research are also given.

8.1 Conclusions

The research presented in this dissertation deals with the gear shift control strategy for conventional and hybrid electric vehicles equipped with discrete ratio transmissions. This resulted in the six research objectives ($\mathbf{O}_1 - \mathbf{O}_6$) as presented in Chapter 1.

- \mathbf{O}_1 : define and address the driveability in a fuel-optimal gear shift strategy for conventional vehicles on drive cycles known a priori.
- \mathbf{O}_2 : design a fuel-optimal control algorithm, including the gear shift strategy, for the hybrid dynamical system of HEVs on drive cycles known a priori.
- \mathbf{O}_3 : develop an online gear shift strategy for conventional and hybrid electric vehicles equipped with discrete ratio transmissions. The strategy improves the fuel economy meanwhile still satisfying an acceptable driveability.
- \mathbf{O}_4 : propose a gear shift strategy for a HEV to further improve the fuel economy by exploiting the route information from the GPS-based onboard navigation system.
- \mathbf{O}_5 : analyze the effect of the gear shift and engine start losses on the control strategy and fuel consumption.
- \mathbf{O}_6 : investigate the sensitivity of an optimal gear shift strategy to the relevant control design objectives, such as fuel economy, driveability, comfort, etc.

The six research objectives were addressed in six research chapters, from Chapter 2 till Chapter 7, respectively. The first four objectives were fulfilled by developing various gear shift strategies for automotive transmission. The last two objectives focussed on i) investigating the effect of the discrete state variable-dependent losses (gear shift, clutch losses and engine start) on the control strategy, and ii) analyzing the consequences on the control design objectives (fuel economy, driveability, comfort) with respect to the optimal gear shift strategy. In summary, the research presented in this dissertation made a fundamental contribution in the field of the automotive transmission control design and analysis, with six explicit contributions ($C_1 - C_6$):

- C_1 : various optimal gear shift strategies with respect to the fuel economy and driveability are proposed for conventional vehicles. A novel concept of variable power reserve is developed to properly address the driveability, meanwhile guaranteeing the highest achievable fuel economy (Chapter 2).
- C_2 : a novel gear shift control algorithm based on a combination of DP and Pontryagin's Minimum Principle (PMP) is developed for the hybrid dynamical system (consisting of continuous and discrete variables) of HEVs. This so-called DP-PMP algorithm benchmarks the gear shift problem in terms of optimality and computational efficiency (Chapter 3).
- C_3 : a gear shift map design methodology aiming at a realtime solution for discrete ratio transmissions is developed. The methodology exploits the fuel economy and driveability potential of the optimal gear shift strategies (proposed in Chapters 2 and 3) in order to realize an online gear shift strategy for conventional and hybrid electric vehicles (Chapter 4).
- C_4 : a concept of integrated predictive gear shift strategy for HEVs, utilizing route information to further explore fuel economy potential, is demonstrated in simulation (Chapter 5).
- C_5 : an analysis of the effect of gear shift and engine start losses on control strategies for AMT-based HEVs. By taking the gear shift loss into account, this study reveals a perception of a fuel-efficient advantage of powershift transmissions (DCT, PS-AMT) over non-powershift transmissions (MT, AMT) applied for passenger HEVs. Furthermore, the effect of the engine start loss can not be ignored in seeking a fair evaluation of the fuel economy for parallel HEVs. A prediction horizon of few seconds can help a predictive EMS to realize the highest achievable fuel economy (Chapter 6).
- C_6 : a Singular Value Decomposition-based technique is introduced to analyze the correlation among the design objectives of an optimal gear shift problem for conventional and hybrid electric vehicles (Chapter 7).

The main results and conclusions are summarized in the following subsections.

Optimal gear shift strategies for conventional vehicles

In Chapter 2, a systematic approach in order to address the fuel economy and driveability in an optimal gear shift strategy for conventional vehicles equipped with an AMT was proposed.

The fuel-optimal gear shift strategy based on DP benchmarks the fuel economy on a certain drive cycle. The driveability, defined by the power reserve and represented for an acceleration capability, is systematically addressed in the fuel-optimal gear shift problem. The tradeoff between the fuel economy and driveability is investigated by three methods: i) the weighted inverse of power reserve, ii) the constant power reserve, and iii) the variable power reserve. The first two methods provide control laws more sensitive to the design parameters, and the obtained solutions are too conservative on a certain drive cycle. The third method outperforms the first two methods in terms of the fuel economy and driveability improvements, which is explained by a variable characteristic of the power reserve to the vehicle speed such that the gear shift strategy is adapted accordingly. The advantages of the variable power reserve method is reaffirmed through a comparative analysis with a Stochastic Dynamic Programming (SDP)-based gear shift strategy. The SDP algorithm optimizes the gear shift strategy, subject to a stochastic distribution of the power request, to minimize the expected fuel consumption over an infinite horizon. Hence the obtained solution intrinsically respects the driveability and is realtime implementable. The SDP-based strategy nearly results in the same fuel economy, yet in a lower acceleration capability compared to the results obtained from the variable power reserve method.

The variable power reserve method possesses a superior character in dealing with the driveability effectively and adaptively over a wide range of driving profiles, meanwhile still improving the fuel economy. Hence, it is highly suitable for a realtime application, e.g. a predictive gear shift strategy, or an optimization-based gear shift map design.

Optimal gear shift strategies for HEVs

For HEVs, a DP-based EMS, including the gear shift strategy, is proved to be only useful for benchmarking a globally optimal solution, yet requires an intensive computation. Therefore, the DP-PMP control algorithm is considered as a novel method for the constrained optimal control problem of the hybrid dynamical system in terms of optimality and computational efficiency. PMP is used in the inner loop of the control algorithm to obtain the instantaneous optimal solution for the continuous control variable. Meanwhile, DP is applied in the outer loop of the control algorithm to define the optimal solution for the discrete control variable(s). The main insights related to the

application of this novel method for the hybrid powertrain system are given next.

- For the hybrid powertrain without a start-stop functionality, the DP-PMP approach optimizes the power split and gear shift command. It is found that a unique constant Lagrange multiplier exists, such that the end constraint of the battery state-of-energy is respected and a globally optimal solution is guaranteed.
- For the hybrid powertrain with a start-stop functionality, the DP-PMP approach optimizes the engine start-stop command, power split and gear shift command. It reveals that finding a constant Lagrange multiplier is not possible for this non-smooth optimization problem. A battery state-of-energy feedback controller, e.g. proportional integral controller, is used to adapt the Lagrange multiplier over time. Therefore the obtained solution is in principle suboptimal, despite the fact that it is very close to the globally optimal solution based on DP.

From an engineering point of view, the DP-PMP algorithm can be considered as a globally optimal method applied for HEVs. The algorithm is executed fast enough such that it can be seen as a potential candidate, which can be used in a realtime implementable control algorithm, e.g. a predictive gear shift strategy, or an optimization-based gear shift map design method.

Gear shift map design methodology

Chapter 4 developed a gear shift map design methodology for conventional and hybrid electric vehicles equipped with discrete ratio transmissions. By applying the two-step design procedure: i) utilize an optimal gear shift strategy to derive the optimal gear shift patterns; and ii) use statistical theory to analyse the optimal gear shift patterns and extract the shift lines; the gear shift map is obtained. Through various application and validation in both simulation and experimental environments, it is proved that the obtained gear shift map is acceptably optimized with respect to maximizing the fuel economy and driveability. Furthermore, the obtained gear shift pattern is guaranteed to be consistent and robust. More importantly, the design methodology is:

- flexible (easy adaptable) with changes and modifications during the design process;
- time-efficient for the design process;
- applicable to various powertrain configurations with discrete ratio transmissions.

In summary, the design methodology forms a theoretical and quantified way to generate the commonly used gear shift map for automotive transmissions based on the powertrain system modeling and control and statistical analysis.

Integrated predictive gear shift strategy

Chapter 5 presented an integrated predictive gear shift strategy concept for HEVs. It consists of two algorithms exploiting route information and complementing each other: i) a predictive algorithm controls the gear shift command, beside the power split and engine on-off decision by utilizing route information given in the form of a priori velocity profile; ii) the velocity algorithm derives a fuel-optimal velocity trajectory by utilizing route information given in the form of the road characteristics, speed limits, and average traveling time, etc. The concept has been demonstrated and validated in a simulation environment. The velocity algorithm improves the fuel economy considerably by proposing a fuel-optimal velocity trajectory over a certain driving horizon for the vehicle to follow. The predictive algorithm successfully utilizes a predefined velocity profile over a certain horizon to realize a fuel economy improvement very close to that of the globally optimal algorithm.

Hence, the velocity algorithm is seen as a promising solution to be implemented on the onboard navigation system to yield a velocity profile over a horizon, which is sequentially fed to the predictive algorithm implemented on an EMS. The two algorithms complement each other to create an integrated predictive gear shift strategy realizing the highest fuel economy potential for HEVs.

Effect of gear shift and engine start losses

In Chapter 6, the energy losses involved with the gear shift and engine start processes of an AMT-based HEV were modeled and incorporated in the design of an EMS in order to analyze their influences on the fuel economy, respectively.

Design of the EMSs for passenger HEVs equipped with discrete ratio transmissions requires an optimal gear shift strategy for a fuel economy benefit. One gear up or down per shift is the most optimum gear shift command in terms of the fuel economy and engine operation comfort. Gear shift hysteresis strategy plays a crucial role in reducing the shift busyness and hunt in a way not deteriorating the fuel economy.

Regarding the loss involved with the gear shift, it is found by simulation that a perception of a fuel-efficient advantage of powershift transmissions (DCT, PS-AMT) over non-powershift transmissions (MT, AMT) is realized for passenger HEVs.

In relation with the engine start, it is found that the induced energy loss can not be ignored in a proper design of the EMS to guarantee a fair evaluation on the fuel economy of parallel HEVs. Furthermore, the model predictive control algorithm utilized the engine start loss model effectively in yielding the possible shortest prediction horizon of 5s such that the highest fuel economy can be realized.

Structural analysis of the control design objectives

Chapter 7 discussed a method to analyze the sensitivity of an optimal gear shift strategy to the control design objectives. The method utilizes the Singular Value Decomposition-based structural analysis approach to objectively and quantitatively study the possible correlations among the control design objectives. It is found that the objective function, originally comprised of the fuel consumption, driveability (the weighted inverse of power reserve), and comfort (the weighted gear shift frequency), can be simplified to the one consisting of only the fuel consumption and comfort. The analysis results show that the driveability is interdependent with the comfort. The SVD-based method is able to identify the possible dependent control design objective(s). Hence, a design decision to omit the dependent design objective(s) can be realized. This will allow to build a proper objective function for the optimal control problem, thus reducing the design complexity.

8.2 Recommendations

In light of the findings of the study presented in this dissertation, directions for future research are given next.

1. *Powertrain component size study*

Within the context of designing discrete ratio transmissions for road vehicles primarily powered by internal combustion engines, the gear shift strategy has a vital position in improving the fuel economy, see Chapters 2 and 3. Furthermore, the gear number together with the ratios are also a decisive factor in defining the optimal shift points. The greater the gear number, the better the engine will exploit its efficiency by adhering to the ideal tractive effort. Nonetheless, the fuel economy potential comes at a price of a possible high shifting frequency, an increase of weight and size of the gearbox. From a powertrain system design point of view, there are: i) a possibly strong interdependency among the design parameters (the supervisory control strategy and component size), and ii) an unknown sensitivity of the design parameters to the design objectives (fuel economy and driveability) [49]. Hence, in pursuit of the advantages offered by an optimal gear shift strategy, the follow-up research is defined as follows:

- search for an optimum design of the gear number, ratios and ratio coverage for the transmission used in conventional vehicles to improve the fuel economy and/or driveability;
- study the optimal power specifications (sizes) of the engine, electric machine and transmission parameters (the number of gears, step value and ratio coverage) for HEVs to improve the fuel economy.

2. *Gear shift map generation tool*

As stated in Chapter 1, a strong segmentation of the vehicle classes has led to a variety of the transmission technologies and applications. Furthermore, it is necessary to assess the impact of different powertrain systems and the corresponding control strategies, including the gear shift strategy, on the design objectives at a very early stage of the development process. Therefore, an optimized gear shift map in terms of the fuel economy and driveability for automotive transmissions is highly fitted for the purpose of accelerating the development process and application. Motivated by the very positive outcomes and insights of the gear shift map design methodology, presented in Chapter 4, development of a tool to formally generate the gear shift map for a given powertrain system is seen as a promising prospect in terms of practical applicability.

3. *Towards preview route-based driving*

Recently, the trend in automotive control technology development is to utilize route information obtained from the GPS-based onboard navigation system in order to improve the fuel economy [2, 93, 96, 151]. In line with this, Chapter 5 demonstrated an integrated predictive gear shift strategy which also exploits route information to realize the fuel benefit for HEVs. Ultimately, this trend will result in autonomous driving, wherein the vehicle can brake, accelerate and steer by its own to obtain the maximum possible fuel saving, while even improving (lowering) trip time. This represents an ideal situation where a pre-computed optimal velocity trajectory is exactly followed by the vehicle, wherein the powertrain system is governed by an optimal supervisory control algorithm accordingly. However, in real-life traffic situations, it might not be possible to track the optimal profile due to the upcoming traffic disturbances. Therefore, driving the vehicle with a preview route horizon and cooperating (using communication systems) with the vehicle(s) in front are seen as a solution for this problem. The vehicle will switch from a velocity tracking mode to a vehicle following mode, thus making the optimal algorithm in former mode is not optimal for later mode. Moreover, implementation of the control algorithm on a relatively short driving horizon, e.g. an acceleration horizon, a cruise horizon, and a deceleration horizon, etc., is also required to point out the practical relevance, such as the horizon length, constraints on the battery state-of-energy, and estimation of the Lagrange multiplier on various driving profiles, etc. These challenges are recommended for future research.

4. *Powershift transmissions vs. non-powershift transmissions*

The research in this dissertation has demonstrated by simulation that powershift transmissions (DCT, PS-AMT) are more fuel-efficient than non-powershift transmissions (MT, AMT) applied for passenger HEVs, see Chapter 6. This is proved by modeling and incorporating the gear shift loss into the design of an optimal

EMS. From the large margin of relative fuel difference of powershift transmissions over non-powershift ones, it can set preliminary inferences of:

- a fuel benefit property of the AT over the MT or AMT;
- a fuel benefit of powershift transmissions (AT, DCT, PS-AMT) over non-powershift transmissions (MT, AMT) applied for commercial vehicles, wherein the large drivetrain component inertias and reliable operation of transmissions usually require the interruption time of shifting to be in the order of 0.5-1.0s and longer.

Apparently, these preliminary inferences are contrary to the fact that, for example the AT is considered to have a moderate efficiency compared to the MT or AMT. Therefore, to reinforce the hypothesis, a simulation study for the intended vehicle classes equipped with powershift transmissions is required. Experimental study is also needed to prove the hypothesis.

Optimal Power Split Control of HEVs

Problem A.1. *Given a drive cycle $v(k)$ with time length N , with a given certain admissible gear sequence $n_g(k)$ along this drive cycle, find an instantaneous optimal engine power $P_e^*(k)$ that minimizes the cost function of fuel consumption over the entire drive cycle,*

$$\mathbf{J} = \sum_{k=0}^{N-1} \mathcal{F}_r(P_e(k), k) \Delta t, \quad (\text{A.1})$$

subject to constraints:

$$e_s(k+1) = e_s(k) + \mathcal{P}_s(P_e(k), k) \Delta t, \quad (\text{A.2})$$

$$P'_{e,min}(k) \leq P_e(k) \leq P'_{e,max}(k). \quad (\text{A.3})$$

To apply Pontryagin's minimum principle to solve this optimal control problem, the constraint on engine power is rewritten as an equality constraint by introducing a parameter $p(k)$,

$$P_e^2(k) + \mathbb{A}(k) \cdot P_e(k) + \mathbb{B}(k) + p^2(k) = 0, \quad (\text{A.4})$$

wherein:

$$\mathbb{A}(k) = -(P'_{e,min}(k) + P'_{e,max}(k)),$$

$$\mathbb{B}(k) = P'_{e,min}(k) \cdot P'_{e,max}(k).$$

The augmented cost function \mathbf{J}' is constructed by using Lagrange multipliers $\lambda(k)$ and $\gamma(k)$ to take into account the constraints, thus giving,

$$\mathbf{J}' = \sum_{k=0}^{N-1} \left[\begin{array}{c} \mathcal{F}_r(P_e(k), k) \Delta t \\ -\lambda(k) \left(e_s(k+1) - e_s(k) - \mathcal{P}_s(P_e(k), k) \Delta t \right) \\ -\gamma(k) \left(P_e^2(k) + \mathbb{A}(k) P_e(k) + \mathbb{B}(k) + p^2(k) \right) \end{array} \right]. \quad (\text{A.5})$$

Optimality condition with respect to the constraint on engine power is defined as,

$$\frac{\partial \mathbf{J}'}{\partial p(k)} = 0 \quad \Leftrightarrow \quad 2\gamma(k)p(k) = 0 \quad \Leftrightarrow \quad \begin{cases} \gamma(k) = 0, \\ p(k) = 0. \end{cases} \quad (\text{A.6})$$

According to (A.6), we have two cases needed to be considered as follows:

- **case 1:** $p(k) = 0$,

$$P_{e,1}^*(k) \in \{P'_{e,min}(k), P'_{e,max}(k)\}. \quad (\text{A.7})$$

In this case the optimal engine power is at its bounds, either at the lower bound or at the upper bound.

- **case 2:** $\gamma(k) = 0$,
the inequalities described by (A.3) are inactive. Therefore, we have the Hamiltonian function as,

$$\mathbf{H}(P_e(k), \lambda(k), k) = \left[\mathcal{F}_r(P_e(k), k) + \lambda(k) \mathcal{P}_s(P_e(k), k) \right] \Delta t. \quad (\text{A.8})$$

According to the Pontryagin's minimum principle, the necessary optimality conditions are defined by the followings:

$$\begin{aligned} \lambda(k) - \lambda(k+1) &= \frac{\partial \mathbf{H}(P_e(k), \lambda(k), k)}{\partial e_s(k)} = 0 \\ &\Leftrightarrow \lambda(k) \triangleq \lambda_{opt}, \quad \forall k \in [0, 1, \dots, N-1], \end{aligned} \quad (\text{A.9})$$

$$\begin{aligned} \frac{\partial \mathbf{H}(P_e(k), \lambda(k), k)}{\partial P_e(k)} &= 0 \\ &\Leftrightarrow \frac{\partial \mathcal{F}_r(P_e(k), k)}{\partial P_e(k)} + \lambda(k) \frac{\partial \mathcal{P}_s(P_e(k), k)}{\partial P_e(k)} = 0. \end{aligned} \quad (\text{A.10})$$

From approximations of the engine fuel rate (3.1) and the battery efficiency model (3.5), $\mathcal{F}_r(P_e(k), k)$ and $\mathcal{P}_s(P_e(k), k)$ can be approximated as affine piecewise second-order functions of the engine power at a certain engine speed [25, 73]. So, the Hamiltonian function at each time step is continuous and quadratic. Therefore, there exists such a constant Lagrange multiplier denoted as λ_{opt} (see, [149]), such that the final state of $e_s(N)$ meets a specifically predefined value. The globally optimal solution of the engine power $P_{e,2}^*(k)$ is derived analytically. The two-point boundary value problem is solved.

For both cases 1 and 2, by using (A.9), the cost function (A.5) can be rewritten as,

$$\mathbf{J}' = \sum_{k=0}^{N-1} \left[\mathcal{F}_r(P_e(k), k) + \lambda_{opt} \mathcal{P}_s(P_e(k), k) \right] \Delta t - \lambda_{opt} (e_s(N) - e_s(0)) \Delta t. \quad (\text{A.11})$$

Therefore, the globally instantaneous optimal solution of engine power is defined as,

$$P_e^*(k) = \arg \min_{P_e(k) \in \left\{ \begin{array}{l} P_{e,1}^*(k) \\ P_{e,2}^*(k) \end{array} \right\}} \left[\mathcal{F}_r(P_e(k), k) + \lambda_{opt} \mathcal{P}_s(P_e(k), k) \right]. \quad (\text{A.12})$$

State Constrained Optimal Control of the Power Split for HEVs

Under optimally controlled, the EMS will drive the battery state-of-energy around its initial value and ensure its end constraint to be respected. This appendix reformulates the optimization problem described in Appendix A if the bounds on the battery state-of-energy are taken into account in the control design.

Problem B.1. *Given a drive cycle $v(k)$ with time length of N , with a given certain admissible gear sequence $n_g(k)$ along this drive cycle, find an instantaneous optimal engine power $P_e^*(k)$ that minimizes the cost function of fuel consumption over the entire drive cycle,*

$$\mathbf{J} = \sum_{k=0}^{N-1} \mathcal{F}_r(P_e(k), k) \Delta t, \quad (\text{B.1})$$

subject to constraints:

$$e_s(k+1) = e_s(k) + \mathcal{P}_s(P_e(k), k) \Delta t, \quad (\text{B.2})$$

$$E_{s,min} \leq e_s(k) \leq E_{s,max}, \quad (\text{B.3})$$

$$P'_{e,min}(k) \leq P_e(k) \leq P'_{e,max}(k). \quad (\text{B.4})$$

The constraint on engine power $P_e(k)$ must be rewritten as an equality constraint by introducing a parameter $p(k)$,

$$P_e^2(k) + \mathbb{A}(k) \cdot P_e(k) + \mathbb{B}(k) + p^2(k) = 0, \quad (\text{B.5})$$

wherein:

$$\mathbb{A}(k) = -(P'_{e,min}(k) + P'_{e,max}(k)),$$

$$\mathbb{B}(k) = P'_{e,min}(k) \cdot P'_{e,max}(k).$$

The constraint on battery state of energy $e_s(k)$ must be rewritten as an equality constraint by introducing a parameter $q(k)$,

$$e_s^2(k) + \mathbb{C} \cdot e_s(k) + \mathbb{D} + q^2(k) = 0, \quad (\text{B.6})$$

wherein:

$$\mathbb{C} = -(E_{s,min} + E_{s,max}),$$

$$\mathbb{D} = E_{s,min} \cdot E_{s,max}.$$

The new cost function \mathbf{J}' is constructed by using Lagrange multipliers $\lambda(k)$, $\gamma(k)$ and $\beta(k)$ to take into account the constraints, thus giving,

$$\mathbf{J}' = \sum_{k=0}^{N-1} \begin{bmatrix} \mathcal{F}_r(P_e(k), k)\Delta t - \\ -\lambda(k) \left(e_s(k+1) - e_s(k) - \mathcal{P}_s(P_e(k), k)\Delta t \right) \\ -\gamma(k) \left(P_e^2(k) + \mathbb{A}(k)P_e(k) + \mathbb{B}(k) + p^2(k) \right) \\ -\beta(k) \left(e_s^2(k) + \mathbb{C} \cdot e_s(k) + \mathbb{D} + q^2(k) \right) \end{bmatrix}. \quad (\text{B.7})$$

Optimality conditions are defined as,

$$\frac{\partial \mathbf{J}'}{\partial p(k)} = 0 \Leftrightarrow 2\gamma(k)p(k) = 0 \Leftrightarrow \begin{cases} p(k) = 0, \\ \gamma(k) = 0. \end{cases} \quad (\text{B.8})$$

$$\frac{\partial \mathbf{J}'}{\partial q(k)} = 0 \Leftrightarrow 2\beta(k)q(k) = 0 \Leftrightarrow \begin{cases} q(k) = 0, \\ \beta(k) = 0, \end{cases} \quad (\text{B.9})$$

$$\frac{\partial \mathbf{J}'}{\partial e_s(k)} = 0 \Leftrightarrow \lambda(k+1) = \lambda(k) - \beta(k)(2e_s(k) + \mathbb{C}), \quad (\text{B.10})$$

$$\begin{aligned} \frac{\partial \mathbf{J}'}{\partial P_e(k)} &= 0 \\ &\Leftrightarrow \frac{\partial \mathcal{F}_r(P_e(k), k)}{\partial P_e(k)} + \lambda(k) \frac{\partial \mathcal{P}_s(P_e(k), k)}{\partial P_e(k)} - \gamma(k)(2P_e(k) + \mathbb{A}(k)) = 0, \end{aligned} \quad (\text{B.11})$$

and the second derivative,

$$\frac{\partial^2 \mathbf{J}'_1}{\partial P_e^2(k)} \geq 0 \Leftrightarrow \frac{\partial^2 \mathcal{F}_r(P_e(k), k)}{\partial P_e^2(k)} + \lambda(k) \frac{\partial^2 \mathcal{P}_s(P_e(k), k)}{\partial P_e^2(k)} - 2\gamma(k) \geq 0. \quad (\text{B.12})$$

According to (B.8) and (B.9), we have four cases needed to be considered as follows:

- **case 1:** $q(k) = 0$ & $p(k) = 0$,
with condition $q(k) = 0$ we have,

$$e_{s,1}^*(k) \in \{E_{s,min}, E_{s,max}\}. \quad (\text{B.13})$$

- if $e_{s,1}^*(k) = E_{s,min}$, from (B.10) we have:

$$\lambda(k+1) = \lambda(k) - \beta(k)(E_{s,min} - E_{s,max}), \quad (\text{B.14})$$

$$e_s(k+1) \geq E_{s,min} \Leftrightarrow \mathcal{P}_s(P_e(k), k) \geq 0. \quad (\text{B.15})$$

- if $e_{s,1}^*(k) = E_{s,max}$, from (B.10) we have:

$$\lambda(k+1) = \lambda(k) - \beta(k)(E_{s,max} - E_{s,min}), \quad (\text{B.16})$$

$$e_s(k+1) \leq E_{s,max} \Leftrightarrow \mathcal{P}_s(P_e(k), k) \leq 0. \quad (\text{B.17})$$

with condition $p(k) = 0$, we have the optimal engine power $P_{e,1}^*(k)$

$$P_{e,1}^*(k) \in \{P'_{e,min}(k), P'_{e,max}(k)\}, \quad (\text{B.18})$$

and the optimal battery power defined correspondingly with respect to (B.15) and (B.17).

- **case 2:** $q(k) = 0$ & $\gamma(k) = 0$,

with condition $q(k) = 0$ we have still approach the conditions of next values of $\lambda(k+1)$ and $\mathcal{P}_s(P_e(k), k)$ as in (B.14)-(B.17) of case 1.

with condition $\gamma(k) = 0$, the engine power $P_e(k)$ is in its boundary. The optimal engine power $P_{e,2}^*(k)$ is obtained by solving,

$$\begin{aligned} \frac{\partial \mathcal{F}_r(P_e(k), k)}{\partial P_e(k)} + \lambda(k) \frac{\partial \mathcal{P}_s(P_e(k), k)}{\partial P_e(k)} &= 0, \\ \frac{\partial^2 \mathcal{F}_r(P_e(k), k)}{\partial P_e^2(k)} + \lambda(k) \frac{\partial^2 \mathcal{P}_s(P_e(k), k)}{\partial P_e^2(k)} &\geq 0, \end{aligned}$$

and the optimal battery power defined correspondingly with respect to conditions (B.15) and (B.17).

- **case 3:** $\beta(k) = 0$ & $p(k) = 0$,

for this case, the optimal control problem now returns to problem described in Appendix A. Therefore the same procedure is applied to define the optimal engine power $P_{e,3}^*(k)$ and $P_{e,4}^*(k)$ correspondingly.

- **case 4:** $\beta(k) = 0$ & $\gamma(k) = 0$,

this case is similar to case 3.

For cases 1, 2, 3 and 4, the cost function (B.7) becomes,

$$\mathbf{J}' = \sum_{k=0}^{N-1} \left[\begin{array}{c} \mathcal{F}_r(P_e(k), k) \Delta t - \lambda(k) (e_s(k+1) - \\ - e_s(k) - \mathcal{P}_s(P_e(k), k) \Delta t) \end{array} \right], \quad (\text{B.19})$$

or

$$\begin{aligned} \mathbf{J}' = & \sum_{k=0}^{N-1} \left[\mathcal{F}_r(P_e(k), k) + \lambda(k) \mathcal{P}_s(P_e(k), k) \right] \Delta t - \\ & - \sum_{k=0}^{N-1} \lambda(k) (e_s(k+1) - e_s(k)) \Delta t. \end{aligned} \quad (\text{B.20})$$

In (B.20), the first summation term is the augmented Lagrange cost functional which is continuous at every time step; the second summation term describes the demand constraint on the state variable. In this study, this demand constraint denotes the variation of battery state of energy at the beginning and the end of the drive cycle. Therefore, the globally instantaneous optimal solution of engine power is defined as,

$$P_e^*(k) = \arg \min_{P_e(k) \in \left\{ \begin{array}{l} P_{e,1}^*(k), \\ P_{e,2}^*(k), \\ P_{e,3}^*(k), \\ P_{e,4}^*(k) \end{array} \right\}} \left\{ \mathcal{F}_r(P_e(k), k) + \lambda(k) \mathcal{P}_s(P_e(k), k) \right\}. \quad (\text{B.21})$$

Apparently, from (B.14) and (B.16) it is observed that when the battery state of energy reaches its bounds, then the Lagrange multiplier $\lambda(k)$ changes its value. Between the two consecutive points of reaching the bounds of the battery state-of-energy, the Lagrange multiplier $\lambda(k)$ is kept constant.

APPENDIX C

Drive Cycles

This appendix shows the standard drive cycles used throughout chapters of this dissertation.

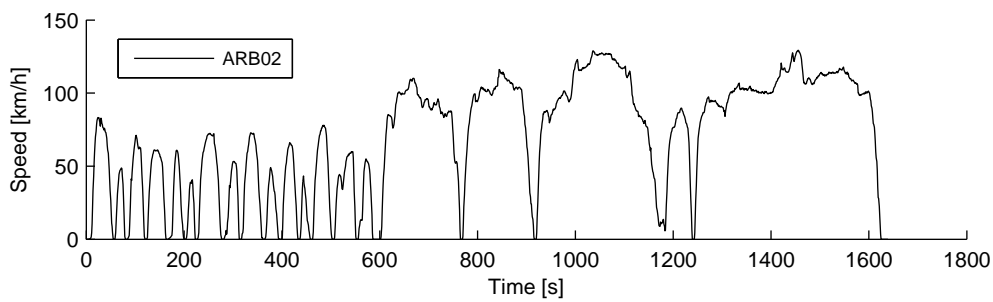


Figure C.1: Drive cycle: Air Resources Board No. 2 (ARB02).

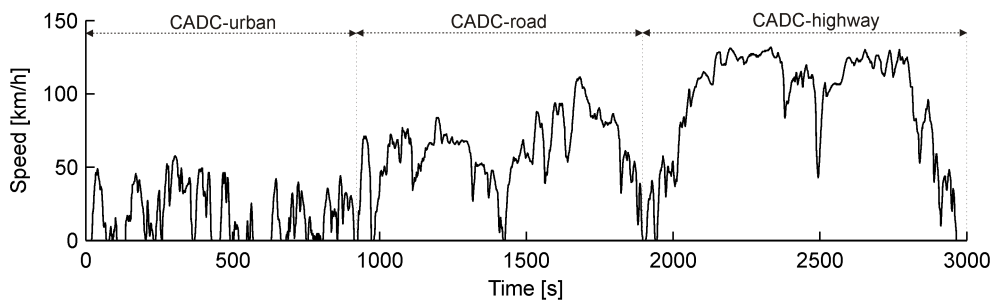


Figure C.2: Drive cycle: Common Artemis Driving Cycles (CADC).

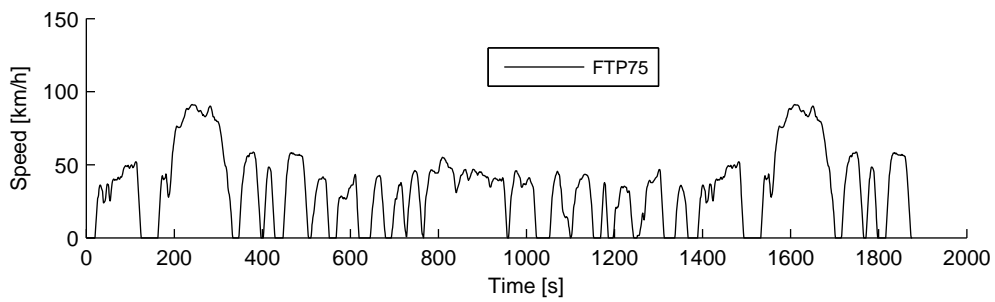


Figure C.3: Drive cycle: Federal Test Procedure 75 (FTP75).

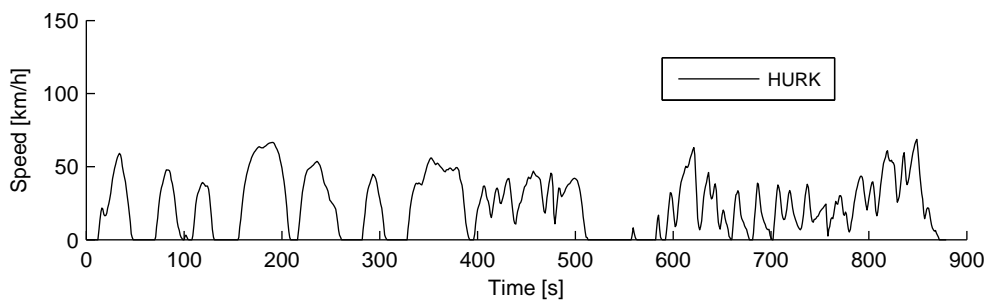


Figure C.4: Drive cycle: Hurk (in Eindhoven, The Netherlands).

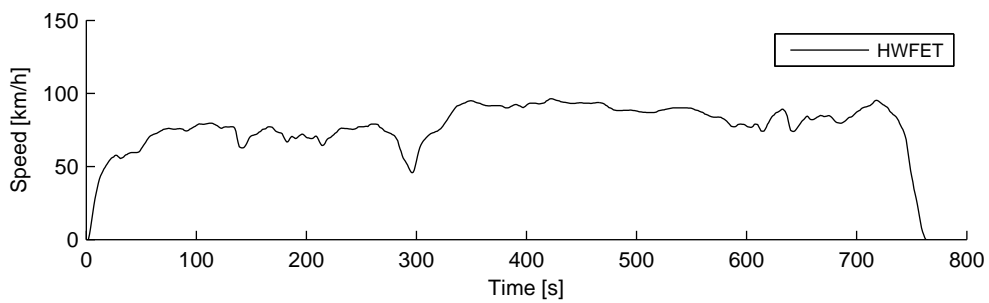


Figure C.5: Drive cycle: Highway Fuel Economy Driving Cycle (HWFET).

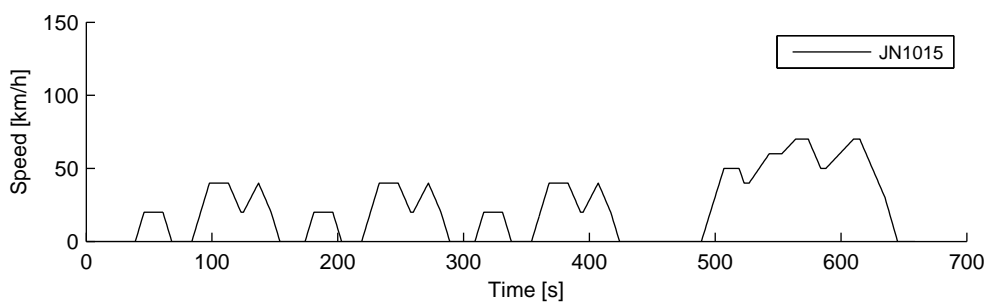


Figure C.6: Drive cycle: Japan 1015 (JN1015).

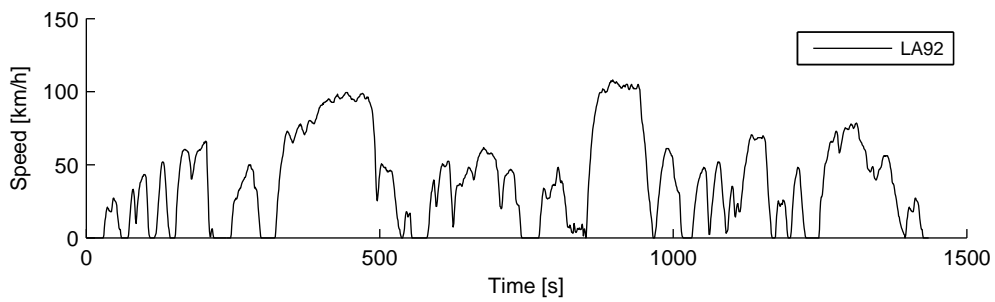


Figure C.7: Drive cycle: Los Angeles 92 (LA92).

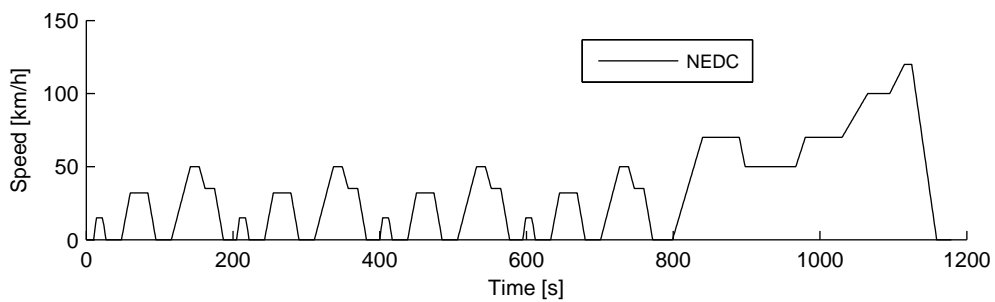


Figure C.8: Drive cycle: New European Drive Cycle (NEDC).

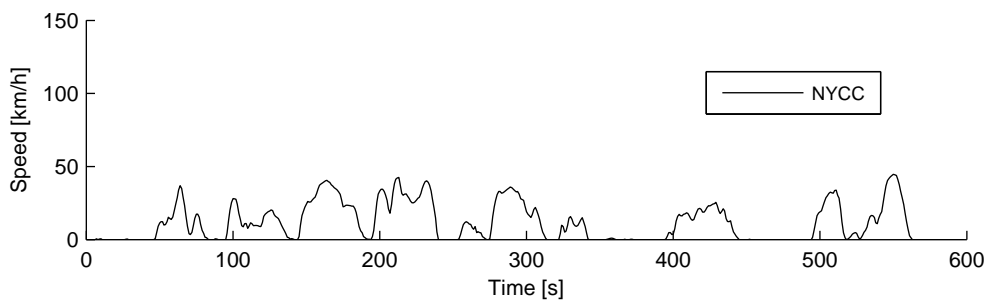


Figure C.9: Drive cycle: New York City Cycle (NYCC).

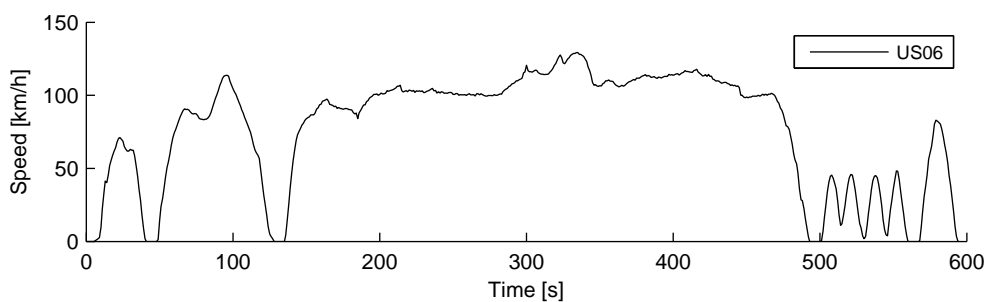


Figure C.10: Drive cycle: US06.

Bibliography

- [1] F. Alkhalisi. Are automotive suppliers prepared for a new era in transmission technology? In *Electric & Hybrid Vehicle Technology International*. UKIP Media & Event Ltd, 2012.
- [2] D. Ambuhl and L. Guzzella. Predictive reference signal generator for hybrid electric vehicles. *IEEE Transactions on Vehicular Technology*, 58(9):4730–4740, 2009.
- [3] D. Ambuhl, O. Sundstrom, A. Sciarretta, and L. Guzzella. Explicit optimal control policy and its practical application for hybrid electric powertrains. *Control Engineering Practice*, 18:1429–1439, 2010.
- [4] I. Arsie, M. Graziosi, C. Pianese, and M. Rizzo, G. and Sorrentino. Optimization of supervisory control strategy for parallel hybrid vehicle with provisional load estimate. In *Proceedings of the 7th International Symposium on Advanced Vehicle Control - AVEC04*, 2004.
- [5] M. Back, M. Simons, F. Kirschbaum, and V. Krebs. Predictive control of drivetrains. In *Proceedings of the 15th IFAC World Congress*, 2002.
- [6] S. Bai, K. V. Hebbale, and C. J. Lee. Automatic transmission shift point control system and method of use, 2008.
- [7] S. Bai, J. Maguire, D. K. Kim, and H. Peng. Dynamic programming based motor vehicle shift map generation. In *Proceedings of the world automotive congress 2006 - FISITA 2006*, 2006.
- [8] S. Barsali, C. Miulli, and A. Possenti. A control strategy to minimize fuel consumption of series hybrid electric vehicles. *IEEE Transactions on Energy Conversion*, 19(1):187–195, 2004.
- [9] R. Bartholomaeus, M. Klingner, and M. Lehnert. Prediction of power demand for hybrid vehicles operating in fixed-route service. In *Proceedings of the 17th IFAC World Congress*, pages 5640–5645, Seoul, Korea, 2008.
- [10] R. Beck, A. Bollig, and D. Abel. Comparison of two real-time predictive strategies for the optimal energy management of a hybrid electric vehicle. *Oil and Gas Science and Technology–Rev. IFP*, 62:635–643, 2007.
- [11] R.E. Bellman. *Dynamic Programming*. Princeton University Press, Princeton, USA, 1957.
- [12] A. Bemporad, P. Borodani, and M. Mannelli. Hybrid control of an automotive robotized gearbox for reduction of consumptions and emissions. *Springer Berlin -Heidelberg*, 2623:81–96, 2003.
- [13] J. Bernard, S. Delprat, T. M. Guerra, and F. N. Buchi. Fuel efficient power management strategy for fuel cell hybrid powertrains. *Control Engineering Practice*, 18:408–417, 2010.
- [14] D. P. Bertsekas. *Dynamic Programming and Optimal Control*. Athena Scientific, Belmont, USA, 2000.
- [15] I. J. M. Besselink, P. F. Van Oorschot, E. Meinders, and H. Nijmeijer. Design of an efficient, low weight battery electric vehicle based on a VW Lupo 3L. In *Proceedings of the 25th Electric Vehicle Symposium*, Shenzhen, China, 2010. 10 pages.

-
- [16] H. A. Borhan, A. Vahidi, A. M. Phillips, M. L. Kuang, and I. V. Kolmanovsky. Predictive energy management of a power-split hybrid electric vehicle. In *Proceedings of 2009 American Control Conference*, pages 3970–3976, St. Louis, MO., USA, 2009.
- [17] L. Buie, M. Fry, P. Fussey, and C. Mitts. An application of cost-based power management control strategies to hybrid fuel cell vehicles. In *Proceedings of 2004 SAE International*, 2004.
- [18] A. Casavola, G. Prodi, and G. Rocca. Efficient gear shifting strategies for green driving policies. In *Proceedings of 2010 American Control Conference*, pages 4331–4336, 2010.
- [19] M. Ceraolo, A. di Donato, and G. Franceschi. A general approach to energy optimization of hybrid electric vehicles. *IEEE Transactions on Vehicular Technology*, 57(3):1433–1441, 2008.
- [20] F. H. Clarke. *Necessary Conditions in Dynamic Optimization*. Vol. 173, Nr 816. American Mathematical Society, Providence, Rhode Island, USA, 2005.
- [21] R. Cook, A. M. Cristobal, G. Parks, C. O. Correa, and P. J. Clarkson. Multi-objective optimization of a hybrid electric vehicle - drive train and driving strategy. *Springer Berlin*, 4403, 2007.
- [22] J. Dai. Isolated word recognition using Markov chain models. *IEEE Transactions on Speech and Audio Processing*, 3(6):458–463, 1995.
- [23] B. de Schutter and W. P. M. H. Heemels. *Modeling and Control of Hybrid Systems*. Lecture Notes of the DISC Course, 2008. DISC: Dutch Institute of Systems and Control.
- [24] S. Delprat, T. M. Guerra, and J. Rimaux. Optimal control of a parallel powertrain: From global optimization to real time control strategy. In *Proceedings of 2002 IEEE Vehicular Technology Conference*, pages 2082–2088, Birmingham, Al., USA, 2002.
- [25] S. Delprat, J. Lauber, T. M. Guerra, and J. Rimaux. Control of a parallel hybrid powertrain: Optimal control. *IEEE Transactions on Vehicular Technology*, 53:872–881, 2004.
- [26] Luc Devroye. *Non-Uniform Random Variate Generation*. Springer-Verlag, 1986.
- [27] R. Edwards, J. F. Larive, V. Mahieu, and P. Rouveïrolles. Well-to-wheels analysis of future automotive fuels and powertrains in the European context, WELL-TO-TANK report version 2b. European Commission Joint Research Centre, Institute for Environment and Sustainability, 2006.
- [28] M. Ehsani, Y. Gao, and A. Emadi. *Modern Electric, Hybrid Electric, and Fuel Cell Vehicles - Fundamentals, Theory, and Design*. CRC Press, September 2009.
- [29] B. S. Everitt, S. Landau, and M. Leese. *Cluster Analysis*. Arnold, 4th edition, 2001.
- [30] B. C. Fabien. Numerical solution of constrained optimal control problems with parameters. *Applied Mathematics and Computation*, 80:43–62, 1996.
- [31] S. A. Fayazi, S. Farhangi, and B. Asaei. Power delivery co-ordination to meet driver’s demand in a mild hybrid vehicle with automated manual transmission. In *Proceedings of the 34th Annual Conference of IEEE Industrial Electronics*, pages 327–332, 2008.
- [32] Z. Filipi and Y.J. Kim. Hydraulic hybrid propulsion for heavy vehicles: Combining the simulation and engine-in-the-loop techniques to maximize the fuel economy and emission benefits. *Oil and Gas Science and Technology—Rev. IFP*, 65:155–178, 2009.
- [33] Z. Filipi, L. Louca, B. Daran, C. C. Lin, U. Yildir, B. Wu, M. Kokkolaras, D. Assanis, H. Peng, P. Papalambros, J. Stein, D. Szkubiel, and R. Chapp. Combined optimisation of design and power management of the hydraulic hybrid propulsion system for the 6x6 medium truck. *International Journal of Heavy Vehicle Systems*, 11:372–402, 2004.
- [34] D. G. Florencio, E. R. Assis, and C. H. F. Amendola. The manual transmission automated - gearshift quality comparison to a similar manual system. In *Proceedings of 2004 SAE International*, 2004.

- [35] D. Foster, R. Cloudt, and F. Willems. Towards integrated powertrain control: exploiting synergy between a diesel hybrid and aftertreatment system in a distribution truck. In *Proceedings of IEEE Intelligent Vehicles Symposium*, pages 1021–1026, Eindhoven, the Netherlands, 2008.
- [36] ZF Friedrichshafen. ZF develops 9-speed automatic transmission for passenger cars. Press Information, 11 2011.
- [37] T. Gassman and C. Gasch. Transmission technology for hybrid and electric vehicle. In *Proceedings of 2012 SAE International*, 2012.
- [38] H.P. Geering. *Optimal Control with Engineering Applications*. Springer-Verlag, Berlin, Heidelberg, Germany, 2007.
- [39] L. Glielmo, L. Iannelli, V. Vacca, and F. Vasca. Gearshift control for automated manual transmissions. *IEEE/ASME Transactions on Mechatronics*, 11(1):17–26, 2006.
- [40] Q. Gong, Y. Li, and Z.R. Peng. Trip-based optimal power management of plug-in hybrid electric vehicles. *IEEE Transactions on Vehicular Technology*, 57:3393–3401, 2008.
- [41] Qiuming Gong, Yaoyu Li, and Zhong-Ren Peng. Optimal power management of plug-in HEV with intelligent transportation system. In *Proceedings of IEEE/ASME international conference on advanced intelligent mechatronics*, pages 1–6, 2007.
- [42] L. Guzzella and A. Sciarretta. *Vehicle Propulsion Systems: Introduction to Modeling and Optimization*. Springer-Verlag, Berlin, Heidelberg, Germany, 2007.
- [43] K. W. Gwak and G. Y. Masada. Structural analysis and optimization of nonlinear control systems using singular value decomposition. *Journal of Dynamic Systems, Measurement, and Control*, 127, 2005.
- [44] R. F. Hartl, S. P. Sethi, and R. G. Vickson. A survey of the maximum principles for optimal control problems with state constraints. *SIAM Review*, 37:181–218, 1995.
- [45] K. Hayashi, Y. Shimizu, Y. Dote, A. Takayama, and A. Hirako. Neuro fuzzy transmission control for automobile with variable loads. *IEEE Transactions on Control Systems Technology*, 3(1):49–53, 1995.
- [46] R. P. G. Heath and A. J. Child. Zeroshift - a seamless automated manual transmission with no torque interrupt. In *Proceedings of 2007 SAE International*, 2007.
- [47] E. Hellstrom. *Look-ahead Control of Heavy Vehicles*. PhD thesis, Linköping University Institute of Technology, Linköping, Sweden, 2010.
- [48] E. Hellstrom, J. Aslund, and L. Nielsen. Management of kinetic and electric energy in heavy trucks. *SAE International Journal of Engines*, 3:1152–1163, 2010.
- [49] T. Hofman. *Framework for Combined control and design optimization of hybrid vehicle propulsion systems*. PhD thesis, Technische Universiteit Eindhoven, The Netherlands, 2007.
- [50] T. Hofman, M. Steinbuch, R. Van Druten, and A. Serrarens. Rule-based energy management strategies for hybrid vehicles. *International Journal of Electric and Hybrid Vehicles*, 1:71–94, 2007.
- [51] T. Hofman, M. Steinbuch, R. van Druten, and A. Serrarens. Design of CVT-based hybrid passenger cars. *IEEE Transactions on Vehicular Technology*, 58(2):572–587, 2009.
- [52] X. L. Hu, Z. F. Wang, and L. Y. Liao. Multi-objective optimization of HEV fuel economy and emissions using evolutionary computation. In *Proceedings of 2004 SAE International*, 2004.
- [53] M. Huang. Optimal multilevel hierarchical control strategy for parallel hybrid electric vehicle. In *Proceedings of 2006 IEEE Vehicle Power and Propulsion Conference*, pages 1–4, 2006.
- [54] International Energy Agency. Hybrid and electric vehicles - the electric drive plugs in. Technical report, International Energy Agency, 2011.

-
- [55] B. Jacobson and M. Spickenreuther. Gearshift sequence optimisation for vehicles with automated non-powershifting transmissions. *International Journal of Vehicle Design*, 32:187–207, 2003.
- [56] S. I. Jeon, S. T. Jo, Y. I. Park, and J. M. Lee. Multi-mode driving control of a parallel hybrid electric vehicle using driving pattern recognition. *Journal of Dynamic Systems, Measurement, and Control*, 124:141–149, 2002.
- [57] L. Johannesson, M. Asbogard, and B. Egardt. Assessing the potential of predictive control for hybrid vehicle powertrains using stochastic dynamic programming. *IEEE Transactions on Intelligent Transportation Systems*, 8:71 – 83, 2007.
- [58] V. H. Johnson, K. Wipke, and D. Rausen. HEV control strategy for real-time optimization of fuel economy and emissions. In *Proceedings of 2000 SAE International*, 2000.
- [59] R. Johri, S. Baseley, and Z. Filipi. Simultaneous optimization of supervisory control and gear shift logic for a parallel hydraulic hybrid refuse truck using stochastic dynamic programming. In *Proceeding of the 4th Annual Dynamic Systems and Control Conference*, VA, USA, 2011.
- [60] J. M. Kang, I. Kolmanovsky, and J. W. Grizzle. Dynamic optimization of lean burn engine aftertreatment. *Journal of Dynamic Systems, Measurement, and Control*, 123:153–160, 2001.
- [61] G. E. Katsargyri, I. V. Kolmanovsky, J. Micheline, M. L. Kuang, A. M. Phillips, M. Rinehart, and M. A. Dahleh. Optimally controlling hybrid electric vehicles using path forecasting. In *Proceedings of 2009 American Control Conference*, pages 4613–4617, 2009.
- [62] J. T. B. A. Kessels. *Energy Management for Automotive Power Nets*. PhD thesis, Eindhoven University of Technology, The Netherlands, 2007.
- [63] J. T. B. A. Kessels, M. W. T. Koot, P. P. J. van den Bosch, and D. B. Kok. Online energy management for hybrid electric vehicles. *IEEE Transactions on Vehicular Technology*, 57(6):3428–3440, 2008.
- [64] J. T. B. A. Kessels and P. Van den Bosch. Electronic horizon: Road information used by energy management strategies. *Journal of Intelligent Information and Database Systems*, 2:187–203, 2008.
- [65] H. K. Khalil. *Nonlinear Systems*. Third edition. Prentice-Hall, Inc., New Jersey, USA, 2002.
- [66] D. K. Kim, H. Peng, S. Bai, and J. M. Maguire. Control of integrated powertrain with electronic throttle and automatic transmission. *IEEE Transactions on Control Systems Technology*, 15(3):474–482, 2007.
- [67] N. Kim, S. Cha, and H. Peng. Optimal control of hybrid electric vehicles based on Pontryagin’s minimum principle. *IEEE Transactions on Control Systems Technology*, 19(5):1279–1287, 2011.
- [68] F. Kirschbaum, M. Back, and M. Hart. Determination of the fuel-optimal trajectory for a vehicle along a known route. In *Proceedings of the 15th IFAC Triennial World Congress*, Barcelona, Spain, 2002. 5 pages.
- [69] A. Kleimaier and D. Schroder. An approach for the online optimized control of a hybrid powertrain. In *Proceeding of the 7th International Advanced Motion Control Workshop*, pages 215–220, 2002.
- [70] I. Kolmanovsky, I. Siverguina, and B. Lygoe. Optimization of powertrain operating policy for feasibility assessment and calibration: stochastic dynamic programming approach. In *Proceedings of 2002 American Control Conference*, volume 2, pages 1425–1430, 2002.
- [71] I. V. Kolmanovsky and V. Winstead. A receding horizon optimal control approach to active state and parameter estimation in automotive systems. In *Proceedings of 2006 IEEE Conference on Control Applications*, pages 2796–2801, Munich, Germany, 2006.
- [72] M. Koot. *Energy Management for Vehicular Electric Power Systems*. PhD thesis, Technische Universiteit Eindhoven, The Netherlands, 2006.

- [73] M. Koot, J. T. B. A. Kessels, B. de Jager, W. Heemels, P. van den Bosch, and M. Steinbuch. Energy management strategies for vehicular electric power systems. *IEEE Transactions on Vehicular Technology*, 54:771–782, 2005.
- [74] M. Koot, J.T.B.A. Kessels, and B. De Jager. Fuel reduction of parallel hybrid electric vehicles. In *Proceedings of 2005 IEEE Vehicle Power and Propulsion Conference*, pages 26–31, Chicago, IL, USA, 2005.
- [75] D. S. Kum, H. Peng, and N. K. Bucknor. Supervisory control of parallel hybrid electric vehicles for fuel and emission reduction. *Journal of Dynamic Systems, Measurement, and Control*, 133(6):10, 2011.
- [76] O. Kyoungcheol, J. H. Min, D. H. Choi, and H. S. Kim. Optimization of control strategy for a single-shaft parallel hybrid electric vehicle. *Proceedings of the Institution of Mechanical Engineers, Part D - Journal of Automobile Engineering*, 221:555–565, 2007.
- [77] D. le Guen, T. Weck, A. Balihe, and B. Verbeke. Definition of gearshift pattern: Innovative optimization procedures using system simulation. *SAE International Journal of Engines*, 4:412–431, 04 2011.
- [78] H. D. Lee, S. K. Sul, H. S. Cho, and J. M. Lee. Advanced gear-shifting and clutching strategy for a parallel-hybrid vehicle. *IEEE Industry Applications Magazine*, 6(6):26–32, 2000.
- [79] Robert D. Leopold. A new definition of ‘fuel efficiency ’ in commercial vehicles. In *Proceedings of 2009 SAE International*, 2009.
- [80] W. Li, G. Xu, Z. Wang, and Y. Xu. Dynamic energy management for hybrid electric vehicle based on adaptive dynamic programming. In *Proceeding of 2008 IEEE International Conference on Industrial Technology*, pages 1–6, 2008.
- [81] C. C. Lin, S. Jeon, H. Peng, and J. M. Lee. Driving pattern recognition for control of hybrid electric trucks. *Vehicle System Dynamics*, 42:41–58, 2004.
- [82] C. C. Lin, H. Peng, and J. W. Grizzle. A stochastic control strategy for hybrid electric vehicles. In *Proceedings of 2004 American Control Conference*, volume 5, pages 4710–4715, 2004.
- [83] C. C. Lin, H. Peng, J. W. Grizzle, and J. M. Kang. Power management strategy for a parallel hybrid electric truck. *IEEE Transactions on Control Systems Technology*, 11:839–849, 2003.
- [84] S. Lin, S. Chang, and B. Li. Gearshift system design for automated manual transmission based on an electromagnetic actuator. In *Proceedings of 2011 International Electrical and Control Engineering Conference*, pages 2250–2253, 2011.
- [85] B. W. Lindgren. *Statistical theory*. Chapman & Hall, 4th edition, 1993.
- [86] S. M. Lukic and A. Emadi. Effects of drivetrain hybridization on fuel economy and dynamic performance of parallel hybrid electric vehicles. *IEEE Transactions on Vehicular Technology*, 53:385–389, 2004.
- [87] B. Mashadi, A. Kazemkhani, and R. B. Lakeh. An automatic gear-shifting strategy for manual transmissions. *Proceedings of the Institution of Mechanical Engineers, Part I - Journal of Systems and Control Engineering*, 221:757–768, 2007.
- [88] C. Musardo, G. Rizzoni, and B. Staccia. A-ECMS : An adaptive algorithm for hybrid electric vehicle energy management. In *Proceedings of the 2005 IEEE Conference on Decision and Control, and the European Control Conference*, pages 1816–1823, Seville, Spain, 2005.
- [89] H. Naunheimer, B. Bertsche, J. Ryborz, and W. Novak. *Automotive Transmissions: Fundamentals, Selection, Design and Application*. Springer, 2 edition, 2011.
- [90] G. J. L. Naus, R. P. A. Vugts, J. Ploeg, M. J. G. Van de Molengraft, and M. Steinbuch. String-stable CACC design and experimental validation, a frequency-domain approach. *IEEE Transactions on Vehicular Technology*, 59:4268–4279, 2010.

-
- [91] V. Ngo, T. Hofman, M. Steinbuch, and A. Serrarens. Performance indices for vehicular propulsion systems. In *Proceedings of the 15th Asia Pacific Automotive Engineering Conference*, 2009.
- [92] V. Ngo, T. Hofman, M. Steinbuch, and A. Serrarens. Shifting strategy for step change transmission vehicle – a comparative study and design method. In *Proceedings of the 24th International Battery, Hybrid and Fuel Cell Electric Vehicle Symposium*, 2009.
- [93] V. Ngo, T. Hofman, M. Steinbuch, and A. Serrarens. An optimal control-based algorithm for hybrid electric vehicle using preview route information. In *Proceedings of 2010 American Control Conference*, 2010.
- [94] V. Ngo, T. Hofman, M. Steinbuch, and A. Serrarens. Optimal shifting strategy for a parallel hybrid electric vehicle. In *Proceedings of the 25th World Battery, Hybrid and Fuel Cell Electric Vehicle Symposium and Exhibition - EVS25*, 2010.
- [95] V. Ngo, T. Hofman, M. Steinbuch, and A. Serrarens. Analyses of the performance index for a hybrid electric vehicle. In *Proceedings of 2011 American Control Conference*, 2011.
- [96] V. Ngo, T. Hofman, M. Steinbuch, and A. Serrarens. Predictive gear shift control for a parallel hybrid electric vehicle. In *Proceedings of 2011 IEEE Vehicle Power and Propulsion Conference*, pages 1–6, 2011.
- [97] V. Ngo, T. Hofman, M. Steinbuch, and A. Serrarens. Effect of gear shift and engine start losses on control strategies for hybrid electric vehicles. In *Proceedings of the 26th Electric Vehicle Symposium - EVS26*, 2012.
- [98] V. Ngo, T. Hofman, M. Steinbuch, and A. Serrarens. Optimal control of the gear shift command for hybrid electric vehicles. *IEEE Transactions on Vehicular Technology*, 61, 2012.
- [99] V. Ngo, T. Hofman, M. Steinbuch, A. Serrarens, and L. Merckx. Improvement of fuel economy in power-shift automated manual transmission through shift strategy optimization – an experimental study. In *Proceedings of 2010 IEEE Vehicle Power and Propulsion Conference*, pages 1–5, 2010.
- [100] D. F. Opila, D. Aswani, R. McGee, J. A. Cook, and J. W. Grizzle. Incorporating drivability metrics into optimal energy management strategies for hybrid vehicles. In *Proceedings of the 47th IEEE Conference on Decision and Control*, pages 4382–4389. IEEE, 2008.
- [101] G. Paganelli, G. Ercole, A. Brahma, Y. Guezennec, and G. Rizzoni. General supervisory control policy for the energy optimization of charge-sustaining hybrid electric vehicles. *JSAE Review*, 22:511–518, 2001.
- [102] G. Paganelli, T.M. Guerra, S. Delprat, Y. Guezennec, and G. Rizzoni. Optimal control theory applied to hybrid fuel cell powered vehicle. In *Proceedings of the 15th IFAC Triennial World Congress*, Barcelona, Spain, 2002. 6 pages.
- [103] M. F. Pan and C. C. Ku. Application of singular value decomposition for structural modal analysis. *The Japanese Journal of Applied Physics*, 30:2626–2635, 1991.
- [104] B. Passenberg, P. Kock, and O. Stursberg. Combined time and fuel optimal driving of trucks based on a hybrid model. In *Proceedings of 2009 European Control Conference*, pages 4955–4960, Budapest, Hungary, 2009.
- [105] R. Pfiffner and L. Guzzella. Optimal operation of CVT-based powertrains. *International Journal of Robust and Nonlinear Control*, 11(11):1003–1021, 2001.
- [106] P. Pisu, K. Koprubasi, and G. Rizzoni. Energy management and drivability control problems for hybrid electric vehicles. In *Proceedings of the 44th IEEE European Control Conference on Decision and Control*, pages 1824–1830, 2005.
- [107] P. Pisu and G. Rizzoni. A comparative study of supervisory control strategies for hybrid electric vehicles. *IEEE Transactions on Control Systems Technology*, 15:506–518, 2007.

- [108] V. Pop, H. J. Bergveld, D. Danilov, P. P. L. Regtien, and P. H. L. Notten. *Battery Management Systems*. Philips Research Vol. 9. Springer, New York, USA, 2008.
- [109] M. Prasad, A. Sardar, and S. Mubashir. Transmission technologies : An Indian perspective. *SAE International*, 01 2011.
- [110] G. Qin, A. Ge, J. Zhao, and J. J. Lee. Cruise control of automated manual transmission vehicles. *Computing & Control Engineering Journal*, 14(2):18–21, 2003.
- [111] A. Rajagopalan and G. Washington. Intelligent control of hybrid electric vehicles using GPS information. In *Future Car Congress 2002*, 2002.
- [112] A. Rajagopalan, G. Washington, G. Rizzoni, and Y. Guezennec. Development of fuzzy logic control and advanced emissions modeling for parallel hybrid vehicles. Technical report, NREL Technical Report, 2003.
- [113] A. C. Rencher. *Methods of Multivariate Analysis*. Wiley, second edition, 2002.
- [114] G. Ripaccioli, A. Bemporad, F. Assadian, C. Dextreit, S. Di Cairano, and I. V. Kolmanovsky. Hybrid modeling, identification, and predictive control: An application to hybrid electric vehicle energy management. *Hybrid Systems: Computation and Control, Lecture Notes in Computer Science*, 54:321–335, 2009.
- [115] G. Rizzoni, L. Guzzella, and B. M. Baumann. Unified modeling of hybrid electric vehicle drivetrains. *IEEE/ASME Transactions on Mechatronics*, 4:246–257, 1999.
- [116] P. Rodatz, G. Paganelli, A. Sciarretta, and L. Guzzella. Optimal power management of an experimental fuel cell/supercapacitor-powered hybrid vehicle. *Control Engineering Practice*, 13:41–53, 2005.
- [117] A. P. Ronald and D. I. Osita. Interaction analysis for multivariable systems. In *Proceedings of IEEE International Conference on Systems Engineering*, 1990.
- [118] G. Rousseau, D. Sinoquet, and P. Rouchon. Constrained optimization of energy management for a mild-hybrid vehicle. *Oil and Gas Science and Technology—Rev. IFP*, 62:623–634, 2007.
- [119] SAE Standard J2711. Recommended practice for measuring fuel economy and emissions of hybrid-electric and conventional heavy-duty vehicles, 2002.
- [120] B. Saerens, M. Diehl, J. Swevers, and E. Van den Bulck. Model predictive control of automotive powertrains - first experimental results. In *Proceedings of the 2008 IEEE Conference on Decision and Control*, pages 5692–5697, Cancun, Mexico, 2008.
- [121] F. R. Salmasi. Control strategies for hybrid electric vehicles: Evolution, classification, comparison, and future trends. *IEEE Transactions on Vehicular Technology*, 56(5):2393–2404, 2007.
- [122] H. Scherer, M. Bek, and S. Kilian. ZF new 8-speed automatic transmission 8HP70 - basic design and hybridization. *SAE International Journal of Engines*, 2:314–326, 04 2009.
- [123] N. J. Schouten, A. Salman, and N. A. Kheir. Energy management strategies for parallel hybrid vehicles using fuzzy logic. *Control Engineering Practice*, 11:171–177, 2003.
- [124] A. B. Schwarzkopf and R. B. Leipnik. Control of highway vehicles for minimum fuel consumption over varying terrain. *Transportation Research*, 11:279–286, 1977.
- [125] A. Sciarretta, M. Back, and L. Guzzella. Optimal control of parallel hybrid electric vehicles. *IEEE Transactions on Control Systems Technology*, 12:352–363, 2004.
- [126] A. Sciarretta and L. Guzzella. Control of hybrid electric vehicles: optimal energy management strategies. *IEEE Control Systems Magazine*, 27:60–70, 2007.
- [127] L. Serrao, S. Onori, and G. Rizzoni. ECMS as a realization of Pontryagin’s minimum principle for HEV control. In *Proceedings of 2009 American Control Conference*, pages 3964–3969, 2009.

-
- [128] L. Serrao, S. Onori, A. Sciarretta, Y. Guezennec, and G. Rizzoni. Optimal energy management of hybrid electric vehicles including battery aging. In *Proceedings of 2011 American Control Conference*, pages 2125–2130, 2011.
- [129] A. Serrarens. *Coordinated Control of The Zero Inertia Powertrain*. PhD thesis, Eindhoven University of Technology, The Netherlands, 2001.
- [130] A. Serrarens. Roadmap of DTIs efficient power shift transmissions. In *Proceedings of the 2009CTI Symposium on Innovative Automotive Transmissions*, 2009.
- [131] A. Serrarens, R. van Druten, W. van Liempt, N. Weel, P. Kumar, L. Rmrs, and D. V. Ngo. Light hybridisation of diesel powertrains: The most cost-effective route towards 120 g/km CO_2 and below. In *Proceedings of the 2008 VDI Conference Innovative Powertrains*, 2008.
- [132] A. Serrarens, W. van Liempt, N. Weel, and L. Merckx. Powershift module combination of friction brake and planetary gearset. *ATZ Magazine*, 112:5, 2010.
- [133] A. F. Simon, L. Guzzella, C. H. Ondera, and C. Nizzolab. Improved dynamic performance of turbocharged SI engine powertrains using clutch actuation. *Control Engineering Practice*, 14:363–373, 2006.
- [134] D. Sinoquet, G. Rousseau, and Y. Milhau. Design optimization and optimal control for hybrid vehicles. *Optimization and Engineering*, 12:199–213, 2009.
- [135] M. H. Smith, E. J. Barth, N. Sadegh, and G. J. Vachtsevanos. The horsepower reserve formulation of driveability for a vehicle fitted with a continuously variable transmission. *Vehicle System Dynamics*, 41(3):157–180, 2004.
- [136] G. Steinmauer and L. del Re. Optimal control of dual power sources. In *Proceedings of the 2001 IEEE International Conference on Control Applications*, pages 422–427, 2001.
- [137] S. Stockar, V. Marano, G. Rizzoni, and L. Guzzella. Optimal control for plug-in hybrid electric vehicle applications. In *Proceedings of 2010 American Control Conference*, pages 5024–5030, Baltimore, MD., USA, 2010.
- [138] A. P. Stoicescu. On fuel-optimal velocity control of a motor vehicle. *International Journal of Vehicle Design*, 16:229–256, 1995.
- [139] O. Sundstrom, D. Ambuhl, and L. Guzzella. On implementation of dynamic programming for optimal control problems with final state constraints. *Oil and Gas Science and Technology—Rev. IFP*, 65:91–102, 2010.
- [140] O. Sundstrom, L. Guzzella, and P. Soltic. Torque-assist hybrid electric powertrain sizing: From optimal control towards a sizing law. *IEEE Transactions on Control Systems Technology*, 18:837–849, 2010.
- [141] O. Sundstrom, P. Soltic, and L. Guzzella. A transmission-actuated energy-management strategy. *IEEE Transactions on Vehicular Technology*, 59(1):84–92, 2010.
- [142] S. Suzuki. The development of new hino hybrid commercial vehicles. In *Proceedings of 2011 SAE International*, 2011.
- [143] L. Tan, D. Cameron, and C. McCorkell. Multivariable decoupling control system design for the plasma etching process. In *Proceedings of International Industrial Electronics, Control and Instrumentation*, volume 3, pages 1971–1976, 1994.
- [144] E. Tate and S. Boyd. Finding ultimate limits of performance for hybrid electric vehicles. In *Proceedings of 2000 SAE International*, 2000.
- [145] H. Vahabzadeh and S. Linzell. Modeling, simulation, and control implementation for a split-torque, geared neutral, infinitely variable transmission. In *Proceedings of 1991SEA International*, 1991.

- [146] A. Vahidi, A. Stefanopoulou, and H. Peng. Recursive least squares with forgetting for online estimation of vehicle mass and road grade. *Vehicle System Dynamics*, 43:31–55, 2005.
- [147] H. J. Valeri, B. W. Keith, and J. R. David. HEV control strategy for real-time optimization of fuel economy and emissions. In *Proceedings of 2000 SAE International*, 2000.
- [148] T. J. J. van den Boom and A. A. Stoorvogel. *Model Predictive Control*. DISC Course-Lecture Notes, 2010.
- [149] P. P. J. van den Bosch and F. A. Lootsma. Scheduling of power generation via large-scale nonlinear optimization. *Journal of Optimization Theory and Applications*, 55:313–326, 1987.
- [150] T. van Keulen. *Fuel Optimal Control of Hybrid Vehicles*. PhD thesis, Eindhoven University of Technology, The Netherlands, The Netherlands, 2011.
- [151] T. van Keulen, B. de Jager, and M. Steinbuch. Optimal trajectories for vehicles with energy recovery options. In *Proceedings of the 18th IFAC World Congress*, volume 18, 2011.
- [152] T.A.C. van Keulen, A.G. de Jager, A.F.A. Serrarens, and M. Steinbuch. Optimal energy management in hybrid electric trucks using route information. *Oil and Gas Science and Technology—Rev. IFP*, 65:103 – 113, 2010.
- [153] P. Varaiya. Lecture notes on optimization. Technical report, University of California at Berkeley, 1998.
- [154] M. Vasak, M. Baotic, N. Peric, and M. Bago. Optimal rail route energy management under constraints and fixed arrival time. In *Proceedings of 2009 European Control Conference*, pages 2972–2977, Budapest, Hungary, 2009.
- [155] F. Vasca, L. Iannelli, A. Senatore, and M. T. Scafati. Modeling torque transmissibility for automotive dry clutch engagement. In *Proceedings of 2008 American Control Conference*, pages 306–311, 2008.
- [156] F. Wang, X. J. Mao, B. Zhuo, H. Zhong, and Z. L. Ma. Parallel hybrid electric system energy optimization control with automated mechanical transmission. *Proceedings of the Institution of Mechanical Engineers, Part D - Journal of Automobile Engineering*, 222:499–513, 2008.
- [157] W. Wang, Q. Wang, and X. Zeng. Automated manual transmission shift strategy for parallel hybrid electric vehicle. In *Proceedings of 2009 SAE International*, 2009.
- [158] X. Wei. *Modeling and Control of a Hybrid Electric Drivetrain for Optimum Fuel Economy, Performance and Driveability*. PhD thesis, Ohio State University, US, 2004.
- [159] X. Wei, L. Guzzella, V. I. Utkin, and G. Rizzoni. Model-based fuel optimal control of hybrid electric vehicle using variable structure control systems. *Journal of Dynamic Systems, Measurement, and Control*, 129:13–19, 2007.
- [160] F. Willems and R. Cloudt. Experimental demonstration of a new model-based SCR control strategy for cleaner heavy-duty diesel engines. *IEEE Transactions on Control Systems Technology*, 19:1305–1313, 2011.
- [161] S. S. Williamson and A. Emadi. Comparative assessment of hybrid electric and fuel cell vehicles based on comprehensive well-to-wheels efficiency analysis. *IEEE Transactions on Vehicular Technology*, 54:856–862, 2005.
- [162] J. S. Won and R. Langari. Intelligent energy management agent for a parallel hybrid vehicle-part ii: torque distribution, charge sustenance strategies, and performance results. *IEEE Transactions on Vehicular Technology*, 54(3):935–953, 2005.
- [163] J. S. Won, R. Langari, and M. Ehsani. An energy management and charge sustaining strategy for a parallel hybrid vehicle with CVT. *IEEE Transactions on Control Systems Technology*, 13(2):313–320, 2005.

- [164] W. Xiong, Y. Zhang, and C. Yin. Optimal energy management for a series-parallel hybrid electric bus. *Journal of Energy Conversion and Management*, 50:1730–1738, 2009.
- [165] M. Yamasaki, H. Konno, H. Kuroiwa, and N. Ozaki. Automated manual transmission with torque assist mechanism for reducing shift shock. In *Proceedings of 2005 SAE International*, 2005.
- [166] Z. G Yang, C. X Cao, and Y. Su. A method of optimal shift control based on pattern recognition and learning algorithm. In *Proceedings of the 4th World Congress Intelligent Control and Automation*, volume 2, pages 955–959, 2002.
- [167] X. Yin, D. Xue, and Y. Cai. Application of time-optimal strategy and fuzzy logic to the engine speed control during the gear-shifting process of AMT. In *Proceedings of the 4th International Conference of Fuzzy Systems and Knowledge Discovery*, volume 4, pages 468–472, 2007.
- [168] Z. Yong, S. Jian, W. Di, and Xu C. Automatic transmission shift point control under different driving vehicle mass. In *Proceedings of 2002 SAE International*, 2002.
- [169] H. J. Yoon and C. J. Lee. An optimized control strategy for parallel hybrid electric vehicle. In *Proceedings of 2003 SAE International*, 2003.
- [170] R. Zhang and Y. Chen. Control of hybrid dynamical systems for electric vehicles. In *Proceedings of 2001 American Control Conference*, volume 4, pages 2884–2889, 2001.
- [171] Y. Zhang, H. Lin, B. Zhang, and Mi C. Performance modeling and optimization of a novel multi-mode hybrid powertrain. *Journal Mechanical Design*, 128:79–89, 2006.
- [172] Y. Zhu, Y. Chen, Z. H. Wu, and A. H. Wang. Optimization design of an energy management strategy for hybrid vehicles. *International Journal of Alternative Propulsion*, 1:47–62, 2006.

Acknowledgements

It has been a great privilege for me to be with the Control Systems Technology Group at Mechanical Engineering Department, Eindhoven University of Technology, as a PhD candidate. The PhD journey is probably the most challenging one with which I have ever been. By organizing the study, planing the project, doing research, and realizing fruitful results, a dissertation has finally come up. The research as presented in this dissertation has been made possible by the contributions of numerous people to whom I would like to acknowledge.

First of all, I would like to express my deep gratitude to my supervisor Prof. Maarten Steinbuch, for offering me the opportunity to work on such an interesting project as a PhD candidate. He has patiently provided the vision, encouragement and advise necessary for me to proceed through the doctoral program and complete my dissertation. I am totaly delighted with his efficient, pragmatic, direct and honest guidance and supervising approach. He has always given me a freedom to do research in the academic environment. I have learnt a lot from him, not only the knowledge but also the communication, organization and management skills, which will definitely benefit my future career.

I am very much grateful to my co-supervisor Dr. Theo Hofman, with whom I work closely during my PhD candidacy. He has guided me openly and critically and motivated me to pursue independent, innovative research. I am much indebted to him for his valuable advice in my work, spending his precious times at regular meetings, reading papers and dissertation. I am totally undoubted to say that he is a strong and supportive advisor, very enthusiastic and energetic. Beside the academic world, we have shared together a lot of fun, life, conference time, etc. I am very happy of having had the opportunity to work with him.

The research project is proposed by Drivetrain Innovations B.V. (DTI) together with Eindhoven University of Technology. Herewith, I would like to send special thanks to DTI in general, and to Dr. Alex Serrarens in particular. The guidance, support, helpful suggestions and critical comments for papers and dissertation from him has served me well throughout my PhD. He was the source of inspiration in the early days of my PhD.

I owe him my heartfelt appreciation. Moreover, we have also had very good moments together, not only at DTI but also at conferences.

This dissertation would not have been possible without the thoroughly reading of manuscript together with valuable feedbacks, and the approval for technological designs from the core committee. Therefore, I am very much grateful to Prof. Hyunsoo Kim, Prof. Huei Peng and Prof. Paul van den Bosch for their time and participation. I also thank Prof. L.P.H. de Goey, Dr. P.A. Veenhuizen and Prof. W.P.M.H. Heemels for their willingness to participate in the doctoral committee. The road to my PhD in automotive engineering started with my master in Korea. Therefore, I take this opportunity to say heartfelt thanks to Prof. Hyunsoo Kim again for introducing me to this interesting field and for being my master advisor.

Working on and finishing a PhD require more than only research. My (former) roommates, Niels, Bart, Ismail, Tom, have been the sources of laugh, joy and support. They have helped me much more than I can imagine, especially in creating a nice working environment and adhesive substances to integrate me to the groups. They deserve my sincere thanks. However, all (former) members of the CST, D&C, and H&NS groups will always remain dear to me. I also thank Antonio Colin for the fruitful cooperation during his master project. We achieved nice results and worked well together.

Coming and staying at The Netherlands for my PhD would have been more difficult without the help of Hetty, Thea, Mariken from HR department, since the early contact emails when I were in Vietnam until the end of my PhD tenure. My job would not have gone smoothly without the help of Lia, Petra, Geertje at the secretariat for practical issues. I extend my warm thanks to the Vietnamese friends in Eindhoven, who have created and shared a warm, joyful, and supportive life, making it homely feeling at Eindhoven. Therefore, it is also a pleasure to mention some good friends like Dung, Hai, Phuoc, Anh Van for their love, care, support that have gone to a certain extend beyond normal. All other people who were involved are equally acknowledged.

Above all, I would like to pay the highest regards to my parents due to their many years of unconditional love, wholehearted support, and guidance. I owe them everything. My grandfather has showed a genuine interest in my PhD and continuously motivated me to pursue with it. I thank my brothers (and their families), for their love, continuous support during my study and work far away home. I would like to express my sincere thanks to my parent in-law, my brothers in-law (and their families) for their love, help and support during my PhD research.

Finally, my special and heartfelt thanks go to my wife, Phan Tran Duc Lien, for her endless love, support and great patience at all times. She has always been along with me during the happy and hard moments to encourage and push me up. My beloved daughter, Ngo Duc Ngoc Han, has been an unlimited energy source, a great inspiration for me to overcome difficulties and challenges to be able to go ahead during this journey.

Việc tiếp tục học tập nâng cao chuyên môn, nghiên cứu tiến sĩ sẽ không suôn sẻ nếu thiếu sự giúp đỡ, tạo điều kiện thuận lợi của TS. Lê Vinh Danh ở Đại học Tôn Đức Thắng. Tôi xin chân thành cảm ơn sự quan tâm, và những động viên quý báu của Thầy trong thời gian vừa qua. Tôi cũng xin cảm ơn sự giúp đỡ của các đồng nghiệp ở phòng KHCN-HT-SĐH và khoa Điện-Điện tử. Nhân đây, tôi cũng xin gửi lời cảm ơn đến PGS. TS. Phạm Xuân Mai (ĐHBK Tp.HCM) vì những trao đổi hữu ích, các hoạt động chuyên môn, sự quan tâm, và chia sẻ chân thành trong nhiều năm qua, góp thêm gia vị cuộc sống cho việc nghiên cứu.

Đạt được thành quả hôm nay, trước tiên tôi xin bày tỏ lòng biết ơn đến ông nội. Mặc dù tuổi đã trên 80, nhưng ông nội luôn luôn son sắt động viên, khích lệ và bày tỏ sự mong đợi thành công trên con đường nghiên cứu của tôi. Mong ông luôn luôn mạnh khỏe và minh mẫn. Bằng cả tấm lòng, điều mà khó diễn tả thành lời, tôi xin gửi lời tri ân đến ba mẹ, vì tình yêu thương vô bờ, sự nuôi nấng, dạy dỗ, hỗ trợ vô điều kiện, sự tận tâm hướng dẫn và động viên không ngừng. Bên cạnh đó, tôi xin gửi lời cảm ơn đến anh Thủy (và gia đình) và em Triều, vì những thương yêu, tin tưởng và hỗ trợ vai trò trong quá trình tôi học tập và làm việc xa nhà, xa quê hương. Tôi cũng xin chân thành biết ơn ba mẹ vợ, anh Đức Anh (và gia đình) và em Hiếu (và gia đình), đã luôn quan tâm, động viên, giúp đỡ với sự yêu thương, tạo thuận lợi cho quá trình nghiên cứu này.

Cuối cùng là những lời cảm ơn đặc biệt dành cho vợ tôi, Đức Liên, vì sự yêu thương không điều kiện, hỗ trợ, lo lắng và kiên nhẫn trong mọi thời gian, đồng hành và động viên trong mọi khó khăn. Con gái yêu quý, Ngọc Hân, thật sự là nguồn năng lượng vô tận, là sự động viên lớn lao để tôi có thể vượt qua những khó khăn, thách thức và tiến lên phía trước trong suốt chặng đường nghiên cứu tiến sĩ.

Ngo Duc Viet

Eindhoven, The Netherlands.

July, 2012.

Curriculum Vitae

Ngo Dac Viet was born on 9 September 1980 in Thua Thien Hue, Vietnam. He graduated from Quoc Hoc - Hue high school, Thua Thien Hue in 1998. He received a bachelor degree with honor in Electrical and Electronics Engineering from HoChiMinh City University of Technology, Vietnam in 2003. He continued his study at Sungkyunkwan University, South Korea, where in 2007 he obtained a master degree in Mechanical Engineering. His master's thesis was entitled 'Torque Smoothing of Clutch by Active Motor Control' and carried out at Dynamic System Design Lab, Sungkyunkwan University.

In May 2008, he started as a Ph.D candidate in the Control Systems Technology Group at Mechanical Engineering Department of Eindhoven University of Technology. The Ph.D project focuses on designing the energy management strategies for vehicular propulsion systems, including conventional and hybrid electric vehicles. The results of his Ph.D project are presented in this dissertation, entitled 'Gear Shift Strategies for Automotive Transmissions'. During his Ph.D candidacy, he followed the courses from the Graduate School of Dutch Institute of Systems and Control (DISC). He won the 'Best Paper Prize' for the paper 'Predictive Gear Shift Control for a Parallel Hybrid Electric Vehicle' at the 7th IEEE Vehicle Power and Propulsion Conference - (VPPC 2011), Chicago, USA in 2011.

